Imperial College London

Stretch Sensors to Measure Knee Kinematics in Sports

Yewande Adebola Adesida

April 2023

A thesis submitted in fulfillment of the requirements

for the degree of Doctor of Philosophy

in the

Department of Surgery and Cancer

IMPERIAL COLLEGE LONDON

Declaration of Originality

I declare that to the best of my knowledge, all work included in this thesis is my own, and that any other work that has been included has been duly acknowledged and appropriately referenced.

Yewande Adesida

February 2023

Copyright Statement

The copyright of this thesis rests with the author. Unless otherwise indicated, its contents are licensed under a Creative Commons Attribution-Non Commercial 4.0 International Licence (CC BY-NC).

Under this licence, you may copy and redistribute the material in any medium or format. You may also create and distribute modified versions of the work. This is on the condition that: you credit the author and do not use it, or any derivative works, for a commercial purpose.

When reusing or sharing this work, ensure you make the licence terms clear to others by naming the licence and linking to the licence text. Where a work has been adapted, you should indicate that the work has been changed and describe those changes.

Please seek permission from the copyright holder for uses of this work that are not included in this licence or permitted under UK Copyright Law.

Acknowledgements

I would like to start off by thanking my supervisors: Professor Alison McGregor and Dr Enrica Papi, without whom I do not think this process would have been possible. They have been excellent guides but have also encouraged my independence, believing in my ability to carry out this extensive research project when I did not have the same self-belief. Alison especially took a leap of faith (at least that is what it feels like), convincing me to enrol on the PhD programme when I was fully convinced I was only going to do an MPhil and spent the first two years telling everyone so.

This project was not solely a biomechanics endeavour (especially considering my background as a Materials Scientist and Engineer) – there here was involvement from other departments at Imperial, indicating the development of wearable technology as a truly multi-disciplinary field. That being said, I would also like to thank the following people (some of whom have now moved on from their positions): Dr Cecilia Mattevi and Dr Peter Sherrell for their help with access to the Materials department, and the knowledge and expertise that led to the creation of the strain sensors that formed the basis for this project; Dr Noelia Rubio Carrero from Chemistry for her help in preliminary investigations of sensor coating options; and finally Dr Matthew Hopkins for aiding me with all my sensor and circuitry woes, even if he did laugh at my initial attempts at soldering.

Next, even though they started after me and finished before me (my excuse being that this was a part-time endeavour!): thanks goes to Shruti Turner, Birana Sivapuratharasu and Caryn Urbanczyk for their encouragement, giving me a reason to come into the office, and then indulging me when I suggested that we start a virtual reading and writing group when we went into lockdown. This group gave me the motivation to start working on my thesis and to get two chapters written while waiting to get back onto campus.

Special shout outs go to Dr Rebecca Howard and (soon to be Dr!) Claire Baker: Rebecca for being my PhD and cycling guru; and Claire for being my S&C buddy and someone I could relate to about balancing PhD life and sporting commitments at Imperial. I am grateful to the chance encounters in sports that have led to these friendships.

Finally, thank you to my family (Mum, Dad and Busoye) for your support during the past few years while I undertook something that I am not sure any of us knew quite knew the intensity of. Also, for actually remembering what my subject topic is when you told other people about my research.

Abstract

The popularity of wearable technology in sport has increased, due to its ability to provide unobtrusive monitoring of athletes. This technology has been used to objectively measure kinetic and kinematic variables, with the aim of preventing injury, maximising athletic performance and classifying the skill level of athletes, all of which can influence training and coaching practices. Wearable technologies overcome the limitations of motion capture systems which are limited in their capture volume, enabling the collection of data in-field, during training and competition. Inertial sensors are a common form of technology used in these environments however, their high-cost and complex calibration due to multiple sensor integration can make them prohibitive for widespread use.

This thesis focuses on the development of a strain sensor that can be used to measure knee range of motion in sports, specifically rowing and cycling, as a potential low-cost, lightweight alternative to inertial sensors which can also be integrated into clothing, making them more discreet. A systematic review highlighted the lack of alternate technologies to inertial sensors such as strain sensors, as well as the limited use of wearable technologies in both rowing and cycling.

Strain sensors were fabricated from a carbon nanotube-natural rubber composite using solvent exchange techniques and employed a piezoresistive sensing mechanism. These were then characterised using mechanical testing, to determine their electrical properties under cyclical strain. The strain sensors displayed hysteretic behaviour, but were durable, withstanding over 4500 strain cycles. Statistical analysis indicated that over 60% of the tests conducted had good intra-test variability with regards to the resistance response range in each strain cycle and sensor response deviating by less than 10% at strain rates below 100 mm/min and less than 20% at a strain rate of 350 mm/min.

These sensors were integrated into a wearable sensor system and tested on rowing and cycling cohorts consisting of ten athletes each, to assess the translational use of the strain sensor. This preliminary testing indicated that strain sensors were able to track the motion of the knee during the rowing stroke and cycling pedalling motion, when compared to the output of a motion capture system. Perspectives of participants on the wearable system were collected, which indicated their desire for a system that they could use in their sport, and they considered the translation of this system for real-life use with further development to improve comfort of the system and consistency of the sensor response. The strain sensors developed in this project, when integrated into a wearable sensor system, have the

potential to provide an unobtrusive method of measuring knee kinematics, helping athletes, coaches and other support staff make technical changes that can reduce injury risk and improve performance.

Contents

Title Page **1**

Declaration of Originality **2**

Copyright Statement **3**

Acknowledgements **4**

Abstract **5**

Table of Contents **11**

List of Tables **15**

List of Figures **21**

List of Acronyms **22**

1 Introduction **25**

1.1 Project Background and Motivation 25

1.2 Thesis Aims 27

1.3 Summary of Contributions 27

1.4 Publications 28

1.4.1 Publications to Date 28

1.4.2 Proposed Publications 28

1.5 Thesis Structure 28

2 Literature Review **30**

2.1 Introduction 30

2.2 Overview of Sports Biomechanics 31

2.3 Systematic Review 32

2.3.1 Abstract 32

2.3.2 Introduction . . . 32
2.3.3 Materials and Methods . . . 34
2.3.4 Results - Summary of Original Review . . . 36
2.3.5 Results - Updated Review . . . 37
2.3.6 Discussion . . . 43
2.3.7 Limitations . . . 47
2.3.8 Conclusions . . . 47
2.4 Gap in the field - rowing and cycling focus . . . 48
2.4.1 Current Uses of Technology . . . 48
2.4.2 Movement Patterns . . . 50
2.4.3 Research Focus . . . 50

3 Sensor Development **51**
3.1 Introduction . . . 51
3.2 Literature Review . . . 52
3.2.1 Strain Sensor Technology . . . 52
3.2.2 Sensor Classifications . . . 53
3.2.3 Strain Sensor Performance Parameters . . . 61
3.3 Piezoresistive Sensors . . . 65
3.3.1 Material Choice . . . 65
3.3.2 Summary . . . 70
3.4 Materials, Methods and Results . . . 71
3.4.1 Preparation of Carbon Nanotube Dispersion . . . 71
3.4.2 Expansion of Rubber Bands . . . 72
3.4.3 Solvent Exchange Process . . . 72
3.5 Exploration of Different Materials and Methods . . . 73
3.5.1 Conductive Material and Solvent Choice . . . 73
3.5.2 CNT Concentration . . . 75
3.5.3 Fabrication Steps . . . 77
3.6 Discussion . . . 78
3.6.1 Limitations . . . 80
3.7 Conclusion . . . 81

4 Sensor Characterisation **82**
4.1 Introduction . . . 82
4.2 Literature Review . . . 83
4.2.1 Mechanical and electrical characterisation of strain sensors . . . 83

4.2.2 Effects of Temperature and Humidity (Environmental Considerations) 87
4.2.3 Summary 91
4.3 Mechanical Testing 91
4.3.1 Intoduction 91
4.3.2 Materials and Methods 92
4.3.3 Data Processing 95
4.3.4 Statistical Analysis 98
4.4 Protocol 1 99
4.4.1 Repeatability and Durability 99
4.4.2 Drift 106
4.4.3 Hysteresis, Linearity and Sensitivity 108
4.4.4 Further Discussion and Limitations 111
4.5 Protocol 2 111
4.5.1 Testing Protocols 112
4.5.2 Repeatability 112
4.5.3 Limitations 114
4.6 Conclusions 115

5 Wearables Development **116**
5.1 Introduction 116
5.2 Knee Sleeve Design 117
5.3 Sensor Configuration 118
5.4 Final Design 120

6 Cohort Study **122**
6.1 Introduction 122
6.2 Methods 123
6.2.1 Study Populations 123
6.2.2 Equipment 124
6.2.3 Testing Protocol 126
6.2.4 Data Processing and Analysis 126
6.3 Rowing Cohort Study 127
6.3.1 Study Population 127
6.3.2 Results 128
6.3.3 Discussion 138
6.3.4 Summary 141
6.4 Cycling Cohort Study 141

6.4.1 Study Population . . . 141
6.4.2 Results . . . 141
6.4.3 Discussion . . . 164
6.4.4 Summary . . . 166
6.5 Further Discussion . . . 166
6.5.1 Limitations . . . 168
6.6 Conclusion . . . 169

7 Cohort Study - Questionnaire Responses 170
7.1 Introduction . . . 170
7.2 Methods . . . 171
7.2.1 Data Analysis . . . 172
7.3 Results . . . 172
7.3.1 Descriptive Statistics . . . 172
7.3.2 Thematic Analysis . . . 178
7.4 Discussion . . . 183
7.4.1 System Design and Impact on Performance . . . 184
7.4.2 Use Environment . . . 186
7.4.3 Cost, Investment and Accessibility . . . 187
7.4.4 Metrics and Communicaiton . . . 187
7.4.5 Further Perspectives on Wearable Technology . . . 189
7.4.6 Limitations . . . 190
7.5 Conclusion . . . 190

8 Conclusions and Future Work 191
8.1 Introduction . . . 191
8.2 Summary of Work . . . 191
8.2.1 Review of the Literature . . . 191
8.2.2 Sensor Development and Characterisation . . . 193
8.2.3 Wearable Technology Development and Cohort Testing . . . 194
8.3 Future Work . . . 195
8.3.1 Sensor Coating . . . 195
8.3.2 Further Sensor Characterisation . . . 196
8.3.3 Wider Cohort Testing . . . 196
8.4 Research Contributions . . . 197

Appendices 197

A Systematic Review Published in 2019 **223**

B Inter-test variability results for all strain sensors **248**

B.1 Sensor S1 . . . 248

B.2 Sensor S2 . . . 249

B.3 Sensor S3 . . . 250

B.4 Sensor S4 . . . 252

B.5 Sensor S5 . . . 253

B.6 Sensor S6 . . . 254

B.7 Sensor S7 . . . 256

B.8 Sensor S8 . . . 258

B.9 Sensor S9 . . . 260

C Wearable Sensor System Design Iterations **262**

C.1 Knee Sleeve Design . . . 262

C.1.1 Iteration 1 . . . 262

C.1.2 Iteration 2 . . . 263

C.1.3 Iteration 3 . . . 264

C.2 Sensor Configuration . . . 264

C.2.1 Configuration 1 . . . 265

C.2.2 Configuration 2 . . . 265

D Ethics Documents **266**

D.1 Cycling Documents . . . 266

D.1.1 Approval Letter . . . 266

D.1.2 Participant Information Sheet . . . 268

D.1.3 Feedback Questions . . . 275

D.2 Rowing Documents . . . 277

D.2.1 Approval Letter . . . 277

D.2.2 Participant Information Sheet . . . 278

D.2.3 Feedback Questions . . . 282

E Squat Calibration **284**

E.1 Participant 34943, visit 1 . . . 284

E.2 Participant 77344, visit 1 . . . 285

E.3 Participant 48896, visit 2 . . . 286

List of Tables

2.1 Boolean Search Strategy. 35
2.2 List of Olympic Sports. 36
2.3 Sports studied in selection of incldued articles. 37
2.4 Measuring systems used in included articles to evaluate biomechanical parameters. . . 40

3.1 Advantages and disadvantages of different sensing classifications. 60
3.2 Advantages and disadvantages of different conductive materials used as fillers in strain sensors. 67
3.3 Conductive filler and solvent combinations for the different dispersions prepared. . . . 73
3.4 Mean resistance value (over three readings) over 8 cm for strain sensors fabricated with each dispersion concentration. 77
3.5 Hansen solubility parameters for substances used. 79

4.1 Summary of key metrics from cyclic strain sensor testing that has been reported in the literature. 88
4.2 Details of temperature and humidity testing performed on different carbon nanotube/polymer composite strain sensors. 90
4.3 Testing order for Protocol 1, indicating the number of cycles and strain rates for each test carried out. 94
4.4 Example of randomised testing order for Protocol 2. 95
4.5 Number of values extracted from raw datasets. 98
4.6 Greenhouse-Geisser p-values associated with sensor intra-test variability. Significant values have been highlighted in red. 101
4.7 Mean of the sensor resistance range, standard deviation and percent deviation for sensor S10. 102
4.8 Inter-test variability results from comparisons between tests of the same cycle length on sensor S10 (including post-hoc analysis). Significant values have been highlighted in red. The test number within Protocol 1 has been used to distinguish between comparisons. 104
4.9 Mean hold compared to cyclic max and min resistance (S10). 107

4.10 Average hysteresis, corresponding Gauge Factor and Coefficient of determination for each test type. Original and adjusted values are reported for each metric. 108
4.11 Testing order for each strain sensor. 112
4.12 P-values from the inter-test variability statistics carried out at a significance level of 0.025. Significant values have been highlighted in red. 114

6.1 Vicon marker locations. 125
6.2 Testing protocol for the rowing cohort study. 126
6.3 Testing protocol for the cycling cohort study. 127
6.4 Participant and sensor details for rowing cohort study. 128
6.5 Mean maximum and minimum knee flexion angles for each participant during each rowing step. 137
6.6 Mean knee flexion angle range for each participant during each rowing step. 138
6.7 Participant and sensor details for cycling cohort study. 142
6.8 Sections of data extraction for analysis, showing the average cadence for that section and the time period this corresponds to within the testing protocol. 143
6.9 Mean maximum and minimum knee flexion angles for each participant during each 1-min extract of cycling data. 163
6.10 Mean knee flexion angle range for each participant during each 1-min extract of cycling data. 163

7.1 Breakdown of questionnaire responses vs. total number of participants. 172
7.2 Overview of user experiences with the WSS. Outcomes for the 10-point Likert scale are given by the median and range. 173
7.3 Overview of participants' responses on wearable technology in general. . Outcomes for the 10-point Likert scale are given by the median and range. 176

B.1 Mean of the sensor resistance range, standard deviation and percent deviation for sensor S1 248
B.2 Inter-test variability results from comparisons between tests of the same cycle length on sensor S1 (including post-hoc analysis). Significant values have been highlighted in red and non-significant values in green. The test number within Protocol 1 has been used to distinguish between comparisons. 249
B.3 Mean of the sensor resistance range, standard deviation and percent deviation for sensor S2 249

B.4 Inter-test variability results from comparisons between tests of the same cycle length on sensor S2 (including post-hoc analysis). Significant values have been highlighted in red and non-significant values in green. The test number within Protocol 1 has been used to distinguish between comparisons. 250
B.5 Mean of the sensor resistance range, standard deviation and percent deviation for sensor S3 250
B.6 Inter-test variability results from comparisons between tests of the same cycle length on sensor S3 (including post-hoc analysis). Significant values have been highlighted in red and non-significant values in green. The test number within Protocol 1 has been used to distinguish between comparisons. 251
B.7 Mean of the sensor resistance range, standard deviation and percent deviation for sensor S4 252
B.8 Inter-test variability results from comparisons between tests of the same cycle length on sensor S4 (including post-hoc analysis). Significant values have been highlighted in red and non-significant values in green. The test number within Protocol 1 has been used to distinguish between comparisons. 252
B.9 Mean of the sensor resistance range, standard deviation and percent deviation for sensor S5 253
B.10 Inter-test variability results from comparisons between tests of the same cycle length on sensor S5 (including post-hoc analysis). Significant values have been highlighted in red and non-significant values in green. The test number within Protocol 1 has been used to distinguish between comparisons. 253
B.11 Mean of the sensor resistance range, standard deviation and percent deviation for sensor S6 254
B.12 Inter-test variability results from comparisons between tests of the same cycle length on sensor S6 (including post-hoc analysis). Significant values have been highlighted in red and non-significant values in green. The test number within Protocol 1 has been used to distinguish between comparisons. 255
B.13 Mean of the sensor resistance range, standard deviation and percent deviation for sensor S7 256
B.14 Inter-test variability results from comparisons between tests of the same cycle length on sensor S7 (including post-hoc analysis). Significant values have been highlighted in red and non-significant values in green. The test number within Protocol 1 has been used to distinguish between comparisons. 257
B.15 Mean of the sensor resistance range, standard deviation and percent deviation for sensor S8 258

B.16 Inter-test variability results from comparisons between tests of the same cycle length on sensor S8 (including post-hoc analysis). Significant values have been highlighted in red and non-significant values in green. The test number within Protocol 1 has been used to distinguish between comparisons. 259
B.17 Mean of the sensor resistance range, standard deviation and percent deviation for sensor S9 260
B.18 Inter-test variability results from comparisons between tests of the same cycle length on sensor S9 (including post-hoc analysis). Significant values have been highlighted in red and non-significant values in green. The test number within Protocol 1 has been used to distinguish between comparisons. 261

C.1 Summary of main features of design iteration 1. 262
C.2 Summary of the positive and negative factors of design iteration 1. 263
C.3 Summary of main features of design iteration 2. 263
C.4 Summary of the positive and negative factors of design iteration 2. 263
C.5 Summary of main features of design iteration 3. 264
C.6 Summary of the positive and negative factors of design iteration 3. 264
C.7 Summary of the positive and negative factors of sensor configuration 1. 265
C.8 Summary of the positive and negative factors of sensor configuration 2. 265

E.1 Mean max and min knee flexion angles during squatting and rowing trials (Participant 34943) 284
E.2 Mean max and min knee flexion angles during squatting and rowing trials (Participant 77344) 285
E.3 Mean max and min knee flexion angles during squatting and rowing trials (Participant 48896) 286

List of Figures

2.1 PRISMA chart detailing the article selection process. 38

3.1 Schematic of the resistive sensing mechanism and the change in conductive network when strain is applied. 54
3.2 Schematic of the capacitive sensing mechanism and the change in sensor dimensions when strain is applied. 55
3.3 Schematic of the optical sensing mechanism and change in transmitted and reflacted light due to the fibre Bragg grating. 56
3.4 Schematic of the piezoelectric sensing mechanism and the separation of charges when strain is applied (direct effect). 58
3.5 Schematic of the various triboelectric sensing modes: a)vertical contact-separation mode, b) contact-sliding mode, c) single-electrode mode and d) freestanding triboelectric-layer mode. 58
3.6 Round nanoparticles under strain. 62
3.7 Load-unload behaviour of a polymer. 62
3.8 Stress-relaxation behaviour of a polymer. 64
3.9 Dispersion (A) pre-homogenisation and (B) post-homogenisation. 71
3.10 (A) dispersion in centrifuge vial (B) sedimentation remaining after centrifugation (C) final dispersion. 72
3.11 Sensor drying made from dispersion of CNT in water. 74
3.12 Side by side comparison of dispersions (L-R) MWCNT in water (x2), graphene in NMP (x1), MWCNT in NMP (x2) at different stages of drying. 74
3.13 A cross-sectional image of the fabricated sensor using a FEGSEM. The featureless region at the top of the image represents the amorphous rubber band. The conductive networks formed by the carbon nanotubes can be seen in the lower two thirds of the image, indicating the uptake of nanotubes into the pores of the rubber band. This image was false-coloured using ImageJ. 75
3.14 CNT dispersion destabilised by toluene. 76

3.15 Side by side comparison of sensors made with different dispersion concentrations - (L-R) 1mg/mL (x2), 5mg/mL (x2), and 10mg/mL (x2). The highest uptake of CNTs was as a result of a 5mg/mL dispersion concentration, indicated by the mostly black appearance of the sensor. A concentration of 10mg/mL resulted in the lowest uptake of CNTs as the rubber band surface is still approximately 50% visible. A concentration of 1mg/mL provided results between these two. 77

4.1 A) Set up of Instron testing, with the sensor placed between grips and connected to an external instrumentation circuit and B) close-up of the sensor with connective attachments. 93

4.2 Schematic of the testing profile, the sensor is held at rest for 10 seconds, followed by 100 cycles between 0-12.8mm displacement at a strain rate of 350 mm/min, ending with a hold at the maximum displacement for a period before being allowed to rest. 94

4.3 Noise extraction for raw sensor data from sensors S2 and S3, sampling frequency of 100 Hz. 96

4.4 Noise extraction for raw sensor data from sensors S8 and S9, sampling frequency of 200 Hz. 96

4.5 Raw and filtered sensor response for sensor S2 with different cut-off frequencies (5, 10 and 20 Hz). 97

4.6 Raw and filtered sensor response for sensor S8 with different cut-off frequencies (5, 10 and 20 Hz). 97

4.7 Sensor response for 100-cycle tests on the same sensor (S10) carried out at different strain rates a) 350 mm/min, b) 100 mm/min c) 50 mm/min. 99

4.8 Change in output range over the course of a 100-cycle test repeats at 350 mm/min strain rate on the same sensor (S10). 100

4.9 Change in output range as a function of strain rate over differing cycle-length tests on sensor S10 at a) 100 cycles, b) 200 cycles, c) 500 cycles and d) 1000 cycles. 101

4.10 Mean sensor output range at different strain rates, grouped by the number of testing cycles. 103

4.11 Mean sensor output range of tests over 100 cycles at different strain rates. 103

4.12 Hysteresis loops plotted for a strain cycle test carried out on S10 for 100 cycles at 350 mm/min. a) original plot featuring spikes in the sensor response at minimum and maximum extension b) adjusted plot, accounting for the data spikes. 109

4.13 Mean sensor resistance range for each test carried out on sensors a) S12, b) S13, c) S14, d) S15 and e) S16. 113

5.1 PCB assembly used during the cohort study with a ruler for scale: a) side on view showing the on/off switch, b) top-down view of the connector PCB with resistors and connecting ports for the jumper wires and c) additional top-down view showing length of PCB assembly. 119
5.2 Strain sensor as incorporated into the WSS, with clincher connector boards clamped around the strain sensor at each end and the male snap fastener end secured to these with superglue and electrical tape. The top sensor is the longer sensor used on larger knee warmers, the bottom sensor is the regular length sensor used on smaller knee warmers. A ruler is shown at the bottom for scale. 119
5.3 Final WSS design used for cohort testing. 120

6.1 Location of Vicon markers and clusters on participant. 125
6.2 Normalised sensor response for the middle minute of each step during the rowing trials performed by participant 34943. 129
6.3 Overlaid time-normalised response for each rowing stroke in the middle minute of each step in the protocol. Knee angles from Vicon on the left and strain sensor response on the right for participant 34943. 130
6.4 Normalised sensor response for the middle minute of each step during the rowing trials performed by participant 77344. 131
6.5 Overlaid time-normalised response for each rowing stroke in the middle minute of each step in the protocol. Knee angles from Vicon on the left and strain sensor response on the right for participant 77344. 131
6.6 Normalised sensor response for the middle minute of each step during the rowing trials performed by participant 48896. 132
6.7 Overlaid time-normalised response for each rowing stroke in the middle minute of each step in the protocol. Knee angles from Vicon on the left and strain sensor response on the right for participant 48896. 133
6.8 Normalised sensor response for the middle minute of each step during the rowing trials performed by participant 69340. 134
6.9 Overlaid time-normalised response for each rowing stroke in the middle minute of each step in the protocol. Knee angles from Vicon on the left and strain sensor response on the right for participant 69340. 135
6.10 Normalised sensor response for the middle minute of each step during the rowing trials performed by participant 22341. 136

6.11 Overlaid time-normalised response for each rowing stroke in the middle minute of each step in the protocol. Knee angles from Vicon on the left and strain sensor response on the right for participant 22341. 137
6.12 Example of clipless foot retention used in cycling a) pedal attached to bike, b) cycling shoes with the left hand shoe showing the cleat on the underside that clips into the pedal.142
6.13 Normalised sensor response for 3 × 1-min segments at 80, 90 and 100 rpm during the cycling protocol, performed by participant 50560. 144
6.14 Overlaid time-normalised response for each pedal revolution for 3 × 1-min segments at 80, 90 and 100 rpm during the cycling protocol. Knee angles from Vicon on the left and strain sensor response on the right for participant 50560. 144
6.15 Normalised sensor response for for 3 × 1-min segments each at 80 rpm during the cycling protocol, performed by participant 50560. 145
6.16 Overlaid time-normalised response for each each pedal revolution for 3 × 1-min segments each at 80 rpm during the cycling protocol. Knee angles from Vicon on the left and strain sensor response on the right for participant 50560. 145
6.17 Normalised sensor response for 3 × 1-min segments at 80, 90 and 100 rpm during the cycling protocol, performed by participant 39683. 147
6.18 Overlaid time-normalised response for each pedal revolution for 3 × 1-min segments at 80, 90 and 100 rpm during the cycling protocol. Knee angles from Vicon on the left and strain sensor response on the right for participant 39683. 147
6.19 Normalised sensor response for for 3 × 1-min segments each at 80 rpm during the cycling protocol, performed by participant 39683. 148
6.20 Overlaid time-normalised response for each each pedal revolution for 3 × 1-min segments each at 80 rpm during the cycling protocol. Knee angles from Vicon on the left and strain sensor response on the right for participant 39683. 148
6.21 Normalised sensor response for 3 × 1-min segments at 80, 90 and 100 rpm during the cycling protocol, performed by participant 69013. 150
6.22 Overlaid time-normalised response for each pedal revolution for 3 × 1-min segments at 80, 90 and 100 rpm during the cycling protocol. Knee angles from Vicon on the left and strain sensor response on the right for participant 69013. 150
6.23 Normalised sensor response for for 3 × 1-min segments each at 80 rpm during the cycling protocol, performed by participant 69013. 151
6.24 Overlaid time-normalised response for each each pedal revolution for 3 × 1-min segments each at 80 rpm during the cycling protocol. Knee angles from Vicon on the left and strain sensor response on the right for participant 69013. 151

6.25 Normalised sensor response for 3 × 1-min segments at 80, 90 and 100 rpm during the cycling protocol, performed by participant 60435, visit 1/2. 152
6.26 Overlaid time-normalised response for each pedal revolution for 3 × 1-min segments at 80, 90 and 100 rpm during the cycling protocol. Knee angles from Vicon on the left and strain sensor response on the right for participant 60435, visit 1/2. 153
6.27 Normalised sensor response for for 3 × 1-min segments each at 80 rpm during the cycling protocol, performed by participant 60435, visit 1/2. 153
6.28 Overlaid time-normalised response for each each pedal revolution for 3 × 1-min segments each at 80 rpm during the cycling protocol. Knee angles from Vicon on the left and strain sensor response on the right for participant 60435, visit 1/2. 154
6.29 Normalised sensor response for 3 × 1-min segments at 80, 90 and 100 rpm during the cycling protocol, performed by participant 60435, visit 2/2. 155
6.30 Overlaid time-normalised response for each pedal revolution for 3 × 1-min segments at 80, 90 and 100 rpm during the cycling protocol. Knee angles from Vicon on the left and strain sensor response on the right for participant 60435, visit 2/2. 155
6.31 Normalised sensor response for for 3 × 1-min segments each at 80 rpm during the cycling protocol, performed by participant 60435, visit 2/2. 156
6.32 Overlaid time-normalised response for each each pedal revolution for 3 × 1-min segments each at 80 rpm during the cycling protocol. Knee angles from Vicon on the left and strain sensor response on the right for participant 60435, visit 2/2. 156
6.33 Normalised sensor response for 3 × 1-min segments at 80, 90 and 100 rpm during the cycling protocol, performed by participant 59445, visit 1/2. 158
6.34 Overlaid time-normalised response for each pedal revolution for 3 × 1-min segments at 80, 90 and 100 rpm during the cycling protocol. Knee angles from Vicon on the left and strain sensor response on the right for participant 59445, visit 1/2. 158
6.35 Normalised sensor response for for 3 × 1-min segments each at 80 rpm during the cycling protocol, performed by participant 59445, visit 1/2. 159
6.36 Overlaid time-normalised response for each each pedal revolution for 3 × 1-min segments each at 80 rpm during the cycling protocol. Knee angles from Vicon on the left and strain sensor response on the right for participant 59445, visit 1/2. 159
6.37 Normalised sensor response for 3 × 1-min segments at 80, 90 and 100 rpm during the cycling protocol, performed by participant 59445, visit 2/2. 160
6.38 Overlaid time-normalised response for each pedal revolution for 3 × 1-min segments at 80, 90 and 100 rpm during the cycling protocol. Knee angles from Vicon on the left and strain sensor response on the right for participant 59445, visit 2/2. 161

6.39 Normalised sensor response for for 3 × 1-min segments each at 80 rpm during the cycling protocol, performed by participant 59445, visit 2/2. 161
6.40 Overlaid time-normalised response for each each pedal revolution for 3 × 1-min segments each at 80 rpm during the cycling protocol. Knee angles from Vicon on the left and strain sensor response on the right for participant 59445, visit 2/2. 162

7.1 Participant experiences with WSS in a) cycling study and b) rowing study. The distribution of scores on the 10-point Likert scale are shown in each bar chart (very much [1] – not at all [10]). 173
7.2 Box plots representing the distribution of scores from both cohorts - the red line represents the median, the top and bottom edges of the box are the 75th and 25th percentiles respectively. The whiskers extend to the extreme, non-outlier points. Outliers are represented by the + symbol. 174
7.3 Results of participants using the WSS in a) cycling and b) rowing i) in training, ii) in competition and iii) to adjust their technique after the first testing session and iv-vi) after the second testing session. 175
7.4 Box plots representing the distribution of scores from both cohorts - the red line represents the median, the top and bottom edges of the box are the 75th and 25th percentiles respectively. The whiskers extend to the extreme, non-outlier points. Outliers are represented by the + symbol. 177
7.5 Participants' views on a) data storage, b) using a device without assistance and c) learning to use a new device. 177
7.6 Thematic map showing the two main themes and linked sub-themes identified from the questionnaire responses. 178

C.1 Different designs trialled for the WSS a) iteration 1, b) iteration 2 and c) iteration 3. . 262
C.2 Schematic of the two sensor configurations tested on the knee warmer a) one sensor was placed on the anterior and the second on the posterior b) both sensors were placed side-by-side on the anterior. 264

E.1 Example of sensor response normalised by the sensor signal range in dynamic squat trial performed at the beginning of the testing protocol (Participant 34943) 284
E.2 Example of sensor response normalised by the sensor signal range in dynamic squat trial performed at the beginning of the testing protocol (Participant 77344) 285
E.3 Example of sensor response normalised by the sensor signal range in dynamic squat trial performed at the beginning of the testing protocol (Participant 48896) 286

List of Acronyms

0D Zero-dimensional

1D One-dimensional

2D Two-dimensional

3D Three-dimensional

ACL Anterior cruciate ligament

CAI Chronic ankle instability

CB Carbon black

CSV Comma separated variable

CNT Carbon nanotubes

CPC Conductive polymer composite

DAQ Data acquisition board

DTFT Discrete-time Fourier transform

FBG Fibre Bragg grating

GF Gauge factor

HW Heavyweight

IMU Inertial measurement unit

JAAF Japanese Associations of Athletic Federations

LCR Inductance capacitance resistance

LED Light-emitting diode

LW Lightweight

MARG Magnetic, angular rate and gravity

MCU Microcontroller unit

MEMS Microelectromechanical systems

MIMU Miniature inertial measurement unit

MWCNT Multi-walled carbon nanotube

NCPF Nanocomposite piezoresistive foam

NMP 1-Methyl-2-pyrrolidinone

NR Natural rubber

NW Nanowire

PANI polyaniline

PBS Phosphate-buffered saline

PCB Printed circuit board

PDMS Polydimethylsiloxane

PEDOT:PSS poly(3,4- ethylenedioxythiophene) polystyrene sulfonate

POF Plastic optical fibre

PP Polypropylene

PPy Polypyrrole

PVDF Polyvinylidene flouride

PZT Lead zirconate titanate

RMSE Root mean square error

rpm Revolutions per minute

SBR Styrene-butadiene rubber

SEBS m poly[styrene-b-(ethylene-co-butylene)-b-styrene]

SEM Scanning electron microscope

spm Strokes per minute

SWCNT Single-wall carbon nanotube

TCR Temperature coefficient of resistance

TENG Triboelectric nanogenerator

TPU Thermoplastic polyurethane

UCI Union Cycliste Internationale

UTS Ultimate tensile stress

UV-Vis Utraviolet-Visible

vGRF Verical ground reaction force

VO_2 Rate of oxygen

WSS Wearable sensor system

Chapter 1

Introduction

Introducing the motivation behind using wearable technology, specifically strain sensors, to measure biomechanics in a sporting context

1.1 Project Background and Motivation

Wearable technologies are prominent in our daily lives: for the average person, smart watches, fitness trackers and even jewellery can allow them to monitor their heart rate, calorie expenditure [1], sleep and step count [2], among other metrics. The unobtrusive measurement of these metrics over a long period (months or even years), could help track trends that can help these individuals or healthcare professionals with health monitoring, early disease identification and thus early management.

These technologies have also been used in sports to individualise training programmes and help maximise athletic performance [3]. Athletic performance and biofeedback comprise several factors including: physiological, neurological, biochemical and biomechanical [4]. Monitoring workloads to understand the physical demands on different athletes and conducting tests to measure lactate thresholds, heart rate or electrolytes in sweat are some examples of what can be measured with various sensors concerning physiological and biochemical factors [5].

Biomechanics is highly important to monitor and measure in sports, due to its ability to analyse the movement patterns of highly skilled athletes [6] and influence coaching practice. The use of wearable technology has the potential to make the field of sports biomechanics more accessible, and can be used to assess and quantify: injury prevention; performance assessment and optimisation; movement recognition; and skill level classification [7]. These objective measurement tools can aid those involved in sport, informing decision-making and backing up current coaching methods. There is a willingness to embrace such technologies as they make tracking performance-related metrics more accessible and easier to interpret – coaches and athletes can identify what is being done well and where to improve, particularly at the elite level where marginal gains can be the difference between a gold medal and no medal at all [5]. Understanding how injuries can be prevented and training optimised can give athletes

a competitive advantage with fewer training days missed and more productive training sessions [5].

Wearable technology has the advantage over other objective measurement systems (e.g. camera-based motion capture) as it can be used in different environments, monitoring athletes while they are training or competing. It can help bridge the gap between sports scientists, biomechanists, coaches and athletes, optimising the multi-disciplinary teams that exist in elite training centres. Each person has a unique knowledge that they can contribute towards achieving a common goal, so nurturing these relationships is important [8].

Using wearable technology to measure biomechanics is still an emerging field due to each sport having its specific motor patterns that need to be understood [4, 9]. This leads to challenges that need to be overcome with regards to understanding the performance-related metrics associated with each sport. Inertial measurement units (IMUs) are the most common type of system used and some have been proven to have high accuracy, but are also associated with a high cost when they have been derived from research [9]. They often require multiple sensors to attain kinematic parameters, which also drives the cost up. The cost of these systems may be more than people can afford [9], limiting their usage to elite teams. IMUs are also subject to errors due to signal drift during measurements, which is compounded during processing and signal integration [10]. More complex tasks, such as manual handling compared to joint flexion and extension, can also increase the root mean square error (RMSE) values associated with the device [11].

These challenges drive the motivation to consider other wearable technology systems, which is the focus of this doctoral work. Focusing on joint kinematics, strain sensors have been demonstrated to measure the range of motion for different joints including the ankle, knee [12] and wrist [13], with potential applications in health monitoring and sport [14]. Using multiple inertial sensors requires precise placement and therefore an expert to set up the system; overcoming the need for multiple sensors with a single strain sensor can increase the uptake of a wearable system if any user can set it up themselves.

This work looks to develop a low-cost solution for measuring joint angles which is based on strain sensor technology, and compare its response to motion capture systems. The sports investigated were rowing and cycling: two sports featuring a cyclical motion, where performance improvement can be made from small changes in technique. The focus is on using strain sensors to measure knee kinematics from an injury prevention and performance enhancement perspective. Coaches will often look at angular movements of joints including the knee, to determine whether athletes are moving in an effective way. Considering injury, the knee joint can be a common injury site in both sports due to inadequate equipment set-up or poor technique, with excessive range of motion putting additional force on the patella. There are also performance indicators associated with measuring knee kinematics: in bike-fitting in cycling knee flexion is often used to set saddle height, while in rowing reduction in both knee extension and flexion have been observed in athletes with increasing intensity [15]. Both of

these sports have little in the way of sensors placed on the body to measure biomechanics and so there is scope for athletes and coaches to realise improvements by accessing these kinematic parameters.

1.2 Thesis Aims

Considering the current state of play of wearable technology to measure sports biomechanics, and the gap in the field presented by the need for a low-cost system that can be used in rowing and cycling and potentially other sports, this work sets out to answer the following question: Can flexible strain sensors be used to measure the knee kinematics of athletes during sporting activities?

The overarching aim of this work was: to develop, characterise and validate a flexible strain sensor that can be incorporated into a wearable system; and to assess the translational use of the sensor for measuring knee kinematics of athletes in sports.

From this aim, the following objectives were established:

- Review the current state of play of wearable technology in sports to evaluate performance and injury risk with the use of kinetic and kinematic variables
- Develop a composite strain sensor and optimise the fabrication process
- Characterise the strain sensor and obtain its mechanical and electrical responses under cyclic loading to determine its suitability for sustained use
- Develop a wearable system integrating the stain sensor that can be worn over the knee and used to measure knee flexion angles
- Evaluate the potential of the wearable system against 3D optical motion capture as a means of measuring knee flexion angles in rowers and cyclists

1.3 Summary of Contributions

This thesis contributes to the field of wearable technology for sports biomechanics, by the creation and testing of a prototype wearable sensor system on rowing and cycling cohorts. These contributions are summarised as follows:

- The literature has been systematically reviewed by the author of this thesis, to assess the use of wearable technology that is used in sports biomechanics, while establishing requirements for the development of new technology
- Carbon nanotube-natural rubber composite strain sensors were fabricated and characterised

- Composite strain sensors were integrated into a wearable sensor system in order to measure knee range of motion in rowing and cycling
- The capability of the wearable sensor system to monitor knee range of motion compared to a motion capture system was evaluated
- The perspectives of the study cohort on wearable technology and experiences with the developed wearable sensor system were considered

1.4 Publications

1.4.1 Publications to Date

The following systematic review was published by the author of this thesis while undergoing this doctoral work:

- Adesida, Y.; Papi, E.; McGregor, A.H. Exploring the Role of Wearable Technology in Sport Kinematics and Kinetics: A Systematic Review. Sensors 2019, 19, 1597. [7]

1.4.2 Proposed Publications

It is proposed that publications will be submitted for review based on the work in this thesis:

- A discussion on the fabrication and characterisation of the carbon nanotube-rubber composite strain sensor, while also presenting some preliminary data from the cohort study. Journal for submission - to be determined, but with a focus on materials science and applications
- A qualitative analysis of the views of cohort study participants on the use of wearable technology in sports. Journal for submission - to be determined, but with a focus on sports coaching practices

1.5 Thesis Structure

This thesis is organised into 8 main chapters, including this introductory chapter, as outlined below in this section:

Chapter 2: Literature Review

Chapter 2 provides an overview of the role played by biomechanics in sport, followed by a systematic review that assesses the use of wearable technology to measure kinetic and kinematic parameters. It also highlights the technology gap in cycling and rowing when it comes to measuring these parameters and where opportunities lie for development.

Chapter 3: Sensor Development

Chapter 3 begins with an overview of different strain sensor technologies and narrows the focus onto piezoresistive sensors, which is the chosen sensing mechanism for this doctoral work. The fabrication methods for producing the strain sensors utilised in this work are then detailed, as well as the optimisation of this process.

Chapter 4: Sensor Characterisation

Chapter 4 details the mechanical testing methods developed and conducted on fabricated strain sensors to characterise their mechanical and electrical properties and ascertain their suitability for use within a wearable sensor system.

Chapter 5: Wearables Development

Chapter 5 describes the design of the wearable sensor system which the strain sensor was incorporated into. Different fabrics and sensor configurations were considered for the optimal output.

Chapter 6: Cohort Study

Chapter 6 sets out the testing protocols and equipment set-up used to test the usability of the fabricated strain sensor when incorporated into a wearable sensor system. It also assesses the data capture method and quality of data when compared to the Vicon motion capture system. It details the differences between the testing protocols for rowing and cycling, as well as describing the cohorts that were recruited. The quantitative results from these studies are presented and discussed.

Chapter 7: Cohort Study – Questionnaire Results

Chapter 7 presents an analysis of the questionnaires sent out to participants after testing, to understand the user experience with the wearable sensor system and wearable technology in general. Descriptive statistics and thematic analyses were conducted on this data set.

Chapter 8: Conclusions and Future Work

Chapter 8 summarises the work presented in this thesis and the important findings that were made. Recommendations are suggested for future work that can aid the development of this technology, including sensor coatings and providing live feedback.

Chapter 2

Literature Review

Assessing the need for wearable technology to measure kinetics and kinematics in sports, primarily in the context of rowing and cycling

2.1 Introduction

Sports performance encompasses more than how athletes and teams rank in a competition, or how they perform in distance and time-based events compared to their personal best. There are a number of factors that influence performance such as an athlete's physiological capabilities, including VO_2 max or lactate threshold; or whether an athlete is able to avoid injury and complete as many sessions as possible. Finally there is how an athlete moves and the effective forces they can produce, i.e. their biomechanics. Especially at the elite level, the winning margins are so small that it requires athletes to be at the top of their game. With restrictions in some sports that limit some technological advancements to equipment (swimmers have rules surrounding which parts of their body can and cannot be covered by their swimsuits, while, cycling has minimum weight limits for bicycles and rules around the texture of materials used for clothing), more focus is being placed on whether an athlete is moving effectively and efficiently.

Coaches are able to provide feedback on this, but everyone has their own opinion and the human eye can only see so much. This feedback is subjective, as "Every coach or athlete brings personal interests to the coaching setting" [16]. Technology can help overcome this subjectivity, quantifying biomechanics and ultimately performance in an objective manner.

This chapter provides an overview on the importance of sports biomechanics and the role it plays in sports performance, before moving to a systematic review which assesses the role of wearable technology to measure biomechanics in sport. The focus then narrows onto two sports, rowing and cycling, the technology that is already being utilised and how new innovations can benefit athletes, coaches, and other support staff.

2.2 Overview of Sports Biomechanics

Biomechanics can be defined as 'the science which applies mechanical principles in order to understand the functioning of the biological system' [17]. Sports biomechanics permits the understanding of how someone moves in a sporting context, considering the forces, accelerations, velocities and joint angles involved in these movements. It is a useful tool in improving the technique and performance of athletes, preventing injury and also influencing training protocols [6]. Biomechanics can be used to quantify the movement of skilled athletes, which can help coach those who are less skilled, as well as identify trends and patterns that can be used to predict performance and training outcomes. In addition to skill level, kinetics and kinematics can be influenced by someone's age, sex or anthropometric characteristics.

In Japan, through collaboration between athletics sprint coaches and The Japanese Associations of Athletic Federations (JAAF), the kinematic analysis of World Championship level 100m sprinters by Ito (1994) was performed to understand which motions were biomechanically advantageous, which in turn influenced coaching practice and led to the National record over 100m being broken [6, 18]. In the case of rowing which can be split into two weight classes – lightweight (LW) (where individual rowers must not exceed 59kg and 72.5kg for female and male athletes respectively) and heavyweight (HW) – one might want to understand what, if any, differences there are between weight classes when it comes to motion or forces produced. Doyle et al. (2010) analysed the performance of 24 world class level rowers, split evenly across the two weight classes, and compared force outputs (a common performance indicator) [19]. Although the force outputs of the HW rowers were statistically significantly higher than for LW rowers, two pairs of LW rowers were able to produce boat velocities similar to the HW crews at different stroke ratings [19]. This suggests perhaps there are other factors that come into play and how each rower themselves moves should be considered: biomechanical approaches would permit us to understand movement patterns as well as force outputs.

An area that has not been studied to the same extent is the biomechanics of Paralympic athletes with regards to performance and preparation for events [20]. The use, configuration and structure of a prosthetic lower limb for example, can alter step length and vertical ground reaction force (vGRF). When sprinting around a curve in athletics, a study by Taboga et al. (2016) found that athletes who wore a prosthetic on their inside leg were 3.9% slower than those whose prosthesis was on their outside leg, due to their inability to generate large forces with their inside leg [21]. In para-kayaking, those in the legs/trunk/arms category have lower power outputs (compared to non-para-kayakers) as a result of a reduced range of motion around certain joints [22]. These examples of asymmetry and reduced range of motion, as well as lower force production due to neurological conditions [22] has the ability to, and should, influence training protocols that minimise injury risk whilst enhancing performance.

Despite the wealth of knowledge held by researchers, there is still some disconnect between the work done in academia and those involved in sports on a day to day basis – athletes, coaches and other

support staff – as highlighted by Martindale and Nash in 2013 [23]. The relationship between coaches and biomechanists is one that can be mutually beneficial, with coaches being able to influence research questions and have an understanding of performance indicators, while the biomechanists can provide scientific evidence for how to improve technique or performance [8]. Communication is something important that can help facilitate this relationship, and foster knowledge sharing, requiring a common understanding of both science and coaching or sport jargon. Research needs to be engaging and the translation of this (from the lab to the training or competition environment) is still poor [8, 24].

A way of bridging this gap is through the use of wearable technology to measure biomechanics. Taking technology out of the lab and into the training environment, gives the opportunity for coaches and athletes to interact and become more familiar with technology that could help them improve their performance or prevent injury. The following systematic review explores the role that wearable technology can play in sport, specifically to assess kinetics and kinematics.

2.3 Systematic Review

This section is based on a systematic review that was published in 2019 in Sensors [7], and has since been updated in August 2022 to reflect the progression of the field since the original review. A copy of the orginal review can be found in Appendix A.

2.3.1 Abstract

A systematic review was conducted with the aim of understanding the role that wearable technology plays in sport in injury prevention and performance improvement. Metrics related to these are traditionally measured using optical motion capture systems, however the limited capture volume restricts usage to laboratory environments. Wearable technology is able to overcome this by allowing the same metrics to be measured during training or competition. A search was carried out across seven databases to find articles where wearable technology has been used to assess kinetic and kinematic variables in sport. Eighty eight articles were included for full-text analysis, with wearable technologies used to monitor dynamic movements related to performance of sports participants. A range of devices including magnetic, angular rate and gravity sensors; flex sensors; and inertial measurement units, were used to assess motion in 22 sports. The field of wearable technology is rapidly developing, with useful parameters that can be measured being investigated more widely in order to enhance and improve athletes' technique and coaching practice.

2.3.2 Introduction

Feedback in sports is essential for improving performance and preventing injury. Feedback can be produced in a number of forms, with coaching being the most common, however this can be highly

subjective. Incorporating objective measurements into the feedback loop can enhance the expertise and experience of an athlete or coach, with its ability to inform decision making.

Technology capable of providing objective measurements range from video analysis with software allowing for annotation to measure joint angles; to motion capture systems using cameras and passive or active markers that have been placed on anatomical landmarks for full-body tracking [7]. Optical motion capture systems are considered the gold-standard for analysing movement [25, 26], with Vicon (Oxford Metrics, Oxford, UK) and Qualisys (Qualisys AB, Göteborg, Sweden) the most commonly used systems [27]. However they are unable to provide measurements in training or competition environments because of their limited capture volume, as well as the lengthy times needed to set-up the system and process the data [7, 26]. There is a skill required to run the system and correctly place markers on anatomical landmarks, some of which can obstruct or be occluded by complex sporting tasks [7].

These limitations can be overcome with wearable technology, which has the advantage of being used outside of laboratory environments and the ability to provide concurrent feedback (given in real-time) as well as terminal feedback (given after completing the movement) [28, 29]. The design is such that they are generally small and lightweight, and most importantly unobtrusive to any sporting movements [7]. Examples of such systems include: inertial measurement units (IMUs); flex and strain sensors; pressure insoles; and microelectromechanical systems (MEMS). These systems have the ability to measure joint range of motion, accelerations and impact forces, among other metrics, either directly or indirectly. IMUs are a popular choice, with a number of sports using these to assess biomechanical outcomes including: football, running, figure skating and baseball [9].

There are requirements that wearable technology must meet in order to be well received by those involved in sports. Technology should be validated against gold-standard motion capture systems and tested for reliability, with recommendations made by Düking et al. (2018) with regards to constructing a testing protocol [30]. Being able to recognise key movements in signals produced by any sensor is of high importance, therefore the sampling frequency plays a key role in achieving this. The Nyquist-Shannon sampling theorem provides a starting point for choosing a suitable sampling frequency so that all information can be found in the signal of interest [30–32]. The nature of wearable technology is such that it is not connected to a mains output, so the contained power source must enable data to be recorded for the duration of the measurement period, which will be dependent on the nature of the sport.

Wearable technology is becoming more integrated within sports as an unobtrusive measurement tool for injury prevention or performance improvement that can support athletes or coaches with specific sports metrics related to accelerations, impacts and range of motion. The aim of this review is to identify which forms of wearable technology are being used to achieve this, focusing specifically on kinetic and kinematic variables of sports participants performing sport-specific movements. Using

the review published by the author as a starting point [7], this review seeks to expand upon how the field of wearable technology has progressed in the three years since initial publication.

2.3.3 Materials and Methods

2.3.3.1 Search Strategy

Two systematic searches were carried out in seven databases with articles included from inception until 31st October 2018, and 1st November 2018 to 11th April 2022. The databases used were: Scopus, Medline, Embase, Cochrane Library, IEEE Xplore, Web of Science (Core Collection) and Engineering Village. The Boolean search strategy used was 'wearable AND sensor AND sport' with the search terms grouped under these three key words (see Tables 2.1 and 2.2). Articles were imported into EndNote20 software (Clarivate Analytics, Philadelphia, USA).

2.3.3.2 Eligibility Criteria

Articles were included if they were: published in English; included at least one of the following outcome measures: joint, limb and trunk kinematics and kinetics as obtained from wearable technology; participants took part in a sport (defined as an organized physical activity done alone or with a group); dynamic movement tasks were performed related to performance in the sport studied. Articles were excluded if they were a review or case study; were a conference abstract (except peer-reviewed abstracts); used only non-wearable devices; wearable technology was used to only quantify physical activity or temporal measures; described a potential technology not validated/used with human subjects [7].

2.3.3.3 Selection Process

Duplicates arising from searches in multiple databases were removed, and the titles and abstracts were reviewed for inclusion by two independent reviewers (the author and one supervisor.). Full texts of the remaining articles were retrieved, and these were evaluated against the eligibility criteria [7].

Table 2.1: Boolean Search Strategy [7].

General	Specific	
Wearable	Portable OR worn OR cloth*3 OR "body-mounted" OR "non-invasive" OR mobile OR wearable* OR apparel OR textile OR "electronic skin"	
	Cochrane Library MeSH terms	Wearable electronic devices (exp)
	Embase MeSH terms	Non invasive monitoring ; Clothing
	Medline MeSH terms	Clothing ; Wearable electronic devices
Sensor	Sens*3 OR goniomet* OR acceleromet* OR monitor* OR inertia* OR gyroscope* OR device* OR magnet* OR imu OR telemet* OR pressure OR strain OR conductive OR stretch* OR flexible OR smart OR electronic*1 OR electromagnetic OR microsensor*1 OR microelectronic*1	
	Cochrane Library MeSH terms	Monitoring, ambulatory
	Embase MeSH terms	Ambulatory monitoring ; Sensor ; Devices ; Monitoring
	Medline MeSH terms	Monitoring, ambulatory
Sport	Cochrane Library MeSH terms	Athletes ; Sports ; Exercise ; Athletic performance ; Motor activity
	Embase MeSH terms	Athletes ; Sports ; Exercise ; Training ; Sports medicine ; Motor activity
	Medline MeSH terms	Athletic performance ; Athletes ; Sports ; Exercise ; Motor activity ; Sports medicine

Table 2.2: List of Olympic Sports [7].

archery OR run*4 OR badminton OR basketball OR boxing OR canoe* OR cycl*4 OR bik*3 OR bicycl* OR bmx OR div*3 OR equestrian OR dressage OR fencing OR football OR soccer OR golf OR gymnastics OR handball OR hockey OR judo OR pentathlon OR row*3 OR rugby OR sail*3 OR shoot*3 OR swim*4 OR taekwondo OR tennis OR trampoline OR triathlon OR volleyball OR "water polo" OR weightlifting OR wrestling OR skiing OR biathlon OR bobsleigh OR curling OR skat*3 OR luge OR "Nordic combined" OR skeleton OR snowboard*

2.3.4 Results - Summary of Original Review

This section will summarise the results of the initial review conducted and published in 2019 as part of this project [7]. As part of the article selection process, the search was narrowed down from 27,767 articles (duplicates removed) to the full text of 46 articles were assessed for eligibility. 34 articles met the inclusion criteria. These articles covered 17 sports, an overview of which is listed in Table 2.3. This review highlighted different applications for wearable technology, including: injury prevention; quantifying skill level and expertise; improving technique; and characterizing movements [7]. Included articles were assessed based on the quality of the information provided, including details on sample size, protocol and sensor placement. Eleven articles were deemed to be of high quality, with medium and low quality articles totalling 19 and four respectively.

Systems used to measure kinetic and kinematic variables were dominated by inertial sensors, with individual sensors being mentioned in 13 articles [33–45] and five articles discussing the use of body suits [33, 46–49]. Other systems included accelerometers (used in baseball [50], running [51], table tennis [52], swimming [53] and Nordic walking [54]) magnetic, angular rate and gravity (MARG) sensors (used in football [55] and cricket [56]) and pressure insoles (used in skiing [57, 58]and snowboarding [46]). A flex sensor was incorporated into a glove-like structure in badminton [59]. Studies took place in different environments, but only five of these were within a laboratory setting [36, 40, 47, 55, 60]. There was no mention of location for three studies [35, 59, 61], while the protocols in the remaining studies were conducted in field, allowing a more realistic movement to be performed by participants in their relevant sport.

The most common sampling frequency used for data collection by the wearable technologies was 100 Hz [35, 38, 42, 43, 45, 57, 58, 62], enabling sporting movements to be captured, although sampling frequency was reported to be as low as 10 Hz [33] and as high as 1000 Hz [50]. A number of methods were employed for data transfer, including storing data on a memory card for later upload and transferring data using Bluetooth. Live feedback was only used in two articles, with haptic feedback used in swimming [33] and auditory feedback used in running [60], both to alter technique of the participants.

A number of technologies were validated using gold-standard systems such as the Vicon motion capture system, Kistler force platforms (Kistler Instruments Ltd., Hampshire, UK). Optical based systems were also used to validate technologies, like BTS Bioengineering stereo-photogrammetric system (BTS Bioengineering Corp., Quincy, MA, USA) and XOS Technologies (Wilmington, MA, USA).

At the stage of this review, the use of wearable technology to measure sports biomechanics was in more of an exploratory phase. Devices developed in-house were used more than commercially available technologies, but the translation to general usage was not optimal. It was evident that the potential was there to improve this translation, influencing athlete technique and coaching practice.

2.3.5 Results - Updated Review

The systematic search was updated in April 2022, with 141 full texts assessed for eligibility. From this updated search, a further 54 articles satisfied the inclusion criteria, with the selection process and reasons for exclusion are detailed in Figure2.1. This section will focus on the 54 newly included articles.

22 sports were considered across both sets of included articles, with 14 being discussed in this updated selection of articles. A summary of this is in Table 2.3. Sports that were not included in the previous review are: field athletics, speed skating, tennis, basketball, boxing and gymnastics. An additional 19 articles relating to track athletics and running were included, making this the most popular sport that used wearable technology to assess movement.

Table 2.3: Sports studied in selection of incldued articles.

Sport /Review	Football and rugby	Swimming	Skiing	Equestrian	Cricket	Table Tennis
Original	4	3	6	3	1	1
Updated	1	5	7	0	3	2
Total	5	8	13	3	4	3
Sport	Badminton	Track athletics and running	Rowing	Baseball	Snow-boarding	Golf
Original	1	4	1	3	1	1
Updated	2	19	0	5	0	0
Total	3	23	1	8	1	1
Sport	Netball	Archery	Volleyball	Canoeing	Nordic Walking	Field athletics
Original	1	1	1	1	1	0
Updated	0	0	0	0	0	1
Total	1	1	1	1	1	1
Sport	Speed skating	Tennis	Basketball	Boxing	Gymnastics	
Original	0	0	0	0	0	
Updated	2	2	2	2	1	
Total	2	2	2	2	1	

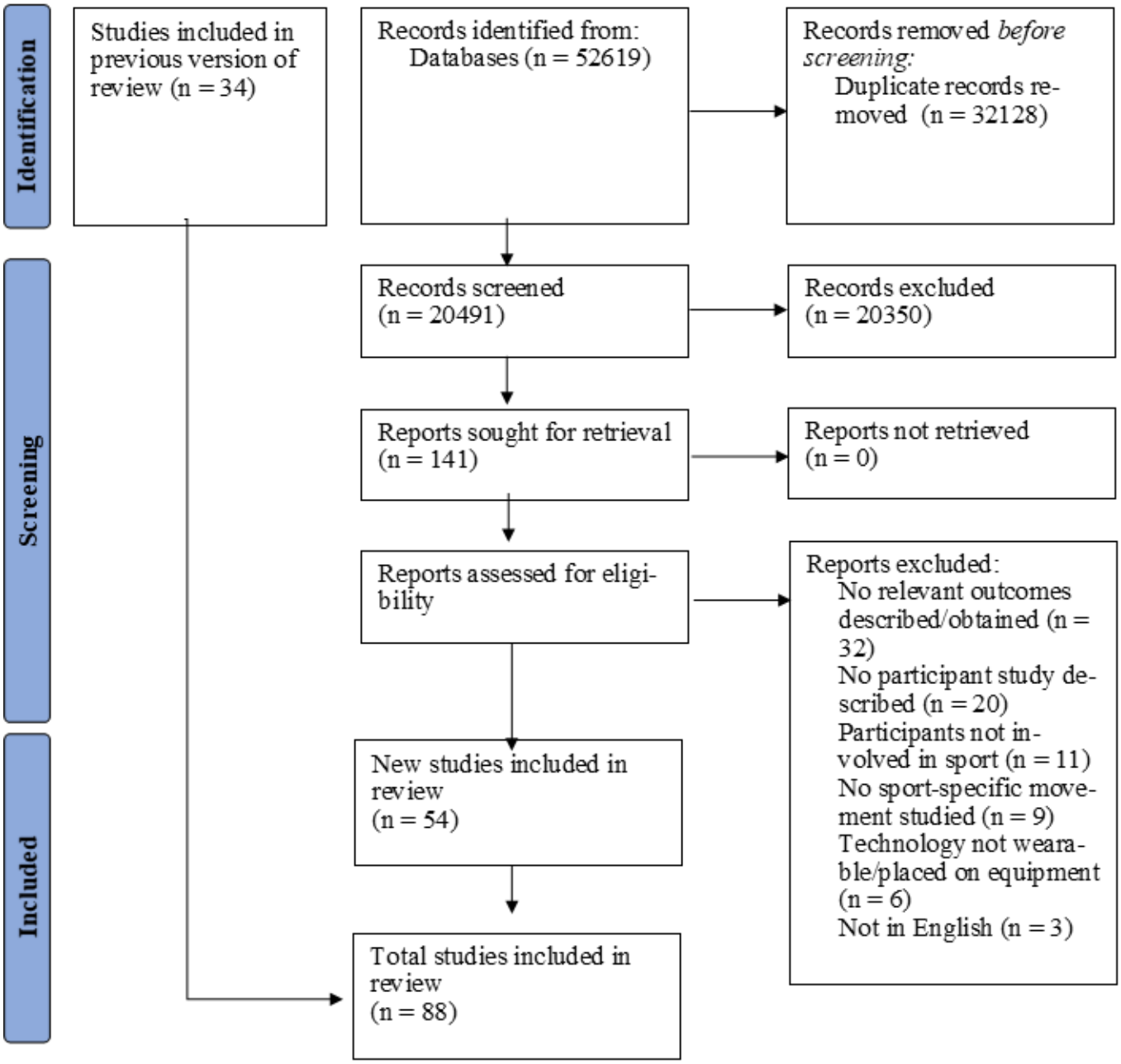


Figure 2.1: PRISMA chart detailing the article selection process [63].

2.3.5.1 Article Quality

When considering the amount of detail provided on the study cohort, experiments conducted and wearable technology used, there is a range in the quality of articles included in this review. Key quality metrics include: stating the research objective; clearly describing the study design and population; giving accurate descriptions of the method, equipment used and location of sensors; and stating the main findings of the study.

Cohort sizes ranged from 1 [64–67] to 100 [68] within the included studies. Kos and Kramberger (2018) used several participants of different experience, but did not provide any specific detail as to the actual number of participants or their background [69]. Bańkosz and Winiarski (2020) on the other hand provided an average weight and height of the cohort consisting of Polish national team tennis players, as well as including their handedness [70].

Although detail was provided by Sha et al. (2021) on their testing cohort, it was not clear what actions from the tennis players took place when data was recorded [71]. Similarly, Shang and Cheng (2021) did not indicate the type of swimming stroke performed when collecting data on hip rotation [72]. In contrast to this, in boxing Menzel and Potthast (2021) gave detail on the four striking techniques used and how many of each strike were performed within the protocol [66].

In addition to experimental details, giving an accurate description of where sensors are allows experiments to be replicated by others. The article by Lapinski et al. (2019) is a good example of this, using images as well as text to give indication of where the sensors are located on the chest, waist and upper limbs [73]. Cottam et al. (2022) also provide a high level of detail, using specific anatomical locations to describe the placement of each MIMU used [74].

2.3.5.2 Types of Measuring Systems Used and Evaluated Variables

The types of wearable systems used in the included articles is overwhelmingly dominated by IMU-based technology, with commercial systems being favoured over those being built in-house, such as Lumo Run (Lumo Bodytech Inc, San Fransisco, California, United States) [75–77], myoMOTION (Noraxon USA Inc., Scottsdale, Arizona, USA) [70, 74, 78, 79] and Optimeye by Catapult (Melbourne, Australia) [80]. Pressure insoles from pedar (Novel GmbH, München, Germany) [65, 81–85] and loadsol (Novel GmbH, München, Germany) [86, 87] were also investigated, as well as nanocomposite piezoresistive foam (NCPF) sensors placed under standard insoles to also measure foot pressure [88]. In addition to this, force sensing resistors [66, 89] and stand-alone accelerometers [88] were used to measure biomechanical variables. A summary of these systems is listed in Table 2.4

Five articles used a combination of systems to increase the number of biomechanical parameters measured. The Xsens Mtw Awinda system (Xsens Technologies B.V., Enschede, Netherlands) and Noraxon MyoMOTION Research Pro system (Noraxon USA Inc., Scottsdale, Arizona, USA) were

used by Cottam et al. (2022) in cricket [74]; Matsumura et al. (2020) used an IMU from Sports Sensing Co. Ltd (Fukuoka, Japan) alongside the pedar system to observe ski movement [84]; and nanocomposite piezoresistive foam (NCPF) sensors placed under shoe insoles were used in running by Seeley et al. (2020) with accelerometers to estimate vertical ground reaction force (vGRF) [88]. Force sensing resistors and IMUs were combined by Menzel and Potthast (2020) to measure punching force and understand technique in boxing [66, 89].

Table 2.4: Measuring systems used in included articles to evaluate biomechanical parameters.

Sensor Category	System	Articles Included
IMU	Lumo Run	3 [75–77]
	IMeasureU	4 [78, 90–92]
	Dialog Semiconductor	1 [93]
	Unspecified	6 [64, 67, 69, 72, 73, 94]
	myoMOTION	4 [70, 74, 78, 79]
	motusBASEBALL	2 [95, 96]
	Wearnotch	2 [97, 98]
	RunScribe	5 [99–103]
	Xsens Mtw Awinda/MTi	2 [74, 104]
	Xsens MVN Link suit	2 [85, 105]
	Optimeye S5 (Catapult)	1 [80]
	Physilog	2 [106, 107]
	InvenSense	1 [108]
	IMU (Sports Sensing Co)	3 [84, 109, 110]
	BTS G-Sensor 2	1 [111]
	WIBASE IMU	1 [112]
	WIMU Pro (RealTrack Systems)	1 [113]
	Movesense IMU	1 [68]
	APDM Opal V2 inertial sensors	1 [114]
	MPU9250 IMU	1 [71]
	miPod	1 [115]
	iSensor	2 [116, 117]
MEMS	Unspecified	1 [93]
Pressure Insoles	loadsol	2 [86, 87]
	pedar	6 [65, 81–85]
Other	Force-sensing resistor	2 [66, 89]
	Accelerometer (Bosch Sensortec)	1 [88]
	Nanocomposite piezoresistive foam (NCPF) sensors	1 [88]

Within the inclusion criteria of joint, limb and trunk kinematic and kinetic outcomes being obtained by wearable technology, a number of different variables were observed. The myoMOTION system comprising 16 inertial sensors was used in table tennis to determine the sagittal plane angles of the knee joints, as well as the shoulder, elbow and wrist of the playing hand [70]. The same system was used to determine knee joint angles in speed skating by Tomita et al. (2021) but with eight inertial sensors [79]; and also in cricket to capture global thorax and lumbar angles, thorax-to-pelvis relative

angles, and lumbar-to-pelvis relative angles in all three planes of motion by Cottam et al. (2022) using MIMUs placed on the pelvis, lower back and thorax [74].

The most popular systems reported are the pedar pressure insoles and the RunScribe sensors (San Fransisco, California, United States), mentioned in six and five articles respectively. While the pedar system was used in a number of different sports – tennis [82], basketball [81], skiing [65, 84], running [83] and speed skating [85] – to measure outcomes such as force, mean and peak pressure at the foot [82]; the RunScribe sensors were only used in a running environment [99–103]. This was to measure ankle pronation excursion [99–103], maximum pronation velocity [100–103] and peak vGRF [103] using a pair of sensors placed either on the heel of running shoes [99–102] or attached to the shoelaces [103].

Also in running, pelvic drop and rotation were evaluated with the Lumo Run sensors [75–77], while sagittal plane kinematics of the left thigh were measured with the IMeasureU IMU (Auckland, New Zealand) [91]. Physilog5 sensors (Gait Up, Lausanne, Switzerland) measured heel-strike pitch and eversion [107] and the Movesense sensor was used to estimate vGRF [68]. This same metric was estimated using the Xsens MVN Link motion capture system [105] and also by using the combination of an accelerometer and novel NCPF sensors [88].

In skiing, normal GRF, and kinematics (flexion/extension, abduction/adduction and rotation) of the knee, hip and ankle joints were quantified by Bessone et al. (2019) using the loadsol wireless insoles [87]; while knee, hip and elbow flexion angles were calculated by Kim et al. (2019) and Choi et al. (2021), both using the Wearnotch wearable motion capture system (Notch Interfaces Inc, Brooklyn, New York, United States) [97, 98]. Inclination of the shank, thigh and trunk, in addition to hip and knee flexion, were determined by Fasel et al. (2018) with Physilog IMUs [106].

Trunk-related parameters were evaluated in cricket with the Optimeye S5 sensors [80]; elbow torque and shoulder rotation were investigated in baseball with the motusBASEBALL sensor (Motus Global, New York, United States) (Camp et al., 2021)and IMUs [73]; and centre of pressure, punch force, wrist trajectory and fist rotation were measured in boxing using force sensing resistors and IMUs [66, 89]. Swimming studies reported a range of parameters, including: lumbar rotation angles [116, 117] and 3D joint kinematics of the hip, knee and ankle [72, 104]. The APDM Opal V2 inertial sensors (APDM Wearable Technologies Inc., Portland, Oregon, United States) were used to evaluate spine extension and flexion for different gymnastics skills [114].

The impact of wearable technology and sensors on its users were considered in swimming and in baseball [73, 108]. One sentence summarised that the Iswim system was not of any inconvenience to the two recreational swimmers that wore it [108]. Lapinski et al. (2019) stated that their sensor system was not designed to be used in baseball competition, acknowledging the constraints associated with this, but that "after a few pitches the player "got used to it" and "did not feel it at all"." [73].

2.3.5.3 Testing Environment

Studies were conducted in a laboratory setting in four sports: boxing [66], cricket [74], tennis [82] and running [68, 88, 90, 94, 102, 105, 107, 111]. All running studies in this environment took place on an instrumented treadmill in order to validate the estimated GRF from the wearable technology. The cricket study allowed the wearable systems from Xsens and Noraxon to be validated against the Vicon motion capture system [74]. The study by Menzel and Potthast (2021) in boxing was also a validation study, using Kistler force plates (Kistler Group, Winterthur, Switzerland) to validate Centre of Pressure (CoP) measurements from an instrumented boxing glove [66]. The study by Chen et al. (2019) in tennis was not used to validate any wearable technology [82]. Four studies did specify where they were conducted. These were boxing [89], tennis [69], table tennis [71] and one baseball [64].

For those studies performed outside a laboratory, a distinction should be made between those that used a normal training or race setting, and those where a specific protocol was developed to measure biomechanical parameters. One study collected data during football matches [113], while in running data collection took placed during training runs [76, 77] and marathon races [75].

2.3.5.4 Application of Technology

The applications of wearable technology considered in the earlier review by Adesida et al. (2019) are still present in this selection of articles: characterising movements; quantifying skill level and expertise of athletes; improving technique; and preventing injury [7], with more crossover between these different applications. There are also studies designed purely to determine the accuracy of or validate wearable technology [66, 95, 102, 105]. In swimming and basketball, the development of technology was considered purely as a performance improvement tool [67, 72].

Injury prevention was the focus in a number of sports: plantar pressure was analysed in tennis and basketball to determine the kinetic links to overuse injuries [81, 82], while knee internal rotation was measured using sensors in speed skating as a predictor for anterior cruciate ligament (ACL) injuries [85]. Different parameters were explored in running in relation to injury: sensors were used to predict vGRF for running performance and injury risk [88]; kinematic differences were measured between men and women to aid practitioners [111]; the effects of strapping and bracing on running biomechanics have been measured [100]; and sensors have been used to determine the differences in runners with and without chronic ankle instability (CAI) [99].

Studies aiming to classify differences in skill level between athletes recruited groups with at least two types of experience levels. Wang et al. (2018) used three levels of athletes (professional, sub-elite and amateur) to determine differences in accelerations obtained from the wrist in various badminton strokes and be able to classify these levels using machine learning [93]. Sub-elite and amateur athletes performed similarly to each other, while consistent differences were found in how professional athletes

performed different badminton strokes [93]. Clermont et al. (2019) started with one cohort of runners and were able to group them into two clusters based on measured biomechanical variables (including pelvic drop and rotation) that were linked to performance level, with one cluster running more consistently in the second half of a marathon than the other, in which runners displayed a more "atypical" approach [75].

Two groups with athletes of different performance levels were studies in skiing [84, 97, 98] and boxing [89]. In boxing, statistically significant results were determined between experienced and non-experienced athletes in rotation around the sagittal axis in the cross, hook and jab punches when the fist moved from a defensive position to a target [89]. Using IMUs in skiing, Choi et al. (2021) quantified the motions of national and college-level skiers, with the national-level skiers having greater flexion angles at the hip and knee joints, allowing them to achieve higher speeds than their counterparts [97].

The effects of different environments and equipment have been investigated, particularly in running. Foot strike patterns while wearing minimalist and traditional running shoes were compared by Jandova et al. (2018), with traditional running shoes being linked to lower peak pressure and deemed better for people with foot pain [83]. The RunScribe sensors used by Hollis et al. (2021) were able to identify changes in maximum pronation velocity and excursion as a result of running on track and grass surfaces and at different speeds, with both parameters increasing with speed and on the harder track surface [101].

Live feedback was employed by Li et al. (2020) in swimming for technique improvement, with the Iswim system recording information on medial-lateral rotation (or roll) angles and audio feedback provided through the use of bone conductors [108]. Feedback to swimmers improved the left side rolls by 29.64% and 17.67% for two athletes, with retention tests showing improvement of 27.86% and 4.68% when compared to no feedback [108].

2.3.6 Discussion

This review set out to determine the application of wearable technology in sport to measure biomechanical parameters. Systems used to measure kinetic and kinematic parameters in 14 sports included inertial based sensors, pressure insoles and resistor-based technology. The common themes established were characterising movements, quantifying skill level and expertise of athletes through technique; and injury prevention.

2.3.6.1 Article Quality

As highlighted in the review by Adesida et al. (2019), the amount of detail provided by authors in this set of included articles regarding methods and participants is variable [7]. When stated, participants ranged from novices or beginners [64, 89, 93, 116] to elite level athletes [72, 73, 86, 93, 107, 114]. A range of participants is important, especially when it comes to skill level quantification, however it is

important that the study population is reflective of the intended user of the wearable technology as movement patterns will differ [30]. Elite athletes are better for observation when looking at performance related metrics, while having a healthy and injured cohort is important for studying differences between the two groups, as in the study by Colapietro et al. (2020) [99]. Cohort sizes ranged from 1 [64–67] to 100 [68] which is important to note, as lower numbers can lead to population bias in the results.

There were also studies lacking appropriate descriptions of the tasks performed by the participants [71, 72] which makes it difficult for them to be repeated by other researchers and confirm the original results. The same can be said about reporting on sensor location as this also affects the ability of experiments to be replicated accurately. Especially in the case where multiple IMUs are used - as anatomical landmarks are specifically chosen for sensor placement in order to reconstruct human motion and trajectories – not knowing these locations can have a negative impact on the accuracy and reliability of the reconstruction [118].

2.3.6.2 Wearable Systems Used

Predominantly inertial sensors were used in the included articles, with commercial systems popular amongst investigators. The most popular were the pedar insoles and RunScribe IMUs, although as the name suggest RunScribe was only used to measure parameters in running [99–103], while the pedar system was used in five sports [65, 81–85]. Another example of a sensor system being used in multiple sports is myoMOTION, utilised in four different sports [70, 74, 78, 79]. Having a wearable technology that transcends sports increases its utility, however, how data is interpreted and the reported metrics will differ between sports. Users outside of a research environment should have confidence that any technology they use, especially the non-sport specific ones, are able to provide them with useful information to help monitor technique and performance.

Only two articles in this updated review used the Xsens MVN Link system comprising a full body suit into which inertial sensors are embedded [85, 105], compared to seven in the review by Adesida et al. (2019) [7, 34, 37, 38, 46, 48, 49, 119], suggesting that they are becoming less popular as a measurement tool. Although these suits allow many inertial sensors to be embedded for full body monitoring, in practice these suits would interfere with normal clothing worn in the sports of running [105] and speed skating [85]. Furthermore, they may not be very comfortable for long durations or aerodynamic, which is not suitable for training or competition environments. Fewer, more compact sensors that provide the same metrics would be able to overcome this problem.

A combination of wearable systems was used in cricket [74], skiing [84], running [88] and boxing [66, 89] – the advantage of this is that you can obtain both kinetic and kinematic outcomes as in the case of skiing and boxing [89]. However, collecting data from two different sources can increase processing and analysis times. Again user comfort must be taken into consideration – it can lead to potentially more interference (whether that be weight or size of the sensors) with their movement,

which can have a negative impact on their performance.

Although inertial sensors and pressure insoles have been used in the majority of these included articles, novel technologies are emerging, such as the nanocomposite piezoresistive foam (NCPF) sensors tested by Seeley et al. (2020) for predicting vGRF in running and placed inside running shoes [88]. Low-profile, lightweight systems such as these can replace the pedar and loadsol systems, however there is still developmental work to be done with regards to accuracy as reported by the authors. For predictions of vGRF impulse and active peak vGRF, per cent error was low at 2-7% and 3-7% respectively, but high for vGRF load rates at 22-29% [88], which currently is not suitable to replace other available systems.

As well as considering the design and accuracy of different technologies, the cost must also be taken into account. At the lower end, the Movesense Developer Kit 2.0 (containing one sensor and a number of attachment options) retails at €149 [120], while the RunScribe Red Gait Lab technology retails at $599 for only foot-related metrics and two sensor pods, and $799 for foot and sacral-related metrics and three sensor pods [121]. A subscription model is offered by IMeasureU of different tiers: the basic plan includes two sensors, offers a basic level of support and metrics but not real-time feedback, and costs $6600 per year [122]. While an individual may be able to afford a one-off payment of $799 for the RunScribe sensor set, the IMeasureU system is not geared at every day athletes, but rather teams or elite groups that have the money to invest into gathering data in this way. The cost of technology can be quite prohibitive, and only allows a small number of people to utilise it, which is not representative of the wider sporting population.

Understanding the unobtrusiveness of a wearable system is also a key factor – a good indicator of this is monitoring an athlete during training or competition. This is because athletes may expect discomfort from sensors in a laboratory setting or their range of motion to be affected, but would not necessarily put up with this when actively practising their sport [7]. Although participants in swimming and baseball studies were stated as not experiencing any inconvenience or grew accustomed to wearing sensors [108], being able to quantify any motion differences with and without sensors would give an understanding of whether they have an impact on any performance parameters or biomechanical movements.

2.3.6.3 Testing Environment

The majority of included studies took place outside of a laboratory setting – 11 studies stated that they were conducted in a laboratory [66, 68, 74, 82, 88, 90, 94, 102, 105, 107, 111] – but very few took place during an actual training or race environment [75–77, 113]. Laboratories are great for validation studies to test the accuracy of wearable technology, but a real-sporting environment is better for understanding kinetic and kinematic factors that relate to performance and injury, and a training session or competition come at the top of this hierarchy. The study conducted by Fantozzi

et al. (2016) is an example of this, where swimmers simulated the swimming stroke on dry land with their pelvis, trunk and upper limbs suspended horizontally while their lower limbs were held down on a box, but this altered their biomechanics [36]. Conditions in an outdoor environment can be unpredictable, so in sports such as running where this can influence biomechanical motions, it is important for wearable technology to be tested in this environment to determine kinematic and kinetic measures more accurately [7].

A change in surface is an example of how running biomechanics can be altered, with stiffer surfaces leading to a higher foot rotation [101, 115]. The ability to quantify water flow or wind resistance can provide useful information when assessing outdoor biomechanics. Increased wind resistance can lead to a cyclist adopting a more aerodynamic position in order to cut a smaller hole in the wind, sometimes at the expense of power output. Rowers may adjust stroke rate or power application in order to adapt to different water flow conditions. Awareness of what is happening in the environment can aid understanding of why athletes sometimes adapt their own technique from what may be considered as typical.

2.3.6.4 Applications of Wearable Technology

There are a number of applications of wearable technology in sport to measure kinetic and kinematic parameters, with the following reported in this study: injury prevention; skill level quantification; technique improvement; and movement characterisation. Sensors were used by athletes of different levels, from novice to elite, which implies that they have a benefit to everyone and not just those looking for marginal gains.

Injury prevention is an important theme to consider within this field, the cost of athletes missing out on training or competition due to injury can be high (whether that is financial or emotional), as well as the physical harm done by the injury itself. The use of technology is able to provide objective and quantifiable evidence for movement patterns that could lead to acute or overuse injuries. This can supplement the anecdotal advice that often forms the basis for injury prevention, which includes stretching and strength training [123]. Colapietro et al. (2020) observed lower pronation excursion in runners with chronic ankle instability (CAI) which became more prominent with increased running distances [99]. This kind of information provided by the RunScribe sensors can influence rehabilitation protocols and monitoring, increasing the ability to identify someone who may suffer from CAI.

Being able to classify skill level of athletes and identify movement patterns associated with each group can be useful for the athletes themselves and also for the coaches. Identifying that professional badminton players have markedly different wrist accelerations [93] can help coaches upskill athletes not already at this level, providing coaching points to aid them in improving their technique. The quantification of a movement and linking it to performance parameters, as done in skiing with hip and knee flexion and speed [97] can help athletes buy into making a technical change if they can understand

what the desired outcome is.

In the case of technical improvement, live feedback is more beneficial than feedback after the fact, as trialled by Li et al. (2020) [108]. A minimum of 17.67% improvement in left side rolls with audio feedback compared to no feedback is significant [108], however a small sample size of two recreational athletes is not suitable to come to a valid conclusion about the influence of this system. A larger cohort, and working with athletes of different experience levels would be helpful in understanding the best target audience for the Iswim system. Offering some type of feedback – whether that is audible, vibratory or visual – is useful for athletes as it allows them to make biomechanical changes even if they do not have a coach present.

2.3.7 Limitations

There are limitations that arose when conducting this review, the first being that it was limited to seven databases, which although returning a high number of results, may have omitted articles from sport-focused journals. The choice of search terms and inclusion criteria, focusing on specific kinetic and kinematic parameters, will have had an impact on the number of articles included. However, with the rapid expansion of the wearable technology field, narrowing the focus slightly allows a deeper investigation to take place. The search terms and criteria were also guided by previously published reviews with a similar interest [7].

2.3.8 Conclusions

The use of wearable technology in sport to measure kinetic and kinematic parameters is a field that is continuing to grow. The emergence of commercially available sensors in running that can be used by individuals and not just research groups is aiding the translation to the wider population.

Inertial measurement units are still the most common type of device being used across different sports, however the utility of force-sensing resistors and piezoresistive technologies are also being investigated as an alternative to the inertial sensors. These devices were reported in a number of applications such as quantifying skill level, characterising movement and preventing injury – these all have the potential to improve athlete technique and influence coaching practices. Using wearable technology for long-term monitoring can aid rehabilitation protocols and serve as an early-warning system, as it allows athletes, coaches and support staff to observe biomechanical risk factors over time.

A primary advantage of using wearable technology is that it allows athletes to be monitored in their sporting environment and not in a laboratory. Many studies have been conducted outside of a laboratory, but few are being conducted in training or competition, which is the environment that would provide the most accurate measurements of biomechanical parameters.

There is scope for wearable technologies to be used more outside of a research environment, however the cost is still prohibitive and the comfort of these systems must also be significantly considered for

there to be a wider uptake.

2.4 Gap in the field - rowing and cycling focus

From the articles included in the systematic review, it is clear that some sports have had more research concerning the use of wearable technology to measure biomechanical parameters. One article discussed the use of inertial sensors to monitor femur and lower back kinematics in rowing [40], while cycling was not mentioned in any. Since the completion of this systematic review, a validation study has been published, investigating the LEOMO system (TYPE-R, LEOMO, Boulder, CO, USA), made up of IMUs, to measure kinematic variables in cycling [124]. However there is still a clear gap in measuring biomechanics in this way compared to sports such as running. Rowing and cycling were therefore chosen to give this project a focus and determine how the impact that wearable technology can have.

2.4.1 Current Uses of Technology

Technology is very prominent in these two sports, which is promising for introducing something new to athletes and coaches. However, this is generally featured as equipment modifications or the use of computers that can measure a range of metrics from power to cadence, or stroke rate to stroke length.

2.4.1.1 Rowing

In rowing, a vast amount of research has been conducted in laboratory environments. Concept2 (Nottingham, UK) ergometers have been modified with the addition of load cells in the handle to measure the force of the arm pull [125, 126]; further load cells or strain gauges on the foot stretcher to measure foot reaction forces, torques and asymmetries [125, 127]; and incremental encoders to measure stroke length and seat position [125]. A combination of four load cells placed under the sliding seat on the ergometer have also been used to measure centre of pressure and the force magnitude on the seat [128].

The Flock of Birds (Ascension Technology Corporation, Shelburne, USA) motion capture system comprises electromagnetic receivers that are connected to a control unit by a long cable and has been used to measure the motion occurring in the lumbopelvic region of rowers [129, 130] alongside capturing data from the various load cells on the ergometer. Similarly, the optical system Optotrak Certus (NDI, Ontario, Canada), comprising of 14 active infrared light-emitting diode (LED) markers, has been used alongside kinetic measures to obtain angles of the hip, knee and ankle during the rowing stroke [125].

Both the sensor and marker based systems have been instrumental in improving the technical aspects of rowing, striving for those marginal gains in performance while minimising the injury risk to athletes, especially in a high performance environment. The problem is that they are constrained to indoor environments due to the bulky nature of the sensors and receivers or the multiple camera

set-up. Using the SIMI motion analysis system, Geng et al. (2012) observed that there was a 60-80% similarity between the kinematics of ergometer and on the water rowing. Differences were observed in the drive length and stroke rate but handle acceleration profiles were similar [131]. There is also the added instability of being in a boat that can alter an athlete's biomechanics.

Outdoor solutions consist of strain gauges and load cells placed on oarlocks, oars and footplates. These form telemetry systems that are able to measure handle force, foot force and blade angles. BioRowTel (BioRow, Cambridge, UK), Powerline (Peach Innovations, Cambridge, UK) and SmartOar (SMART Tracker, B.T.S., Milan, Italy) are examples of such systems that have been used on the water to calculate kinematic differences between elite and sub-elite level rowers [132]. However these systems do not provide outputs related to the body positions that athletes put themselves in, and measures of these motions is needed to maximise an athlete's potential on the water, creating the need for wearable sensors that can do so.

2.4.1.2 Cycling

The cycling landscape is quite similar to rowing in terms of technology usage, however where it is clear how technique can improve performance in rowing, Turpin and Watier (2020) state "the links between technique and performance are poorly understood" in cycling. The same power output can be produced from various combinations of different factors such as joint torque, trunk position and whether a cyclist is seated versus standing [133]. No one factor solely contributes to power output, leading to this statement from the authors.

Looking at indoor environments, bike-fitting is a process in cycling that involves setting up a bicycle to an individual, usually to increase comfort and/or aerodynamics. Systems such as Vantage 3D motion capture system by Retül (Boulder, CO, USA) offer dynamic measurements of joint angles [134], with this particular system using LED markers placed on anatomical points on the body which are tracked by a camera. Wadsworth and Weinrauch (2019) consider how bike-fits can be used to aid cyclists with hip pain which can be caused by different kinematic motions [134]. Posterior pelvic tilt, pelvic rocking and knee external rotation can be associated with a saddle and handlebars that are too low and a crank length that is too long, contributing to this hip pain [134]. Adjusting these components can be a start to eliminating the hip pain felt by cyclists.

On the bike, sensors that measure cadence and power are hugely popular and are used by recreational cyclists up to elite level athletes. Power meters contain strain gauges that are incorporated into pedals, cranksets or wheels, with many having the ability to be used interchangeably across different bikes and allow cyclists to track workloads and monitor their training [135]. As already highlighted, the LEOMO system has the potential to take some of these measurements outdoors, with some Motion Performance Indicators listed on their website as torso angle, pelvic angle and pelvic rotation, but does not include measurements of the knee joint angle that is widely used in bike set-up [136].

2.4.2 Movement Patterns

Both cycling and rowing are sports made up of a repetitive movement: there is minimal upper body movement in cycling, while in rowing the torso and upper limbs do have some contribution to moving a boat through the water. The forwards movement of a bicycle or a rowing boat are primarily driven by the lower-body, with the hip, knee and ankle joints going through a cycle of flexion and extension. In rowing the lower limbs move together in phase, while in cycling they are out of phase with each other. In both sports it is important to optimise this movement pattern that is continuously repeated, not only to improve performance, but to minimise the impact of an injury.

The knee joint and its movement in the sagittal plane is able to influence how boats and bicycles are set up and can link to performance indicators. The knee angle range has value in bike fitting as this can be used to set saddle height, not only to help prevent knee injuries which are the most common overuse injury in cycling, but to improve power output and therefore performance [136]. Being able to measure this in a dynamic situation is important compared to measuring the knee angle while the joint is static – once the pedalling motion starts to take place, increased plantar flexion will increase the knee angle, with more variation among novice cyclists [137]. This will therefore provide a better indicator of the motion that will take place on the bike away from the fitting process.

In rowing, the knee is also a common site of injury [138] often as a result of equipment set-up or lack of mobility that causes the knees to track out of the sagittal plane, as well as the knee going through a substantial range of motion in each stroke, from near-maximal flexion to full extension. Some athletes exceed this range of motion, for example by hyperextending the knee joint, increasing the forces it is already subject to. With regards to performance, the rate of knee extension during the drive phase of the rowing stroke (which contributes to the forward propulsion of a boat) has links to the force output on the foot-stretcher: a higher rate of knee extension increases the horizontal force output [139]. Being able to measure this rate of knee extension, and the joint angles during this movement can inform the power production and allow comparisons to be made between different rowers.

2.4.3 Research Focus

Rowing and cycling have performance improvement and injury prevention metrics associated with the knee joint that are not currently being measured by wearable technologies. Although IMUs are popular and have high accuracy, the limitations associated with cost and signal processing suggest that an alternative solution is needed. By focusing on the knee joint, strain sensors can be explored as a low-cost alternative to IMUs, assessing their feasibility and utility in measuring range of motion.

Chapter 3

Sensor Development

Fabrication, development and optimisation of carbon nanotube-rubber composite strain sensors

3.1 Introduction

Flexible and conductive strain sensors were fabricated in this project, with the aim of using them to monitor knee kinematics during sporting activities such as rowing and cycling. These sensors were created using a commercially available rubber band matrix and a conductive, multi-walled carbon nanotube (MWCNT) filler. The sensors are piezoresistive in nature: applying mechanical strain to the sensor causes a change in electrical resistance. On a microscopic level, there is separation between the conductive elements with the application of strain, contributing to an increase in the overall resistance. There is also a tunnelling effect that contributes to the overall resistance change. Tunnelling describes the transfer of electrons through a non-conductive barrier, such as a polymer matrix, between neighbouring nanoparticles and is best described by Simmon's theory for tunnelling resistance [140]. These resistance change contributions can be measured as a potential difference by means of an external instrumentation circuit, thus permitting assessment of movement.

The method used for fabricating strain sensors involved preparing a conductive filler dispersion, into which swollen rubber bands (expanded with toluene, a solvent) were placed. The nanotubes entered the rubber band pores via a solvent exchange process, before the rubber band was removed and left to dry. A range of dispersions (carbon nanotubes (CNTs) and graphene) and concentrations were employed until an effective selection of materials was found, providing the optimal amount of conductive filler element uptake from visible inspection and verified using scanning electron microscopy. Keeping the cost of fabrication down while ensuring the method was simple and repeatable was of great importance.

This chapter provides an overview of strain sensors, their different classifications and the strain-response mechanisms that can influence material choice and sensor design. There is also a review of the different polymer matrix and nanomaterial filler combinations that have been investigated in previous

literature, before detailing the optimisation of the fabrication process used in this project; investigating the use of different conductive fillers and the concentration of such fillers.

3.2 Literature Review

3.2.1 Strain Sensor Technology

Strain-sensing devices convert an external mechanical deformation produced via a force or temperature variation into a change in electrical properties (for example resistance or capacitance) that can be measured. These devices can be split into strain gauges and strain sensors. They differ in both material choice and deformation response mechanisms, although the terms have been used interchangeably in the literature [141, 142].

3.2.1.1 Limitations of Strain Gauges

Strain gauges are typically made from metal foils or semiconductors such as silicon. Examples of use include structural health monitoring, characterisation of structures and detecting damage in engineering fields. There are numerous advantages such as fabrication costs being low and the fact that the technology is well developed [143, 144]. Strain gauges rely on geometrical changes and the piezoresistivity of their component materials in order to generate an electrical signal during deformation [140].

However, strain gauges are generally limited to strain measurements below 5% and are rigid structures, making them unsuitable for detecting human motion and wearable electronics [145, 146]. Sensors for these applications need to be stretchable and have the ability to conform to different shapes [146]. Strain gauges require extensive cabling and can be difficult to embed in some structural materials [144, 147]. Furthermore, measurements of strain with strain gauges are unidirectional, and the gauge can be subject to transverse sensitivity if used in a biaxial strain field [148]. Strain gauges are only able to provide localised information with regards to strain measurements [149]. They are also susceptible to changes in temperature and humidity, however these can be overcome using a Wheatstone Bridge circuit configuration [150, 151].

3.2.1.2 Strain Sensors

In contrast to strain gauges, strain sensors tend to be made of softer and more robust materials (often a nanomaterial-polymer composite), resulting in more applications and the ability to withstand a higher amount of strain before structural failure compared to their brittle strain gauge counterparts [152]. The mechanisms involved to generate a change in electrical properties also differ: strain sensors utilise the tunnelling effect, crack propagation in thin films and the disconnection between sensing elements [140], allowing more tuning of properties.

It is understandable why there is a driving force behind research into strain sensors, particularly those that can be worn on the body. Traditional electronics based on silicon or metals do not deform appropriately in this kind of application [153]. Wearable strain sensors are rising in popularity across different applications including human motion detection; healthcare monitoring; soft robotics and neuromechanics; gaming and virtual reality; and sport performance monitoring due to their ability to interact easily with the human body [140, 152]. There is little evidence surrounding the use of strain sensors in sports with regards to joint measurements, but cues can be taken from healthcare where there is an overlap between aims such as long-term, remote and unobtrusive monitoring.

Strain sensors can be organised into different classifications which determines material choice and the sensing mechanisms involved. Previously, authors highlighted resistive and capacitive strain sensors being the most popular for wearable applications, with other types having poor dynamic performance and low resolution [140, 154]. A few years after this statement, the most researched sensing methods in the stretchable strain sensor field have expanded to optical, resistive, capacitive, triboelectric and piezoelectric [152], indicating how progressive the field is.

Several authors have discussed the important design parameters that should be considered when developing wearable strain sensors: they should be lightweight and have low power consumption, in addition to flexibility, stretchability and durability, as stated by Amjadi et al. (2016) [140]. Souri et al. (2020) also discussed sensitivity (as quantified by the gauge factor, GF); linearity of the response (quantified by the coefficient of determination, R^2); hysteresis; response and recovery time; and overshoot behaviour [152]. The sensing classification and the sensing mechanisms, as well as the choice of materials used will impact these parameters and there may also be a trade-off, e.g. favouring sensitivity over linearity, when developing new sensor technologies [152].

3.2.2 Sensor Classifications

As discussed in the previous section, there are a number of different classifications of strain sensors. A summary of the advantages and disadvantages of these is displayed in Table 3.1, which also includes important design and performance parameters. Piezoelectric and triboelectric sensors are relatively new technologies compared to resistive, capacitive and optical sensors and so the literature around them and their application as strain sensors is not as extensive.

3.2.2.1 Resistive Sensors

For resistive-based sensors, structural deformation will lead to a change in electrical resistance and this mechanism is known as piezoresistivity. Resistance, R, is given by the following equation:

$$R = \frac{\rho L}{A} \tag{3.1}$$

Where ρ is the electrical resistivity of the material, L is the length of the sensor and A is its cross-sectional area. The relative change in resistance after deformation, ΔR/R, is calculated as:

$$\frac{\Delta R}{R} = (1 + 2\upsilon)\epsilon + \frac{\Delta\rho}{\rho} \tag{3.2}$$

Where υ is Poisson's ratio and ϵ is strain. The first term is linked to the geometrical changes of the sensor and their influence on the change in resistance, while the second term describes the piezoresistivity of the materials themselves [140]. The piezoresistivity of the materials have little effect, therefore the main contribution to the overall resistance are the geometrical changes of the sensor [14].

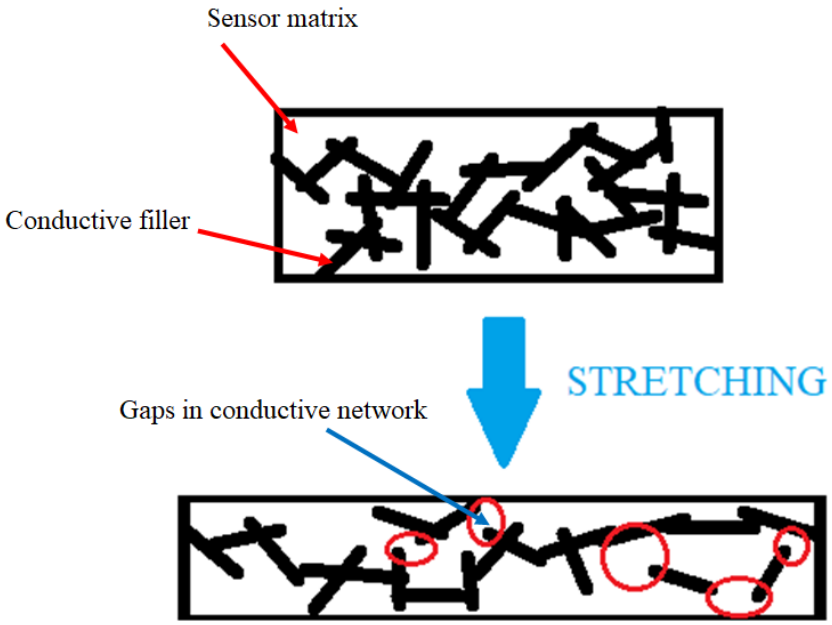


Figure 3.1: Schematic of the resistive sensing mechanism and the change in conductive network when strain is applied.

In this class of sensors, piezoresistive conductive polymer composite (CPC) based strain sensors are very popular due to their simple configuration, fabrication process and read-out system, as well as demonstrating high flexibility and stretchability [14]. Stretching these sensors will increase the separation between these conductive elements (e.g. carbon nanotubes) and increase the overall resistance of the sensor, as demonstrated in Figure 3.1. Upon recovery, the resistance should return to its original value, however resistive sensors are subject to hysteresis which can affect the reported outputs over time [152]. The high stretchability associated with these sensors allows them to be applied in wearable electronic devices that are used for healthcare and human motion monitoring, as well as structural damage monitoring [14, 152].

3.2.2.2 Capacitive Sensors

Capacitive sensors are based on a parallel-plate capacitor structure. Capacitors are devices that store electrical energy and a parallel-plate capacitor will consist of two electrically conductive plates (usually metallic although for stretch sensors this could be a polymer/nanomaterial composite), separated by a dieletric material which is electrically insulating and can exhibit an electric dipole structure (separating positive and negative charged dipole moments) in the presence of an electric field [155].

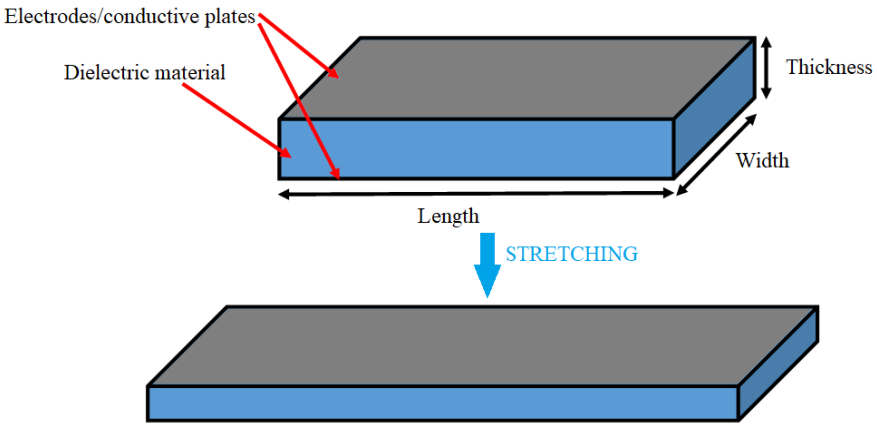


Figure 3.2: Schematic of the capacitive sensing mechanism and the change in sensor dimensions when strain is applied.

A geometrical effect comes into play with this sensing mechanism – when a capacitive sensor is stretched, the change in surface area and reduction in thickness of the dielectric layer will cause a change in capacitance, C, a measure of the amount of charge stored on one of the plates (see Figure 3.2). The original capacitance of the sensor at rest, C_0, can be represented by the following equation:

$$C_0 = \epsilon_0 \epsilon_r \frac{l_0 w_0}{d_0} \tag{3.3}$$

Where ϵ_0 is the permittivity of a vacuum, ϵ_r is the relative permittivity of the dielectric material, and the original length, width and thickness of the dielectric layer are given by l_0, w_0 and d_0 respectively. The application of strain, ϵ, will increase the length of the capacitor, and the thickness and width will decrease according to the material's Poisson's ratio, υ. The capacitance after stretching, C, would therefore be:

$$C = \epsilon_0 \epsilon_r \frac{(1+\epsilon) l_0 (1 - \upsilon_{electrode}) w_0}{(1 - \upsilon_{dielectric}) d_0} \tag{3.4}$$

Assuming that the conductive plates and dielectric layer have the same Poisson's ratio, then Equation 3.4 can be simplified to:

$$C = \epsilon_0 \epsilon_r \frac{(1+\epsilon) l_0 w_0}{d_0} = (1+\epsilon) C_0 \tag{3.5}$$

Equation 3.5 shows that the capacitance of a capacitive strain sensor increases linearly with respect to strain but it is only limited to a certain amount of strain, past which the linear relationship between the Poisson's ratio is no longer valid [140].

The sensitivity of these sensors is limited due to the parallel-plate structure, with the best theoretical gauge factor being 1, however investigation into different structures such as a wrinkled capacitor, has enabled a slightly higher gauge factor of 3 to be achieved [156]. Similar applications are seen with capacitive sensors as with resistive sensors: measuring physiological parameters and body movements are possible as a result of their compatibility with soft materials and easy electronic read-out [152, 157].

3.2.2.3 Optical Sensors

Optical sensors have the potential to overcome the trade-off between sensitivity and stretchability that can be encountered with some resistive and capacitive based sensors, and they do not suffer from electrical safety issues [158]. They are also small, lightweight, biocompatible, have a large bandwidth, are not subject to electromagnetic interference [159] and can be used in harsh environments such as those that are corrosive or of high temperature [160]. As a result, fibre optic sensors were introduced in the 1960s and have been used for in vivo measurements in humans to study bones and muscles since the 1980s [161].

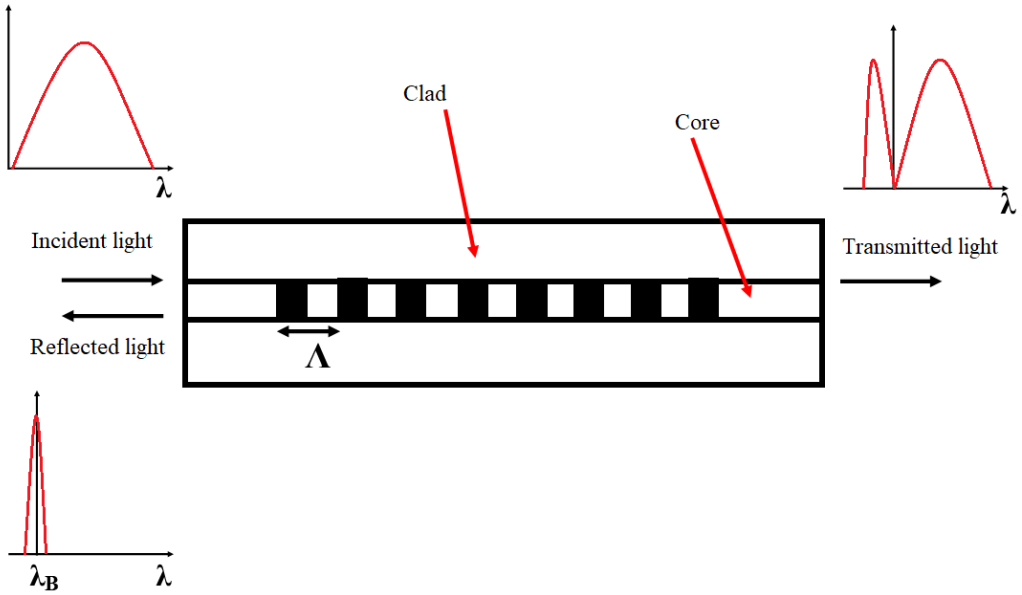


Figure 3.3: Schematic of the optical sensing mechanism and change in transmitted and reflacted light due to the fibre Bragg grating.

For wearable applications, the use of silica fibres in conventional optical sensors is not appropriate as a result of their high stiffness and maximum strain of 1% [162], however several types of optical-based strain sensors have been used in wearable applications [163]. These include a gold nanoparticle-elastomer composite, a notched side-ablated polymer optical fibre on a fabric substrate, a plastic optical fibre (POF), a fibre Bragg grating (FBG) and a side-polished FBG [163].

FBG are the simplest type of optical sensors and work through the wavelength modulation of light [161]. Within the core of an optical fibre are diffractive elements that act like filters when a light packet enters the fibre and reflects the light back according to the Bragg relation [162]:

$$\lambda_B = 2n_{eff}\Lambda \tag{3.6}$$

Where λ_B is the Bragg wavelength, n_{eff} is the effective refractive index of the fibre core and Λ is the grating period or spacing between diffractive elements. When the optical fibre is strained the spatial period is changed, shifting the Bragg wavelength, which can be converted into a measure of strain [164]. Figure 3.3 provides a schematic of the change to incident light when using a FBG.

In the context of human monitoring, FBG optical sensors encased in polyvinyl chloride (PVC) have been used to monitor knee joint motion during gait cycles [165] and more recently a highly flexibile POF sensor has been used to monitor wrist joint motion to aid rehabilitation following a stroke, with low errors in angle measurement [163].

While these sensors can demonstrate flexibility, they are limited by their stretchability. FBG sensors are only able to reach a maximum strain of about 10% [143]. Furthermore, optical sensors are more difficult to integrate with existing software and hardware, leading to an additional cost when using this type of sensor [166].

3.2.2.4 Piezoelectric Sensors

Piezoelectric sensors rely on the use of materials that contain a non-symmetrical distribution of electrical charges within the crystal structure. These charges, or dipole moments will normally cancel each other out, but the application of stress or strain will deform the structure and result in a net electric charge that can be measured (see Figure 3.4). Lead zirconate titanate (PZT) is the most well-known of the piezoelectric materials but is brittle and is cause for concern with regards to safety with the incorporation of lead [167].

Research into polymer-based piezoelectric materials such as polyvinylidene flouride (PVDF) has increased in order to expand the application of this class of sensors. The fabrication processes are of a lower cost and can take place at a lower temperature [168].

Chen at al. (2017) has been able to overcome the limited stretchability that some sensors face, using a $BaTiO_3$ and polydimethylsiloxane (PDMS) composite structure, demonstrating lateral stretching up to 60% and the ability to monitor different human physiological functions [169]. Most applications of piezoelectric sensors focus on energy harvesting: converting applied mechanical energy into electrical energy. This means that devices can be self-powered, but there is little surrounding the use of these sensors as a mechanism for measuring strain in relation to human kinematics.

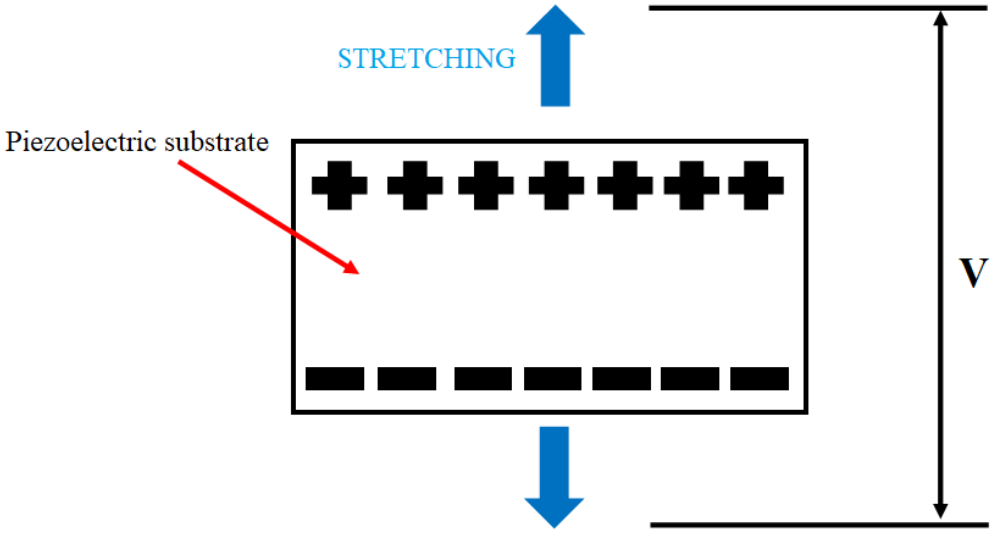


Figure 3.4: Schematic of the piezoelectric sensing mechanism and the separation of charges when strain is applied (direct effect).

3.2.2.5 Triboelectric Sensors

Like piezoelectric sensors, triboelectric sensors are also self-powered and so not limited by their lifetime or mobility like other sensing mechanisms [170]. Triboelectric nanogenerators (TENGs) instead utilise mechanical energy from the surrounding environment [170]. The working principles of TENGs combine triboelectrification and electrostatic induction, mechanisms that are normally avoided in everyday life, and utilise common materials such as paper, fabric and different polymers [171].

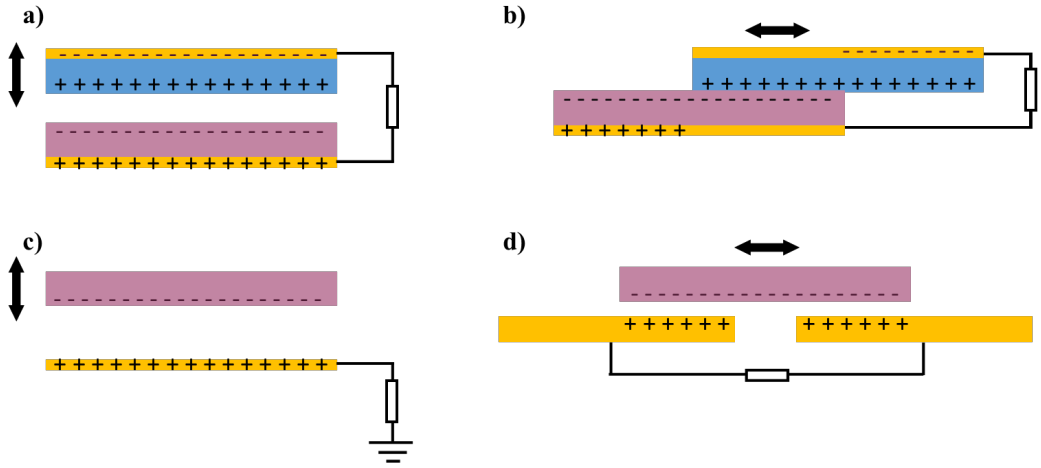


Figure 3.5: Schematic of the various triboelectric sensing modes: a)vertical contact-separation mode, b) contact-sliding mode, c) single-electrode mode and d) freestanding triboelectric-layer mode.

The triboelectric effect is a phenomenon by which a material becomes electrically charged after coming into frictional contact with a different material [172]. An example of this is a balloon sticking to a wall after becoming triboelectrically charged from being rubbed on hair [173]. Materials can be ranked in a triboelectric series and the greater the separation between their rankings in this series, the more effectively charge can be transferred between the two materials [172]. Electrostatic induction

takes place when there is a redistribution of charges in an object as a result of nearby charges.

There are two factors that contribute to the current, I, generated during mechanical compression, and can be explained by the following equation [174]:

$$I = C\frac{\delta V}{\delta t} + V\frac{\delta C}{\delta t} \tag{3.7}$$

Where C is the capacitance of the system, V is voltage across the electrodes and t is time. The first term corresponds to the electrostatically induced charges and the potential drop between the electrodes, while the second term corresponds to the change in capacitance as the distance between the electrodes is reduced during compression.

The four modes of TENGs that were invented by Wang et al. (2014) will vary in how much these terms contribute to the overall current. They are: vertical contact-separation, contact-sliding, single-electrode and freestanding triboelectric-layer mode [171], as presented in Figure 3.5. Each has two electrodes apart from the single-electrode mode. Except in the case of the final mode, electrical charges are generated by contact and friction between different materials which has a downside in that this requires materials to be highly durable to withstand constant friction.

Another disadvantage is that for a common phenomenon, it is not one that is well understood. Contradictory triboelectric series have been published over time, and also researchers do not yet have a complete understanding of the species that transfer charge between materials [173]. TENG sensors have been demonstrated to detect finger bending which can be quite a low frequency movement [175], but the magnitude of the electrical output changes with bending frequency as well as strain [174], increasing the complexity of calibration if the same sensor were to be used for a higher frequency movement.

3.2.2.6 Classifications Summary

The requirements for the use of strain sensors to measure sports kinematics are a dynamic response capable of capturing high-speed motions, ideally with a quick response time; long-term durability so the sensor can withstand repeated use; high stretchability and a large working range. An overview of these properties are listed in Table 3.1 for each sensor classification. Optical sensors fall short on a number of these parameters, coupled with the additional cost of integrating the sensors with existing software and hardware. Although piezoelectric and triboelectric sensors are self-powered, they are limited in their ability to sense static loads – in human monitoring it is important to be able to distinguish when someone is holding a position, at rest, or in motion. This leaves resistive and capacitive-based sensors as the classifications of choice.

There is no clear-cut choice between the two remaining classifications. Resistive-based sensors offer high sensitivity and stretchability at the expense of linearity and non-hysteretical behaviour, while ca-

Table 3.1: Advantages and disadvantages of different sensing classifications.

Sensing method	Advantages	Disadvantages
Resistive	High gauge factors achievable [152] High stretchability and sensitivity [152] Easy and low cost fabrication [14] Simple read-out and uncomplicated sensor configuration [14]	Generally non-linear output [152] viscoelastic behaviour of substrates contributes to hysteresis [152] subject to high overshoot [152]
Capacitive	Higher linearity (compared to resistive sensors) (Souri et al., 2020b) Show less hysteresis than other methods (resistive and optical) [152] Faster response time [152] Simple readout [152]	Maximum theoretical gauge factor = 1 (for parallel-plate structure) [152] Poor sensitivity [152]
Optical	Higher linearity (compared to resistive sensors) [152] Negligible hysteresis [176] Good environmental stability (temperature, humidity) [176]	Poor dynamic performance [152] Long response time [152] Poor long-term durability [152] Fibre Bragg Grating sensors limited to maximum strain of about 10% [143] Difficult to integrate with existing software and hardware [166]
Piezoelectric	High sensitivity and fast response when detecting mechanical deformations [177] Can convert mechanical forces directly into electrical signals [177]	Poor ability to sense static loads [178] Little information regarding kinetics monitoring
Triboelectric	Can convert mechanical forces directly into electrical signals [179] Easy assembly, low cost and high output voltage [179]	Poor ability to sense static loads [178] Residual charges at high frequencies [174] Output affected by humidity levels and ionic particles [180]

pacitive based sensors provide better linearity and minimal hysteresis, however, compromise sensitivity and stretchability. Many resistive sensors have linear output regions that surpass the required working range for measuring joint range of motion [181, 182]. Furthermore, Shintake et al. (2018) highlight that the majority of the literature does not compare how the two classifications respond to strain rate and temperature [183], which are also important factors to consider in a sporting context, and so no distinction can be made here.

All considered, resistive-based sensors are able to provide the high stretchability and sensitivity needed to detect joint motion and accurately distinguish between different joint positions that capacitive-based sensors cannot, suggesting that they are more suitable for this type of application.

3.2.3 Strain Sensor Performance Parameters

When developing sensors for long-term joint measurement, stretchability, durability and stability of the sensor output are very important parameters to consider, among others. Each of these can be affected by the fabrication process, the sensor microstructure and also sensor classification.

Stretchability is defined by Souri et al. (2020) as "the maximum strain where the sensor maintains its physical integrity and response stability" [152] and it can be improved by using high-aspect ratio fillers such as nanotubes, as these form percolation networks more easily than rounder nanoparticles [140]. However achieving high stretchability can come at a detriment, affecting the ability to also achieve high sensitivity, defined as "the relative change in electrical resistance per unit strain" and quantified by the gauge factor (GF) [184]. The gauge factor for a resistive strain sensor can be expressed as:

$$GF = \frac{\frac{(R-R_0)}{R_0}}{\epsilon} \tag{3.8}$$

Where R is the resistance under strain, R_0 is the unstrained resistance and ϵ is the strain. For capacitive sensors, capacitance, C, would replace resistance in Equation 3.8. A higher GF means high sensitivity and for polymer-nanoparticle based sensors it requires a conductive network that can be easily damaged, whereas the requirement for high stretchability is a network that is more stable [185].

Round nanoparticles could be used to make a network but it would be easily damaged; when a sensor is stretched there is separation of these particles and they are unlikely to overlap with other particles with further application of strain and thus the conductive network is lost as indicated in Figure 3.6. Nanotubes provide a more stable network – with the application of strain there will still be overlap between the fillers due to their high aspect ratio and the conductive network is therefore not completely destroyed (see Figure 3.1).

Sensor stability encompasses several behaviours including hysteresis, response time, recovery time and overshoot behaviour. When considering wearable applications, these are especially important as sensors are subject to dynamic load. Hysteresis arises as a result of the viscoelastic nature of polymers,

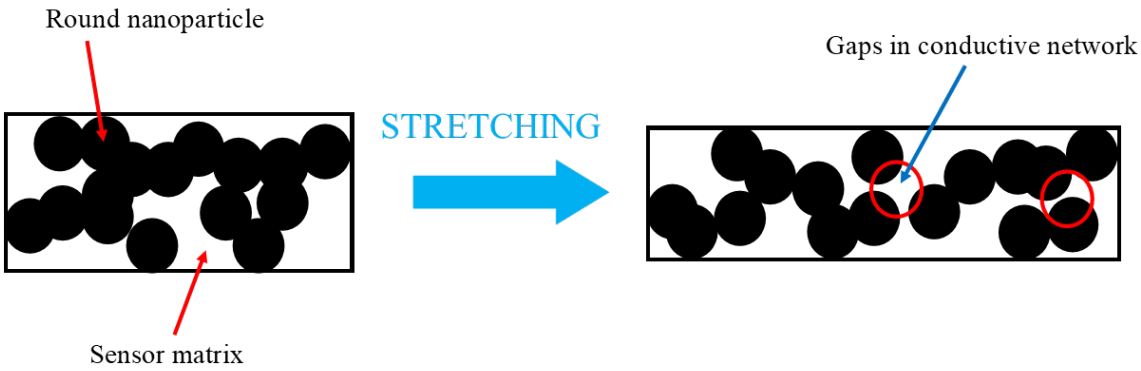


Figure 3.6: Round nanoparticles under strain.

as well as the interaction of those polymer matrices with the nanomaterial fillers [140]. Mechanical hysteresis describes the behaviour of the polymer when loaded and then unloaded. The strain will be recovered but the loading curve will follow a different path to the unloading curve [186] – in one complete cycle there will be two stress values recorded for the same strain value, as represented in Figure 3.7. This can be considered a rate-dependent form of hysteresis and can be defined by the following equation:

$$Hysteresis(\%) = \frac{|R_{load} - R_{unload}|}{R_{max} - R_{min}} \times 100\% \tag{3.9}$$

Where $|R_{load} - R_{unload}|$ corresponds to the greatest difference between the loading and unloading responses, and R_{max} and R_{min} are the resistance values at the maximum and minimum strain respectively.

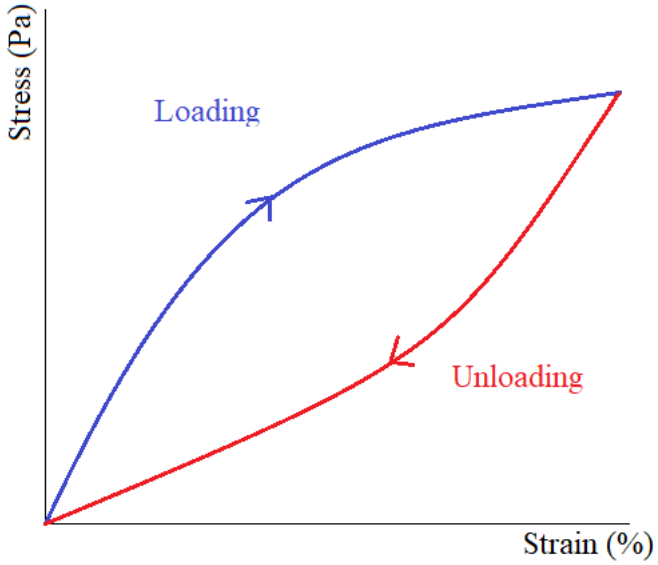


Figure 3.7: Load-unload behaviour of a polymer.

There is a trade-off between hysteresis and recovery: strong interfacial binding between the filler and matrix will minimise hysteresis but a weaker binding between the components will promote better sensor recovery, with nanomaterials returning to their initial positions when strain is released [140]. Between sensor classifications, resistive-type sensors exhibit more hysteresis behaviour compared to their capacitive and optical counterparts [140, 152]. This is an important factor to consider as repeatability of the sensor output can be negatively influenced by high amounts of hysteretic behaviour.

There is also a difference between sensor classifications when observing response and recovery time of strain sensors. Response time is defined as "how quickly the strain sensors move toward steady state response" after experiencing a change in load [140], while recovery is linked to the return of the sensor output to its original, unstrained value. Viscoelasticity has a role to play here too, and so all polymer-based strain sensors will experience some degree of delay in their response. Response times can be calculated theoretically or measured experimentally and the 90% time constant ($\tau_{90\%}$) is often the reported metric [140, 152]. Treating a strain sensor as a first-order dynamic system, the following relationship applies [187]:

$$\frac{C(S)}{R(S)} = \frac{1}{\tau S + 1} \tag{3.10}$$

Where R(S) and C(S) are the Laplace functions for the input and output of the system respectively, and τ is the time constant of the system. For a ramp input (e.g. strain increased from 0 to 16% at a rate of 100 mm/min), R(S) can be defined as:

$$R(S) = \frac{k}{S^2} \tag{3.11}$$

where k is the steady-state gain, and so:

$$C(S) = \frac{k}{S^2(\tau S + 1)} \tag{3.12}$$

A solution for Equation 3.12 is:

$$C(t) = k(t - \tau(1 - e^{-\frac{t}{\tau}})) \tag{3.13}$$

Where t is time. Souri and Bhattacharyya (2018) used the MATLAB curve fitting tool to fit their experimental data to Equation 13 to determine a value for τ [187].

Again capacitive sensors have been shown to be more promising, having a faster response time than resistive sensors [140]. Material choice also impacts response, softer polymers will have a lower recovery force with the removal of strain and so will have a higher response time [152].

Overshoot behaviour is caused by stress-relaxation of polymers and is dependent on both internal and external factors: GF, viscoelasticity and strain rate [140, 152]. An example of this is a carbon

nanotube-Ecoflex composite strain sensor which displayed overshoot behaviour in the sensor response when it was stretched to and held at a strain of 270% [188]. A sudden application or reversal of strain leads to an instant release of stress by polymer matrices which causes this type of behaviour, more prominent in resistive-type sensors compared to capacitive and optical sensors [140, 145, 152]. A schematic representation of stress-relaxation behaviour is shown in Figure 3.8.

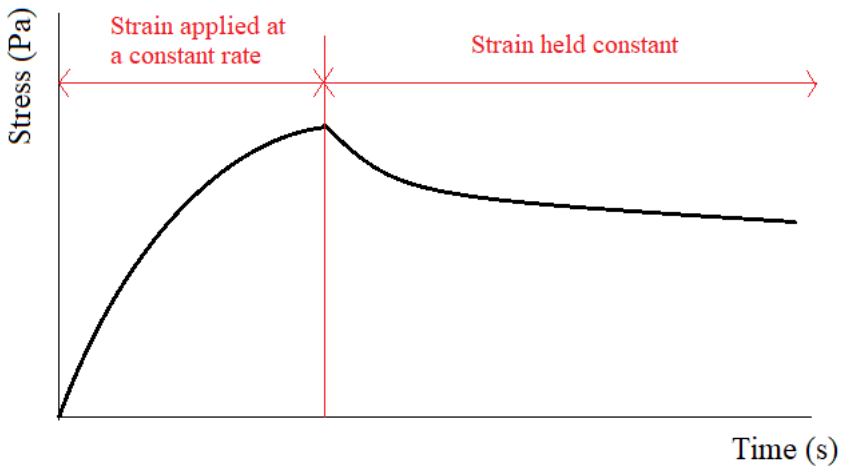


Figure 3.8: Stress-relaxation behaviour of a polymer.

Linearity is another important performance parameter, referring to the relationship between the strain sensor response and the applied strain. A linear sensor response (quantified by a high R^2 value) will make calibration and the subsequent data processing easier when equating it to joint kinematics. Capacitive and optical sensors tend to have higher linearity [152], however capacitive sensors have low sensitivity as a result [140]. Resistive sensors tend to not have a linear response due to the development of an inhomogeneous network after strain is applied, however sensors have now been developed with linear regions and can be applicable to human motion capture if used within this range.

Finally, dynamic durability and the stability of a sensor's structural integrity and output over a number of strain cycles are important to consider. Strain sensors used for wearable applications need to be able to accommodate large and dynamic strains with minimal or no degradation in performance. This degradation is dictated by the materials used to construct these sensors: buckling and fracture of nanomaterial fillers, fatigue and plastic deformation of the polymer matrices, as well as the interaction between filler and matrix are examples of this [140]. Some sensors have reported impressive dynamic durability. For example, a metal nanowire/elastomer composite resistive-based sensor has been developed that displays durability and reliability over 10,000 cycles at 150% strain [189]. However, no indication was given as to the strain rates used when testing this sensor, and this is an important consideration for sports where faster actions may occur and affect the properties of the sensor as a result.

3.3 Piezoresistive Sensors

When considering the performance parameters discussed in Section 3.2.3, piezoresistive conductive polymer composites (CPCs), where the conductive element is a nanomaterial contained in a polymer matrix, are able to provide superior properties such as high stretchability, tuned sensitivity and improved dynamic durability at a high strain when compared to CPCs using alternative sensing mechanisms [14] . These sensors can also have a high signal to noise ratio, as demonstrated by Wichmann et al. (2009) with epoxy-based sensors containing carbon fillers [190]. As briefly discussed in Section 3.2.2.1, deformation will cause a change in electrical resistance in piezoresistive sensors, with the main contribution coming from the geometrical changes experienced by the strain sensor rather than the piezoresistivity of the materials used. This section will focus on CPC composites, material choice, charge transport mechanisms and applications of these sensors.

3.3.1 Material Choice

3.3.1.1 Matrices and Substrates

Polymers are an advantageous choice as a sensor matrix or substrate due to their stretchability and ability to conform to the human body, with elastomers and rubbers being the preferred subsets within this group. Examples of elastomers and rubbers that have been used in strain sensing applications include: natural rubber (NR), styrene-butadiene rubber (SBR), epoxy, Ecoflex, polypropylene (PP), polyvinylidene fluoride (PVDF), thermoplastic polyurethane (TPU) and the most common, PDMS [14].

However, polymers are subject to degradation as a result of long-term cyclic use or environmental factors (such as humidity and temperature), and the viscoelastic behaviour of some polymers can lead to hysteretic behaviour. The choice of polymer will affect the susceptibility to these negative effects, the performance parameters discussed previously, and the ease of fabricating strain sensors.

There is no standardisation when it comes to processing polymers for strain sensor fabrication, and the amount of detail provided in the literature is variable. Whether the polymer is used as a matrix (the conductive material is dispersed) or as a substrate (the conductive material is deposited on the surface) is an important distinction as the fabrication methods used will be different. However, in matrix and substrate applications, several authors have used curing, often a high temperature process that needs to be precisely controlled or it can affect mechanical properties [145, 146, 154]. For example, over curing can lead to a tougher material that is harder to stretch over a large strain range. Methods containing mixing also require precision – the conditions for this and the filler properties have influence over the electrical properties of the final strain sensor [191], such as ease of forming conductive networks.

A simple method has been demonstrated by Boland et al. (2014): a swollen rubber band was placed in a dispersion of exfoliated graphene, enabling a solvent exchange process to take place, and

promoting graphene infusion into the band [153]. Low temperature and uncomplicated methods such as these could help preserve the mechanical properties of the polymer matrix or substrate and enable the fabrication process to be more easily repeated.

3.3.1.2 Conductive Fillers

Like matrices and substrates, there are a number of options when it comes to conductive fillers or thin films which can be separated into three groups: carbon-based, metallic based and conductive polymers. Examples of carbon-based fillers include graphene, carbon black (CB) and CNTs; for metallic materials there are nanowires, nanoparticles and nanosheets made from silver (Ag), gold (Au), copper (Cu) and zinc oxide (ZnO); while conductive polymers include poly(3,4-ethylenedioxythiophene) polystyrene sulfonate (PEDOT:PSS), polyaniline (PANI) and polypyrrole (PPy) [14, 192].

One must not only consider the contribution of these materials to overall strain sensor performance, but their intrinsic properties such as conductivity, as well as the cost of fabrication or obtaining higher purity forms of these materials; and their abundancy. There are advantages that span across the different groups: high-aspect ratio materials (nanotubes and nanowires) form conductive pathways through sensors more easily.

When assessing the benefits and downfalls of conductive fillers, fillers in the same group do not necessarily have the same advantages. For example, the properties of carbon-based fillers are affected by their aspect ratio and ease of processing. For metallic fillers, the abundancy of each one will impact those chosen for use in sensors. As with the strain sensor substrates and matrices, conductive polymer fillers will have different degrees of stiffness that will impact the overall sensor properties. Table 3.2 provides more detail into the advantages and disadvantages of the different conductive filler material prospects.

A possible solution is to use hybrid materials that can overcome the disadvantage of individual materials. An example is combining with CNTs and graphene [14], or silver nanowires (AgNWs) and CNTs where the former provided high conductivity and the latter provided high stretchability within a composite material [197]. However, a hybrid approach could drive up costs in terms of sourcing materials and the fabrication process, which may also become more complex as a result and less repeatable unless the configuration of the conductive elements is precisely controlled.

For human joint monitoring, strain sensors can be subject to high amounts of cyclic strain and in a case of sports, be exposed to different temperatures, levels of humidity and moisture in the case of sweat. Carbon-based fillers have been extensively studied and have demonstrated superior performance compared to other filler types. AgNWs are the most promising out of the metallic based fillers and have numerous advantages, but their cost and low abundancy make them less suitable compared to carbon based fillers. High conductivity is important for sensor performance, which is not guaranteed with conductive polymers. For these reasons, the conductive mechanisms and structures of carbon-based

Table 3.2: Advantages and disadvantages of different conductive materials used as fillers in strain sensors.

Conductive Material	Advantages	Disadvantages
Carbon-based	CB – cheap and good health and safety performance [14]	CB – difficult to achieve a good dispersion; poor electrical conductivity; low sensitivity [14]
	MWCNTs – high purity; large working range, can improve sensitivity and linearity [14]	CNT based sensors – experience hysteresis under cyclic loading; health concerns [14]
	Graphene – non-toxic, good electrical and mechanical properties; high GF, high stretchability and transparency [14]	Graphene – signal may not be repeatable; difficult to achieve high quality in bulk [14]
Metallic-based	Nanowires and nanoparticles have a very high conductivity [14]	Strain range may be limited by irreversible crack formation for nanoparticles [14]
	Nanowires – excellent mechanical compliance [14]	
	AgNW – have high resistance to oxidation and corrosion [14], high transparency [193]	AgNW – expensive, nonabundant [14], weak adhesion on polymer substrates that are flexible [193])
	CuNWs – inexpensive, abundant [14]	CuNWs - poor resistance to oxidation [14]
	AuNWs – biocompatible, chemically inert, NW thin films have high sensitivity	AuNWs – difficult to produce, poor mechanical/electrical properties
Conductive Polymer	Low cost, large-scale fabrication [194]	Poor environmental stability (sensitive to moisture and temperature) [14]
	PEDOT:PSS – high flexibility, processability and conductivity [14, 180]	PPy – concerns surrounding rigidity [195]
	PANI – low cost and easy processing, high conductivity and chemical stability [196]	Fibres produced through electrospinning have poor conductivity

CB – carbon black, MWCNT- multi wall carbon nanotube, AgNW – Ag (silver) nanowire, CuNW – Cu (copper) nanowire, AuNW – Au (gold) nanowire, PEDOT:PSS - poly(3,4-ethylenedioxythiophene): poly(styrene sulfonate), PANI - polyaniline, PPy – polypyrrole

fillers will be explored further.

3.3.1.3 Carbon-based Fillers

Carbon-based fillers used in strain sensors include: carbon black (CB), carbon nanotubes (CNTs) and graphene. Nanomaterials can be classed by their architecture dimensions and in the case of these fillers we have 0D, 1D and 2D respectively. In order to understand the importance of the different dimensional architectures, one must investigate the structure of the conductive networks that are formed and the charge transport mechanisms that take place in these networks.

3.3.1.3.1 Charge Transport Mechanisms

In addition to the geometrical changes and material piezoresistivity highlighted in Section 3.2.2.1 that contribute to overall changes in sensor resistance, there are other mechanisms that come into play which are affected by the choice of conductive fillers: the disconnection mechanism, crack propagation and the tunnelling effect.

The disconnection mechanism refers to the contact between nanomaterials: there needs to be overlap of these particles at rest and with the application of strain, as this area of overlap reduces, the electrical connection reduces, increasing the electrical resistance. On a microstructural level, the driving force behind this mechanism is the weak interfacial binding between the nanomaterial filler and the polymer matrix, as well as the large stiffness mismatch. Under strain, there will be slippage of the nanomaterials within the matrix, causing disconnection [140].

Crack propagation is a mechanism associated with brittle thin films on polymer substrates and less so with conductive fillers in a polymer matrix. When strain is applied, cracks are generated in the thin film in order to release the stress that has been accommodated in concentrated areas. The electrical resistance is increased as cracks are formed but can be recovered when the source of strain is removed. However, these cracks can be irreversible in some cases where a high amount of strain has been applied.

Finally, the tunnelling effect refers to "the crossing of electrons through a nonconductive barrier" [140]). This means that electrons can tunnel through a polymeric matrix between nanomaterials that are separated by a small distance. As the distance between nanomaterials increases so does the tunnelling resistance as it is more difficult for electrons to cross the nonconductive barrier. This can be approximated by Simmon's theory [140], given by the following equation:

$$R_{tunnel} = \frac{V}{AJ} = \frac{h^2 d}{Ae^2\sqrt{2m\lambda}} exp(\frac{4\pi d}{h}\sqrt{2m\lambda}) \tag{3.14}$$

Where V is the electrical potential difference, A is tunnelling junction cross-sectional area, J is the current density for tunnelling, h is Plank's constant, d is the separation distance between adjacent

nanomaterials, e is the charge of a single electron, m is the mass of an electron and λ gives the height of the energy barrier for polymers [140]. The type of polymer used for the matrix will affect tunnelling resistance as well as the dimensional architecture of the conductive filler – the cut-off distance for tunnelling is found to be higher for graphene sheets than for CNTs [140]. The tunnelling effect has been found to be the dominant charge transport mechanism in CPC strain sensors [140].

As the crack propagation mechanism is mostly irreversible and will change the resistance range with each use of a sensor, it is more useful to maximise the resistance changes as a result of the disconnection mechanism and tunnelling effect. This allows the same sensor to be used multiple times to measure joint range of motion, and reducing the frequency for changing resistors to optimise the circuit containing the strain sensor. The various charge transport mechanisms informed the composition of the sensors developed in this work, opting for a matrix and filler-based sensor, instead of a thin-film based technology.

3.3.1.3.2 Optimal Carbon-based Filler

Although carbon-based fillers are superior to other filler types, they are not all made equal, with the dimensional architecture impacting strength, stretchability and the aforementioned charge transport mechanisms. In some cases, there can be a trade-off between these properties. Several authors have demonstrated the effect of different carbon fillers on the stretchability of strain sensors and the change of resistance over this strain range, including Sau et al. (1998) [191], Das et al. (2002) [198], Wichmann et al. (2009) [190] and Zhao et al. (2013) [199].

The properties of different polymer matrices filled with short carbon fibres (SCF) or carbon black (CB) were compared by Das et al. (2002) [198]. The resulting mechanical properties are largely due to how the fillers interact with the matrix on a micro-level. CB creates chemical bonds with the chains of rubber within the matrix, providing mechanical reinforcement, while SCF mainly creates weak physical bonds with the rubber chains. For CB composites, Das et al. (2002) found that the behaviour was similar to that of vulcanized rubber reinforced with CB, and they were able to undergo strains of up to 120% with no tendency to yield [198]. Contrary to this, SCF composites had a much higher tendency to yield, with the irreversible deformation occurring as a result of "total failure of the fibre-rubber interface" [198].

In addition to mechanical reinforcement, CB composites have better sensitivity to mechanical deformation [190]. As strain is applied, the separation distance between CB particles will increase, thus there is less contact between particles and it is more difficult for electron tunnelling to take place, which increases the overall resistance. Nanotubes composites will have a lower sensitivity: as strain increases, because of the random orientation and overlap between the high aspect ratio fillers, interparticle separation may actually decrease. This is exaggerated at higher amounts of CNT-loading

as the two competing processes, network formation and network destruction, are more balanced and mean that conductivity change takes place at a slower rate [198].

For joint monitoring applications where a large strain range is required, CB composites will not do well as once the particles separate with strain, they will not reconnect with each other. Nanotubes are preferable as the conductive network is more stable and resistance changes can be detected over a larger range. Furthermore, CB composites have an exponential resistance vs strain response which can make sensor calibration more difficult, while the response is more linear for nanotube composites [190].

Graphene fillers are a further option, their hexagonally bonded carbon-structured nanosheets can be produced via liquid exfoliation in large quantities. Boland et al. (2014) demonstrated a simple technique using graphene to fabricate strain sensors in this way [153]. The high resulting flexibility is useful for strain sensing applications where conforming to the human body is a requirement. They have high sensitivity like CB, as well as optical transparency compared to CNTs [5, 200, 201].

Despite this, having a lower aspect ratio compared to CNTs means that graphene-based sensors will have a lower stretchability since the percolation networks will not be as easily maintained [140]. This can be overcome using a wrinkled or crumpled graphene nanostructure that becomes less wrinkled with the application of strain, allowing the network to still be maintained at high levels of strain. Moreover, non-linearity is a problem for resistive strain sensors in general, but thin films made from graphene flakes or nanoparticles are more susceptible to it as a result of the generation and propagation of cracks in these films [140].

Even within the resistive-based sensor classification and looking specifically at carbon fillers, the trade-off between certain performance parameters – linearity, sensitivity and stretchability – must still be considered. Non-linearity will affect carbon black, nanotubes and graphene sheets, but nanotubes will be less susceptible. For monitoring human joint range of motion, such as the knee or the elbow, sensor stretchability is more important than sensitivity as the output must be stable over a large strain range, which again favours the use nanotubes for this application. The choice of filler is clearly application dependent and there is no blanket approach when it comes to the development of strain sensors.

3.3.2 Summary

Depending on the application of the strain sensor produced, it is acceptable for there to be some compromises when it comes to some of the sensor performance parameters discussed in Section 3.2.3. When considering the requirements for human joint measurements where sensors are subject to a large strain range, the linearity of sensor output and stretchability are more important metrics than sensitivity (or gaguge factor) and therefore material combinations should be determined based on this.

Carbon nanotube-rubber composite piezoresistive sensors were chosen to be developed in this

project for human joint monitoring in sports. Stretchability has been favoured over sensitivity and the relatively simple construction and fabrication methods that are also low-cost have been deemed suitable for this application.

3.4 Materials, Methods and Results

3.4.1 Preparation of Carbon Nanotube Dispersion

Multi-walled carbon nanotubes (MWCNTs) were obtained from Sigma-Aldrich (>90% carbon basis, D × L 110-170 nm × 5-9 μm; Sigma-Aldrich Corporation, St Louis, Missouri, United States) and used to prepare a dispersion in distilled water at a concentration of 5 mg/mL.

A 250 ml media bottle was used to make up the dispersion. Approximately 1 gram of MWCNTs were weighed out and transferred to the bottle with 200ml of distilled water. 1ml of Triton X-100, a surfactant (Laboratory Grade; Sigma-Aldrich Corporation, St Louis, Missouri, United States), was measured out using a syringe and added to the mixture to help exfoliate the MWCNTs.

An ultrasonic homogeniser (Hielscher Ultrasonic GmbH UP200S, Hielscher Ultrasonics, Teltow, Germany) was used to disperse the MWCNTs in the distilled water. The probe was placed in the middle of the mixture and a water bath was used to regulate its temperature as displayed in Figure 3.9. This was run for 90 minutes (probe settings: 0.6 cycles, 65% amplitude).

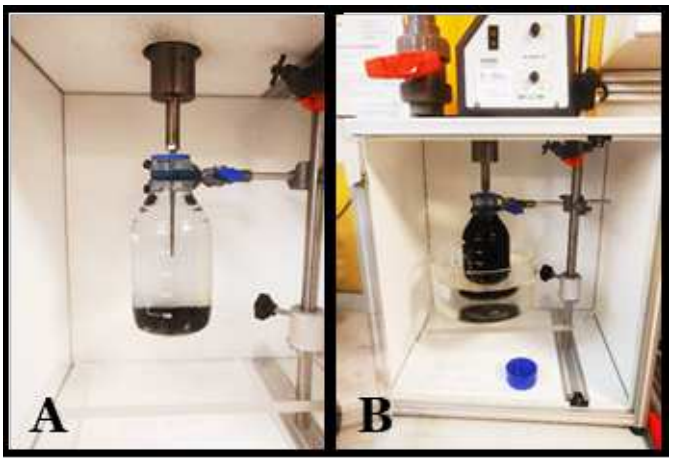


Figure 3.9: Dispersion (A) pre-homogenisation and (B) post-homogenisation.

A centrifuge (Eppendorf Centrifuge 5804 Eppendorf, Hamburg, Germany) was used to separate the resulting dispersion from non-exfoliated MWCNTs (settings: 30 minutes at 2000 rpm). A pipette was then used to transfer the dispersion to another media bottle, taking care not to transfer any of the sedimentation deposited at the bottom of the centrifuge vials, as shown in Figure 3.10. This was then refrigerated for later use.

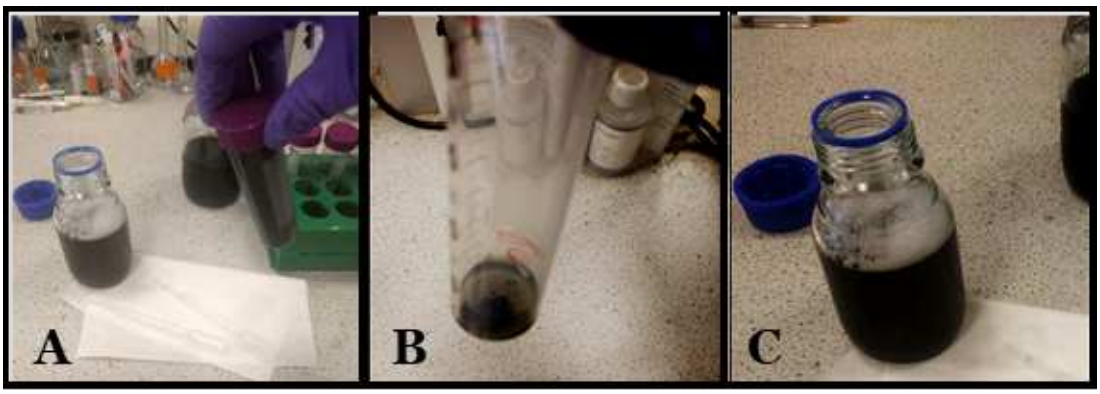


Figure 3.10: (A) dispersion in centrifuge vial (B) sedimentation remaining after centrifugation (C) final dispersion.

3.4.2 Expansion of Rubber Bands

Rubber bands, based on natural rubber, were obtained from Office Depot Inc. (Boca Raton, Florida, United States) with given dimensions 180 mm x 12 mm (length x width). The thickness was measured to be 1 mm. Lengths of 110 mm were cut from the rubber bands, ensuring that they would be able to stretch over the anterior aspect of the knee.

An aromatic solvent, toluene (≥99.5%, AnalaR NORMAPUR® ACS, Reag. Ph. Eur. analytical reagent; VWR International Limited, Leicestershire, England) was used to expand the pores of the rubber band, causing them to swell to approximately one and a half times their original size. This was done in preparation for the solvent exchange process which would form the final composite. Prepared rubber bands were placed in a sealed media bottle of toluene, ensuring that they were completely covered by the solvent, and left submerged for three hours before being removed.

3.4.3 Solvent Exchange Process

Each swollen rubber band was placed in 100 ml of the MWCNT dispersion in 250 ml media bottles. The size of the bottle was chosen so that the rubber band did not come into contact with itself in the dispersion; this would have prevented the MWCNT from entering the rubber matrix in these areas. The sealed bottles were placed in an ultrasonic cleaner (VWR Ultrasonic Cleaner USC -TH, VWR International, Radnor, Pennsylvania, United States) for two hours. This was done to aid the solvent exchange process with vigorous mixing as toluene and water are not miscible. After two hours, a cloudy grey solution was produced indicating successful exchange between the toluene in the pores of the rubber band and the MWCNT dispersion in the bottle.

The rubber band was then removed from the bottle in its swollen state, but black in appearance due to the uptake of MWCNTs, then left to air dry for 48 hours. This allowed the band to return to its original dimensions through evaporation of the residual toluene over time.

Table 3.3: Conductive filler and solvent combinations for the different dispersions prepared.

Dispersion	Conductive Filler	Solvent
1	Graphene	NMP
2	MWCNT	NMP
3	MWCNT	Water

3.5 Exploration of Different Materials and Methods

The above methods describe the optimal fabrication method used to develop CNT- rubber composite strain sensors. However, different conductive fillers and solvents were trialled before settling on the dispersion of carbon nanotubes in water. The concentration of this dispersion was also considered. Steps in the fabrication process of these composites were also evaluated and modified in order to improve and save time within the entire process.

3.5.1 Conductive Material and Solvent Choice

Three combinations of solvent and conductive material were prepared for use in the strain sensor using the following forms of carbon: graphene and MWCNT; and the following solvents: 1-Methyl-2-pyrrolidinone (NMP; ACS reagent, $\geq$ 99.0%, Sigma Aldrich Corporation, St Louis, Missouri, United States) and water. The combinations are displayed in Table 3.3. Equal concentrations of each dispersion were made (1 mg/mL), and a rubber band expanded in toluene was placed in a media bottle with 100 ml of each prepared dispersion.

Each bottle was placed in an ultrasonic cleaner for approximately 30 minutes to encourage the solvent exchange process to take place. The rubber bands were then left to sit in each solution for five days. The bands were removed and left to air dry for approximately 15 minutes while held by a clamp (Figure 3.11), before being transferred to a paper towel to continue drying and to allow them to return to their original size (Figure 3.12).

From visual inspection of the rubber band surfaces as shown in Figure 3.12, the dispersion of MWCNT in water resulted in the best uptake of nanotubes into the rubber band matrix. Almost complete coverage was achieved from the CNT dispersion in water, identified by the black material on the surface. The band placed in the graphene/NMP dispersion had a very similar appearance to a normal rubber band, while the CNT/NMP dispersion resulted in a sensor between the two extremes. As graphene was less promising than CNT when paired with NMP, the decision was made to not explore the combination of graphene with water. The uptake of CNTs by the rubber band using a dispersion in water was later confirmed using Scanning Electron Microscopy.

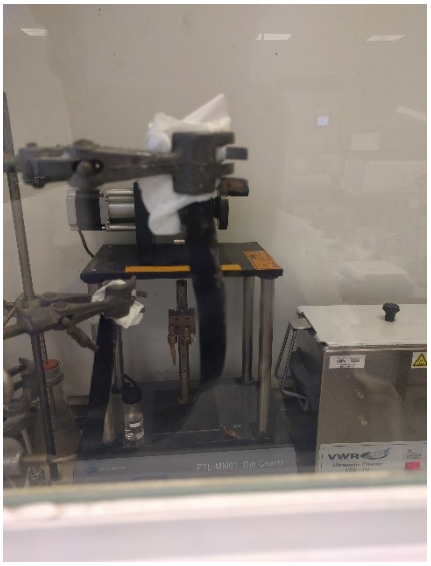


Figure 3.11: Sensor drying made from dispersion of CNT in water.



Figure 3.12: Side by side comparison of dispersions (L-R) MWCNT in water (x2), graphene in NMP (x1), MWCNT in NMP (x2) at different stages of drying.

3.5.1.1 Imaging

A scanning electron microscope (SEM, LEO Gemini 1525 FEGSEM) was used to image a CNT-rubber composite strain sensor fabricated using a water solvent. Approximately 5 mm was cut off one end of the sensor and coated in 5 μm of chromium in order to ensure that the entire sample was conductive. This sample was fixed onto a holder and placed in the SEM. Several images were taken including a cross-section of the bulk. An accelerating voltage of 2kV was used to produce the image in Figure 3.13.

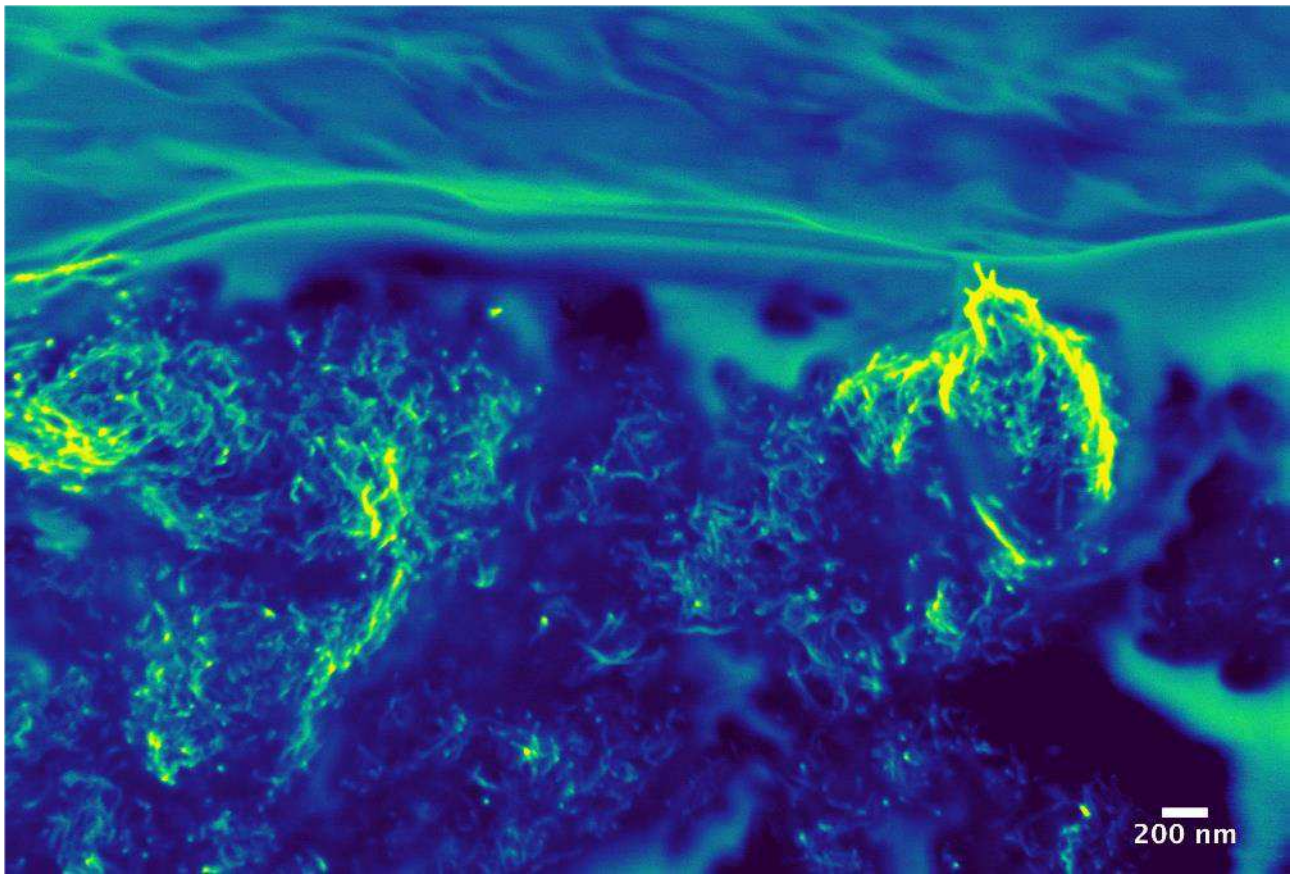


Figure 3.13: A cross-sectional image of the fabricated sensor using a FEGSEM. The featureless region at the top of the image represents the amorphous rubber band. The conductive networks formed by the carbon nanotubes can be seen in the lower two thirds of the image, indicating the uptake of nanotubes into the pores of the rubber band. This image was false-coloured using ImageJ.

The top third of the image is amorphous in nature, consistent with the amorphous structure of the rubber band matrix. A percolating structure can be seen in the lower portion of the image. This structure shows the conductive pathways formed in the sensor by the carbon nanotubes. From this, it can be calculated that the nanotubes have entered the rubber band matrix by a depth of at least 2 μm, which can be assumed to be the same at the opposite end of the sensor cross section, which has a thickness of 100 μm.

3.5.2 CNT Concentration

After determining the optimum dispersion combination, different concentrations of MWCNT (1, 5 and 10 mg/mL) were trialled to observe the effect on MWCNT uptake and overall resistance of the sensor.

Six rubber bands pieces, each cut to a length of 110 mm, were expanded in toluene (left to soak for 48 hours) and then each was placed in a media bottle containing 100 ml of a dispersion (2 bottles for each concentration). The bottles were placed in an ultrasonic cleaner for 30 minutes and then removed, with the rubber bands being left in the solutions for a further 48 hours.

From observing the rubber bands while still in the bottles of each dispersion, there were many aggregates in the high concentration dispersion of 10 mg/mL, compared to the lower concentrations. Liquid in the bottles containing the lowest concentration dispersion had a cloudy grey appearance after removal from the ultrasonic cleaner, indicating most of the MWCNT had entered the rubber band and the remaining solution had been destabilised by the toluene as demonstrated in Figure 3.14. After the 48-hour period, the rubber bands were removed and left to dry. A side-by-side comparison can be seen in Figure 3.15.

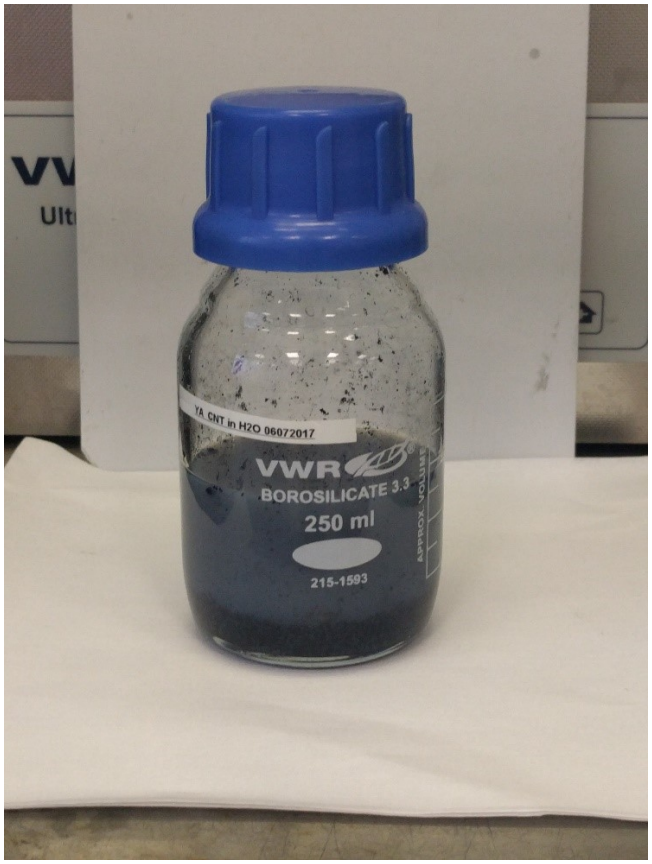


Figure 3.14: CNT dispersion destabilised by toluene.

A multimeter (Edison DM383 digital Multimeter, Edison, Wigston, England) was used to measure resistance over a length of 8 cm on the surface of each rubber band. The resistance was lowest for the 5 mg/mL samples, followed by the 1 mg/mL, with the 10 mg/mL samples recording the highest resistance as listed in Table 3.4. The lower resistance indicates a higher number of conductive pathways present in the sensor that make it easier for charge to flow, and to also detect changes in strain when the sensor is stretched. These results, combined with the observations during fabrication, led to the use of the 5 mg/mL concentration for producing further sensors from rubber bands and MWCNTs.

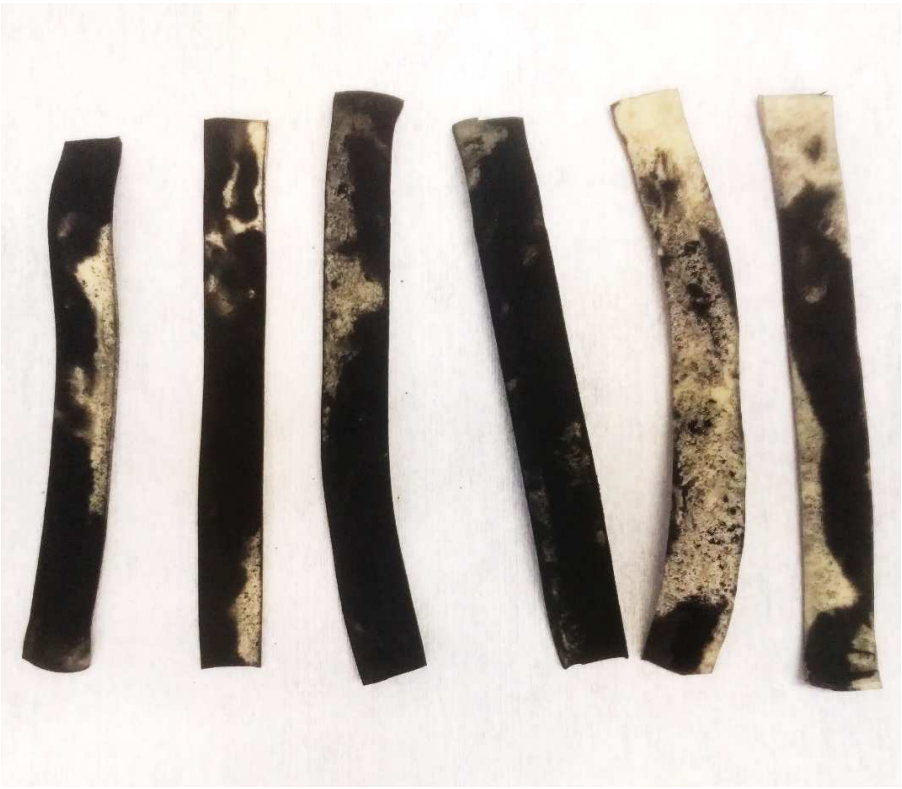


Figure 3.15: Side by side comparison of sensors made with different dispersion concentrations - (L-R) 1mg/mL (x2), 5mg/mL (x2), and 10mg/mL (x2). The highest uptake of CNTs was as a result of a 5mg/mL dispersion concentration, indicated by the mostly black appearance of the sensor. A concentration of 10mg/mL resulted in the lowest uptake of CNTs as the rubber band surface is still approximately 50% visible. A concentration of 1mg/mL provided results between these two.

Table 3.4: Mean resistance value (over three readings) over 8 cm for strain sensors fabricated with each dispersion concentration.

CNT dispersion concentration (mg/mL)	Resistance value ($\times 10^3 \Omega$)
1	1.746
5	0.792
10	447.6

3.5.3 Fabrication Steps

Modifications were made to the fabrication process in order to improve time efficiency during sensor production after noting that the turnaround time to produce sensors was approximately one week. Initially rubber bands were left to soak in toluene for 48 hours in preparation for the solvent exchange process. After some experimentation it was discovered that the bands could be left for as little as three hours to achieve the desired effects with regards to pore expansion. This greatly reduced the length of the fabrication process.

When carrying out the steps for the solvent exchange, initially the rubber band in the MWCNT dispersion was placed in the ultrasonic cleaner for 30 minutes and then removed to allow the exchange process to take place without any outside stimulus over a few days. However, after five days it was found that the exchange had not taken place, with the rubber bands appearing as they did before being placed in the dispersion and only a minimal uptake of nanotubes observed visually. This was

rectified by increasing the sonication duration to two hours, without the need for further immersion of the rubber bands in the MWCNT dispersion afterwards.

3.6 Discussion

The aim of this section of the project was to develop a composite strain sensor and optimise the fabrication process, both in terms of sensor quality and time taken to make the sensors. Carbon nanotubes in water was determined to be the optimal dispersion, prepared using sonication and centrifugation techniques. Toluene was used as a swelling agent to expand the pores in a rubber band. The swollen band was then placed in the nanotube dispersion, with an ultrasonic cleaner used to aid a solvent exchange process.

The solvent exchange process that allows the nanotubes to enter the pores of the rubber band can be better described as liquid-liquid extraction, the transfer of a solute (in this case carbon nanotubes) from one solvent to another. The solvents are immiscible or partially miscible with each other, and typically water is used in conjunction with a non-polar organic liquid [202].

The Hansen solubility parameters can be used to determine the types of interactions that can take place - similar solubility parameters lead to an interaction between substances. The components (which each correspond to a part of total cohesive energy) that make up these parameters are: δ_D, δ_P and δ_H where δ_D is the dispersion cohesion (solubility) parameter, δ_P is the polar cohesion (solubility) parameter and δ_H is the hydrogen bonding cohesion (solubility) parameter (Hansen, 2012). The total solubility parameter, δ_T is given by:

$$\delta_T^2 = \delta_D^2 + \delta_P^2 + \delta_H^2 \tag{3.15}$$

A list of solubility parameters for the different substances used is given in Table 3.5. This indicates that toluene is not miscible with water due to the differing values and therefore satisfying the requirement for liquid-liquid extraction. Toluene does have similar Hansen solubility parameters to natural rubber, meaning that the two can effectively interact with each other, and it is this which allows toluene to open up the pores in the rubber bands.

Considering the solubility parameters for MWCNTs, graphene, NMP and water listed in Table 3.5, one can understand combinations that are energetically favourable for conductive fillers to enter the rubber band. Graphene and MWCNTs have similar Hansen solubility parameters to NMP, making it less energetically favourable for the conductive elements to be surrounded by rubber. However, the use of water as a solvent for the dispersion makes it more energetically favourable for the MWCNTs to enter the pores of the rubber band, because of the differing values. This is clearly demonstrated in Table 3.5.

The dispersions of MWCNTs were considered in two solvents, water and NMP, with a clear im-

Table 3.5: Hansen solubility parameters for substances used.

Substance	$\delta_D(MPa^{1/2})$	$\delta_P(MPa^{1/2})$	$\delta_H(MPa^{1/2})$
Water [203]	15.5	16	42
NMP [204]	18	12.3	7.2
Toluene [204]	18	1.4	2
Natural Rubber [205]	14.4	3.1	4.1
Graphene [206]	18	9.3	7.7
MWCNT [207]	21.3	6.8	3.2

provement of nanotube uptake into the rubber band matrix when water was used. Graphene, however, was only dispersed in NMP. By comparing the solubility parameters in Table 3.5, it would have been more favourable to disperse graphene in water in order to increase the proportion of graphene in the rubber band. In fact, Boland et al. (2014) [153] determined that a mixture of NMP and water (20:80) as a solvent provided the best conditions for graphene to enter a rubber band matrix. For the purposes of this research and with the different combinations of solvent and conductive material tested, a suitable outcome was achieved using MWCNTs dispersed in water as seen in Figure 3.12.

Changing the concentration of MWCNTs in the dispersion directly impacted the filler content in the resulting sensor. A higher concentration dispersion means more available MWCNTs to enter the rubber band, which should result in a higher filler content. As well as visually comparing the sensors fabricated from the different dispersions (see Figure 3.15), the resistance measurements also gave an indication of nanotube uptake. Resistance measurements taken at rest for each of the sensors reported a lower resistance for those made from the 1 mg/mL and 5 mg/mL dispersions and the highest for the 10 mg/mL dispersion.

The formation of aggregates in the 10 mg/mL dispersion hindered the uptake of MWCNTs into the rubber bands, leading to the patchy appearance seen in Figure 3.15. The higher resistance reading can be explained by this: the visual appearance of the sensor indicates fewer conductive pathways, making it difficult for charge to flow through the sensor. If all the nanotubes from this dispersion had entered the rubber matrix it would have become oversaturated, having a negative effect on the sensor output under strain. At rest the resistance would have been lower due to the increased number of conductive pathways, however the sensitivity of the output would have been reduced. With the application of strain, the competing processes of the breakdown and formation of these pathways would balance each other out, leading to a minimal change in resistance output.

There was a drop in recorded resistance from the 1 mg/mL to 5 mg/mL sensors, indicating an increase in conductive pathways through the sensor as a result of more conductive elements in the rubber matrix. The higher filler content also contributes to the tunnelling effect as the nanotubes are likely to be in closer proximity (within the tunnelling cut-off distance), allowing electrons to flow through the sensor via this mechanism as well as through nanotube contact. Similar to the 10 mg/mL

sensors, the patches in the 1 mg/mL sensors indicate fewer conductive pathways in the sensor which increases the resistance and also reduces the working range of the sensor.

The 5 mg/mL dispersion provided a combination of low resistance and high filler content, optimising the electrical and mechanical properties of the sensor. It is expected that the fabricated strain sensor should have a large working range suitable to measuring knee range of motion and high stretchability, but will be affected by hysteresis as a result of the piezoresistive construction.

The SEM image produced in Figure 3.13 provides a visual confirmation of the nanotubes being integrated within the rubber matrix, entering its pores during the solvent exchange process. They have not just been deposited on the surface. As an uncoated sensor is subject to the conductive material rubbing off the surface during handling, having the conductive material within the bulk of the sensor provides increased stability when it undergoes repetitive strain cycles. With the nanotubes being incorporated into the rubber band matrix, the failure of the sensor is dependent on the matrix fatigue properties.

Modifications to sensor fabrication led to a more time efficient process, with the amount of time rubber bands were soaked in toluene from a 48-hour period to just three hours. As well as saving time, this also provides a benefit when it comes to retaining the elastic properties of the rubber band. Prolonged soaking of rubber bands in toluene (i.e. periods of more than 48 hours) can lead to material loss and a decrease in hardness [208]. This would have a negative impact on the durability and use of the sensor under cyclic strain over its lifetime.

3.6.1 Limitations

Despite the fabrication being simple and low cost, there are some limitations to the process. The different steps leading to the final nanotube dispersion result in material loss: transferring the nanotubes from a weighing boat to bottle, then the sedimentation left behind after centrifugation lead to a lower concentration of nanotubes and also volume of surfactant. However, this does not seem to hinder the uptake of nanotubes into the rubber band. The final concentration used could be quantified using ultraviolet-visible light (UV-Vis) spectroscopy.

There is a little control over the solvent exchange process, besides the time the rubber bands spend soaking in the dispersion and immersed in water in an ultrasonic cleaner. This leads to each sensor having its own unique electrical properties that impact sensor calibration.

In Figure 3.15 , it is clear to see that the coverage of the rubber bands is uneven. This is due to the orientation of the rubber bands in the dispersion – any part of the rubber band that is not contained within the carbon nanotube dispersion, is pressed against the side of the bottle or is touching another part of the rubber band, is not able to uptake the carbon nanotubes. Therefore, care needs to be taken in placing the rubber bands in each dispersion bottle before this is put in the ultrasonic cleaner. This can be overcome by changing the orientation of the band in the bottle throughout the solvent

exchange process; using a different shaped vessel which allows the rubber band to lay flat; or in the case of mass-production, using a larger vat to hold the dispersion and multiple rubber band pieces.

3.7 Conclusion

Piezoresistive sensors were determined to be the preferred technology for developing strain sensors that can be used in a sporting context to measure joint range of motion due to their simple configuration, low-cost fabrication and high stretchability. Between multi-walled carbon nanotubes and graphene, the former was able to infiltrate a rubber matrix more easily, which is significant as the uptake of filler will directly impact the flow of conductive elements within a sensor. An optimal nanotube dispersion concentration of 5 mg/mL was achieved, producing a sensor that had a low resistance and visible filler uptake indicating numerous conductive pathways for charge transfer. This low-cost and repeatable method can be used to produce sensors for a biomechanical application.

Chapter 4

Sensor Characterisation

Using mechanical testing to understand the strain sensor response at different strain rates

4.1 Introduction

The use of strain sensors for human movement monitoring requires a system that provides repeatable and accurate measurements, whilst also being durable. When strain sensors are placed on a joint they are unlikely to fail as a result of reaching their maximum strain value, instead, they may fail as a result of numerous cycles at a lower strain value. Therefore, it is important to measure how long it takes for such fatigue to occur: structural failure of the sensor itself and deterioration of its electrical response.

In sports, joints may move through a range of motion more quickly than in a clinical context: for example, a strain sensor placed on the knee will be subject to a higher strain rate during the running motion of a football player on a pitch compared to someone performing a gait study and walking across a laboratory. This means it is important to consider the effect of strain rate on sensor performance as well as the number of cycles – does the fatigue life of the sensor change because of the different strain rates; does it affect the electrical response; or is there a lag between the application of strain and the sensor response?

This chapter reviews carbon nanotube-polymer composite strain sensors that use a resistive-based sensing method and the testing protocols used to assess their mechanical and electrical properties. It then details the development of a mechanical testing protocol to replicate the conditions of rowing or cycling sessions of different lengths and intensities; and determine the durability and robustness of the strain sensor under different strain rate conditions. This testing protocol was carried out on the carbon nanotube-rubber composite sensors developed earlier in this project.

4.2 Literature Review

In the development of conductive polymer composite (CPC) strain sensors, many filler and matrix materials have been considered as the different applications desire certain properties over others. The literature reviewed within this chapter focuses on those sensors with a carbon nanotube (CNT) filler to permit comparisons between the sensors developed in this body of work. As discussed in Chapter 3, there is a distinction between the performance of different carbon fillers – the aspect ratio will influence the sensing mechanisms and properties of a strain sensor under strain. This review aims to address the following questions, which will help inform the characterisation and usability of the nanotube-rubber strain sensors that have been developed:

- How is sensor performance defined – through output stability or structural integrity?
- What level of variability in the sensor output is acceptable from cycle to cycle?
- What are the different testing protocols that have been used (e.g. no. cycles, strain rates), and have they been justified?
- How applicable are these protocols to the real-life use of the sensor? (e.g. clinical, rehabilitation and sporting environments)
- Are there any common testing elements across the literature?
- What are the limitations of the reported methods?

4.2.1 Mechanical and electrical characterisation of strain sensors

The consideration of the mechanical and electrical properties of strain sensors is important as users need to understand whether it is appropriate for their desired application. They will take into account how easy the sensor is to calibrate (aided by the linearity of the signal), and how long it will last before either the sensor output deteriorates too much from its original value or there is structural failure.

Furthermore, the use of polymer matrices means that the effects of viscoelasticity should be quantified as this can result in hysteresis or creep behaviour. Zhao et al. (2013) noted that the strain rate applied to a sensor can impact maximum strength and elongation at failure: elongation is high and strength is low when the strain rate is low as polymer chain segments can relax, while the opposite is seen at higher strain rates [199]. The rate at which strain is applied is equally as important as the number of strain cycles and the degree of strain.

Seventeen articles featuring carbon-based piezoresistive strain sensors were reviewed, considering only those that included cyclic testing in the form of stretching and not bending [141, 146, 182, 188, 199, 209–221]. This distinction is important as bending may only consider the impact of a microstructural

change at a localised point of the strain sensor, whereas stretch testing takes into account changes across the sensor as a whole.

4.2.1.1 Testing equipment

Across the articles considered, a wide range of testing rigs have been used to perform cyclical strain and simple tensile tests on strain sensors. Universal testing machines from Instron (Buckinghamshire, UK) [141, 212, 220] and Suns (Shenzhen Suns Technology Stock Co.Ltd., China) [182, 199] have proved to be popular, as well as the Future Science Motion Controller [188, 210], whilst other systems have been developed in-house [146, 218]. Limitations can arise particularly with in-house systems as the choice of instrument will affect the maximum strain or loading rate that can be applied, the maximum load or strain, the sampling frequency of data that is collected and the protocols that can be programmed. Furthermore, if loading values and ultimately stress are important variables, then so is the choice of load cell: too large a load cell can result in data being lost in the noise range, while too small a load cell may not be able to subject the strain sensor to the desired stress level. Only Lee et al. (2017) indicated the choice of the load cell (4.89N), suggesting they had considered the effects on their results [215].

Electrical measurements have been recorded using various types of equipment: multimeters [182, 211, 214, 215, 219, 221], potentiometers [188, 210], source meters [212], picoammeters [217], inductance capacitance resistance (LCR) meters [218], high resistivity meters [199, 216] and data acquisition (DAQ) boards [141]. None of the authors justified their choice for monitoring electrical output, but factors to consider include: the cost of the set-up, whether the electrical measurement tool can negatively influence the strain measurements, and of course the desired electrical response. This can be current, voltage, resistance or in some cases, capacitance. If considering a wearable system in the future, then a measurement tool that can accommodate this should also be taken into consideration. A more precise measurement system may not be appropriate if it is large and bulky.

To measure the electrical response, electrodes are required to be attached to the sensor. Depending on how this is done, this can create a point of localised failure. To overcome this, Yamada et al. (2011) used a combination of a conductive rubber paste made of single-walled carbon nanotubes (SWCNTs) and a polydimethylsiloxane (PDMS) rubber glue to fabricate stretchable electrodes [146].

4.2.1.2 Testing Protocols

There is no standardisation when it comes to developing strain sensor testing protocols; as a result, the amount of detail provided in the literature on the content and results of each protocol can vary. In an extreme case, two articles did not provide any detail on their protocols, besides what could be determined from the illustrative figures presented [213, 216].

In the reviewed literature, the primary variables that have been considered include strain rate,

amount of strain, and the number of strain cycles. The combination of these variables can help to ascertain the viscoelastic behaviour, durability and sensor response stability, useful for determining any future applications. Not all protocols featured cyclic strain, with some using a step increase in strain instead [182]. Another feature added to some protocols was a holding period at constant strain to determine drift, overshoot behaviour and response time [188, 210].

Strain sensors were subjected to maximum strain values as high as 1380% [210], and cyclic strain values up to 500% [188, 210], but in the case of Amjadi et al. (2015) this was only over the course of 10 cycles [210]. It was more common that strain cycles were applied under 100% strain [141, 211, 212, 218] and the importance here is choosing a degree of strain that is relevant to its use in joint monitoring for example.

Different strain rates were also trialled across the literature, however, the different units (%/s, mm/s and mm/min) make it difficult to compare results between papers. As previously mentioned, the viscoelastic behaviour of the polymer matrices will be influenced by the chosen strain rate, therefore considering a few different rates is of importance, especially when the final environment for use cannot be controlled. Zhao et al. (2013) utilised three different strain speeds to test their strain sensor to failure [199], while Ogasawara et al. (2011) utilised four different loading rates to compare the stress-strain response of their sensors containing different proportions of CNT (and a sample of the unimpregnated polymer matrix) for one load-unload cycle [220]. Fu et al. (2019) also used four strain rates to compare their strain sensors over one loading cycle [211]. Only Guo et al. (2016) chose to compare the response of their strain sensor over more than one cycle (but less than 10) and at different strain rates, noting that the change in resistance ($\Delta R/R_0$) was not affected by stretching speed [212]. Since resistive-based CPC strain sensors are more susceptible to hysteresis [152], different strain conditions should be considered over many cycles, rather than just one.

Finally, considering the number of strain cycles performed: tests of only 1, 5 or 10 strain cycles were common [199, 210, 215, 220], whilst at the other extreme, some tests consisted of over 10,000 cycles [141, 182, 214, 218]. In four studies, sensors were tested between 1000 to 2000 cycles of strain [182, 210–212]. Testing a sensor for over 10,000 cycles without a sign of failure demonstrates excellent durability and reliability for long-term monitoring. However, shorter tests up to 2000 cycles are still able to convey this, perhaps better relating to the end-use of the sensor, for example, a cyclist completing a 20-minute threshold test with a cadence of 90 rpm (1800 cycles), or a rower completing a 7-minute race at a stroke rate of 34 spm (238 cycles). Furthermore, the electrical response of a sensor is more likely to deteriorate over a prolonged test of 10,000 cycles, potentially increasing the complexity of calibration. Protocols must be relevant to the activity to be measured.

Protocols containing fewer than 10 strain cycles are not suitable for observing the change in resistance over a prolonged period, as observed by some authors. For example, Lipomi et al. (2011) observed that the resistance of the strain sensor decreased by 22% over the course of 1500 cycles [218],

which will otherwise not be observed in a short period of cycles. Different sensor structures will lead to different sensor responses, however, the choice of so few strain cycles needs to be justified, especially when the application in healthcare or sport will consist of repeated movements.

4.2.1.3 Key Metrics Reported

In considering the key metrics reported in the literature, the focus was narrowed down to the papers that tested their CPC strain sensors over at least 100 strain cycles. Metrics that were considered include the gauge factor (GF, the sensitivity of the senor response as defined in Equation 3.8), the ultimate tensile stress (UTS) or maximum strain, the sensor response over several cycles (such as stability and hysteresis), and the repeatability of the sensor output. A summary of this can be found in Table 4.1.

Only three studies reported the maximum strain withstood by the sensors [141, 210, 221], with the yield strain and UTS reported in another [214]. Instead, the most commonly reported metric in the studies in Table 4.1 was the GF which ranged from 0.54 to 64 [141]. These two extremes were measured on the same sensor, between different strain values, emphasising the importance of providing a strain range along with a GF value. For MWCNT/PDMS composites Fu et al. (2019) noted that the GF decreased with increasing weight percentage of MWCNT [211], while Wang et al. (2018) observed an increase in GF as the number of printing cycles also increased [221]. It was also noted by Fu et al. (2019) that even though a higher carbon content reduced the GF, it did improve the stability and linearity.

Four studies reported on the linearity of their sensor response with respect to the applied strain. The response observed by Fu et al. (2019) was not linear, especially above 25% strain [211]. Guo et al. (2016) observed linearity in the response up to 11% strain [212], while Amjadi et al. (2015) and Wang et al. (2018) went further to quantify the linearity of the responses, with $R^2 > 0.98$ [210, 221]. A linear sensor response will make the calibration process and deriving a relationship between the sensor response and joint angles much easier.

With regards to hysteresis, three studies reported minimal or negligible hysteresis [210, 214, 221], and one went further to quantify this with a hysteresis error index ranging between 9.3-30.4% over strain values up to 40% [211]. Although the 30.4% error at 20% strain is high, this was deemed comparable to results previously reported in the literature, where sensors made from a carbon black-PDMS composite and a silver nanowire-elastomer composite have errors of approximately 25% and 30% respectively at 10% strain [211].

Mechanical sensor failure was not discussed in any of the selected papers, however, the stability of the sensor response was, with this being another way of considering the lifetime of a strain sensor. In testing sensors for 1000 cycles, observations included an initial drop in resistance and then a further decrease over the course of cycling [211], while another showed good reliability over the same number

of cycles with little variation in the relative change in resistance, however this was not quantified [212]. A third reported an increase in resistance change after 650 cycles, with a 20% upwards drift in resistance change over 1000 cycles which is considered as "good durability for practical applications" [221]. A similar response was noted by Lipomi et al. (2011): over the course of 12500 strain cycles, the resistance decreased by 22% to a minimum value after 1500 cycles, before increasing linearly [218]. This response was observed across three similar experiments [218], however, it is unclear whether these were performed on the same sensor or different sensors. Variation is expected in the response of these strain sensors as a result of the materials used, this may make calibration more complex but it can be accounted for.

4.2.2 Effects of Temperature and Humidity (Environmental Considerations)

In addition to the mechanical and electrical performance under strain, one must consider or be aware of the effects of temperature and humidity when dealing with strain sensors. Laboratory environments are controlled, whilst other environments are not. This means that sensors can be subject to a range of temperatures; and humidity levels; and are susceptible to gas doping, where different compounds can be adsorbed within the structure. Applied to a sporting context, this can present as extreme temperature (e.g. snow sports); indirect contact with liquids (splashing in water sports); and sweat coming into contact with the sensor.

In terms of sensor performance, this will mainly impact the resistance of the sensor. When exposed to different temperature conditions, strain sensors may experience shrinkage or expansion that will be detected as a strain [146]. The relationship may or may not be linear and can be accounted for during sensor calibration. Furthermore, carbon nanotubes can be doped by gases on exposure, impacting their conductivity [146]. Of the selected references, only six, plus another that does not perform strain testing, consider temperature effects on sensor output [146, 209, 210, 214, 216, 219, 221]. These are detailed in Table 4.2.

The temperature coefficient of resistance (TCR) is a measure of the relative change in resistance per degree of temperature, represented mathematically as:

$$TCR = \frac{\Delta R}{R_0} \frac{1}{\Delta T} \tag{4.1}$$

Where ΔR is the change in resistance, R_0 is the initial resistance and ΔT is the change in temperature. Depending on the combination of materials, a temperature rise can lead to an increase in collisions between charge carriers and therefore an increase in resistance. On the other hand, in different materials the same rise in temperature can lead to the release of more charge carriers and reduce the overall resistance, a situation often found in semiconductors.

Of the studies listed in Table 4.2, there is an even split between sensors in which a positive TCR

Table 4.1: Summary of key metrics from cyclic strain sensor testing that has been reported in the literature.

Reference	Materials	Repeatability and Durability	Hysteresis and Linearity	Gauge Factor	Time properties	Max stress and strain
Amjadi et al. (2015) (Ultra) [210]	MWCNT/ Ecoflex	2000 cycles over 0-300% strain at rate 20%/s	$R^2 > 0.98$ for strain up to 100%	1.75	90% time constant 332 ms	Max strain 1380%
Fu et al. (2019) [211]	MWCNT/ PDMS (5, 7 and 9wt% MWCNT)	1000 cycles at 10% strain at 1mm/s	Hysteresis error index – 30.4% at 20%, 16.8% at 10% strain and 9.3% at 40% strain	15 (5wt% MWCNT), 5-9 (7wt% MWCNT), 1 (9wt% MWCNT)	-	-
Guo et al. (2016) [212]	CNT mesh (CNTM)/ PDMS	1000 cycles at 20% strain rate 2%/s	-	4	-	-
Kim et al. (2018) [214]	CNT/PDMS (1-12wt% CNT)	Cycling testing over 10,000 cycles – 4, 8 and 12wt% samples	-	-	-	UTS 7.89 ± 2.33 MPa and yield strain 81.84 ± 20.55% at 1wt% CNT
Lipomi et al. (2011) [218]	CNT/PDMS	12500 cycles at 25% strain	-	-	-	-
Ryu et al. (2015) [141]	CNT fibres/ Ecoflex	10000 cycles	-	Normal Ecoflex: 0.56 (0-200% strain), 47 (200-400% strain) Pre-strained Ecoflex: 0.54 (0-400% strain), 64 (400-960% strain)	Delay – 10 ms (loading), 12 ms (unloading), Recovery time – 12 ms	Max strain 960% (pre-strained Ecoflex)
Wang et al. (2018) [221]	MWCNT/ PDMS (10-50 CNT printing cycles)	45% strain over 1000 cycles – electrical	$R^2 > 0.98$ for all sensors	35.75 (50 printing cycles), 8 (10 printing cycles)	5s response time	Max strain – 45%

has been observed [209, 219, 221] and those where the TCR is negative [210, 214, 216], with the final study not specifying the direction of the resistance change [146]. Even for the same material combination (MWCNTs in a PDMS matrix), there was a difference in the sign attached to the TCR, suggesting that the microstructure of the sensor can also influence this value in addition to the material choice [216, 219]. This is confirmed by Kim et al. (2018) where it is stated that the shrinkage of the PDMS matrix brings the CNTs closer together [214]. Given this, it is important to understand the temperature-related properties of strain sensors being developed, one cannot rely on previously reported results in the literature. A useful indicator alongside the TCR is the relative change in resistance or change in absolute resistance of the strain sensor. A TCR value that leads to a small variation in resistance may not greatly impact sensor calibration when determining joint angles.

Studying the information provided in Table 4.2 further, as well as the difference in reported TCR values, there is also a variation in testing protocols with no standard method being used. Kim et al. (2018) used a hot plate to observe the change in resistance (but did not go on to state a TCR value) [214], while three studies reported the use of an oven or temperature chamber [209, 210, 219]. A concealed chamber is ideal, as it ensures that the sensor is heated to the required temperature and heat is not escaping as it would in an open environment on a hot plate. However, this may be more difficult and expensive to obtain; a hot plate in conjunction with a temperature gauge that directly measures the temperature of the strain sensor can be a cheaper alternative and means that investigators do not need to rely on the temperature reading of the hot plate alone.

The detail provided in the literature is minimal, in most cases, temperature testing was in addition to mechanical testing that formed the main part of a study. For example, the variation in heating ranges, when reported, ranged from 24-42 °C [214] to 33-373 K [209], with the latter range being chosen as this is where MWCNTs show thermal expansion. Any testing range should cover at least the working range of the strain sensor if the equipment can allow it. Prolonged exposure to high temperatures is also a useful indicator of the structural integrity of the sensor.

A consistent element across these studies is a lack of measuring the temperature response of a sensor under strain, however, it is understood that there is some difficulty here in terms of equipment set up to carry this out. This type of testing could indicate whether the linearity of the sensor response changes with temperature and if the range of the measured resistance also changes as a result of temperature. This is certainly a limitation of these studies and a factor that should be considered in the future.

Temperature is not the only environmental factor that is cause for consideration, as highlighted by Yamada et al. (2011) who observe that gases have the ability to dope CNTs and change their conductivity as a result [146]. In this paper, the authors considered the effect of exhaled breath on the resistance of the sensor, reporting a change of approximately 0.6% which in this case was equivalent to 2% strain [146]. Furthermore, Lee et al. (2013) considered the effects of soaking a strain sensor in 1X phosphate-buffered saline (PBS) where a reduction of resistance was observed, due to conductive

Table 4.2: Details of temperature and humidity testing performed on different carbon nanotube/polymer composite strain sensors.

Reference	Sensor composition	Equipment	Temperature testing range	TCR	Resistance observations
Alamusi et al. (2013) [209]	MWCNT/ epoxy (1, 3 and 5wt% MWCNT)	Temperature chamber and LCR meter	33-373K at 1K/min	0.021/K (5wt% MWCNT sensor)	Non-linear increase with temperature. Values stable with slow heat cycling at 1K/min
Amjadi et al. (2015) (Ultra) [210]	MWCNT/ Ecoflex	Convection oven	35-80°C	0.33%/K	Decreases linearly with temperature ($R^2 = 1$)
Kim et al. (2018) [214]	CNT/PDMS (1 – 12wt% CNT)	Hot plate	24-42°C thermal cycles	N/A	Decreases with temperature and subsequent heat cycles
Lee et al. (2013) [216]	MWCNT/ PDMS	-	30-80°C (10°C intervals), constant current (10 μA)	-0.014/°C (5wt% MWCNT) to -0.012/°C (12.5wt% MWCNT)	-
Lu et al. (2007) [219]	MWCNT/ PDMS (4-25wt% MWCNT)	Convection oven, sensor	RT to 80°C (10°C intervals)	$<$ 0.005/°C	-
Wang et al. (2018) [221]	MWCNT/ PDMS (10-50 CNT printing cycles)	-	-	-	Sharply increases from room temperature to 50°C, minimal change at higher temperatures
Yamada et al. (2011) [146]	SWCNT/PDMS	-	RT to 50°C	-	Relative change in resistance of 6%f

ions entering the sensor [216].

A coating can be a way to overcome the effects of gases or solvents on the strain sensors and CNTs in particular, but not necessarily the effects of temperature. If a coating is employed, the mechanical and temperature responses of the combined system must be considered.

4.2.3 Summary

From reviewing the literature around the characterisation of resistive carbon nanotube-polymer composite strain sensors, it is understood that there is not a standard protocol that is used. This does suggest that protocols should be developed based on the intended use of a sensor, however, past authors did not justify their choice of strain rate, strain range or number of strain cycles (which ranged from just one strain cycle to over 10,000).

Across the literature, sensor performance is defined with respect to the sensor response and not its structural integrity, with key metrics reported including the gauge factor, hysteresis and linearity. These are especially relevant as resistive-based strain sensors are more subject to hysteretic behaviour. The quantification of these metrics can aid with comparing the properties of different strain sensors available and with their calibration, however, it is important to understand the conditions under which they were obtained. The lack of quantified metrics or protocol standards makes it difficult to compare results within the literature.

Aside from the choice of testing equipment that may have introduced some limitations, a significant limitation of the reported methods is the lack of repeated testing of the strain sensors developed. In this project, repeated testing on the same strain sensor has been at the centre of the protocols developed to determine its suitability for multiple uses.

4.3 Mechanical Testing

4.3.1 Intoduction

To assess the mechanical and electrical properties of all strain sensors, a mechanical testing system was used to programme and run different cyclic testing protocols. The strain rate and the number of strain cycles were varied to recreate to an extent the varying session lengths and stroke rates or cadences completed by rowers and cyclists respectively. The total number of strain cycles would be equal to the number of completed rowing strokes or pedal revolutions as given by the following equations:

$$number\ of\ strokes = stroke\ rate\ (strokes\ per\ min) \times session\ duration\ (min) \tag{4.2}$$

$$number\ of\ pedal\ revolutions = cadence\ (revolutions\ per\ min) \times session\ duration\ (min) \quad (4.3)$$

For example, in rowing a steady state session lasting 60 minutes at a stroke rate of 18 s/m, the total number of strokes is 1080, while a higher-intensity interval that is 10 minutes long at a stroke rate of 28 s/m consists of 280 strokes. On the bike, a threshold test lasting for 30 minutes at a cadence of 90 rpm consists of 2700 pedal revolutions.

Two protocols were devised: the first, a longer protocol of fifteen tests where both strain rate and the number of cycles were varied and the second, a shorter protocol of nine tests where only strain rate was varied. Both protocols used the same Instron set-up, data processing and statistical analysis steps. Strain sensors were labelled numerically with the prefix S: S1, S2 and so on.

4.3.2 Materials and Methods

4.3.2.1 Equipment Set-Up

An Instron 5866 testing system (Instron, Norwood, Massachusetts, USA) was used to carry out cycling testing, in conjunction with the Bluehill testing software (Instron, Norwood, Massachusetts, USA). Due to the period of time between carrying out tests and the equipment available, the Instron was initially set up with a 50 N load cell (S1-S5) and then a 10 kN load cell (S6 onwards). The Bluehill software was also updated within this time, moving from Bluehill 3 (S1-5) to Bluehill Universal (S6 onwards). Each sensor tested measured 110 mm x 12 mm x 1 mm. Electrodes were placed at a separation distance of 70 mm and the gauge length (distance between Instron grips) was set to 80 mm. The electrodes allowed the electrical resistance of the sensor to be measured as a voltage output using an external circuit.

The maximum extension applied during mechanical testing was identified experimentally by measuring the displacement of the sensor during maximum knee flexion for one test subject. A fabricated strain sensor was placed across the anterior aspect of the knee at full extension in the longitudinal axis. With both ends of the sensor secured, the knee was fully flexed. The original and extended lengths of the sensor were both measured and from this, the strain was calculated to be 16%. A 16% increase in strain (from the gauge length of 80 mm) was calculated as a displacement of 12.8 mm.

At the start of each testing session, the load cell was calibrated and the distance between the grips was set to 80 mm, before zeroing the load and extension values. Physical limits were set on the machine along the scale to protect the machine (preventing the grips from coming into contact with each other). The sensor was then placed between the grips. The Instron set-up and electrode positioning are shown in Figure 4.1.

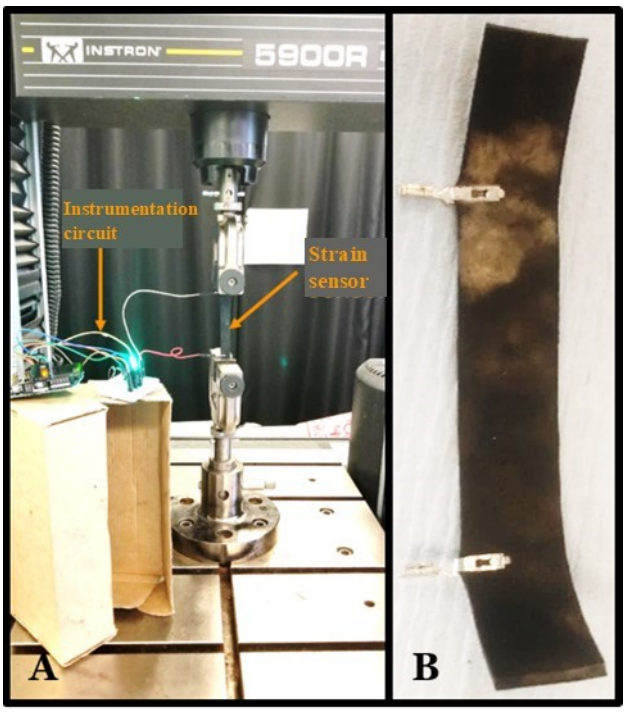


Figure 4.1: A) Set up of Instron testing, with the sensor placed between grips and connected to an external instrumentation circuit and B) close-up of the sensor with connective attachments.

4.3.2.2 Data Collection

Extension and load data were collected at a sampling frequency of 100 Hz and were exported from the Bluehill testing software in comma separated variable (CSV) format. In conjunction with the extension and load measured by the Instron machine, the electrical output of the sensor was measured. An external instrumentation circuit (voltage divider set up on an Arduino microcontroller, 10-bit ADC, +3.3 V supply pins, programmed using Arduino IDE 1.8.5, with resistors on the breadboard, 0.6 mA current) was used to measure the voltage output of the sensor (the circuit also had a sampling frequency of 100 Hz, later increased to 200 Hz for sensors S6 and onwards, and contained a 1 kΩ resistor). The output was recorded using Realterm: Serial Capture Program (2.0.0.70, Baud rate: 115200) on a laptop.

4.3.2.3 Testing Protocols

Each test followed the same structure: a 10-second hold period at rest, followed by a pre-determined number of tensile extension cycles (100, 200, 500 and 1000) up to 12.8 mm displacement at a pre-determined rate (50 mm/min, 100 mm/min and 350 mm/min) to replicate different speeds in a sporting environment, followed by a ramp to the maximum extension used during the cyclic testing portion, where the sensor was held for 5 minutes before being returned to its original length (of 80 mm) by the testing machine. A schematic of the testing profile is shown in Figure 4.2.

The first protocol developed consisted of 15 cyclic tests, from 100 to 1000 cycles, all performed on the same sensor in order of decreasing strain rate listed in Table 4.3. All tests for the second protocol

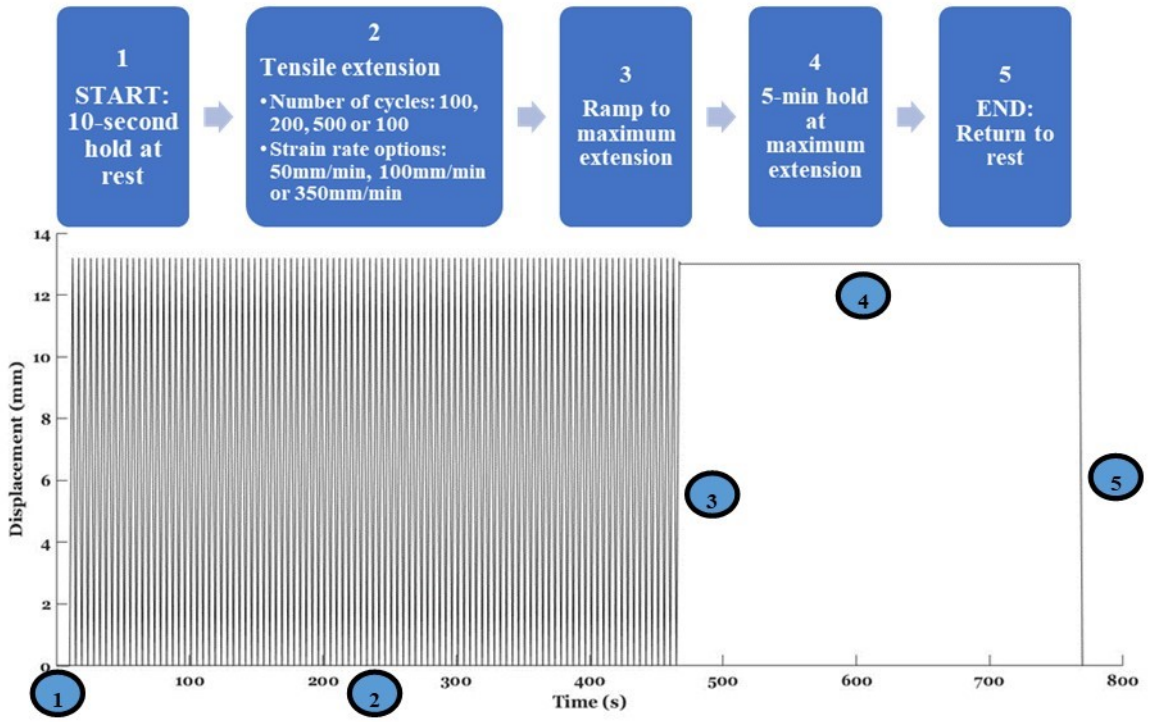


Figure 4.2: Schematic of the testing profile, the sensor is held at rest for 10 seconds, followed by 100 cycles between 0-12.8mm displacement at a strain rate of 350 mm/min, ending with a hold at the maximum displacement for a period before being allowed to rest.

developed were of 100 strain cycles, with three tests carried out at each of the three strain rates in a randomised order. An example of this is listed in Table 4.4.

Table 4.3: Testing order for Protocol 1, indicating the number of cycles and strain rates for each test carried out.

Test number	Number of cycles	Strain rate (mm/min)
1-5	100	350
6	200	350
7	500	350
8	1000	350
9	100	100
10	200	100
11	500	100
12	1000	100
13	100	100
14	200	100
15	500	100

For each test, the Instron protocol was started alongside a stopwatch. When the stopwatch reached ten seconds, the Realterm software was also started to record the voltage output. At least five minutes were allowed between each test being carried out. For Protocol 1, tests on each sensor were carried out over multiple days, while for Protocol 2 this all took place on one day. All tests were carried out at room temperature.

Table 4.4: Example of randomised testing order for Protocol 2.

Test number	Number of cycles	Strain rate (mm/min)
1	100	350
2	100	50
3	100	350
4	100	100
5	100	100
6	100	50
7	100	350
8	100	100
9	100	50

4.3.3 Data Processing

The resistance of the sensor can be calculated using the following relationship for voltage dividers:

$$V_{out} = V_{in}(\frac{R_{pd}}{R_s + R_{pd}}) \tag{4.4}$$

Where R_s is the resistance of the sensor, R_{pd} is the value of the pull-down resistor in the circuit, V_{in} is the voltage supply to the sensor, and V_{out} is the measured voltage.

From this, the resistance of the circuit, R_{pd}, can be optimised for the available voltage range using the following equation:

$$R_{pd} = \sqrt{(R_s^{max} R_s^{min})} \tag{4.5}$$

What Equation 4.4 tells us is that when V_{out} is at its maximum, the resistance of the sensor, R_s is at a minimum, so there is an inverse relationship between the voltage being measured and the resistance of the sensor. Rearranging the equation allows us to calculate R_s:

$$R_s = \frac{R_{pd}(1 - \frac{V_{out}}{V_{in}})}{\frac{V_{out}}{V_{in}}} \tag{4.6}$$

In MATLAB (Mathworks, Natick, Massachusetts), the voltage data collected from the sensor was initially filtered using a Hampel filter to remove any outliers (sharp spikes in the signal), before using a 4th-order zero-lag Butterworth Filter to smooth the voltage signal. A discrete-time Fourier transform (DTFT) was performed on three tests covering the different strain rates from four sensors (a total of 12 tests). Single-sided amplitude spectra were produced (see Figures 4.3 and 4.4), split by the sampling frequency.

Both spectra suggest a high cut-off frequency of 20 Hz due to the high strain rate tests, however in practice, a lower cut-off frequency produced a better signal without losing features from the original signal, as observed in Figures 4.5 and 4.6. A cut-off frequency of 10 Hz was therefore used with the Butterworth filter.

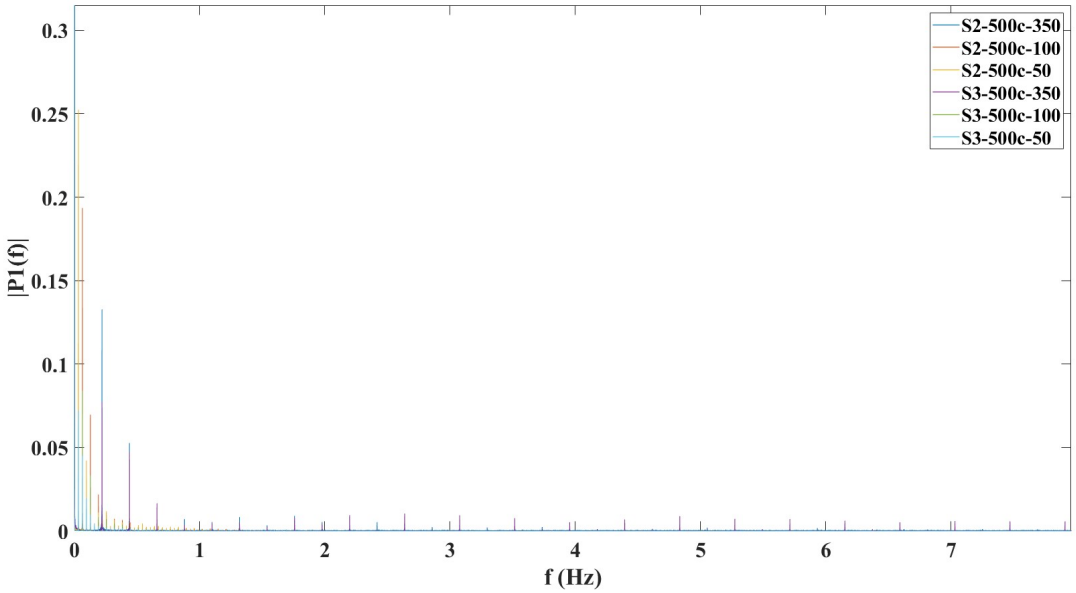


Figure 4.3: Noise extraction for raw sensor data from sensors S2 and S3, sampling frequency of 100 Hz.

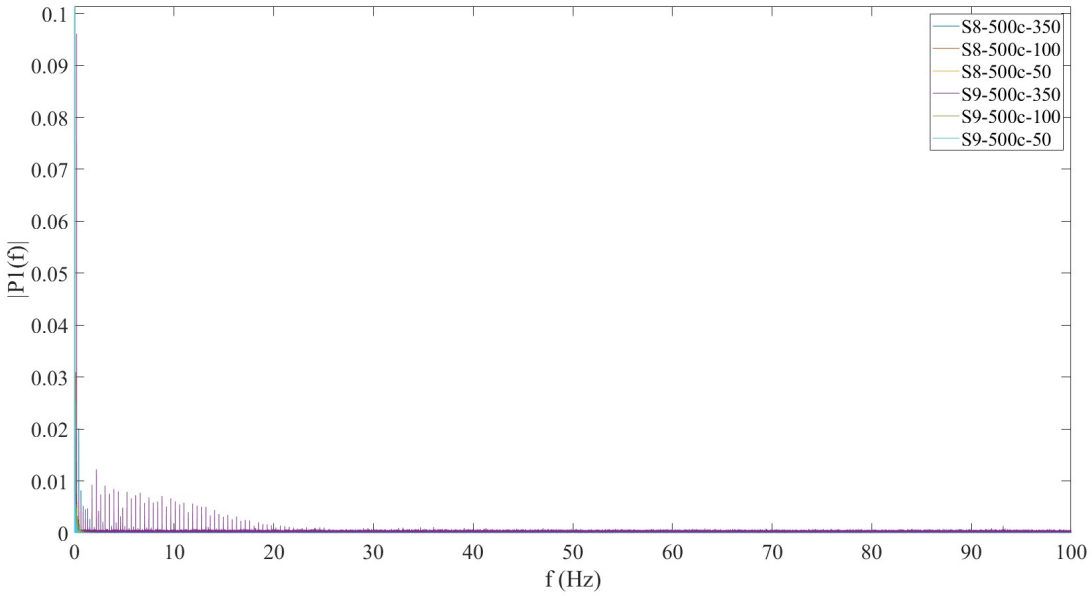


Figure 4.4: Noise extraction for raw sensor data from sensors S8 and S9, sampling frequency of 200 Hz.

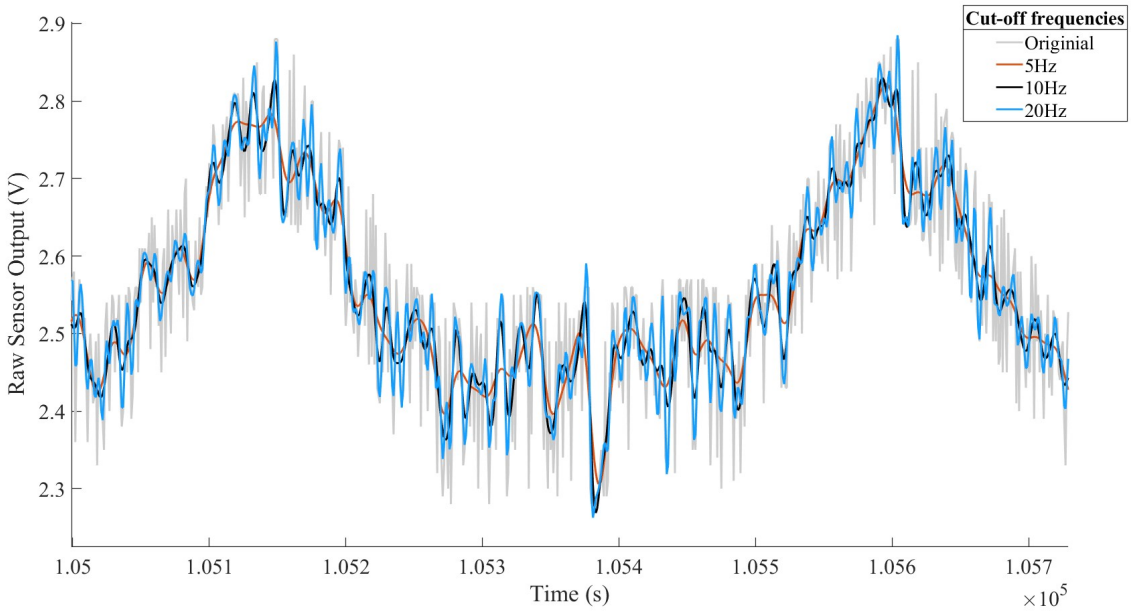


Figure 4.5: Raw and filtered sensor response for sensor S2 with different cut-off frequencies (5, 10 and 20 Hz).

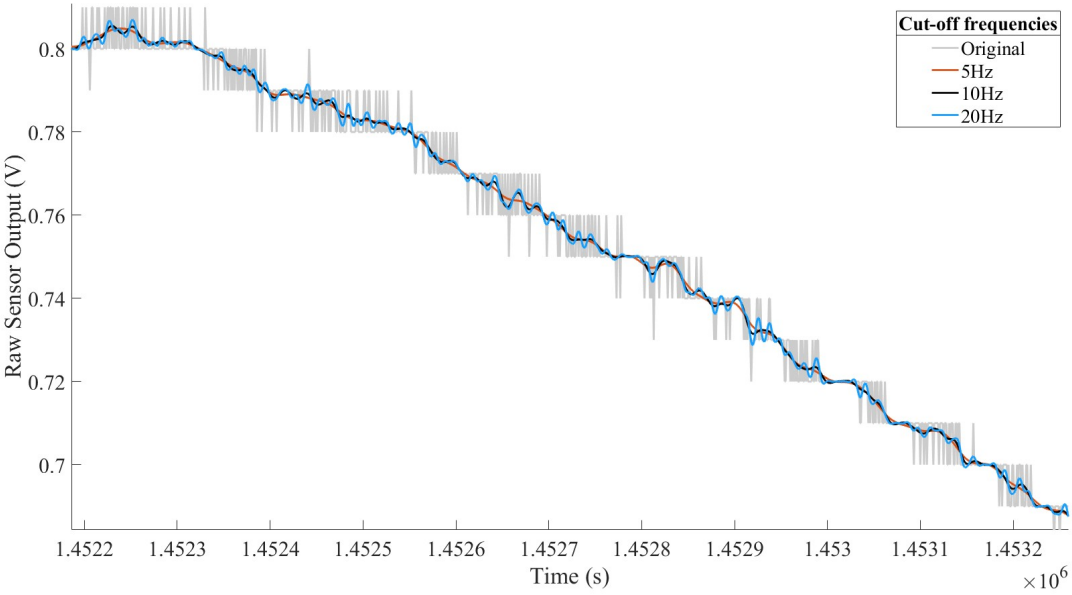


Figure 4.6: Raw and filtered sensor response for sensor S8 with different cut-off frequencies (5, 10 and 20 Hz).

Following filtering, data extraction was performed. Equation 4.6 was used to calculate the sensor resistance from the voltage output collected during testing. A custom MATLAB script was then used to extract the maximum and minimum values from each strain cycle and calculate the resistance range.

Data sets collected from each test contained many values, therefore the decision was taken to extract data from five cycles in every 20 cycles as a representation, up until the holding point in the strain test. The range of the voltage output was calculated for each of the extracted strain cycles, reducing each data set to the lengths seen in Table 4.5. Custom MATLAB scripts were used to perform this extraction and calculate each cycle range. Some incomplete data sets arose from errors in the testing procedure. Custom MATLAB scripts were also used to extract the sensor response during the hold portion of each test.

Table 4.5: Number of values extracted from raw datasets.

Test length (no. cycles)	Extracted data (number of values)
100	6 × 5 cycles (30)
200	11 × 5 cycles (55)
500	26 × 5 cycles (130)
1000	51 × 5 cycles (255)

4.3.4 Statistical Analysis

Statistical analysis was carried out using SPSS (IBM SPSS Statistics Version 25; IBM Corporation, Armonk, New York, United States).

4.3.4.1 Intra-test variability

To determine the consistency of the sensor signal during one cyclical strain test, each set of 5-cycle extracts were compared to each other – six sets for 100 cycle tests, 11 sets for 200 cycle tests and so on (see Table 4.5).

Data normality was verified with the Shapiro-Wilk Test (due to small sample sizes). Repeated Measures ANOVA (a test for repeated measures on the same sample for parametric data) was used to compare the means across the 5-cycle extracts within the same test (significance level = 0.05). Post-hoc analysis was conducted using the Bonferroni Test if significant differences were found.

4.3.4.2 Inter-test variability

Tests of the same cycle length carried out on the same sensor were compared (again using the 5-cycle extracts) to determine inter-test variability. Data normality was again verified with the Shapiro-Wilk Test. The Friedman test (a test repeated measures test on the same sample for non-parametric data) was used if the majority of the variables were not normal, followed by the Wilcoxon signed-rank test for post hoc analysis.

4.4 Protocol 1

Data were collected from ten sensors (labelled S1-S10) which were subject to a series of cyclic strain tests, following the protocol displayed in Table 4.3. The cyclical protocol allowed the determination of several performance parameters. The primary focus of the testing was to determine the repeatability and durability of the sensors, but other parameters determined include sensitivity (measured by the gauge factor), hysteresis, linearity and drift.

4.4.1 Repeatability and Durability

Above all, the repeatability of sensor output and its durability are important considerations in a sporting application, where the sensor is subject to numerous strain cycles. Not only should the output of a sensor be consistent within a test, but ideally it should also be consistent across tests to make calibration easier.

4.4.1.1 Results

Tests were carried out on strain sensors at three different strain rates: 350 mm/min, 100 mm/min and 50 mm/min. Plots of the sensor output in response to these different rates over 100 cycles are displayed in Figure 4.7.

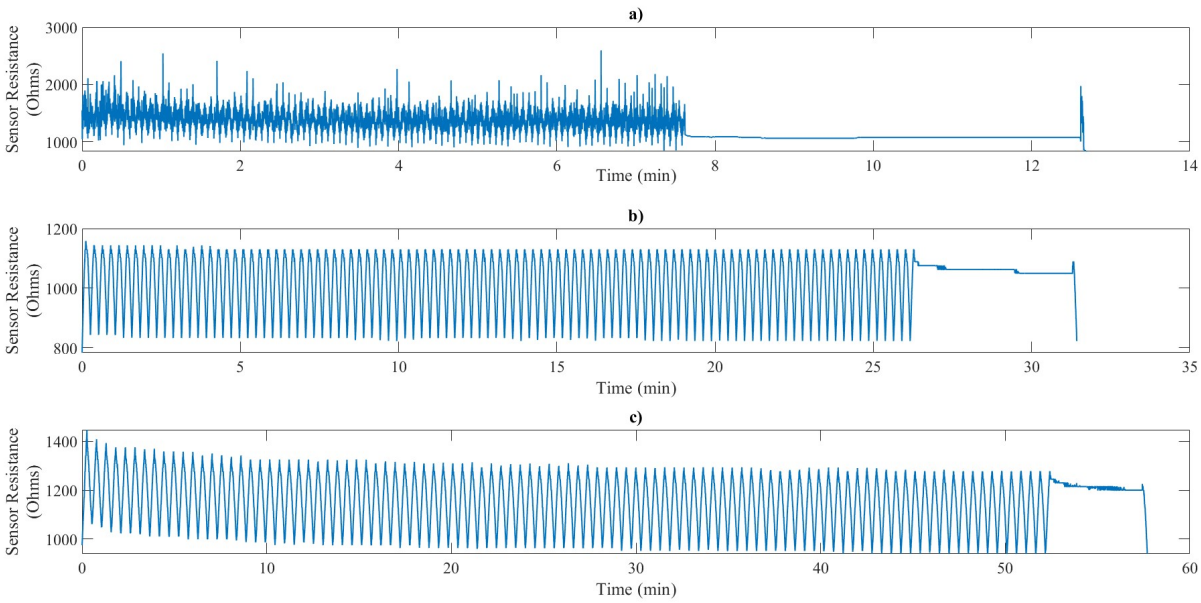


Figure 4.7: Sensor response for 100-cycle tests on the same sensor (S10) carried out at different strain rates a) 350 mm/min, b) 100 mm/min c) 50 mm/min.

At the lowest strain rate of 50 mm/min, the sensor undergoes preconditioning with the maximum and minimum resistance values decreasing together significantly over the first 20 minutes of testing, with a smaller decrease over the next 10 minutes. Visually the range looks to remain steady throughout the cyclic portion of testing. The sensor output at 100 mm/min is the most consistent with the

maximum and minimum values remaining unchanged, while the output at 350 mm/min is much more variable and less predictable than the lower strain rates. At the highest strain rate also, the sensor resistance during the hold period is much more comparable to the minimum values during the cyclic testing when the sensor does not have any load applied to it. For loading at the slower strain rates, the sensor resistance during the hold period is closer to the maximum resistance during the cyclic testing.

4.4.1.1.1 Intra-test variability

Intra-test variability was explored to compare the range of each sensor's resistance response, overcoming the fact that the absolute values change with each subsequent test. The 5-cycle extracted data are used to compare the change in resistance range over the course of one test.

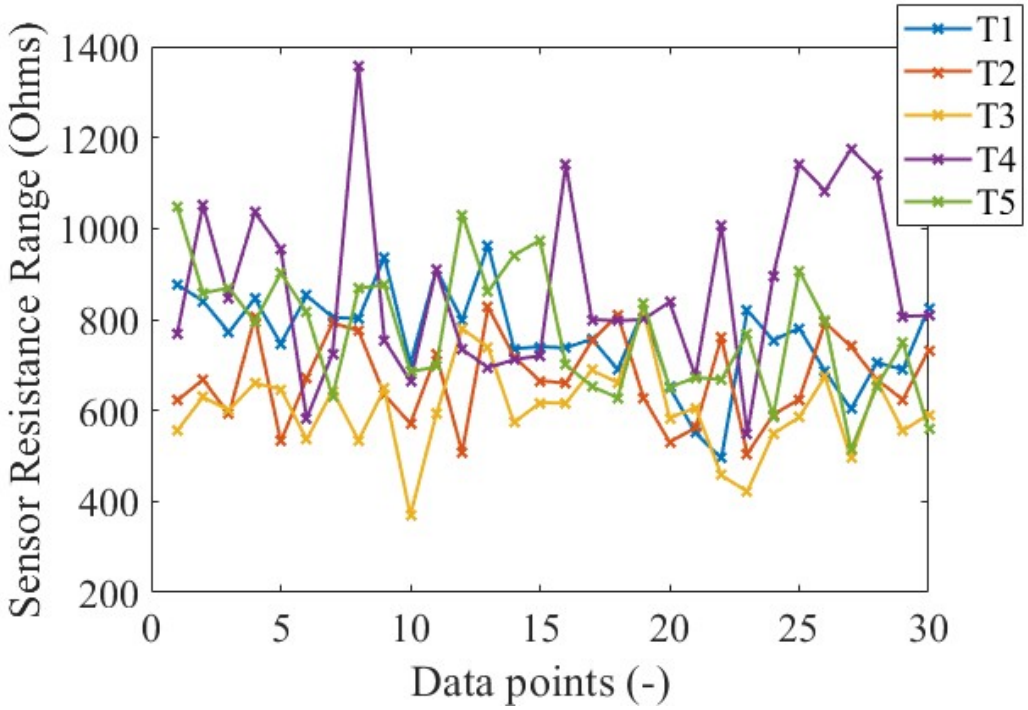


Figure 4.8: Change in output range over the course of a 100-cycle test repeats at 350 mm/min strain rate on the same sensor (S10).

Figure 4.8 compares five tests of 100 cycles at 350 mm/min carried out on the same sensor. T4 is the most variable in its resistance range (almost 800 Ω), however, the average cycle range of the other tests falls between 500 Ω to 1000 Ω. The resistance range does not trend positively or negatively for any of the short, high-speed tests on this sensor.

Figure 4.9 provides a visual representation of the average resistance range of five strain cycles at regular intervals throughout all the tests carried out on sensor S10. Observations can be made on the change in resistance range over one test and comparisons can be made between tests of the same number of cycles but at different speeds. For tests at all cycle lengths, the high-speed tests at a strain rate of 350 mm/min are the most erratic in terms of the resistance range calculated, with values

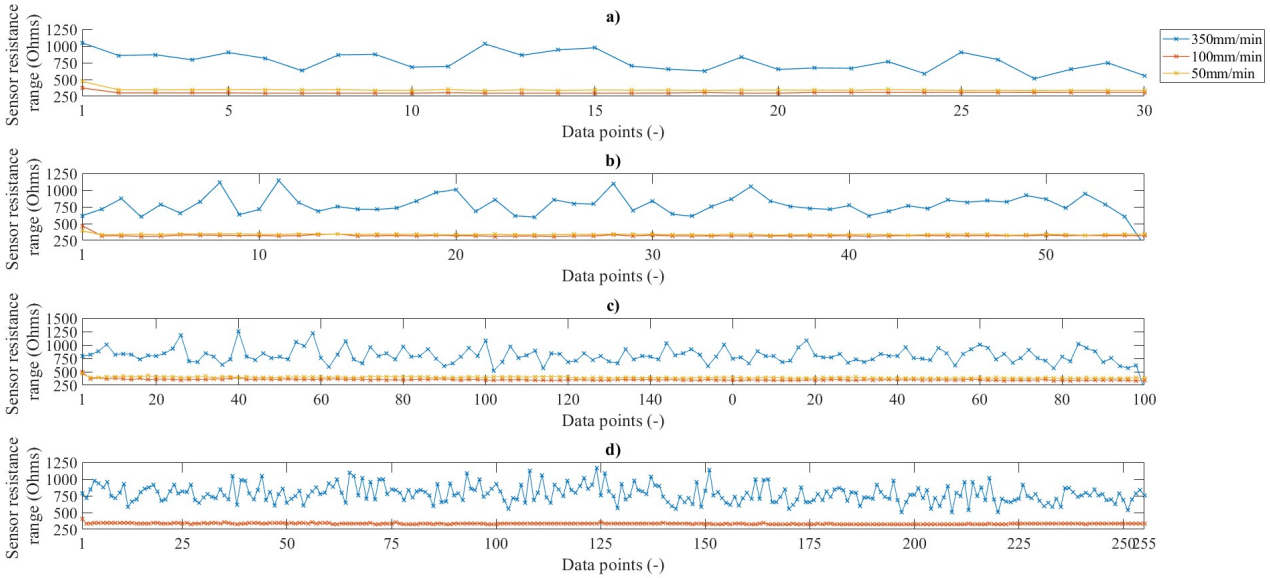


Figure 4.9: Change in output range as a function of strain rate over differing cycle-length tests on sensor S10 at a) 100 cycles, b) 200 cycles, c) 500 cycles and d) 1000 cycles.

between 500-1000 Ω. Tests conducted at 100 mm/min and 50 mm/min are much more consistent at all test lengths with regards to sensor resistance range – similarity is seen both between the two strain rates and the different numbers of cycles applied, with the range just below 500 Ω.

The previous figures summarised results from one sensor (S10). The following statistical results give an overview of the performance of all sensors tested. Intra-test variability, the variability of the range of the sensor resistance during a cyclic test, was determined using statistical tests and based on the 5-cycle extracted data (significance level, $\alpha = 0.05$). The p-values are detailed in Table 4.6.

Table 4.6: Greenhouse-Geisser p-values associated with sensor intra-test variability. Significant values have been highlighted in red.

Test	S1	Test	S2	S3	S4	S5	S6	S7	S8	S9	S10
100c_350_1	0.01	100c_ 350_1	0.003	0.214	0.026	0.433	0.355	0.294	0.144	0.236	0.147
200c_350	0	100c_350_2	0	0.299	0.019	0	0.44	0.176	0.47	0.526	0.569
500c_350	0.002	100c_350_3	0.482	0.557	0.31	0.051	0.116	0.221	0.117	0.213	0.141
100c_50	0.008	100c_350_4	0.012	0.096	0.162	0.268	0.345	0.506	0.359	0.404	0.481
100c_100	0.367	100c_350_5	0.405	0.035	0.255	0.003	0.047	0.18	0.032	0.712	0.057
100c_350_2	0.478	200c_350	0.037	0.015	0.07	0	0.467	0.387	0.327	0.323	0.481
100c_350_3	0.072	500c_350	0.13	0.128	0	0	0.629	0.132	0.056	0.33	0.3
200c_50	0	1000c_350	0.168	0.002	0	0	0.186	0.085	0.166	0.242	0.206
1000c_350	0.006	100c_100	0.268	0.207	0.349	0.05	0.43	0.035	0.158	0.35	0.303
200c_100	0	200c_100	0.266	0.001	0	0.201	0.289	0.218	0.096	0.24	0.443
1000c_100	0	500c_100	0.002	0	0.002	N/A	0.027	0.088	0.042	0.088	0.066
100c_350_4	0	1000c_100	0.204	0	0	N/A	N/A	0.026	0.004	0.017	0.018
500c_100	0.006	100c_50	0	0.047	N/A	N/A	0.157	0.344	0.354	0.255	0.265
100c_350_5	0.236	200c_50	0.001	0.024	N/A	N/A	0.129	0.401	0.232	0.443	0.292
		500c_50	0	0	N/A	N/A	0.032	0.142	0.003	0	0.014

Notation for tests: 100c_350_1 where 100c = 100 cycles, 350 = strain rate of 350 mm/min, 1 = test 1

Over 60% of tests (88 out of 140) reported non-significant p-values, suggesting that the resistance range was consistent over the course of a test. The majority of significant p-values occur for sensors

S1-S5 (39 out of 52) compared to sensors S6-S10 (13 out of 52) which were fabricated from a new batch of rubber bands. The sensors performed best over short cycles (100 and 200) but each sensor responded differently to testing. Sensor S2 showed a consistent response at both 1000-cycle tests at 50 mm/min and 100 mm/min strain rates. Due to the early failure of sensors S4 and S5, statistical analysis could not be carried out for all tests.

4.4.1.1.2 Inter-test variability

Sensor resistance ranges between tests on the same sensor were also compared, calculating the mean and standard deviation for each test. The percent deviation provided another measure of the variation of the resistance across a test. These values are listed in Table 4.7 for sensor S10. The percent deviation is highest for tests conducted at 350 mm/min (22.42% for a 100-cycle test) and lowest for tests at the slower strain rates (2.72-6.98% for tests at 50 mm/min).

Table 4.7: Mean of the sensor resistance range, standard deviation and percent deviation for sensor S10.

	Resistance Range (Ω)		
Test	Mean	Standard deviation	Percent deviation (%)
100 cycles at 350 mm/min, test 1	763.26	105.53	13.83
100 cycles at 350 mm/min, test 2	669.39	96.30	14.39
100 cycles at 350 mm/min, test 3	603.05	95.56	15.85
100 cycles at 350 mm/min, test 4	871.58	195.39	22.42
100 cycles at 350 mm/min, test 5	773.24	140.21	18.13
200 cycles at 350 mm/min	775.25	155.45	20.05
500 cycles at 350 mm/min	799.57	144.16	18.03
1000 cycles at 350 mm/min	780.61	129.64	16.61
100c cycles at 100 mm/min	304.30	13.98	4.59
200c cycles at 100 mm/min	323.31	21.06	6.51
500 cycles at 100 mm/min	353.38	16.12	4.56
1000 cycles at 100 mm/min	333.51	8.50	2.55
100 cycles at 50 mm/min	346.42	24.18	6.98
200 cycles at 50 mm/min	339.63	9.24	2.72
500 cycles at 50 mm/min	394.71	12.00	3.04

The values in Table 4.7 were used to plot Figures 4.10 and 4.11, with the former taking into account the sensor resistance range at differing strain rates and number of cycles, whilst the latter focuses on only the tests over 100 cycles. These figures formed the basis of the inter-test statistics that were then performed. Tests are grouped by cycle length in Figure 4.10 which does not take the testing order into account. The test of 200 cycles at 350 mm/min appears to be an outlier, with other grouped tests having mean resistance ranges within 100 Ω of each other. In Figure 4.11 the mean resistance ranges of Tests 2-4 at 350 mm/min differ the most from the other 100-cycle tests.

Table 4.8 details the results of the inter-test variability statistics and post-hoc analysis. The signficance level ($\alpha = 0.05$) was adjusted based on the Bonferroni correction for each set of tests (divided by the number of comparisons). Tests were grouped by the number of cycles and no similarity

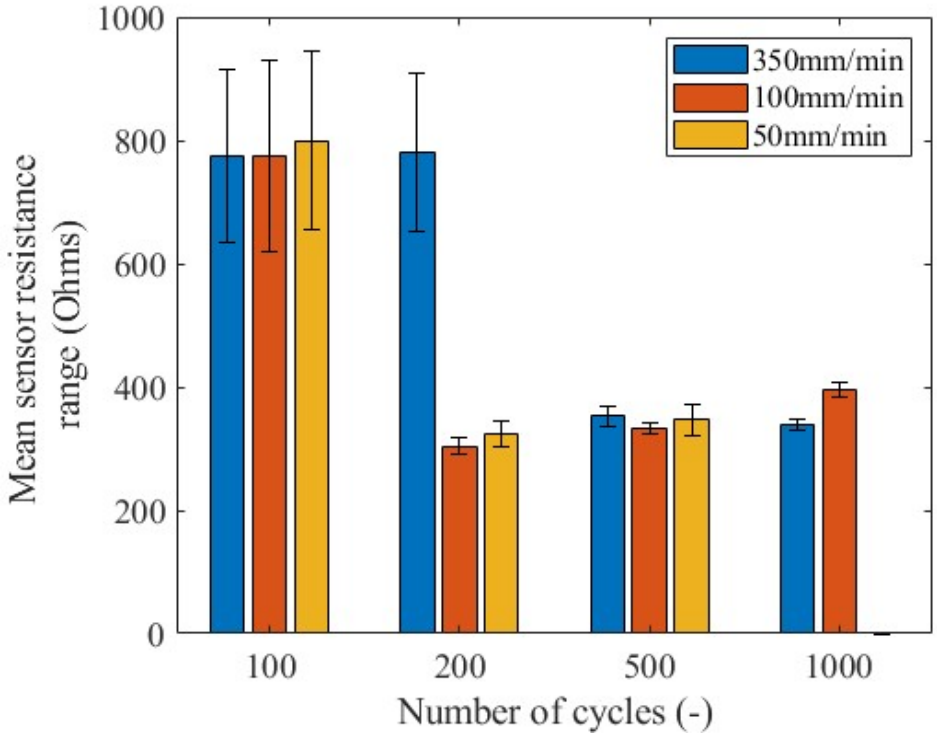


Figure 4.10: Mean sensor output range at different strain rates, grouped by the number of testing cycles.

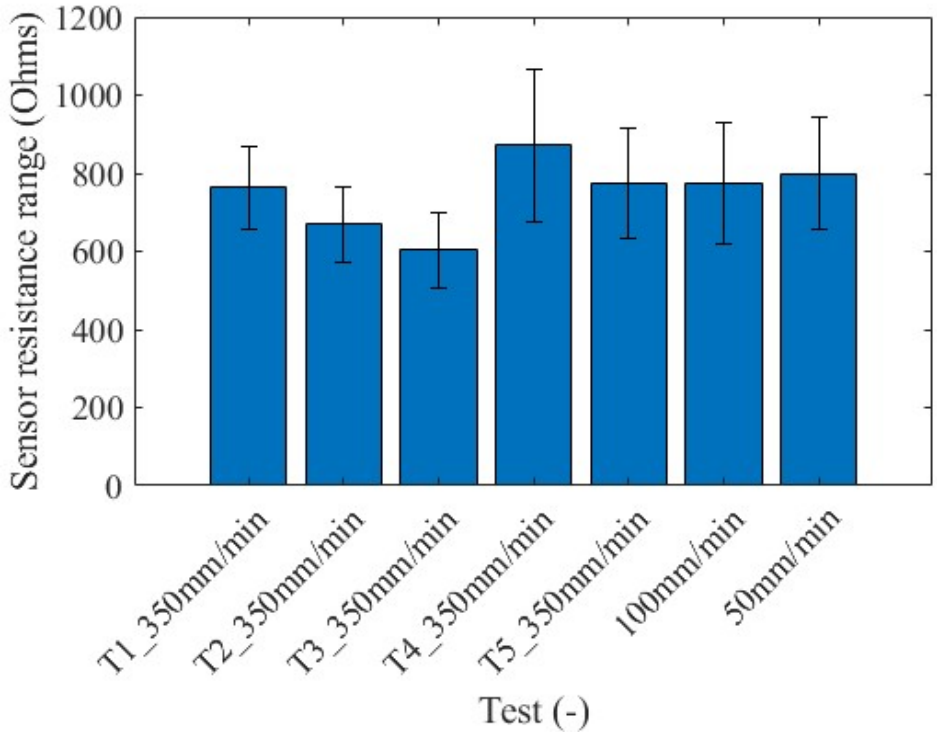


Figure 4.11: Mean sensor output range of tests over 100 cycles at different strain rates.

was seen at a group level on the overall mean resistance range of a sensor. Post-hoc analysis indicated similarity in the overall mean resistance range for tests over 100 cycles at 350 mm/min. Inter-test variability statistics for sensors S1-S9 are listed in Appendix B.

Table 4.8: Inter-test variability results from comparisons between tests of the same cycle length on sensor S10 (including post-hoc analysis). Significant values have been highlighted in red. The test number within Protocol 1 has been used to distinguish between comparisons.

	100 cycles	200 cycles	500 cycles	1000 cycles
No. tests	7	3	3	2
No. comparisons	21	3	3	1
Stats test	Friedman	Friedman	Friedman	Wilcoxon
p-value	0	0	0	0
Post-hoc	Wilcoxon	Wilcoxon	Wilcoxon	-
Adjusted α	0.002	0.017	0.017	-
p-value	(1,4)=0.041, (1,5)=0.688, (2,3)=0.004, (2,5)=0.008, (4,5)=0.063	-	-	-
	(1,2)=0.001, rest=0	All comparisons =0	All comparisons =0	-

4.4.1.2 Discussion

The cyclic testing on the fabricated stain sensors was used to determine the repeatability of the sensor response, by using three different strain rates and four test durations, aiming to replicate conditions during use in a sporting environment.

First considering the behaviour of a strain sensor over 100 cycles at different strain rates, it is clear from Figure 4.7 that the strain rate has an influence on the measured resistance - it becomes more variable as the strain rate increases. This time-dependent strain response is a feature that can be attributed to the viscoelastic behaviour of the rubber matrix. This is also confirmed in Figure 4.9, where the same behaviour is seen as the number of strain cycles increases from 100 to 1000, and in Table 4.7 where the percent deviation is higher for tests conducted at 350 mm/min (13.83-22.42%) compared to tests at 100 mm/min (2.55-6.51% deviation) and 50 mm/min (2.72-6.98% deviation). At the higher strain rates, the CNTs that are responsible for transferring electrical charge are constantly in motion – there is no time for the sensor to relax when the strain is removed and then applied again, leading to this erratic response. Continuing to explore what is happening at a microscopic level, as strain is repeatedly applied to the sensor, the orientation of the CNTs is such that they become more aligned. This leads to increased contact points and makes it easier for a charge to be transferred, leading to a lower resistance and the absolute values decreasing over time as shown at a strain rate of 50 mm/min. Considering the practical application of these sensors, the percent deviation in the resistance range is in line with what is considered as suitable durability by Wang et al. (2018), where

the sensor resistance drifted by 20% over 1000 cycles [221].

It can be observed that the sensor resistance range, maximum and minimum values are not the same for the three strain rates tested and presented in Figure 4.7, with these numbers decreasing as the strain rate reduces from 350 mm/min to 100 mm/min, but then increasing as the strain rate is reduced further to 50 mm/min. This behaviour is not due to the strain rate, but due to the testing protocol and the change in the sensor properties over time, with the three tests not carried out back-to-back (see Table 4.3 for testing order). The lower resistance observed at 100 mm/min can be explained by the microstructural changes discussed earlier. However, the resistance increasing again cannot be explained by this phenomenon. The sensors tested did not have a coating, and so over time there would have been a loss of CNTs certainly from the surface due to handling. Although the CNTs in the sensor bulk would have been mostly responsible for the charge transfer, any loss of CNTs will reduce the number of conductive pathways and therefore increase the resistance, as has happened for the test at 50 mm/min. Having a coating on the sensor would resolve this, but the elastic properties need to be considered and match up with the matrix to prevent sensor failure.

With a total of 15 tests carried out on the same sensor and each being of a different duration, this testing protocol was carried out over multiple days. As discussed before, the handling of the sensor on each day of testing could affect the measured resistance, while the placement of the sensor in the Instron grips also comes into play, as this could not be replicated exactly each time. Any change in pre-strain as a result of sensor placement would lead to resistance changes throughout the testing process. Not being able to control this at this moment suggests that it is preferential to use the resistance range and normalise it to aid with calibration when integrated into a wearable technology system. This argument is backed up by the data presented in Figure 4.8 where the resistance range is between 600-1000 Ω. It is expected that the electrical properties of the sensor will change between tests because of the nature of its structure, but visually there is similarity across the test repeats and normalising the output would help aid comparisons between the tests.

It is important to consider the intra-test variability of the strain sensors: how the sensor resistance range changes from cycle to cycle. A minimal variation would aid the calibration process and suggest its suitability for translation in measuring knee flexion-extension angles. Visually, consistency can be seen in the sensor resistance range from cycle to cycle in Figure 4.9, especially in the longer duration tests at the lower strain rates of 50 mm/min and 100 mm/min where tests were in the region of four hours at the two strain rates for 500 strain cycles and 1000 strain cycles respectively. This indicates suitability for use over longer periods for a rowing or cycling session that could last for this amount of time.

Statistical analysis confirms these visual observations, with p-values presented in Table 4.6, particularly for sensors S6-S10 compared to S1-S5. The difference between these two groups of five sensors can partly be explained by the fabrication process, with the purchase of new rubber bands to be used

as the matrix. Rubber bands will degrade over time, with molecular bonds breaking and reducing the elasticity of the material. Reduced elasticity will mean that after strain is removed, the rubber band will not return to its original dimensions, also impacting the reformation of the CNT conductive pathways.

For all sensors, but especially focusing on sensors S6-S10, the significant p-values referring to a lack of consistency within the cyclical testing are generally amongst the tests towards the end of the testing protocol: 500 cycle and 1000 cycles at 100 mm/min, and 500 cycles at 50 mm/min. Due to the design of the protocol, it cannot be assumed that this is due to testing speed. Sensor degradation is taking place, no matter how minimal, and this can be contributing to the behaviour – a testing protocol randomising the testing speed order could help to rule out this variable.

Good inter-test variability is dependent on the parameter being measured and the context of this use, but indicates the ability to obtain similar or the same results when a measurement is repeated. In the case of using these strain sensors to detect knee range of motion, good inter-test variability should be less than 5% variation between measurements, enabling comparisons between repeated measurements of a person's range of motion. Statistical analysis was carried out on the mean resistance range for each test, grouped by the number of strain cycles as represented visually in Figure 4.10. At a group level, no similarity was seen between tests of the same cycle length conducted at different strain rates. Post-hoc analysis suggested similarity between all tests of 100 cycles at a strain rate of 350 mm/min – these tests were conducted back-to-back without the strain sensor being removed from the Instron grips. These results emphasise the need for a different protocol to rule out testing speed as an influence in the significant statistical results.

4.4.2 Drift

The second part of each test consisted of a 5-minute hold period at constant strain to determine how much variation there was in the sensor output during this period. This strain was equal to the maximum cyclical strain of 16%. Figure 4.7 shows visually how this hold period compares to the cyclic portion of each test.

4.4.2.1 Results

As the sensor is stretched to the maximum value used in the cyclic portion of the test, it is suggested that the mean output value in the hold should be similar to the mean of the max output in the cyclic portion of the test. The values for each test carried out on sensor S10 are displayed in Table 4.9. The mean resistance during the hold period typically falls between the mean and max resistance values during the strain cycles, with the first test of 100 cycles at 350 mm/min being the exception and the mean hold resistance of 881.01 Ω falling below the minimum resistance during cyclic testing of 1058.40 Ω. The standard deviation for the mean hold resistance is low, with the maximum value being 11.48

Table 4.9: Mean hold compared to cyclic max and min resistance (S10).

Test	Mean Resistance (Ω)					
	cyclic max		hold		cyclic min	
	mean	std	mean	std	mean	std
100c_350_1	1821.70	181.09	881.01	6.74	1058.40	150.66
100c_350_2	1476.30	93.39	861.21	7.79	806.90	40.51
100c_350_3	1391.20	93.58	858.41	6.50	788.18	31.62
100c_350_4	1863.60	193.21	1073.79	7.59	991.98	69.04
100c_350_5	1784.40	156.41	1127.12	9.29	1011.10	59.18
200c_350	1741.30	150.32	1121.47	8.35	966.02	22.74
500c_350	1733.70	148.29	1119.09	6.72	934.15	40.86
1000c_350	1683.20	129.73	1092.93	7.72	902.54	27.51
100c_100	1132.80	6.71	1060.19	9.26	828.46	11.64
200c_100	1221.70	40.33	1113.72	10.18	898.35	36.24
500c_100	1358.00	52.01	1238.08	9.71	1004.60	43.18
1000c_100	1277.20	15.34	1183.44	9.34	943.68	12.23
100c_50	1314.30	43.22	1212.77	11.48	967.87	33.15
200c_50	1262.10	10.16	856.67	4.71	922.45	7.83
500c_50	1438.50	61.44	1320.59	11.39	1043.80	55.54

Notation for tests: 100c_350_1 where 100c = 100 cycles, 350 = strain rate of 350 mm/min, 1 = test 1

Ω, compared to the maximum and minimum mean cyclic resistance values which are as high as 193.21 Ω and 150.66 Ω respectively.

4.4.2.2 Discussion

The hold period within this testing protocol was used to understand the strain sensor drift behaviour if it was held under constant tension for an extended period of time, the translation of this being that if an athlete holds a static position then any measurements of joint angles taken during this time should be the same. The low standard deviation of the sensor resistance during the 5-min hold period (calculated and displayed in Table 4.9) suggests the strain sensor's ability to meet this requirement.

The plotted data in Figure 4.7 adds an extra layer of detail to the observations of drift that the numerical data does not. At the start of the hold, there is a reduction in the sensor resistance which can be attributed to stress relaxation. This response is well explained by Amjadi et al. (2014), where the tensile stress in the rubber band matrix is reduced over time as a result of the stress relaxation effect, which leads to a partial restoration in the orientation of the CNTs within the matrix [193]. Conductive networks are reformed and the electrical resistance decreases slightly as a result. This behaviour also explains why the mean resistance during this hold period does not correspond with the mean maximum cyclic resistance. This behaviour is an inherent property of the matrix material and cannot be changed, so needs to be accounted for when taking any constant strain measurements.

4.4.3 Hysteresis, Linearity and Sensitivity

Resistive-based strain sensors can be prone to hysteresis which means the response of the sensor when strain is applied and then released will not follow the same trajectory, impacting sensor calibration. This also links to the linearity of the sensor response with a more linear response simplifying the calibration process, as well as the sensitivity of the sensor and how the electrical resistance changes with strain.

4.4.3.1 Results

For each test, all cycles were averaged to determine the average load-unload cycle. From this, a hysteresis loop was plotted, which forms the basis of the results in this section. Plotting an average strain cycle revealed spikes in the data at maximum and minimum strain (as also seen in the raw data) for the high strain rate tests, which is seen in Figure 4.12a. This has the potential to skew any further calculations for hysteresis, linearity (using the coefficient of determination, R^2) and the gauge factor (GF). The decision was therefore made to crop the data at each end to account for these data spikes (as displayed in Figure 4.12b) and produce adjusted values for each of the metrics mentioned, which are presented in Table 4.10.

The loading and unloading curves in Figure 4.12 are close together, with an overlap between signals at some points. Visually it can be seen that the maximum separation between the two signals does not fall at 8% strain which is the midway point.

Table 4.10: Average hysteresis, corresponding Gauge Factor and Coefficient of determination for each test type. Original and adjusted values are reported for each metric.

Test	Hysteresis (%)		Gauge Factor (-)		Coefficient of determination - Adjusted R^2 load (-)		Coefficient of determination - Adjusted R^2 unload (-)	
	Original	Adjusted	Original	Adjusted	Original	Adjusted	Original	Adjusted
100c_350_1	99.60	11.51	11.87	3.14	0.488	0.933	-0.002	0.909
100c_350_2	99.73	30.70	17.65	3.48	0.541	0.933	0.036	0.806
100c_350_3	99.56	14.54	10.44	3.05	0.681	0.953	0.011	0.927
100c_350_4	75.07	49.84	5.22	2.95	0.787	0.940	0.410	0.720
100c_350_5	31.72	26.27	4.38	2.50	0.833	0.954	0.854	0.929
100c_100	18.74	19.03	2.28	2.24	0.978	0.982	0.945	0.948
100c_50	14.89	15.10	2.17	2.13	0.995	0.996	0.980	0.981
200c_350	99.47	22.96	8.21	2.86	0.810	0.957	0.081	0.930
200c_100	14.53	14.74	2.18	2.14	0.990	0.992	0.979	0.980
200c_50	15.31	15.48	2.24	2.21	0.995	0.996	0.979	0.979
500c_350	72.89	17.40	5.28	3.31	0.851	0.975	0.606	0.948
500c_100	15.93	16.23	2.15	2.09	0.959	0.963	0.920	0.921
500c_50	15.16	15.34	2.34	2.30	0.983	0.985	0.965	0.966
1000c_350	42.66	13.25	5.46	3.87	0.899	0.980	0.806	0.940
1000c_100	17.46	17.73	2.18	2.14	0.943	0.949	0.902	0.905

Notation for tests: 100c_350_1 where 100c = 100 cycles, 350 = strain rate of 350 mm/min, 1 = test 1

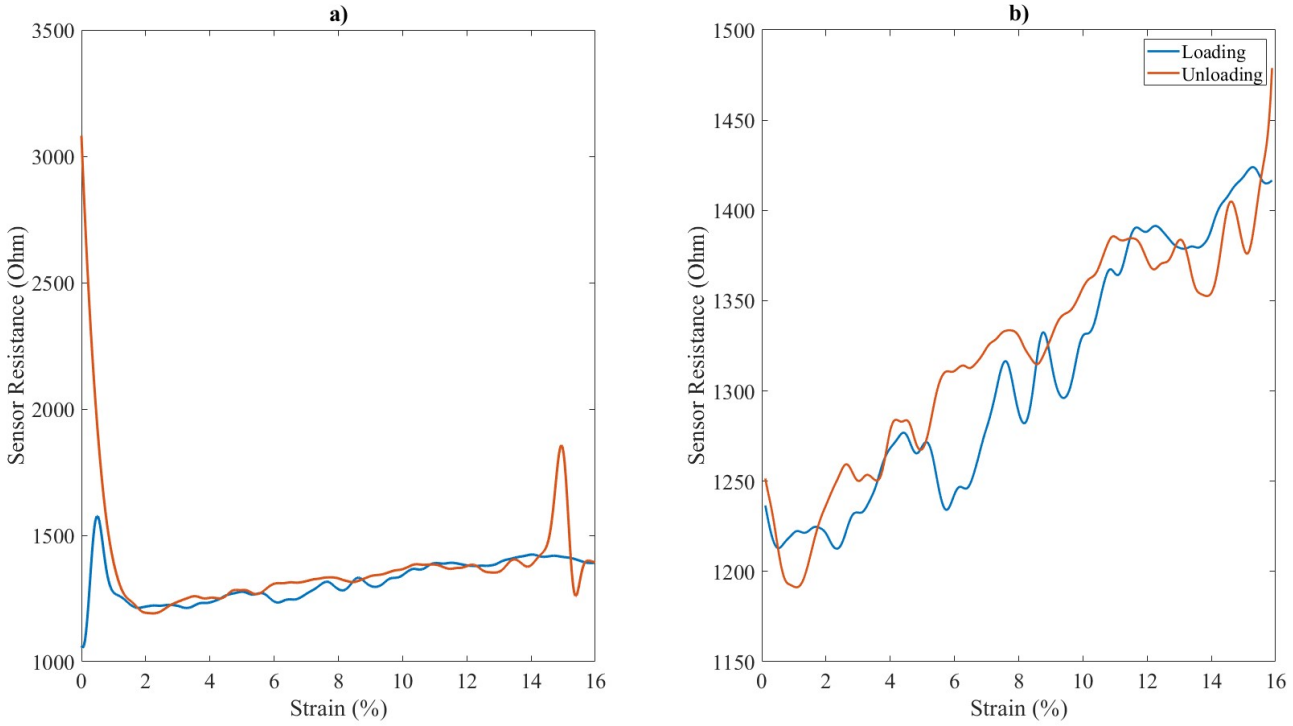


Figure 4.12: Hysteresis loops plotted for a strain cycle test carried out on S10 for 100 cycles at 350 mm/min. a) original plot featuring spikes in the sensor response at minimum and maximum extension b) adjusted plot, accounting for the data spikes.

Hysteresis values in Table 4.10 were calculated using the following equation:

$$Hysteresis(\%) = \frac{|R_{load} - R_{unload}|}{R_{max}R_{min}} \times 100\% \tag{4.7}$$

Where $|R_{load} - R_{unload}|$ corresponds to the greatest difference between the loading and unloading responses, and R_{max} and R_{min} are the resistance values at the maximum and minimum strain respectively.

Adjusted hysteresis values at the highest strain rate of 350 mm/min are much lower than the original values, in one instance falling from 99.56% to 14.54% (test T3_100c_350). A similar observation can be made for the GF, falling from 10.44 to 3.05 for the same test. Accounting for the data spikes at minimum and maximum extension, a difference can also be seen in the coefficient of determination, with the adjusted R^2 values increasing for both the loading and unloading responses. Original and adjusted values for all metrics remain similar for tests conducted at the lower strain rates (100 mm/min and 50 mm/min). Adjusted hysteresis values are below 20% for eleven out of fifteen tests on this particular sensor, the lowest being 11.51%. Adjusted GF values range between 2.09-3.87 and R^2 is as high as 0.996 and 0.981 for loading and unloading respectively, which both suggest a good linear relationship between strain applied to the strain sensor and the electrical resistance response.

4.4.3.2 Discussion

The cyclic portion of the testing protocol was used to determine the linearity and sensitivity of the strain sensor response, as well as understand any irreversible changes or energy losses due to the material properties of the composite.

From the average strain cycle loop plotted in Figure 4.12, it can be seen that the resistance of the sensor follows a similar pattern when strain is applied and then released, however, the loading and unloading curves do not overlay exactly. This suggests that the sensor is exhibiting hysteretic behaviour. The loading and unloading curves however are close together, indicating that little energy is dissipated as heat during the testing process.

Within the literature, there are different ideas as to what constitutes low (and therefore acceptable) hysteresis. A composite made from poly[styrene-b-(ethylene-co-butylene)-b-styrene] (SEBS) and carbon black (CB) was reported to have a low hysteresis below 7% [222] at up to 80% strain, while 30.4% hysteresis at 20% strain was considered tolerable by Fu et al. (2019) for a strain sensor fabricated from MWCNTs and PDMS [211]. The original hysteresis values calculated for tests at strain rates of 100 mm/min and 50 mm/min fall within this range, the highest being 18.74% for a test over 100 cycles at 100 mm/min. Adjusted hysteresis values for the highest strain rate also fall within this range, except for two tests. The results for this particular strain sensor are comparable to those reported in the literature that have been fabricated using more complex and costly techniques involving the curing and layering of polymers [211].

The GF indicates the sensitivity of the strain sensor, reporting the "ratio of the relative change of the output signal to the applied strain" [152]. For this developed strain sensor, the adjusted values range from 2.14 – 3.48 for up 16% strain. Although high GF have been reported such as 1.13 x 10^5 for a MWCNT-SEBS composite [223], strain sensors have also been fabricated with GF as low as 1.55 from a PDMS-MWCNT composite [224]. This PDMS-MWCNT has been used to detect small hand movements in stroke patients, as well as hand and arm movements in badminton [224]. The GF of the sensor developed in this project is therefore suitable for detecting knee range of motion in rowing and cycling, however, the resolution of the measurement may not be as good as a sensor with a higher GF that is more sensitive.

The linearity of the sensor response is also an important feature, with a more linear response aiding the calibration and data processing [152]. Within this strain range of 0-16%, the adjusted R^2 is high, with all values associated with loading above 0.9 and all but two above 0.9 for unloading, indicating that the sensor response has good linearity within this strain range. The R^2 values are lower for the unloading curve – this mismatch is due to the hysteretic behaviour as a result of the viscoelastic properties of the rubber matrix. It is therefore necessary to consider the load and unload sections of the strain cycle separately during any further calibration of the strain sensor.

4.4.4 Further Discussion and Limitations

Outside of the earlier key metrics discussed, there are other elements from the sensor testing process that are important to highlight. There are some gaps in the dataset due to sensor failure. Two sensors (S4 and S5) were found to have failed structurally whilst in storage. Failure was at the point of contact with the electrodes. These sensors were tested and stored during a period of a heatwave that may have contributed to their demise. The electrodes have teeth that clamp onto the elastic matrix of the sensor, increasing stress localisation and the potential for failure after numerous cycles. However, the eight other sensors were tested for over 4500 cycles and did not show any signs of failure.

With the same resistor combination in the external circuit being used for each sensor, and each sensor having different electrical properties, the instrumentation circuit was not optimised for each sensor. This led to different output ranges for each sensor, limiting comparisons between them. Outputs may be optimised in the future by changing the resistor combination for each sensor based on Equation 4.5.

It became apparent during testing that the protocol did not allow the properties of the sensor to be fully exploited and linked to each other. The lengthy protocol meant that all tests on one sensor could not be carried out on the same day. Each sensor was removed from the Instron grips and then replaced on a different day to continue testing. Ensuring the consistent placement of the sensors was difficult and will have impacted the amount of pre-strain and ultimately, the resistance values. A shorter protocol that does not require the sensor to be removed from the Instron grips would provide a better indication of the effect of strain rate and accumulated fatigue on the sensors' properties.

The measurements from the instrumentation circuit and Instron testing machine were not able to be synced and so a manual process was instead used. This made it unsuitable to compare the resistance and load outputs or determine whether the resistance lagged in relation to the strain applied. It also prevented the calculation of time-dependent variables such as response time, recovery and overshoot behaviour. Having a synchronised start of the data collection would have allowed any inherent phase shift to have been observed.

The intended use of this strain sensor is in rowing and cycling where the conditions can be very changeable in an outdoor environment. For this reason, exploring different testing conditions such as temperature and humidity (whether of the environment or sensor itself) would have been beneficial to determine the effect on sensor properties. However, it was observed that a higher storage temperature did decrease the lifetime of the sensor.

4.5 Protocol 2

The original sensor testing protocol gave insight into certain properties, including the durability, repeatability and hysteresis of the carbon-based strain sensors. However, with this protocol being carried

out over multiple days, it made it difficult to make comparisons between each test, specifically tests of the same cycle length, yet different strain rates.

To eliminate the variable of pre-strain and to allow comparisons to be made between tests of different strain rates, a new protocol was devised: sensors underwent 100 strain cycles at loading rates of 50, 100 and 350 mm/min, with three repetitions at each strain rate. These were all carried out on the same day without removing the sensor from the Instron grips. The order of these tests was randomised to ensure that sensor fatigue was not affecting results. Five samples were tested using this new protocol.

4.5.1 Testing Protocols

A random sequence generator was used to determine the testing order for four of the five sensors (labelled S12-S16) used for this new testing protocol. The testing for S12 was developed based on the original protocol order, with the strain rates grouped together for comparison. The testing orders are listed in Table 4.11.

Table 4.11: Testing order for each strain sensor.

Test\Sensor	S12	S13	S14	S15	S16
1	T1_350	T1_50	T1_50	T1_100	T1_100
2	T2_350	T1_100	T1_100	T1_350	T1_350
3	T3_350	T2_100	T2_50	T2_100	T2_350
4	T1_100	T1_350	T1_350	T1_50	T1_50
5	T2_100	T2_350	T2_350	T3_100	T2_100
6	T3_100	T3_100	T3_50	T2_50	T2_50
7	T1_50	T2_50	T2_100	T3_50	T3_350
8	T2_50	T3_50	T3_100	T2_350	T3_50
9	T3_50	T3_350	T3_350	T3_350	T3_100

Notation for tests: T1_350 where T1 = test number, 350 = strain rate

4.5.2 Repeatability

The decision was made to focus only on the repeatability of the sensor output for this testing protocol as it was a limitation of Protocol 1, while the other considered metrics were able to be determined.

4.5.2.1 Results

Figure 4.13 contains plots of the mean sensor resistance range for all the tests carried out on each sensor. As for Protocol 1, the resistance range differs from sensor to sensor, meaning comparisons cannot be made between each sensor. For sensors S14-S16 the resistance range for tests at a strain rate of 350 mm/min is much higher than for tests conducted at a lower strain rate.

Statistical analysis was performed to determine inter-test variability for each sensor using the same mean resistance range used for the plots in Figure 4.13. Friedman tests were performed, grouping

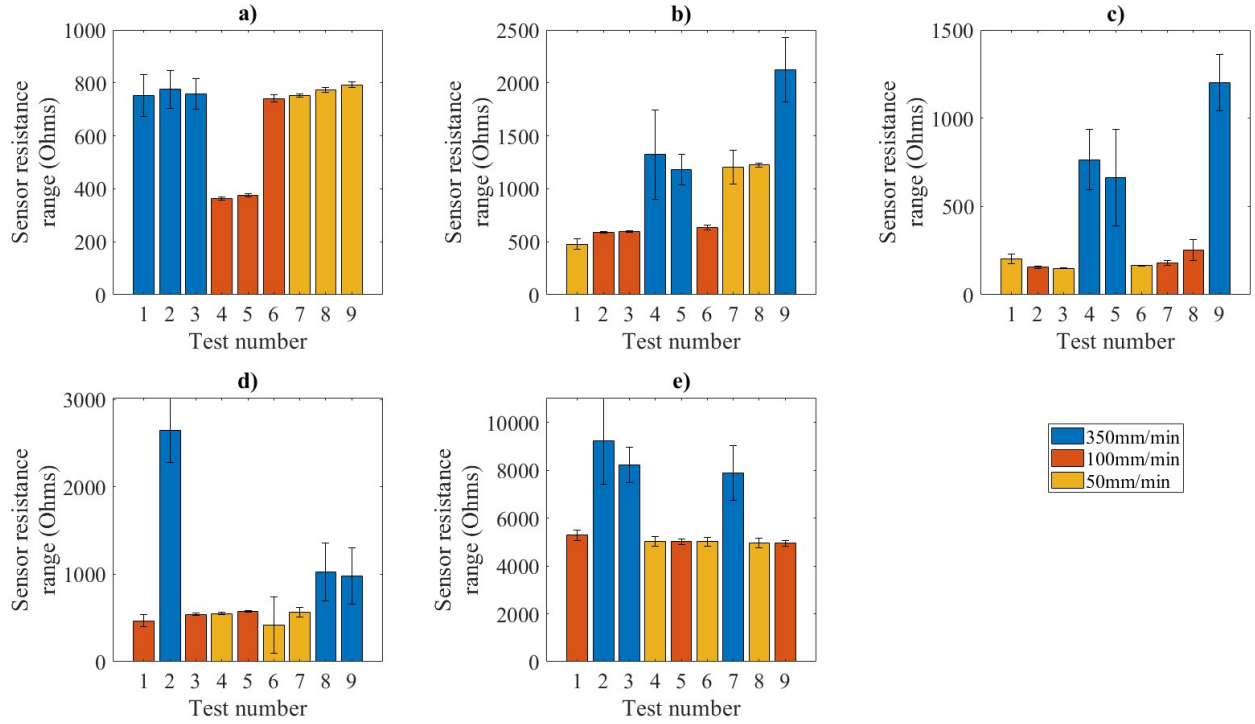


Figure 4.13: Mean sensor resistance range for each test carried out on sensors a) S12, b) S13, c) S14, d) S15 and e) S16.

the protocol tests by strain rate. At a group level, the results showed that there was no similarity between the tests. Post-hoc analysis was performed across all nine tests, with some correlation found as detailed in Table 4.12. The α value was adjusted based on the number of comparisons in each group to be 0.025.

Table 4.12: P-values from the inter-test variability statistics carried out at a significance level of 0.025. Significant values have been highlighted in red.

	S12	S13	S14	S15	S16
350 mm/min	1,2,3	4,5,9	4,5,9	2,8,9	2,3,7
100 mm/min	4,5,6	2,3,6	2,7,8	1,3,5	1,5,9
50 mm/min	7,8,9	1,7,8	1,3,6	4,6,7	4,6,8
Non-significant p-values	(1,2)=0.453, (1,3)=0.926, (1,6)=0.6, (1,7)=0.877, (1,8)=0.116, (2,3)=0.504, (2,6)=0.033, (2,7)=0.254, (2,8)=0.688, (2,9)=0.159, (3,6)=0.09, (3,7)=0.572, (3,8)=0.141,	(5,4)=0.213, (4,7)=0.845, (4,8)=0.943, (5,7)=0.125,	(4,5)=0.079	(1,6)=0.072, (3,4)=0.136, (3,6)=0.229, (4,6)=0.405, (5,7)=0.593, (8,9)=0.405	(5,4)=0.943, (4,6)=0.992, (4,8)=0.063, (5,6)=0.066, (5,6)=0.992, (5,8)=0.06, (6,8)=0.045, (8,9)=0.704
Significant p-values	(1,9)=0.007, (3,9)=0.002, all other comparisons	(7,8)=0.002, all other comparisons	(1,7)=0.004, all other comparisons	all other comparisons	(3,7)=0.023, (5,9)=0.001, (6,9)=0.01, all other comparisons

4.5.2.2 Discussion

Protocol 2 was developed to overcome some of the limitations that arose during Protocol 1, namely the impact of removing strain sensors from the Instron grips (resulting in material loss and different amounts of pre-strain) and the inability to determine the impact of strain rate on sensor behaviour.

By randomising the testing order, it is clear visually from Figure 4.13 that the sensor resistance range does have some dependency on strain rate – with the sensor resistance range generally being higher at a strain rate of 350 mm/min. Sensor S12 is an exception to this. This is reflected in the statistics, with seven out of nine tests on S12 bearing some relationship with each other. Post-hoc analysis for all sensors did not reveal a relationship between tests conducted at different strain rates and also tests conducted at the same strain rate. On a practical level, this suggests that it may be difficult to compare data from one testing session to another unless the sensor resistance is normalised.

4.5.3 Limitations

The randomised testing order in this protocol showed that there is a strain rate dependency on the sensor output, but the response from each sensor was not cohesive with the others tested under this new protocol. Imaging sensors could aid the understanding of how sensors may perform or have performed. Increasing the number of sensors tested under this protocol would also have helped solidify the strain rate dependency observation.

All tests were short, lasting 100 cycles, meaning that the strain sensors were subject to a total of 900 cycles which cannot be used to determine the role of fatigue on the sensor response. Either increasing the testing length (200 cycles would still fit the requirement to do all testing back to back) or adding in more 100-cycle tests would help improve the statistical analysis also.

4.6 Conclusions

The strain sensors developed in this doctoral project were characterised using an Instron machine to understand the key properties required for application in wearable technology. Each sensor displayed different resistance responses, indicating that individual calibration is required for each one. Eight sensors showed good durability when tested over 4800 strain cycles, and good intra-test variability was also observed in relation to the sensor resistance response during a cyclical test, with resistance range deviating by no more than 10% when the strain rate was 100 mm/min or lower and approximately 20% at 350 mm/min. The inter-test variability was poor as the resistance response range varied between tests on the same sensor, but this can be overcome by normalising the resistance response of the sensor.

Adjusted hysteresis values below 20%, gauge factor of 2-3 and R^2 above 0.9 are comparable with other strain sensors that have been developed, and suggest the suitability of this particular sensor for measuring knee range of motion in sports.

Chapter 5

Wearables Development

Integrating the strain sensors into wearable equipment that can be used to monitor knee flexion of athletes

5.1 Introduction

The purpose of developing and characterising carbon nanotube (CNT)-rubber composite strain sensors in this project was to integrate the sensors into clothing or a wearable accessory to measure knee kinematics during sporting activities. This wearable sensor system (WSS) has to meet certain requirements including being comfortable and easy to wear; compatible with other sportswear; easy to modify; secure and unobtrusive. Findings from the systematic review of the literature conducted in Chapter 2 and the previously published review by the author of this thesis [7] were used to establish some of these requirements. Discussions between the author (who has experience as a coach and athlete in both rowing and cycling), their supervisor and other athletes and coaches were used to inform the design and development of the WSS. As the developed sensors do not have a coating, they cannot be washed and so sensor removal from the WSS must be considered. A coating was not used due to the time-frame available to complete this project, as well as disruptions as a result of Covid-19, that prevented a suitable coating from being developed and characterised. Coating development would have delayed the conduction of the cohort study and the collection of data from a real-life scenario.

Athletes have different physiques, especially in rowing and cycling where lightweight rowers and endurance road cyclists are much slighter than their heavyweight rower and track sprint cyclist counterparts. This means that the WSS needs to accommodate different thigh and calf circumferences or be available in different sizes.

Strain sensors have been integrated into different pieces of clothing, using a variety of fixation approaches. Papi et al. (2018) attached their carbon black/polyurethane (CB/PU) sensor to a pair of commercially available leggings using super glue, which was positioned over the anterior aspect of the knee [225], while the strain sensor developed by Nakamoto et al. (2015) from the same materials, was

attached directly to the skin using tape [12, 226]. Integrating a strain sensor into leggings can allow the placement of the sensor across the knee to be replicated over different testing sessions, but attaching it with super glue makes removing and replacing the sensor problematic if the leggings need to be washed or the sensor fails. Furthermore, the lycra material used to make the leggings will stretch but only to a certain extent, meaning that multiple sizes are needed to accommodate different participants. Whilst attaching a strain sensor directly to the skin overcomes the issue of any fabric bunching up and interfering with the signal, it is difficult to replicate the sensor positioning unless done by a trained professional using anatomical landmarks, limiting subsequent translation.

An alternative approach was taken by Munro et al. (2008): they attached their polypyrrole-coated nylon-lycra sensor to a fabric sleeve with press studs, that could be positioned over the anterior aspect of the knee [227]. The press studs allow for easy removal and replacement of the strain sensors, however, the positioning of the fabric sleeve over the knee can change with each wear. Helmer et al. (2013) also used press fasteners to attach their electronic textile strain sensors to compression leggings, which had been purchased in various sizes to accommodate their testing cohort [228].

With regard to sensor configuration, placing a single strain sensor across the anterior aspect of the knee to measure flexion and extension is a common approach [12, 225, 227, 229–231]. Other sensor placements and configurations have been explored, such as placing the strain sensor on the side of the knee to minimise contact with other objects and to reduce displacement artefacts [232]. Hermann et al. (2020) chose to use two sensors positioned over the patella in parallel, using the sensor with the greatest change in resistance to calculate knee angles [233]. It was acknowledged by Hermann et al. (2020) that to measure rotation, adduction and abduction, multiple sensors are required. However, this increases the complexity of calibration and any algorithms that are to be used [233], impacting useability and translation.

Placing a strain sensor on the anterior aspect of the knee is the most direct way of measuring flexion and extension, however, its integration into clothing can vary depending on the requirements of the researchers.

5.2 Knee Sleeve Design

Taking into account the approaches to wearable systems integrating strain sensors considered in previous literature, as well as the requirements stated in the introduction, knee sleeves were chosen as the basis for integrating the developed strain sensor into a wearable device for use in the next phase of this project. It permitted participants to wear clothing that they were familiar with during testing, they were easy to wear and remove, and it allowed multiple sizes to be purchased at a low cost to accommodate a range of participants.

Full leggings were not chosen as different leg lengths as well as femur and tibia proportions, could

mean that the strain sensor does not sit well over the knee joint, being too high or low. Preliminary testing indicated that the knee sleeve permitted easier adjustment and positioning. An iterative approach was used to improve the design of the system, considering different materials and knee sleeve lengths, as well as the attachment of a printed circuit board (PCB) assembly that was used to obtain the strain sensor signal. Section C.1.1 of Appendix C provides details of the different iterations trialled in this project, with Figure C.1 showing a side-by-side comparison.

Throughout this iterative process, the design of the strain sensor and PCB assembly remained unchanged. The PCB was developed and used to measure sensors lined in a socket worn by people with an amputated lower limb [234]. The PCB assembly consisted of a main PCB (containing processing components) and a connector PCB (which was altered for this project). The connector PCB allowed different resistor combinations to be used and facilitated the connection between the assembly and strain sensor.

The assembly was powered by a 3.7 V mAh lithium-ion battery, limited to a supply voltage of 3.3 V. A DSPIC33EP512GM306 microcontroller unit (MCU) was used to capture and process sensor data. The MCU included an analogue-to-digital converter (ADC) with a 10-bit ADC resolution, set to a sampling rate of 200 Hz [234]. A total of four channels were sampled via the connector PCB. A voltage divider circuit was used as the instrumentation circuit for each channel.

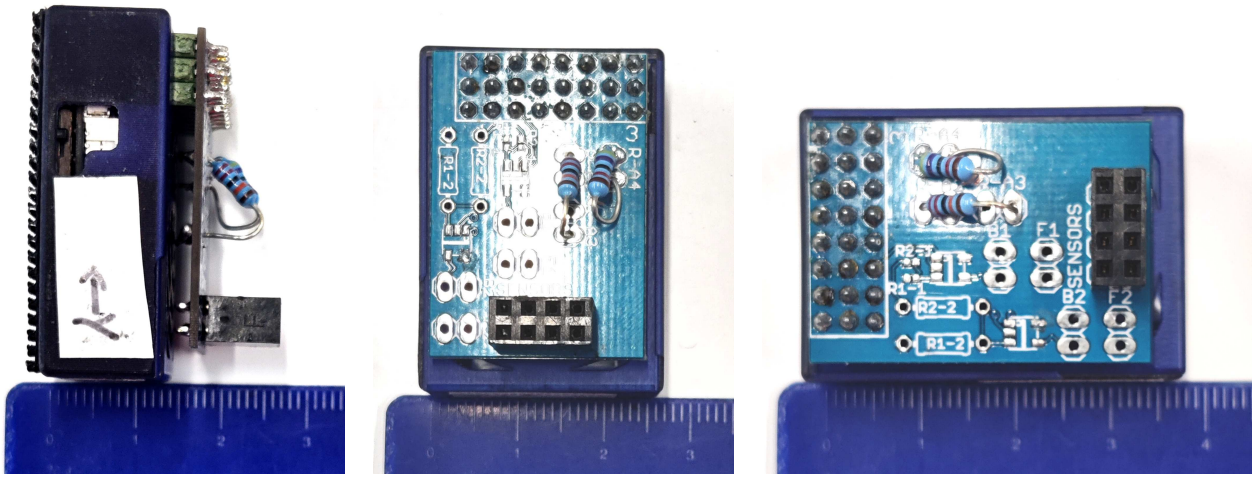
Other features of this assembly include an SD-card and inertial measurement capabilities, a micro-USB port for charging and a switch so that the device could be turned off when not in use. The IMU (LSM9DS0, iNEMO inertial module, STMicroelectronics, Geneva, Switzerland) comprised 3-axis accelerometer ($\pm$ 2g), 3-axis magnetometer ($\pm$ 2 gauss) and 3-axis gyroscope ($\pm$ 500 °/s). Data were recorded from the IMU but they were not analysed as it was outside the scope of this project.

Figure 5.1 shows these different features of the PCB assembly. Data was transmitted from the sampling hardware within the PCB assembly to a receiving device (laptop) via Bluetooth communication (PAN1322-SPP module), in a packeted binary format.

Clincher board connectors were used as electrodes and were clamped at each end of the strain sensor. Snap fasteners were used to attach the strain sensor to the knee sleeve, with the male end secured to the clincher board connectors with superglue and electrical tape. This can be seen in Figure 5.2. These allowed for sensors to be easily removed and replaced during the data collection process. Jumper wires were used to connect the strain sensor to the PCB assembly.

5.3 Sensor Configuration

This project focused solely on measuring knee flexion/extension and not movement in any of the other planes of motion. As discussed earlier in this chapter, placing the strain sensor on the anterior aspect of the knee can accurately track the movement of the joint below. However, it was considered whether



(a) Side view **(b)** Top-down view 1 **(c)** Top-down view 2

Figure 5.1: PCB assembly used during the cohort study with a ruler for scale: a) side on view showing the on/off switch, b) top-down view of the connector PCB with resistors and connecting ports for the jumper wires and c) additional top-down view showing length of PCB assembly.

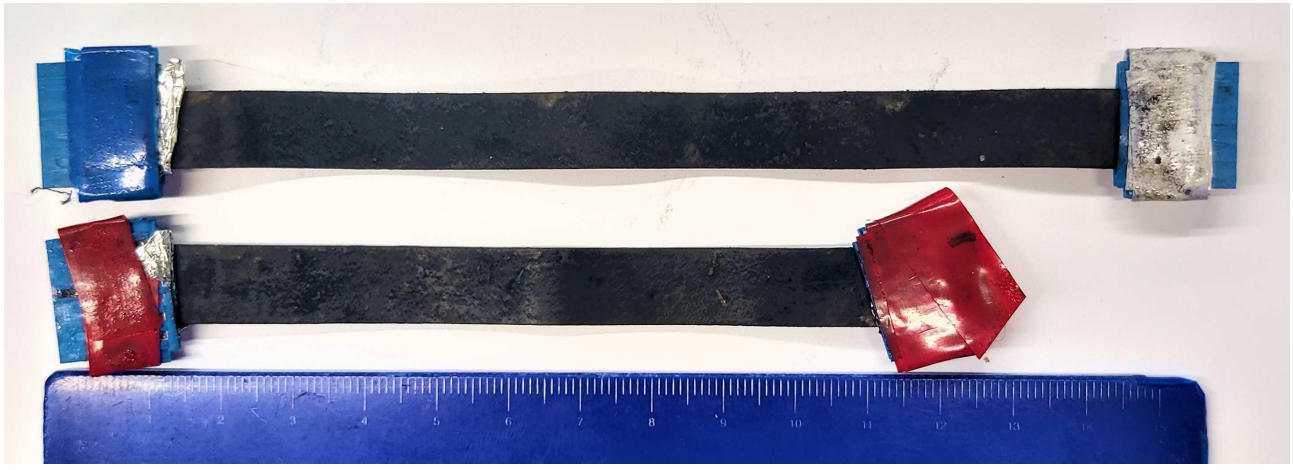


Figure 5.2: Strain sensor as incorporated into the WSS, with clincher connector boards clamped around the strain sensor at each end and the male snap fastener end secured to these with superglue and electrical tape. The top sensor is the longer sensor used on larger knee warmers, the bottom sensor is the regular length sensor used on smaller knee warmers. A ruler is shown at the bottom for scale.

additional sensors and different configurations could help improve the signal obtained from one sensor alone, leading to more accurate and reliable measures of knee angles.

Two configurations using two sensors were explored, with details in Section C.2 of Appendix C, with sensors attached to the knee warmer such that there was always some pre-strain.

5.4 Final Design

Taking into account the various knee sleeve iterations and sensor configurations, a final design was settled on, striking a balance between development costs, being able to attach and remove the sensor easily, capturing data consistently through the sensor being attached securely and a connection being maintained between the sensor, electrodes and circuit. This is shown in Figure 5.3, with a cycling knee warmer used as the basis and only one sensor attached to the anterior of the clothing.

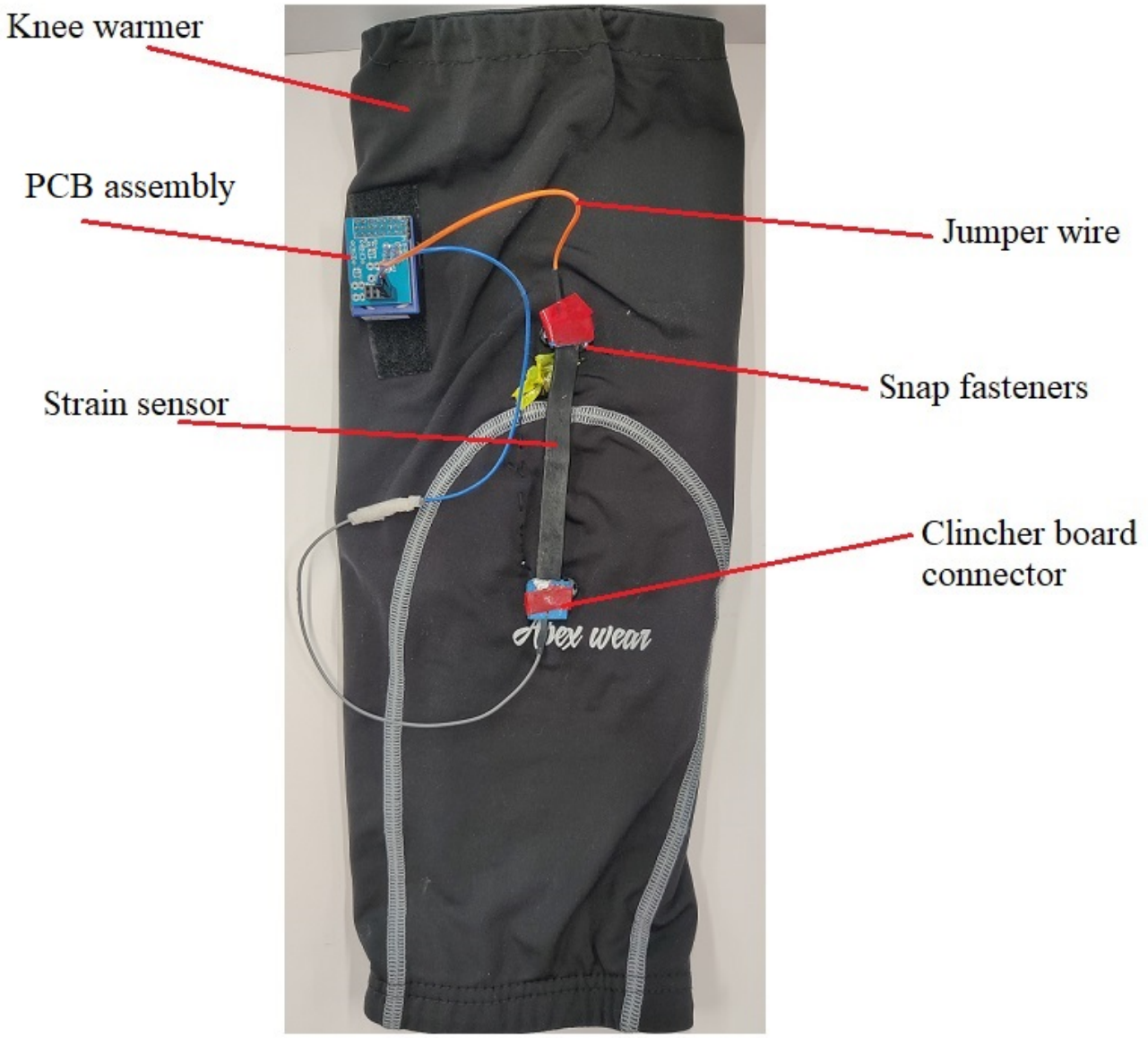


Figure 5.3: Final WSS design used for cohort testing.

This was deemed to be the best solution, with just one strain sensor used to track knee motion as tested in previous literature. Using a simpler configuration for proof of concept reduced the number of variables and therefore increased the amount of control over what was happening during testing. Having just one sensor (which was more visible by being on the anterior of the knee joint) made it easier to make replacements and spot if there were any issues during testing. As previously discussed, the use of knee warmers allowed different sizes to be purchased, accommodating a wider range of participants.

Chapter 6

Cohort Study

Testing and assessing the translational use of the wearable sensor system in rowing and cycling studies alongside a motion capture system

6.1 Introduction

To test the strain sensors developed in this project when integrated into the wearable sensor system (WSS) discussed in Chapter 5, two cohort studies were developed and approved by the Imperial College Research Ethics Committee (ICREC Reference number: 17IC4173) and the Science Engineering Technology Research Ethics Committee (SETREC number: 21IC6651).

These studies were exploratory in nature, conducted to build on the characterisation work carried out in Chapter 4 and gauge the strain sensor's ability to respond to dynamic testing in real-life scenarios. These scenarios were rowing and cycling, two sports highlighted in Chapter 2 for their limited use of wearable technology to measure knee kinematics, despite the knee being a common site of injury.

Participants were recruited from the local community for the rowing and cycling studies, with informed written consent obtained from all. The cohorts included participants over the age of 18 with previous experience of the sport (a minimum of one year), to make sure they met the fitness and technical requirements required for the relevant study. No further restriction on experience was made to allow for data to be collected from a wide range of experience levels, from recreational to elite. The inclusion of a range of experience allowed the evaluation of the technology to be able to distinguish between technical abilities and identify optimal and suboptimal technique. Rowing and cycling are sports that have members of all ages and abilities; one of the recognised successes of wearable technology uptake is reaching a large audience instead of targeting a small minority. However, depending on age and/or experience level, people may have different ideas as to how they want the technology to benefit them in their sport.

The two protocols were designed to consider the response of the strain sensors at different rates of knee flexion, using cadence in cycling and stroke rate in rowing. The rowing protocol was adapted

from a previous study by Buckeridge et al. (2016) [235], with participants completing four 3-minute efforts at increasing stroke rates and intensities. The cycling protocol adapted a pre-existing warm up [236], ramping cadences up from 80 rpm and building towards a maximal effort. Data from the strain sensor were collected simultaneously with the Vicon motion capture system (Oxford Metrics, Oxford, UK). Repeated visits allowed data to be compared between different testing sessions, and a follow-up questionnaire was used to allow experience with the wearable sensor system to be captured in a qualitative manner.

The desired outcomes of these studies were to:

- Test the use of the strain sensor when integrated into the wearable sensor system
- Observe the response of the strain sensor to high-rate cyclic strain as a result of the knee flexion motion
- Compare the strain sensor response to an established motion capture tool (Vicon motion capture system)
- Consider how the strain sensor could be calibrated and the sensors graded based on the quality of its response
- Explore the interpretation of the signals from both the strain sensor and the Vicon motion capture system, in relation to the knee kinematics of the rowing and cycling movements
- Understand the motions that occur during rowing and cycling and their relevance to the development of a tool to measure knee kinematics
- Consider any post-processing needs to facilitate signal interpretation

6.2 Methods

6.2.1 Study Populations

For both studies, participants were recruited through word of mouth and the university rowing and cycling clubs. Information sheets were shared and written informed consent was obtained from all participants. All data collected throughout the study was anonymised. Ethical documentation can be found in Appendix D.

6.2.1.1 Rowing Study

Ten rowers were recruited for this study, consisting of six male athletes (age: 24.0 ± 3.8 years; height: 184.7 ± 6.3 cm; mass: 86.5 ± 7.8 kg) and four female athletes (age: 33.3 ± 18.0 years; height: 168.5 ± 3.9 cm; mass: 65.2 ± 6.8 kg).

Within the cohort, information on main discipline, experience level and number of years in the sport was collected from seven athletes. An amendment to the ethical documentation allowed for this information to be collected but only after two athletes had already completed the study. One athlete did not fill out this information on the online questionnaire. Five athletes listed their main discipline as sweep rowing and two listed their main discipline as sculling. Six athletes listed their experience level as competitive, one as recreational and no answer was recorded for the remaining three athletes. Number of years rowing ranged from 1-15 years, with the mean being 7.3 ± 4.6 years.

6.2.1.2 Cycling Study

Ten cyclists were recruited for this study, consisting of six male athletes (age: 27.0 ± 5.8 years; height: 183.7 ± 8.2 cm; mass: 77.8 ± 6.9 kg) and four female athletes (age: 24.3 ± 3.0 years; height: 165.3 ± 1.5 cm; mass: 60.3 ± 8.9 kg).

Out of the ten athletes, seven stated road cycling as their main discipline, two stated track cycling and one stated spinning. Six athletes described themselves as recreational and the other four described themselves as competitive. The mean number of training hours across the cohort (including cross training) was 7.7 ± 3.1 hours per week. Number of years cycling ranged from 1.5-34 years, with the mean being 10.1 ± 9.6 years.

6.2.2 Equipment

Data were recorded simultaneously from the printed circuit board (PCB) assembly connected to the strain sensor and from Vicon's Nexus programme. Details of the PCB assembly used are described in Chapter 5.

Data from the PCB assembly were transmitted via Bluetooth (BT900, Laird Technologies, Inc., Chesterfield, Missouri, USA) to a receiving laptop and processed via a C# graphical user interface (GUI). These data were synchronised with that from Nexus, using Nexus' automatic capture system, sending a UDP signal (internet type signal) across to the GUI via an Ethernet cable, signifying when capture in Nexus started and stopped.

6.2.2.1 Wearable Sensor System (WSS)

For both studies, participants wore a modified cycling knee warmer that will be referred to as the wearable sensor system (WSS). The knee warmer was modified such that strain sensors could be attached using snap fasteners to the posterior or anterior aspect of the joint. Hook and loop tape was also used to attach the PCB assembly laterally along the thigh. The PCB assembly was placed on the thigh to ensure that it did not interfere with the rowing stroke through potential contact with the ergometer handle.

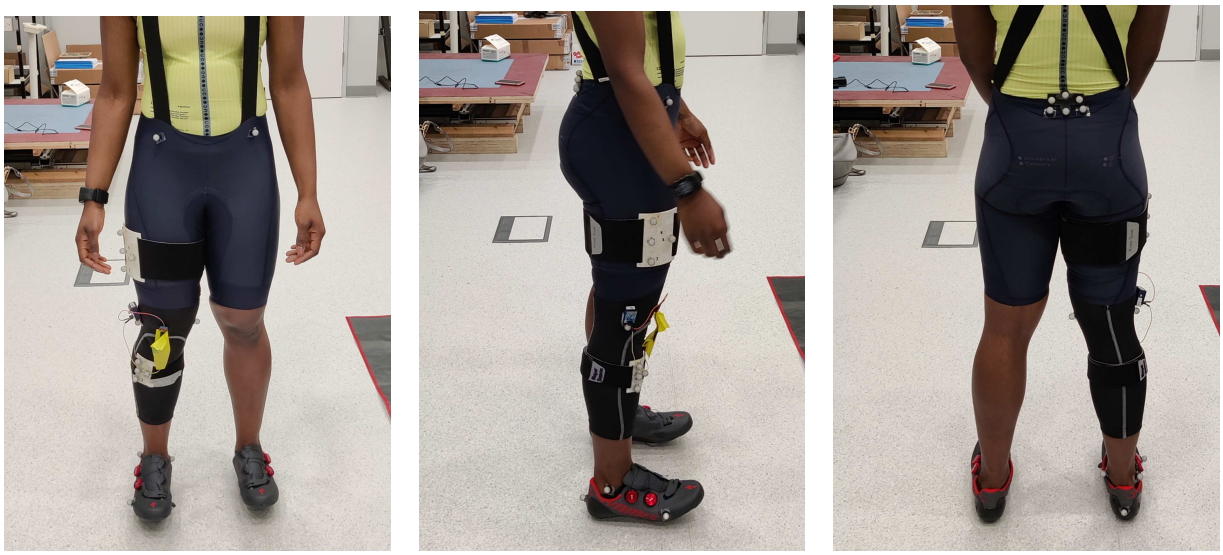
Electrodes at the end of each strain sensor allowed them to be connected to the PCB assembly using jumper wires. Bluetooth technology was used to collect data from the PCB assembly through a laptop, with a sampling rate of 200 Hz.

6.2.2.2 Motion Capture System

Data were also acquired from the Vicon motion capture system, with a 28-camera set-up used to detect the reflective markers placed on the participant. The marker set consisted of 3 cluster sets and 11 individual markers, placed around the pelvis and right leg, as detailed in Table 6.1 and Figure 6.1. Markers were attached to the participant's skin or clothing with double-sided tape.

Table 6.1: Vicon marker locations.

Segment	Cluster location	Individual marker location
Pelvis	Posterior (3 markers)	Right anterior superior iliac spine (RASIS)
		Left anterior superior iliac spine (LASIS)
		Right posterior superior iliac spine (RPSIS)
		Left posterior superior iliac spine (LPSIS)
Right thigh	Distal lateral side (4 markers)	Femur laterial epicondyle (RLEPI)
		Femur medial epicondyle (RMEPI)
Right shin	Distal lateral side (4 markers)	Lateral malleolus (RLMAL)
		Medial malleolus (RMMAL)
Foot	N/A	First metatarsal (RMET1)
		Fifth metatarsal (RMET5)
		Calcaneus (RHEEL)



(a) **(b)** **(c)**

Figure 6.1: Location of Vicon markers and clusters on participant.

6.2.3 Testing Protocol

Upon arrival, participants were instructed to set up the Concept 2 (Morrisville, Morristown, Vermont, United States) rowing ergometer (footplate height and drag factor) or Wattbike Pro (Nottingham, United Kingdom) indoor bike trainer (saddle and handlebar height and fore/aft positioning, and resistance) as required. They were then fitted with the WSS and reflective marker set.

All participants wore suitable sports clothing for the protocols (e.g. rowing all in one, padded cycling shorts) and footwear varied from barefoot (rowing) to cycling shoes with cleats. The Wattbike was fitted with different pedals to allow participants to clip in, or wear trainers and use toe straps.

Two static calibration trials were collected (participants stood in a neutral position), and one dynamic trial of ten bodyweight squats, before completing the appropriate testing protocol. Participants were guided through the protocol by the researcher.

After completing the protocol, participants were sent a link an online questionnaire, to gather their experiences on the WSS and thoughts on wearable technology in general.

6.2.3.1 Rowing Study

Participants performed a step-test protocol described in Table 6.2, with each step lasting for three minutes. The stroke rate was increased, correlating to an increase in intensity. For each step, the distance rowed, average 500m pace and stroke rate were recorded by the ergometer and noted by the researcher. Participants were allowed to recover for as long they needed between each step.

Table 6.2: Testing protocol for the rowing cohort study.

Step	Duration	Stroke rate (spm)
1	3 mins	18
2	3 mins	24
3	3 mins	28
4	3 mins	Free rate

6.2.3.2 Cycling Study

Participants performed a 20-minute warm-up (modified from the British Cycling procedure [236] and described in Table 6.3), that consisted of a cadence ramp and then three maximal sprint efforts. No rest was permitted between any of the different steps. Four out of the ten participants were familiar with the British Cycling warm-up prior to completing this testing.

6.2.4 Data Processing and Analysis

Vicon Nexus 2.12.1 software (Oxford Metrics, Oxford, UK). was used to reconstruct the motion data files, label and gap-fill marker trajectories. Custom MATLAB (Mathworks, Natick, Massachusetts) scripts were used to generate the desired Model Outputs from Nexus, these being the right knee Euler

Table 6.3: Testing protocol for the cycling cohort study.

Duration	Cadence (rpm)
5 mins	80
2 mins	85
2 mins	90
2 mins	95
1 min 30 secs	100
2 mins	80
6 secs	Max
1 min	80
6 secs	Max
1 min	80
6 secs	Max
2 mins 42 secs	80

angles. Data were then exported to MATLAB for further processing, alongside the data collected from the strain sensor. Only sagittal plane knee angles were considered for analysis.

Data from Vicon and the strain sensor were filtered with a zero-phase 4th order low-pass Butterworth filter, with cut-off frequencies of 3 Hz and 5 Hz respectively. Cut-off frequencies were determined using a discrete-time Fourier transform (DTFT). Custom MATLAB scripts were also used to process the sensor data (using the voltage divider relationship), determine offset between the two signals and produce time-normalised plots to compare them.

Preliminary plots were used to assess the quality of the collected data and calculate the mean temporal offset between the Vicon and strain sensor signals from the plots where the sensor response signal was aligned with the Vicon output (such as Figure 6.5). This mean offset value was calculated to be 63 data points and calculated from eight sets of participant data (each having four pairs of Vicon and strain sensor signals).

6.3 Rowing Cohort Study

Due to the cohort size and exploratory nature of this study, generalisations on the knee kinematics of the members of this cohort and their related sub-groups in the wider sport cannot be made. Therefore, a few examples of the sensor performance are presented, highlighting testing where the sensor signal profile is in line with the Vicon signal, in addition to areas where improvements are required in relation to sensor design and performance.

6.3.1 Study Population

The data of five participants are presented to highlight differences in technique that can be observed from the Vicon motion capture system from monitoring sagittal knee angles. It also demonstrates the relationship between the strain sensor signal and the Vicon output. The details of these five

participants are presented in Table 6.4, listing anthropometric details, rowing experience and details of the strain sensor used during testing.

Table 6.4: Participant and sensor details for rowing cohort study.

Participant details								Sensor details	
ID	Sex	Age (years)	Height (cm)	Body mass (kg)	Rowing experience (years)	Preferred discipline	Participation	Sensor number	Sensor use
34943	Female	28	166	70.8	6	Sculling	Recreational	3	1/8
77344	Male	22	194	77	9	Sweep	Competitive	3	2/8
48896	Female	21	168	60	1	Sweep	Competitive	3	6/8
69340*	Male	29	178	102	-	-	-	1	1/3
22341	Male	19	189	86	3	Sculling	Competitive	4	2/2

*Data missing as before ethics amendment including questionnaire was approved

6.3.2 Results

The results are divided into two sections, the first focusing on the strain sensor response and how it compares to the Vicon output, and the second focusing solely on the kinematics extracted from the Vicon output. Over the four rowing steps, the stroke rate was increased from 18 strokes per minute, to 24, then to 28 and the final step was at free rate at the choice of each participant. Data have been extracted from each step to determine if the increase in stroke rate and rowing intensity has an influence on knee kinematics.

6.3.2.1 Analysis of Strain Sensor Response

In this section, data for each participant has been summarised into two sets of plots, focusing on the middle minute of each 3-minute step. The first set of plots includes the strain sensor signal which has been normalised by its own range. The original intention was to use the squatting dynamic trial to calibrate and normalise the sensor response, however the range of the sensor signals during the squatting and rowing motions were not aligned. Examples of the sensor signal in the rowing trials normalised by the range of the signal in the squatting step is presented in Appendix E. Despite a similar knee range of motion being covered by participant 34943 in both motions, the normalised range signal was found to have a range greater than 1 for some of the rowing steps. This can be attributed to the overshoot behaviour of the strain sensor at a higher strain rate while rowing. The inconsistencies between participants in how the sensor signal was transformed after being normalised by the squat signal range meant that it was therefore better to consider each rowing trial in isolation and normalise it by its own range.

The second set of plots compares the Vicon and strain sensor signals, with each cycle being time-normalised and overlaid on top of each other. The catch position, corresponding to maximal knee

flexion, was chosen as the start and end of each cycle.

6.3.2.1.1 Participant 34943 - visit 1/1

The range-normalised strain sensor response for participant 34943 is displayed in Figure 6.2. Higher frequency spikes at the top end of the range in the signal for Step 1 are representative of overshoot behaviour; these spikes are less prominent in the subsequent steps conducted. There is some variation in peak height, especially in Step 1 due to the spikes, but without the spikes the peaks are of similar amplitude. Double peaks can also be observed in the signal, which are more prominent in Steps 3 and 4 as the rowing stroke rate increases. In each step, the sensor was able to detect the following number of strokes: 19, 23, 27 and 29 strokes in the middle minute extracted.

From the time-normalised plots in Figure 6.3, it can be seen that the profile of the sensor response follows that of the Vicon output. The higher frequency spikes in the strain sensor signal carry across to the time-normalised plots, with more variation between strokes seen in the upper range of the strain sensor plots. The Vicon plots show that the rower is able to achieve close to or full extension at the end of the drive phase of the rowing stroke, however as the stroke rate increases, the period for which the rower holds their knees in full extension starts to decrease.

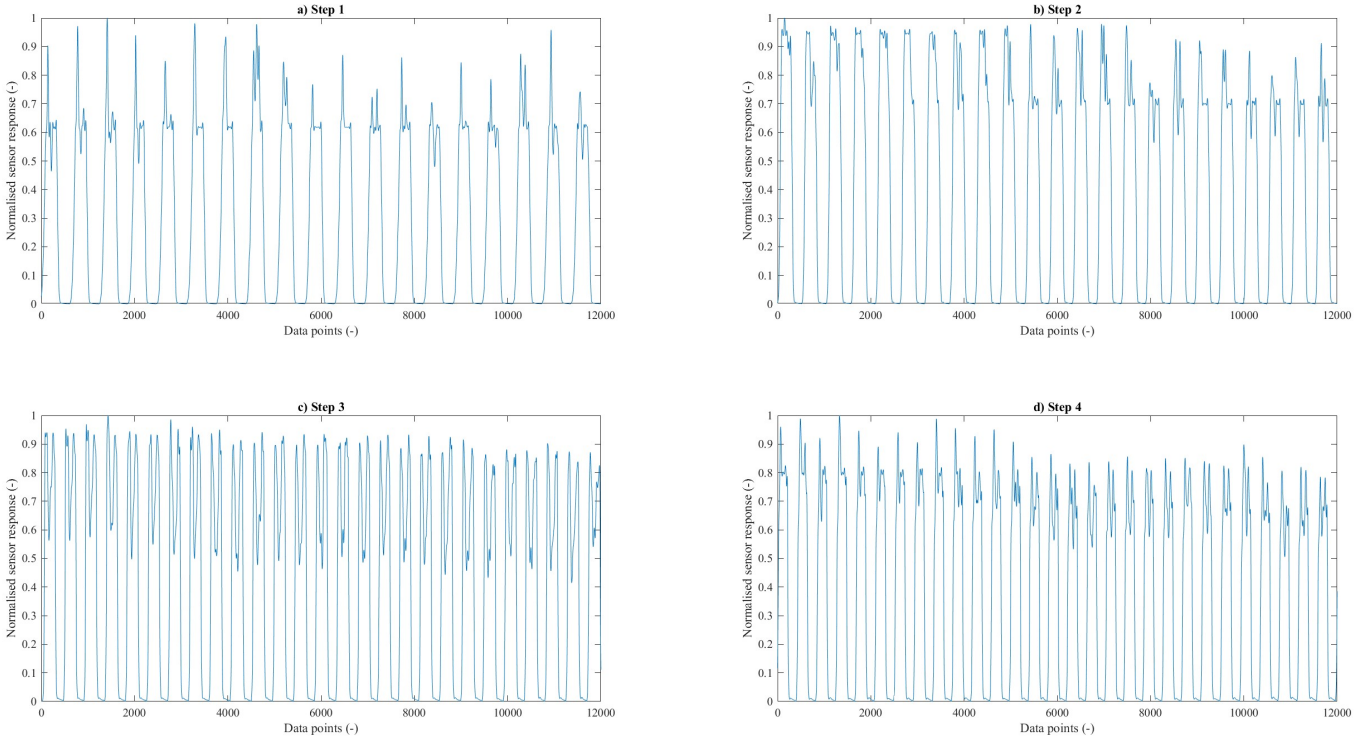


Figure 6.2: Normalised sensor response for the middle minute of each step during the rowing trials performed by participant 34943.

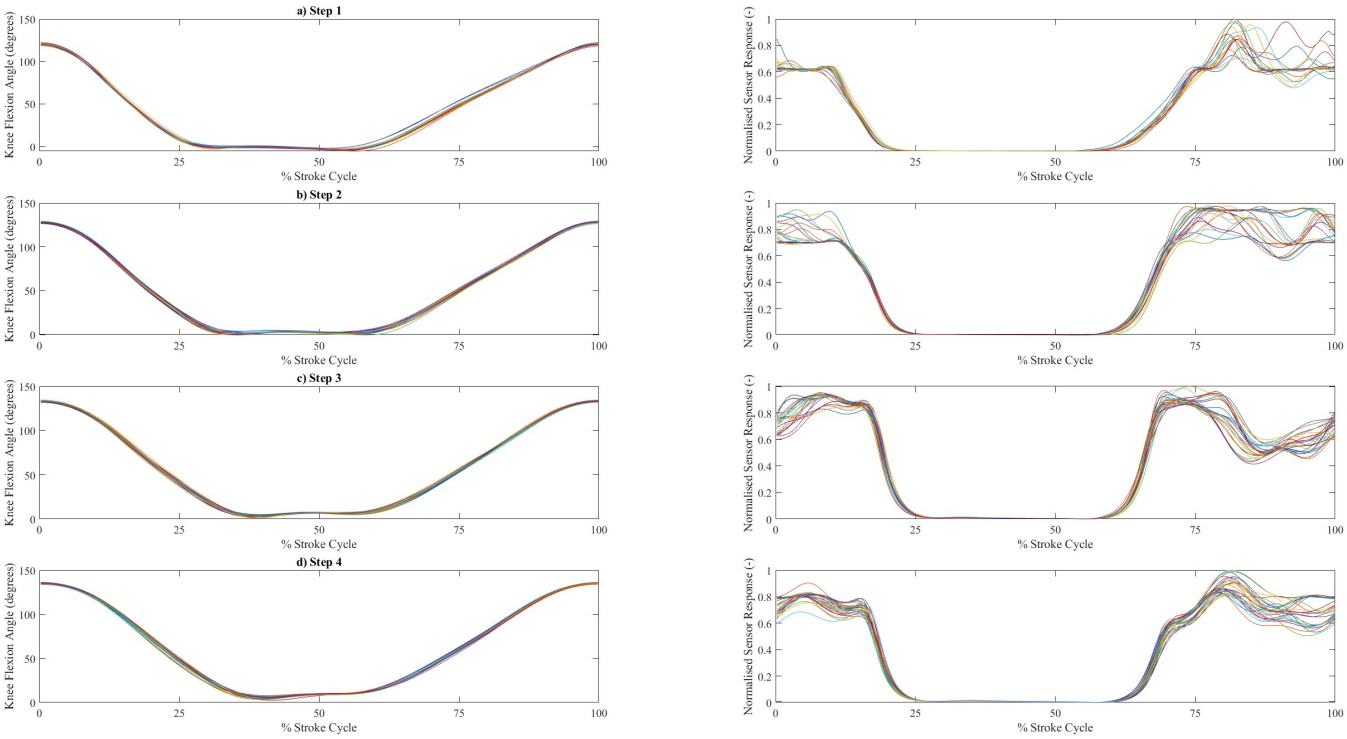


Figure 6.3: Overlaid time-normalised response for each rowing stroke in the middle minute of each step in the protocol. Knee angles from Vicon on the left and strain sensor response on the right for participant 34943.

6.3.2.1.2 Participant 77344 - visit 1/2

Double peaks are present in all rowing steps, however there is less overshoot behaviour observed in the range-normalised strain sensor response in Figure 6.4 for participant 77344. This is suggested by the double peaks being of similar amplitude in each strain cycle. Apart from the first three strokes in Step 1, there is a good consistency in peak height throughout the middle minute of rowing in each step with approximately 10% variation. From the extracted signal, the number of strokes taken were 18, 24.5, 28 and 31 for Steps 1-4 respectively.

From the time-normalised plots in Figure 6.5, it can be seen once again that the profile of the sensor response is similar to the Vicon output, with less variation between strokes at maximum knee flexion due to the minimised overshoot behaviour. The Vicon output shows that the rower does not achieve full knee extension at any point during the rowing stroke.

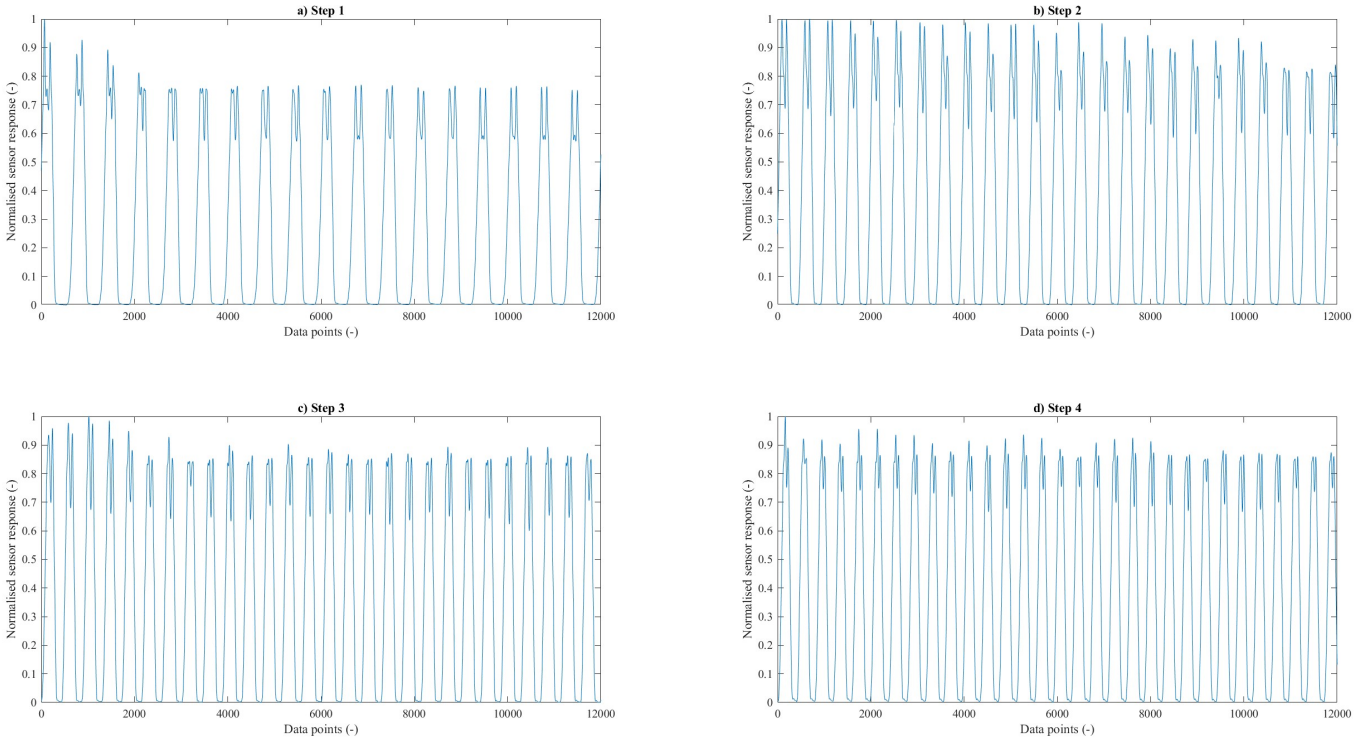


Figure 6.4: Normalised sensor response for the middle minute of each step during the rowing trials performed by participant 77344.

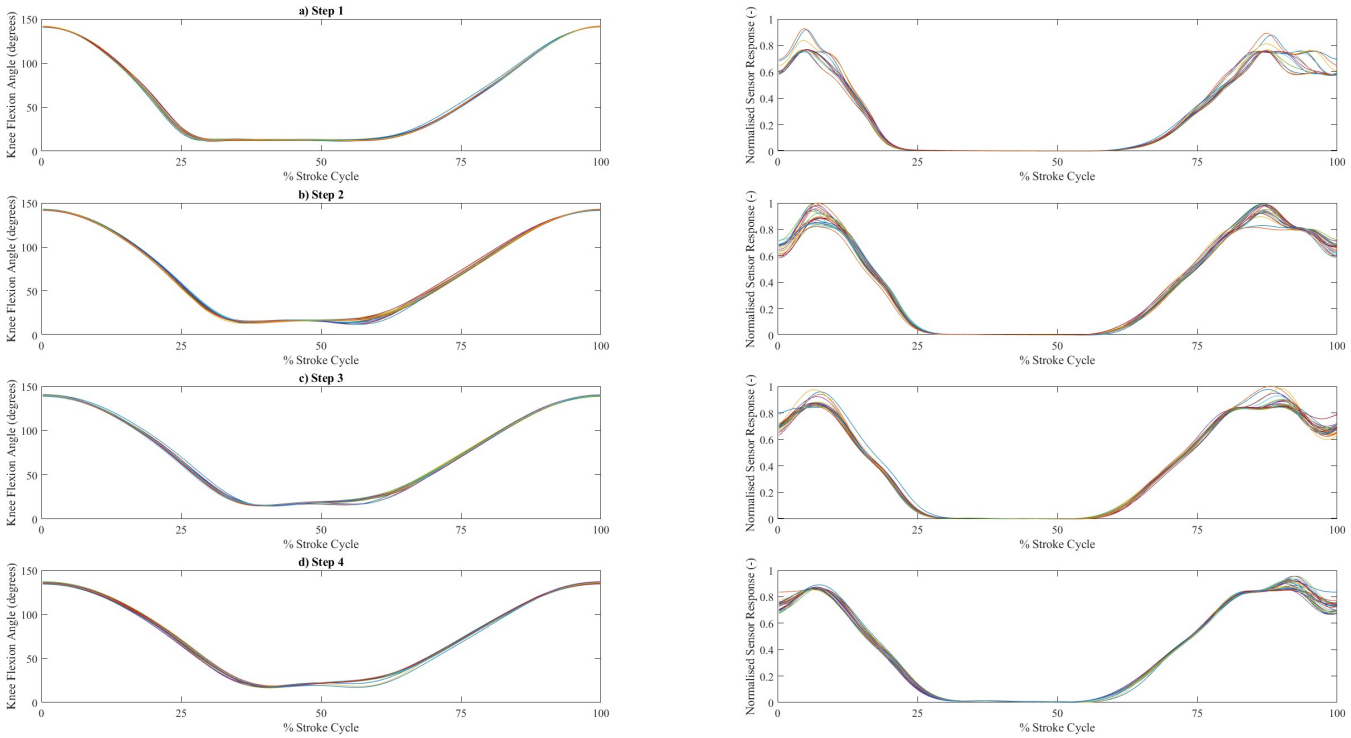


Figure 6.5: Overlaid time-normalised response for each rowing stroke in the middle minute of each step in the protocol. Knee angles from Vicon on the left and strain sensor response on the right for participant 77344.

6.3.2.1.3 Participant 48896 - visit 2/2

The normalised sensor signal for participant 48896 in Figure 6.6 features the double peaks that have been observed in the previous participants, however, they only become prominent in Step 4. There is consistency in peak height for each of the steps, and the number of strokes as determined by the signal are 18, 24, 27 and 32 strokes within the middle minute of each step.

The profile of the signal extracted from Vicon differs in Step 1 compared to the later, higher stroke rate steps, as displayed in Figure 6.7. The bottom of the curve between 25-60% in Step 1 is much flatter, indicating that knee angle (in extension) is remaining constant around the back end of the rowing stroke. However, from Step 2 onwards, less time is spent with the knees maximally extended for this participant, suggesting that knee flexion is occurring as the arms are stretched out away from the trunk and the trunk rotates anteriorly. In this instance, although the strain sensor signal values in the second half of the stroke cycle increase earlier with subsequent rowing steps as in the Vicon signal, it is not able to detect that gradual change in knee flexion between about 30-55% of the stroke cycle.

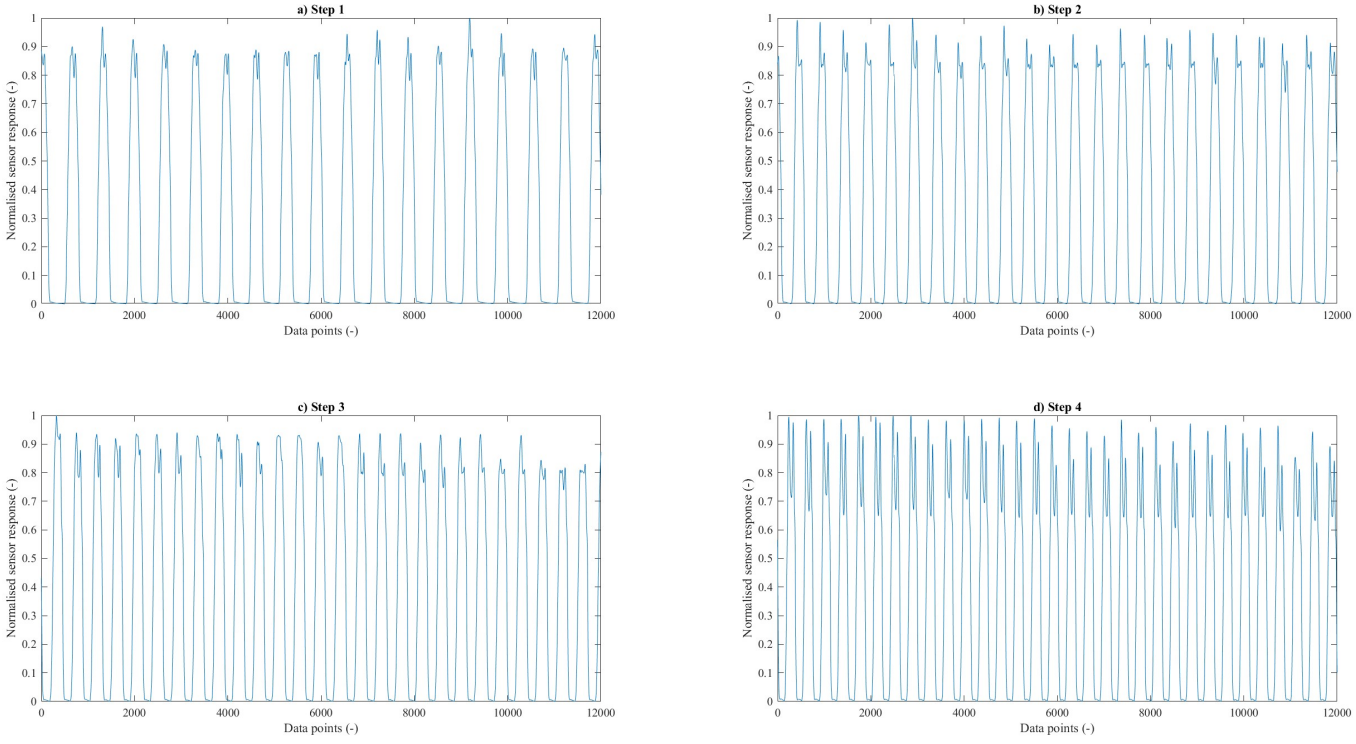


Figure 6.6: Normalised sensor response for the middle minute of each step during the rowing trials performed by participant 48896.

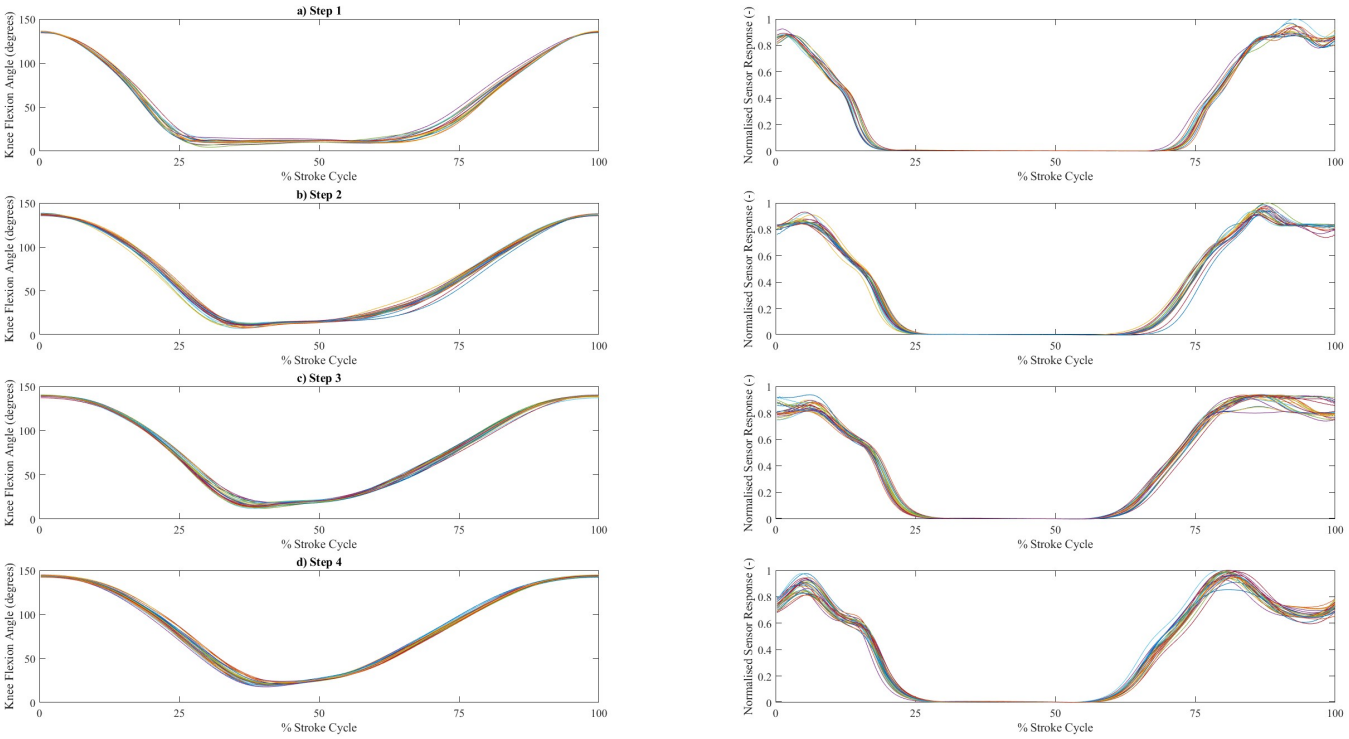


Figure 6.7: Overlaid time-normalised response for each rowing stroke in the middle minute of each step in the protocol. Knee angles from Vicon on the left and strain sensor response on the right for participant 48896.

6.3.2.1.4 Participant 69340 - visit 1/2

In the data presented, that from participant 69340 is the first example of a smoother strain sensor signal without any double peaks, as seen in Figure 6.8. In all four steps, particularly in Step 1, there is less consistency from stroke to stroke when looking at the height of each peak, suggesting that the participant does not always achieve the same amount of knee flexion and therefore the stroke length is quite variable. The number of strokes detected by the strain sensor in each of the steps were 18, 24.5, 27 and 30 during the middle minute.

The time-normalised Vicon plots in Figure 6.9 agree with what is seen in the raw sensor signal, in that there is variation in each stroke taken, including when looking at the higher angle values which indicate maximum flexion for this participant. Another observation that can be made is that this participant initially achieves maximum extension at around 25% of the stroke cycle in Step 1, however in the subsequent steps this becomes much later, at around 50% of the stroke cycle, meaning less time proportionally is dedicated to the end of the drive phase and the entire recovery phase of the rowing stroke as the intensity and stroke rate increases.

The curves representing the strain sensor signal in Figure 6.9 have a very flat bottom, which is not representative of the knee kinematics taking place in this protocol as displayed by the Vicon signal. This participant indicated experiencing discomfort with the knee warmer, and the poor fit led to

bunching: the strain sensor would, therefore, not have been under strain for a significant portion of the rowing stroke, leading to this particular signal profile.

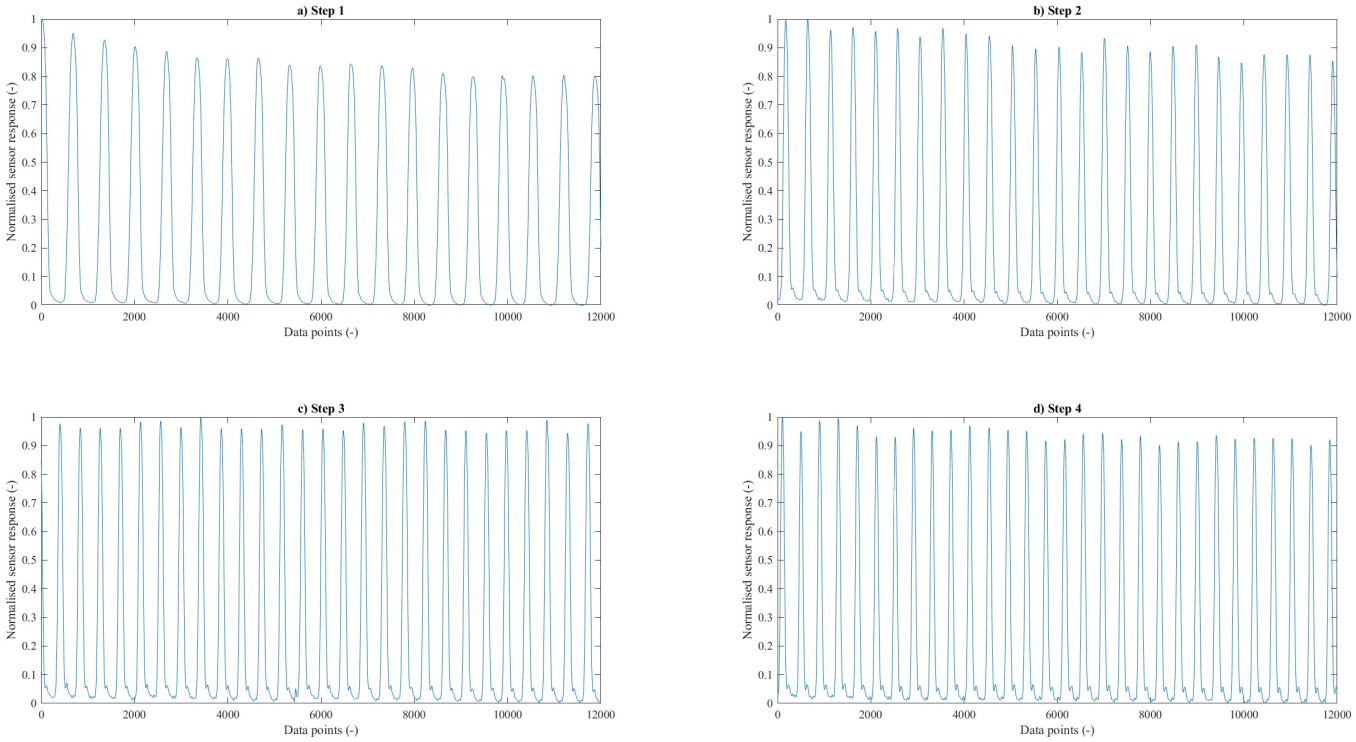


Figure 6.8: Normalised sensor response for the middle minute of each step during the rowing trials performed by participant 69340.

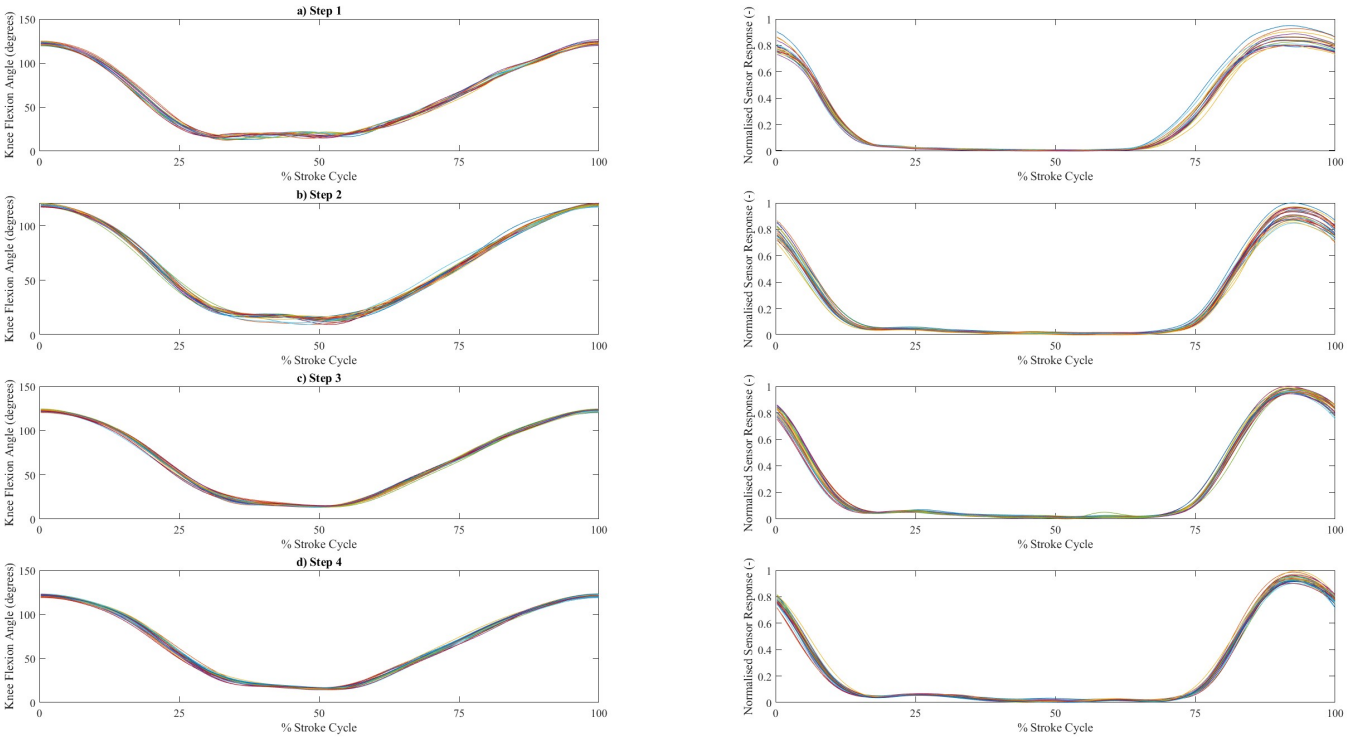


Figure 6.9: Overlaid time-normalised response for each rowing stroke in the middle minute of each step in the protocol. Knee angles from Vicon on the left and strain sensor response on the right for participant 69340.

6.3.2.1.5 Participant 22341 - visit 1/1

The strain sensor data presented for participant 22341 is an example of a poor signal, which has been distorted by noise and does not align with the Vicon profile, and the subsequent implications of this on data extraction. Each sensor plot in Figure 6.10 features a signal of two parts: lower amplitude waves (peaking at 0.4 in Step 1, at 0.25 in Step 2 and 0.2 in Steps 3 and 4), and higher frequency spikes (typically around 0.8-1). There is noise that has been introduced into the signal, but it is not clear which part relates to the noise and which part is the main signal to be analysed. This noise could have been generated from a loose connection between the stain sensor and PCB assembly, via the jumper cables, or by the knee warmer bunching up during the rowing stroke.

In each step, for each smaller wave in the signal there is also one spike of larger amplitude. The number of rowing strokes taken can still be calculated, either using the smaller waves or the larger spikes. In Steps 1-4, the number of strokes were calculated as 18, 23, 27 and 34 respectively using the larger spikes. In Steps 2-4, there are double peaks in the signal produced by the larger spikes, with the first peak spiking up much higher than the second, leading to variation in peak heights during each step.

Looking at the time-normalised Vicon signal in Figure 6.11, the profiles of Steps 1 and 2 are similar, with the knees of this participant in maximum extension for a sustained period (25-55% in Step 1 and

35-55% in Step 2). Steps 3 and 4 follow a similar profile to participant 48896, where maximum knee extension is held for a minimal amount of time before the knee begins to flex again. The strain sensor signal is distorted by the noise that was visible in Figure 6.10 and cannot be compared to that from Vicon.

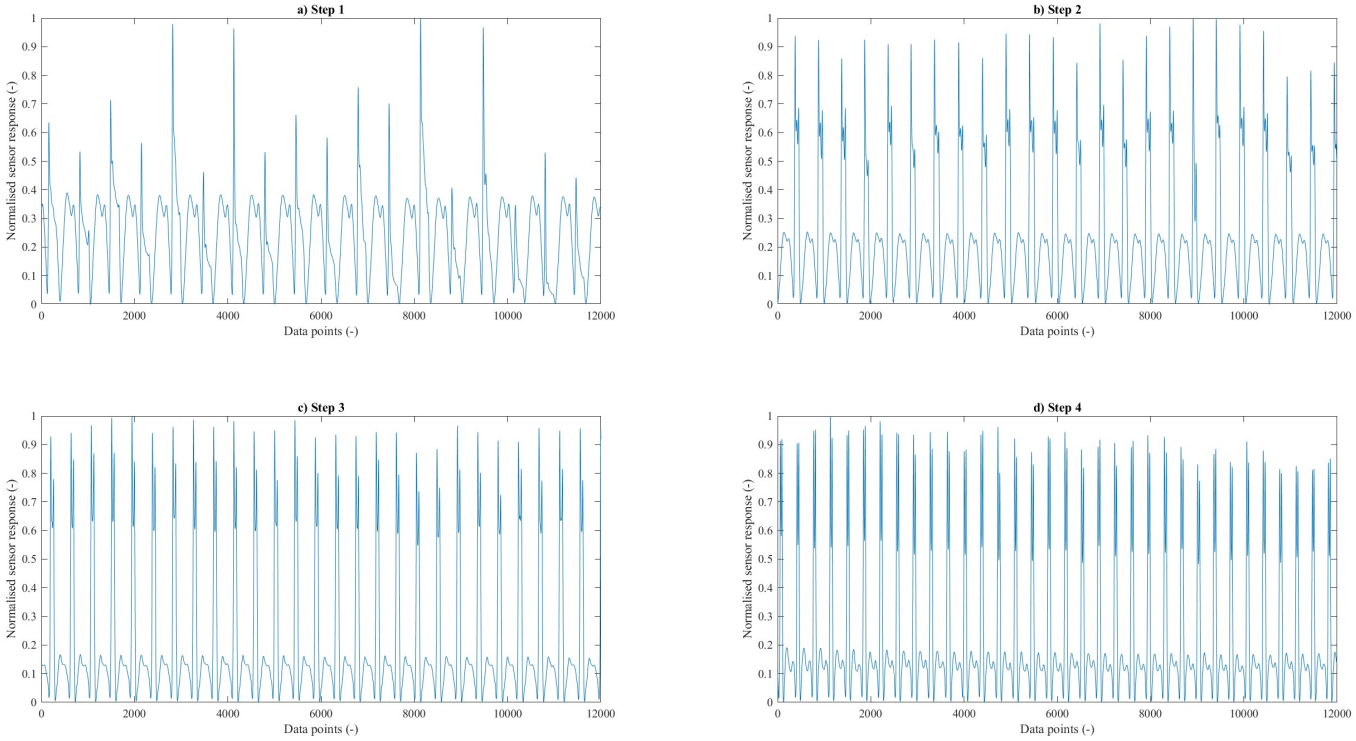


Figure 6.10: Normalised sensor response for the middle minute of each step during the rowing trials performed by participant 22341.

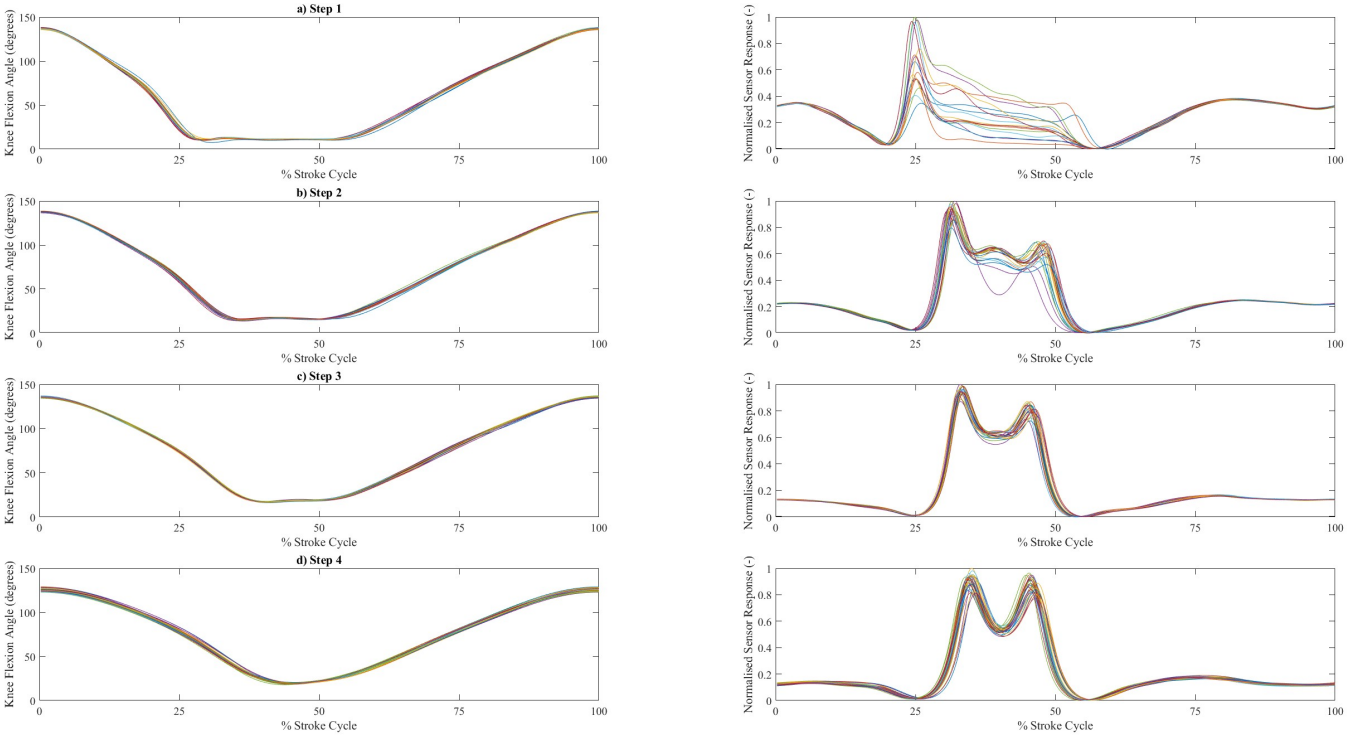


Figure 6.11: Overlaid time-normalised response for each rowing stroke in the middle minute of each step in the protocol. Knee angles from Vicon on the left and strain sensor response on the right for participant 22341.

6.3.2.2 Kinematics Analysis of Vicon Signal

In this section, the mean maximum and knee flexion angles for each participant in the middle minute of each step have been extracted from the Vicon signal (see Table 6.5). This allows comparisons to be made between the knee flexion angles with increasing stroke rate and from participant to participant. The overall knee flexion range has also been calculated for each step (see Table 6.6).

Table 6.5: Mean maximum and minimum knee flexion angles for each participant during each rowing step.

Partici-pant ID	Mean knee flexion angle (degrees)							
	Step 1		Step 2		Step 3		Step 4	
	Max	Min	Max	Min	Max	Min	Max	Min
34943	120.96 ± 0.93	-3.55 ± 0.83	127.95 ± 0.65	0.87 ± 0.92	133.52 ± 0.75	3.50 ± 1.00	135.66 ± 0.57	5.06 ± 1.33
77344	141.29 ± 0.30	12.10 ± 0.65	142.45 ± 0.25	14.18 ± 0.88	140.09 ± 0.33	15.37 ± 0.37	136.03 ± 0.69	17.76 ± 0.56
48896	129.16 ± 0.45	-0.17 ± 1.19	127.51 ± 0.55	3.55 ± 1.43	129.07 ± 0.66	2.48 ± 0.96	129.60 ± 0.62	3.46 ± 1.52
69340	123.40 ± 0.60	18.09 ± 0.75	121.25 ± 0.70	16.53 ± 0.44	123.52 ± 0.53	17.89 ± 0.94	123.18 ± 0.98	19.99 ± 0.88
22341	137.28 ± 0.74	10.26 ± 0.82	137. 93 ± 0.49	14.98 ± 0.58	136.03 ± 0.72	17.03 ± 0.41	126.09 ± 1.49	19.37 ± 0.70

Table 6.6: Mean knee flexion angle range for each participant during each rowing step.

	Mean knee flexion angle range (degrees)			
ID	Step 1	Step 2	Step 3	Step 4
34943	124.51	127.09	130.02	130.60
77344	129.19	128.27	124.72	118.28
48896	129.33	123.96	126.58	126.14
69340	105.31	104.72	105.63	103.19
22341	127.03	122.95	119.01	106.72

Hyperextension is exhibited by two participants in Step 1 as indicated by the mean minimum knee flexion angle (-3.55 ± 0.83° for participant 34943 and -0.17 ± 1.19° for participant 48896). For all participants, the mean minimum knee flexion angle increases from Step 1 to Step 4, suggesting that the ability to achieve full knee extension is linked to stroke rate and intensity.

The changes in mean maximum knee flexion angle with increasing stroke rate differ from participant to participant. It increases for participant 34943 (from 120.96 ± 0.93° to 135.66 ± 0.57°) while for participants 77344 and 22341 it decreases (from 141.29 ± 0.30° to 136.03 ± 0.69°, and from 137.28 ± 0.74° to 126.09 ± 1.49° respectively). For the final two participants (48896 and 69340) there is minimal change in knee angle between Steps 1 and 4 (from 129.16 ± 0.45° to 129.60 ± 0.62°, and from 123.40 ± 0.60 ° to 123.18 ± 0.98° respectively).

When looking at the overall knee flexion angle range and the change between Steps 1 and 4, this decreases for participants 77344, 48896, 69340 and 22341 by 10.91°, 3.19°, 2.12° and 20.31° respectively. For participant 34943, the knee flexion range increases between Steps 1 and 4 by 6.09°.

6.3.3 Discussion

The purpose of this rowing protocol was to establish the response of the strain sensor in a real-life setting and compare it to the Vicon motion capture system as a reference. This cohort study gave an opportunity to comprehend the suitability of the strain sensors developed and characterised in Chapters 3 and 4, as the settings of the Instron testing machine used for characterisation were limited and not able to fully exploit the capabilities of the strain sensors. In all examples presented, the three strain sensors used were able to detect each rowing stroke, indicating as a minimum that the WSS can be used to count strokes.

Comparing the signals obtained from the strain sensor and Vicon, the profile of the strain sensor signal follows that of Vicon: from the catch position as the knee joint is extended, the strain sensor is under less tension, decreasing the resistance measured and the normalised response presented in the figures. This is best represented in Figure 6.5 where not only the profile is similar, but visually the amount of variation between stroke cycles is similar for both Vicon and the strain sensor. More

variation can be seen at the upper end of the sensor response (between 0.7-1) which is at the front end of the rowing stroke where the knee is flexed and the sensor is under the most strain. This could lead to less accuracy in determining the maximal amount of knee flexion when correlating the sensor response to Vicon, compared to the knee flexion at other points during the rowing stroke, as the overshoot behaviour leads to multiple values in the sensor signal corresponding to the same knee angle. Despite this, the data from each of the participants shows that the strain sensor is able to track the motion of the knee during the rowing stroke.

Overshoot behaviour can explain some of the variation in the strain sensor signal at maximal knee flexion. This is particularly noticeable for participant 34943 (see Figure 6.2) in Step 1, where the first peak within the double peak is much higher than the second. At the catch position, a change in direction of the rower is taking place, and so the strain applied to the strain sensor is reversed, leading to stress-relaxation which causes this overshoot behaviour [140, 152]. This helps to explain why strain sensor signal is much more variable, in comparison to that from Vicon, from cycle to cycle at the upper end of the normalised sensor response. However, this does lead to difficulty in determining whether there has been a change in stroke length throughout the protocol as the stroke rate and intensity increase.

This type of behaviour is more pronounced in resistive-based strain sensors, which is the category this developed sensor falls into, and is affected by the viscoelasticity of the rubber matrix, the gauge factor (GF) of the strain sensor, and the strain rate that is applied to it [140, 152]. The intended application of this strain sensor means that there is little control over the applied strain rate, however there are modifications that can be made to the fabrication of the strain sensor which can help address the other factors. The movement of polymeric molecules within the strain sensor will lead to the movement of the carbon nanotubes (CNTs) responsible for charge transfer. Reducing the movement of the polymeric molecules would reduce the impact they have on overshoot behaviour, however this would negatively impact the elastic properties of the strain sensor. An alternative solution would be to improve the GF (currently 2-3), leading to a more sensitive strain sensor, by lowering the concentration of the CNT dispersion from 5 mg/mL, while also increasing the length of the strain sensor so that it experiences less overall strain during the knee flexion process [152].

The knee angles calculated from the Vicon output show that there is a change in knee range of motion between rowing steps, the most significant being for participant 22341 where there is a difference of 20.31° between the mean range of motion for Step 1 (127.03°) and Step 4 (106.72°). Murphy (2009) discusses the compensations made to technique to maintain stroke length when knee range of motion is reduced at higher rowing intensities, such as increased spinal flexion – this is a sign of technique deterioration that not only has an impact on performance but can also be a precursor to injury [15]. Observations regarding knee kinematics have also been made by Buckeridge et al. (2012) who noted that rowers become less effective at flexing their knees and hips at the catch and extending their knees

at the finish of the rowing stroke when work rate is increased, with anterior rotation of the pelvis on the recovery being linked to effective knee extension at the finish [237].

These previous findings and the results of this study indicate the benefits that can arise from monitoring knee range of motion in rowing. For participant 34943, this range of motion increased (from 124.51° to 130.60°) as the intensity increased with more knee flexion at the catch (from 120.96° to 135.66°), termed over-compression in rowing, which could be a result of this athlete having some level of hypermobility and less control of their movements. Over-compression can place additional stress on the knee joint and cause injury and so being able to monitor this is important. On the other hand, for participant 77344, knee flexion decreases from 141.29° to 136.03° and knee extension increases from 12.10° to 17.76° The range of motion is shortened at both ends, which will have a negative impact on the kinematics of the pelvis and trunk. As previously mentioned, currently the squat calibration does not allow for comparisons to be made between each of the rowing steps with regards to how knee range of motion is altered, as they have all been normalised individually. Altering the initial calibration step by conducting knee flexion at a higher speed, would enable the WSS to make relative comparisons of knee ROM as a function of rowing intensity that can already be ascertained from the Vicon output.

As discussed earlier, less knee extension at the finish of the rowing stroke can hinder anterior rotation of the pelvis [237]. This then impacts the sequence of movements on the recovery of the stroke. Looking at Step 1 for participant 48896 in Figure 6.7, between 25-60% of the stroke cycle the knee flexion angle remains approximately constant, which is accounted for by the movement of the trunk and the arms before and after the finish of the stroke. As the intensity increases, most noticeably in Steps 3 and 4, alongside there being less knee extension the amount of time spent with the knees extended is significantly reduced, accounting for about 5% of the stroke cycle. This suggests that this particular rower is flexing their knees while their upper body is still moving into a rocked over position. This improper sequencing of movements can make it more difficult for rowers to achieve higher stroke rates and also lead to the body mass of the rower crashing into the stern of the boat when on the water, negatively impacting boat speed. Although this is something that can be observed visually by coaches, being able to back up what they are saying with data from another source such as the WSS, can have more of an impact in creating change in the technique of some athletes.

With the knee warmer being the basis of the WSS, it is important that it fits well, otherwise it can distort the response of the strain sensor as seen for participant 69340 where the ill-fitting knee warmer led to bunching and the sensor not always being under tension. Data for participant 22341 may have been impacted by the knee warmer, with potentially some buckling of the strain sensor leading to noise in the signal, although nothing was observed by the participant or researcher. Different sized knee warmers were purchased in order to accommodate different leg sizes, however in future more time needs to be taken to ensure that the participant is comfortable with what they are wearing and not finding it restrictive in any way.

6.3.4 Summary

In this particular cohort study observing the rowing motion, the strain sensors used were able to detect all rowing strokes in all of the 25 of the steps presented here. With a well-fitting knee warmer as part of the wearable sensor system, the profile of the strain sensor is similar to that of Vicon and able to track knee flexion during the rowing stroke, but poor-fitting knee warmers can distort the results meaning they do not reflect the actual motion taking place.

A change in overall knee range of motion was observed from analysing the Vicon output, decreasing for several of the participants as the intensity increased, which can negatively impact rowing performance and also lead to injury. It is important to be able to monitor these changes outside of a laboratory environment with a system such as the one developed in this project, however small changes are needed to the design and fabrication to help facilitate this.

6.4 Cycling Cohort Study

As with the data presented in Section 6.3, the data related to the cycling study will include a few examples collected from the cohort of where the strain sensor response aligned with that of the motion capture system, as well as areas for improvement.

6.4.1 Study Population

The data of five participants are presented in this section, with repeat testing sessions for two participants, leading to a total of seven data sets. The details of each of these participants are listed in Table 6.7, including anthropometric details, cycling experience and the strain sensor used during testing. All participants used clipless foot retention (cycling specific shoes with cleats that clipped into pedals). An example of this is shown in Figure 6.12.

6.4.2 Results

Data were extracted from both the Vicon and sensor signals at different points to compare the response at the lowest cadence of 80 rpm, and at the higher cadences of 90 and 100 rpm. The points at which these sections of data were extracted within the testing protocol are listed in Table 6.8. Three sections of data capture at 80 rpm were also extracted to allow the signals to be compared at different points in the testing protocol: at the start of the protocol when the strain sensor has been subject to little strain; after the cadence ramp and approximately halfway through the protocol; after the maximal sprints towards the end of the protocol.

These results are split into two sections: the first visually compares the signals from the strain sensor and Vicon, while the second details the mean maximum and minimum knee flexion angles as obtained from the Vicon signal.



(a) **(b)**

Figure 6.12: Example of clipless foot retention used in cycling a) pedal attached to bike, b) cycling shoes with the left hand shoe showing the cleat on the underside that clips into the pedal.

Table 6.7: Participant and sensor details for cycling cohort study.

Participant details										Sensor details	
Partici-pant ID	Test ses-sion	Sex	Age (years)	Height (cm)	Body mass (kg)	Cycling expe-rience (years)	Preferred disci-pline	Participation	Training (hours)	Sensor num-ber	Sensor use
50560	1	Male	29	175	75	14	Road	Leisure Rider	12	1	1
39683	2	Female	26	163	48	4	Road	Leisure Rider	9	1	4
69013	1	Male	26	196	69	20	Road	Leisure Rider	10	1	9
60435	1	Male	38	180	79	34	Road	Leisure Rider	7	3	4
60435	2	-	-	-	-	-	-	-	-	3	5
59445	1	Female	28	166	71.6	5	Track	Competitive (racer)	7	3	6
59445	2	-	-	-	-	-	-	-	-	3	7

The start of the pedal stroke cycle was taken to be when the right knee (instrumented with markers and the WSS) was most flexed and the foot was in the 12 o'clock position. One full revolution of the pedal and foot was equal to one pedal stroke cycle. The notation used for the sensors in this results section is S1-004, where S1 = the sensor number and 004 is the use number of the sensor.

Table 6.8: Sections of data extraction for analysis, showing the average cadence for that section and the time period this corresponds to within the testing protocol.

Average cadence (rpm)	Time period in protocol (min)
80 rpm (1)	2:00 - 3:00
90 rpm	7:30 - 8:30
100 rpm	11:15 - 12:15
80 rpm (2)	13:30 - 14:30
80 rpm (3)	18:03 - 19:03

6.4.2.1 Analysis of Strain Sensor Response

This section compares the signals from the strain sensor and the Vicon motion capture system. For each participant (and testing visit) there are four sets of plots, with two plots showing only the strain sensor signal and the remaining two showing the overlaid time-normalised response from both Vicon and the strain sensor. Within each plot type, comparisons are made between the sensor response at each cadence (80 rpm - first extract, 90 rpm and 100 rpm), as well as the three 80 rpm data extracts.

6.4.2.1.1 Participant 50560 - visit 1/2

Looking at the normalised sensor response as the cadence increases from 80 rpm to 100 rpm in Figure 6.13, double peaks can be observed in the signal. The cycle for each pedal stoke is distinguishable at the lowest and highest cadences, however at 90 rpm the drop in sensor response between the double peak is so low that it is difficult to establish where each cycle starts and ends. As the cadence increases, the signal range decreases from approximately 0.7 to 0.4.

The double peaks become less prominent as the protocol continues, as seen in the second and third 80 rpm data extracts in Figure 6.15. The overall signal range is still low in the second 80 rpm extract, but has increased slightly to approximately 0.5 in the third data extract.

Comparing the time-normalised strain signal to Vicon in Figures 6.14 and 6.16, it can be seen that there is much more variation between pedal strokes for the strain sensor, especially at the upper end of the response values which corresponds to the knee being most flexed. In Figure 6.16 for the final 80 rpm extract, even at the bottom of the pedal stroke where knee is extended and the strain sensor values are low, there is significantly more variation in the sensor signal.

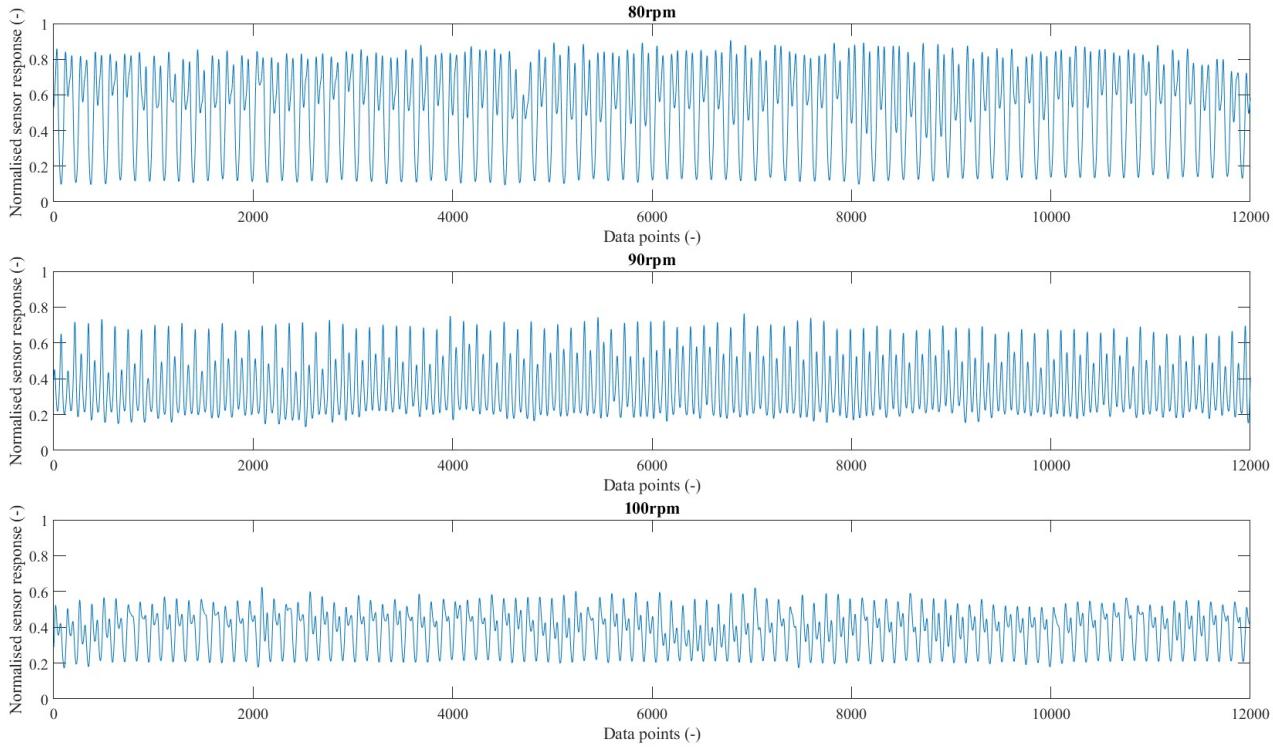


Figure 6.13: Normalised sensor response for 3 × 1-min segments at 80, 90 and 100 rpm during the cycling protocol, performed by participant 50560.

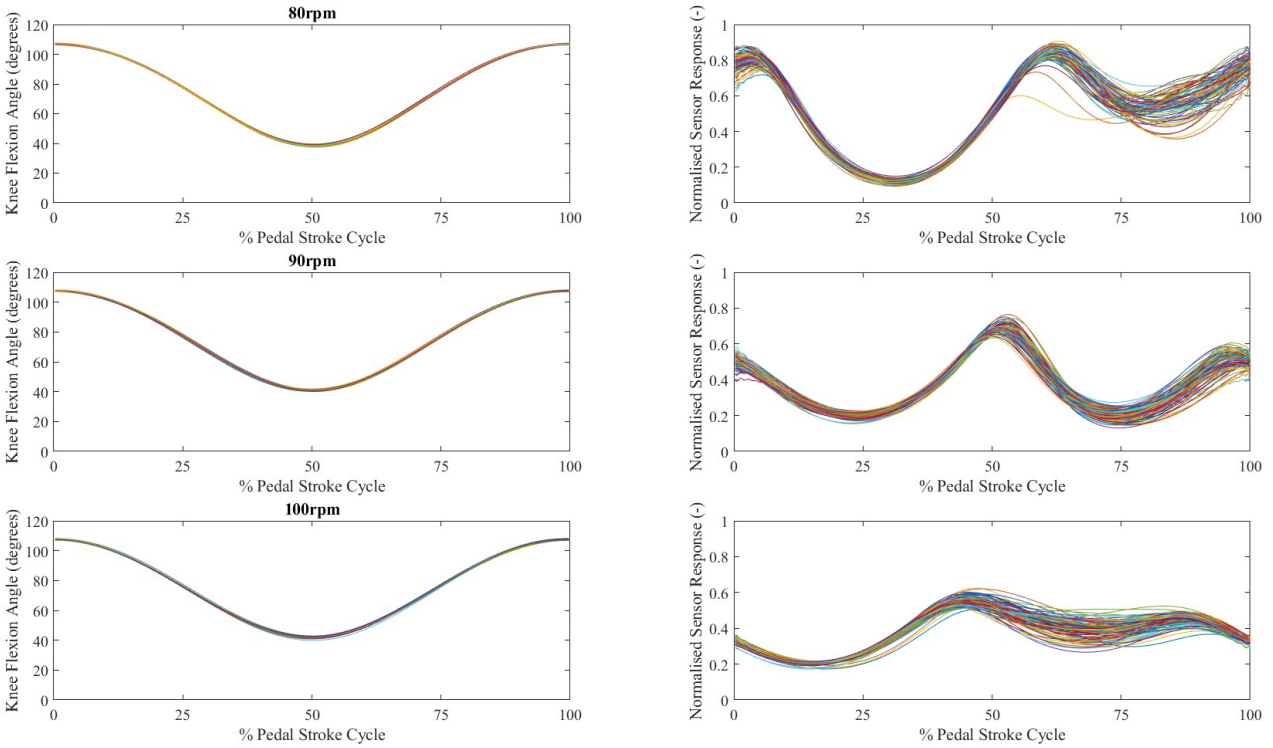


Figure 6.14: Overlaid time-normalised response for each pedal revolution for 3 × 1-min segments at 80, 90 and 100 rpm during the cycling protocol. Knee angles from Vicon on the left and strain sensor response on the right for participant 50560.

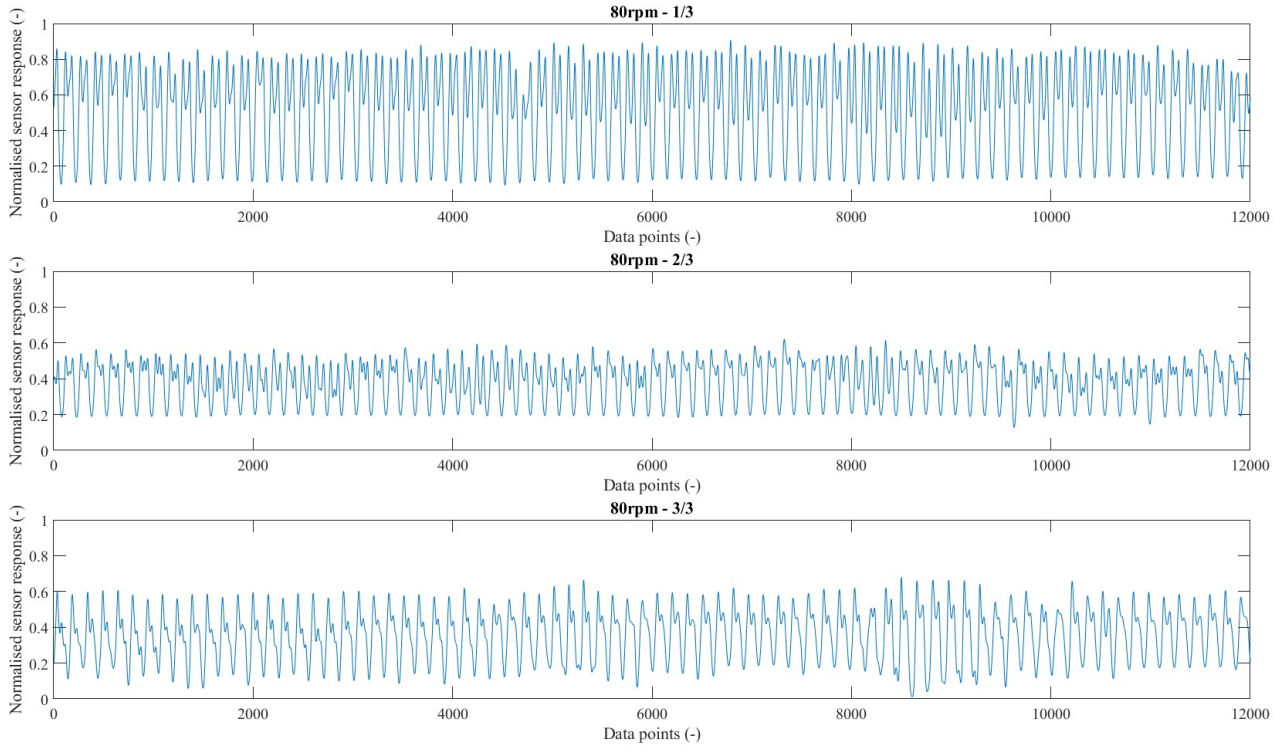


Figure 6.15: Normalised sensor response for for 3 × 1-min segments each at 80 rpm during the cycling protocol, performed by participant 50560.

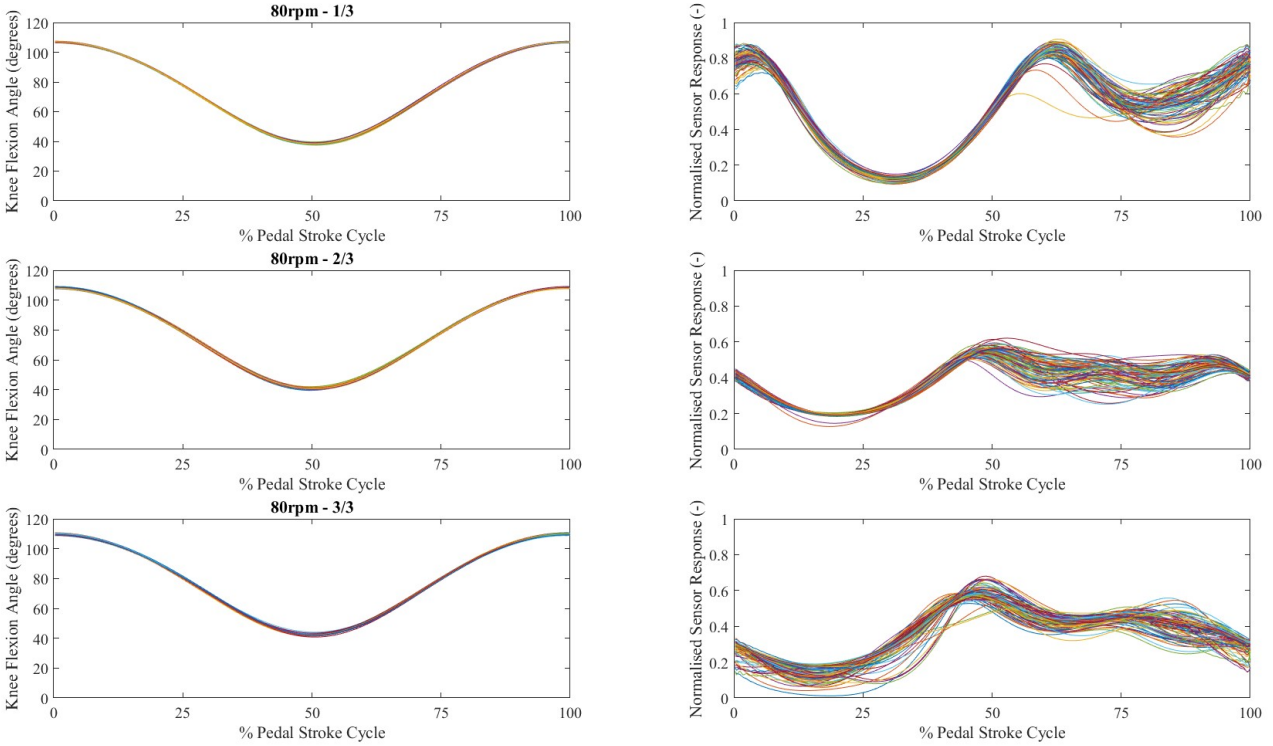


Figure 6.16: Overlaid time-normalised response for each each pedal revolution for 3 × 1-min segments each at 80 rpm during the cycling protocol. Knee angles from Vicon on the left and strain sensor response on the right for participant 50560.

6.4.2.1.2 Participant 39683 - visit 2/2

The same strain sensor used for participant 50560 (S1-001) was also used for participant 39683 (S1-004), with this being the fourth use of this particular sensor. Double peaks are still present in the sensor signal and their range is significant (more than half of the overall signal range), as seen in Figure 6.17, however it is clear where the start and end of each cycle is for all three cadences. The time-normalised plots in Figure 6.18 emphasise just how prominent these double peaks are in the sensor signal – for the one cycle seen in the Vicon plots, there seems to be two cycles in the strain sensor plots with the signal more varied in the second cycle.

For this particular participant, it can be seen that the there is less consistency in the knee angle measured by Vicon at the bottom of the pedal stroke when the knee is extended compared to the top of the pedal stroke, especially at 80 rpm in Figure 6.18. This is not a feature that is noticeable in the strain sensor signal.

Returning to the normalised strain sensor signal, the response range is similar across the three plots in Figure 6.17 and also during the second 80 rpm extract in Figure 6.19. It is then almost halved in the plot for the third 80 rpm extract from approximately 0.8 to 0.4. This reduced range is more noticeable when comparing the time-normalised plots in Figure 6.20 – the curve for the third 80 rpm extract is almost flattened compared to the other 80 rpm extracts. Again in the Vicon signal for all three 80 rpm extracts, there is more dissimilarity in the knee angles measured at the bottom of the pedal stroke when the knee is extended.

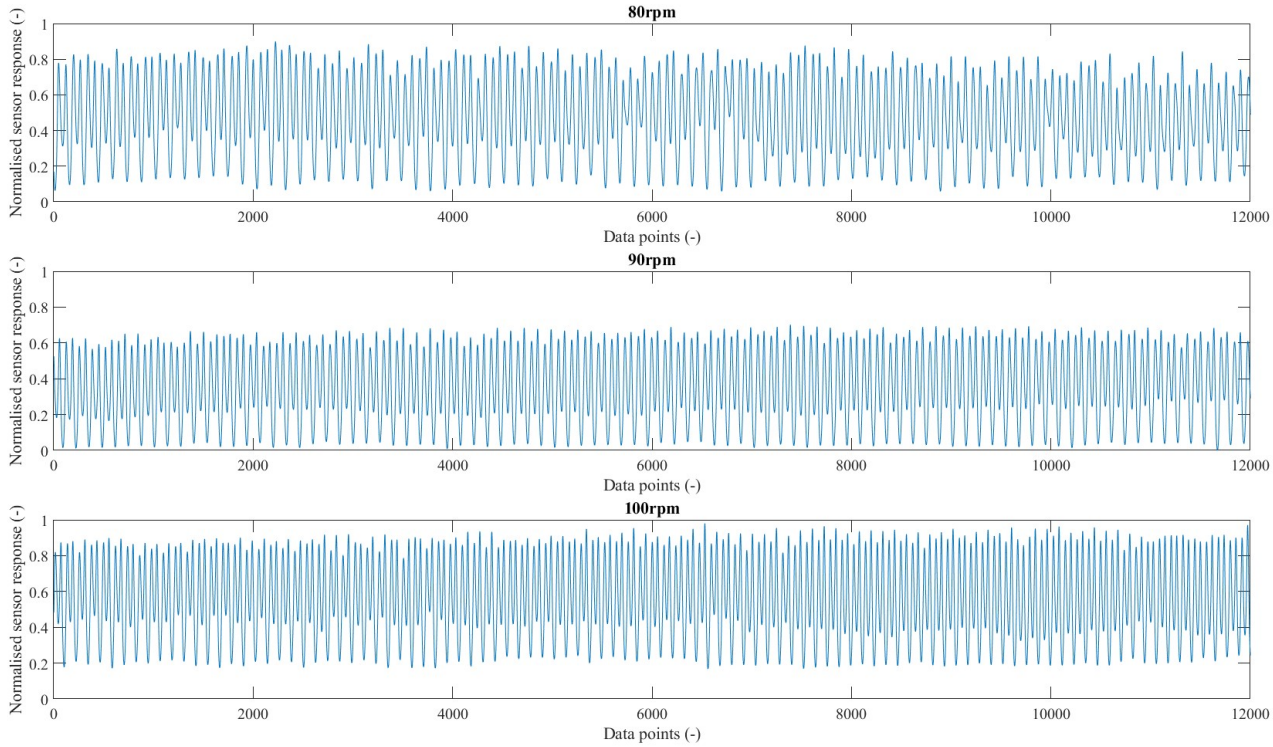


Figure 6.17: Normalised sensor response for 3 × 1-min segments at 80, 90 and 100 rpm during the cycling protocol, performed by participant 39683.

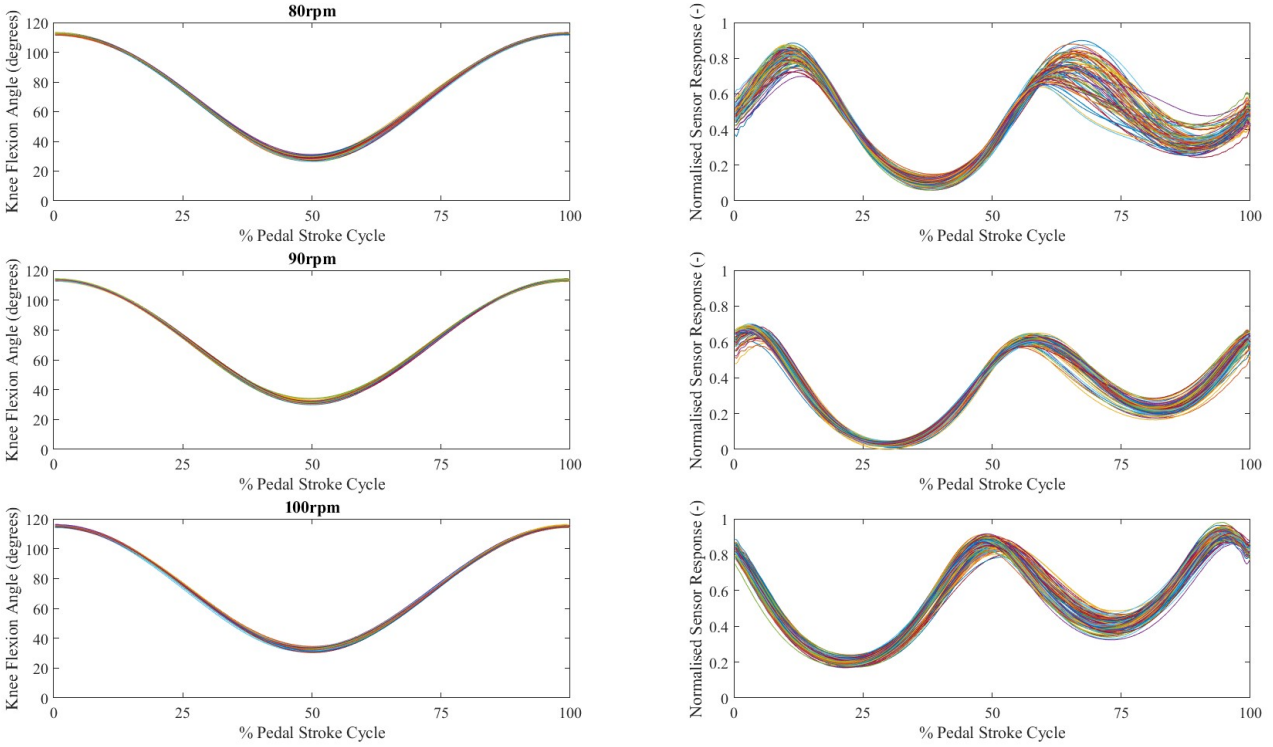


Figure 6.18: Overlaid time-normalised response for each pedal revolution for 3 × 1-min segments at 80, 90 and 100 rpm during the cycling protocol. Knee angles from Vicon on the left and strain sensor response on the right for participant 39683.

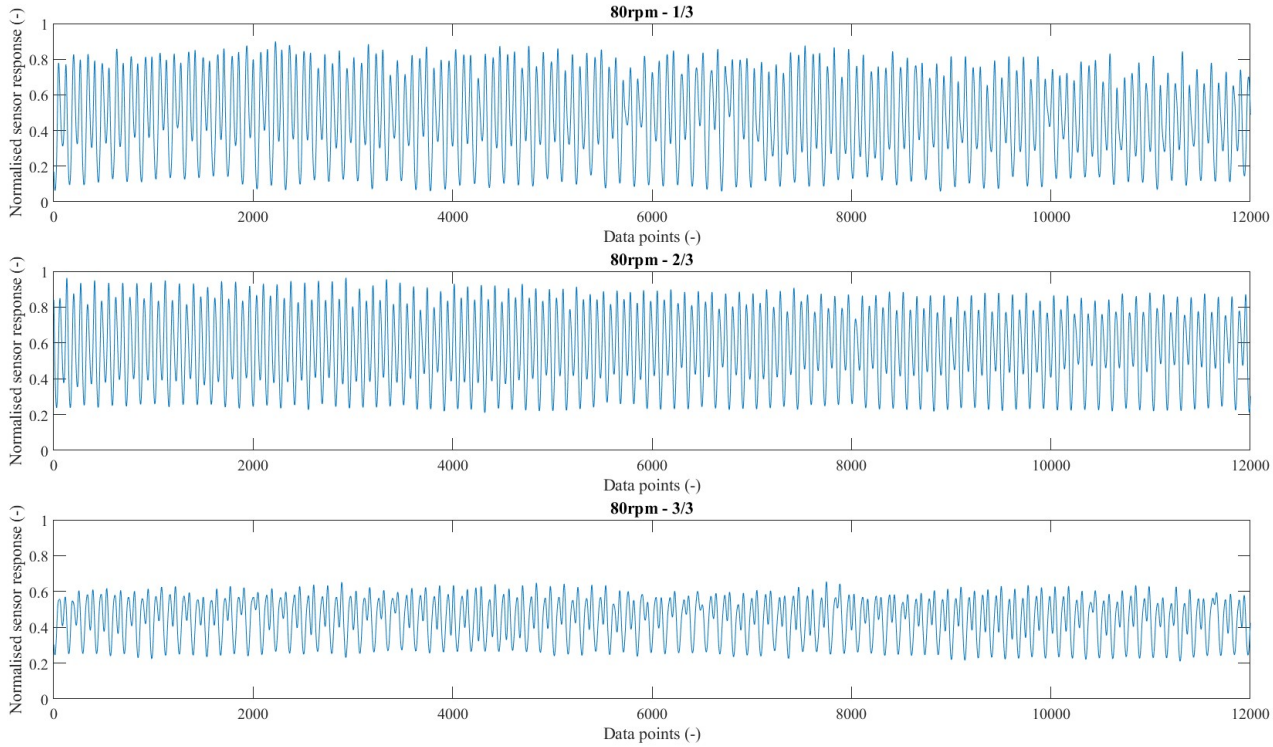


Figure 6.19: Normalised sensor response for for 3 × 1-min segments each at 80 rpm during the cycling protocol, performed by participant 39683.

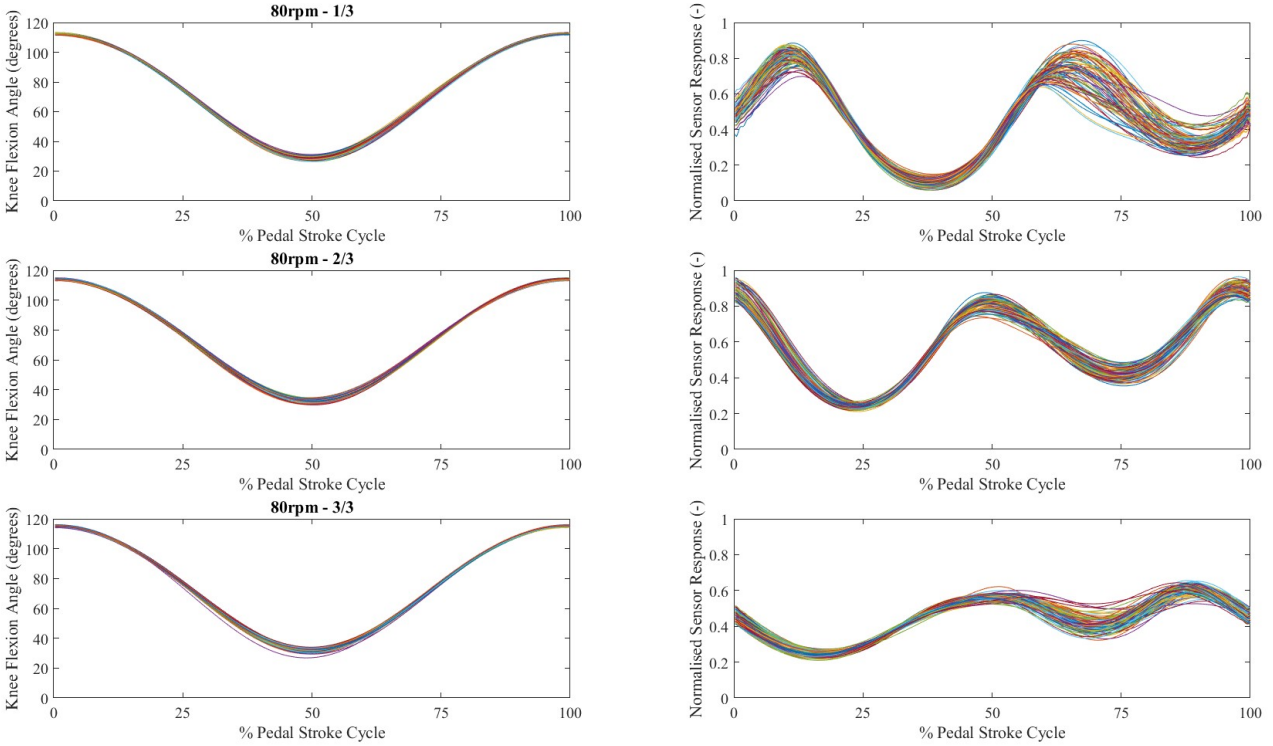


Figure 6.20: Overlaid time-normalised response for each each pedal revolution for 3 × 1-min segments each at 80 rpm during the cycling protocol. Knee angles from Vicon on the left and strain sensor response on the right for participant 39683.

6.4.2.1.3 Participant 69013 - visit 1/2

The same strain sensor was used for participant 69013 as for the previous two participants already presented, with this being the ninth use of the sensor (S1-009). The double peaks in each cycle of the normalised sensor response in Figure 6.21 are less prominent, even as the overall signal range decreases slightly with increasing cadence. This carries across to the time-normalised plots in Figure 6.22 where one wave can be seen in the sensor signal, but still the presence of the double peak means that the profile does not match that of Vicon which is a much smoother sinusoidal wave. Although the profiles from the two signals do not match, the signal from the strain sensor is less varied compared to the previous two participants presented. The knee angles measured by Vicon in each of the plots in Figure 6.22 remain consistent throughout the pedal strokes and across the different cadences also.

Comparing the 80 rpm repeats and the signal plots in Figure 6.23, the sensor response range decreases slightly from the first to second 80 rpm repeat (approximately 0.5 to 0.4) and the entire signal is also shifted down (with the minimum values lowering from approximately 0.3 to 0.1). The range decreases again between the second and third repeats by approximately 0.05. This is represented in the time-normalised plots in Figure 6.24 with a flatter curve in plots two and three compared to the first plot.

For this participant, there is more disparity in the measured knee angle at the bottom of the pedal stroke when it is extended within the second and third 80 rpm extracts compared to the first 80 rpm extract. For the third 80 rpm extract, there appears to be more disparity throughout the entire pedal stroke and not just at the bottom of it.

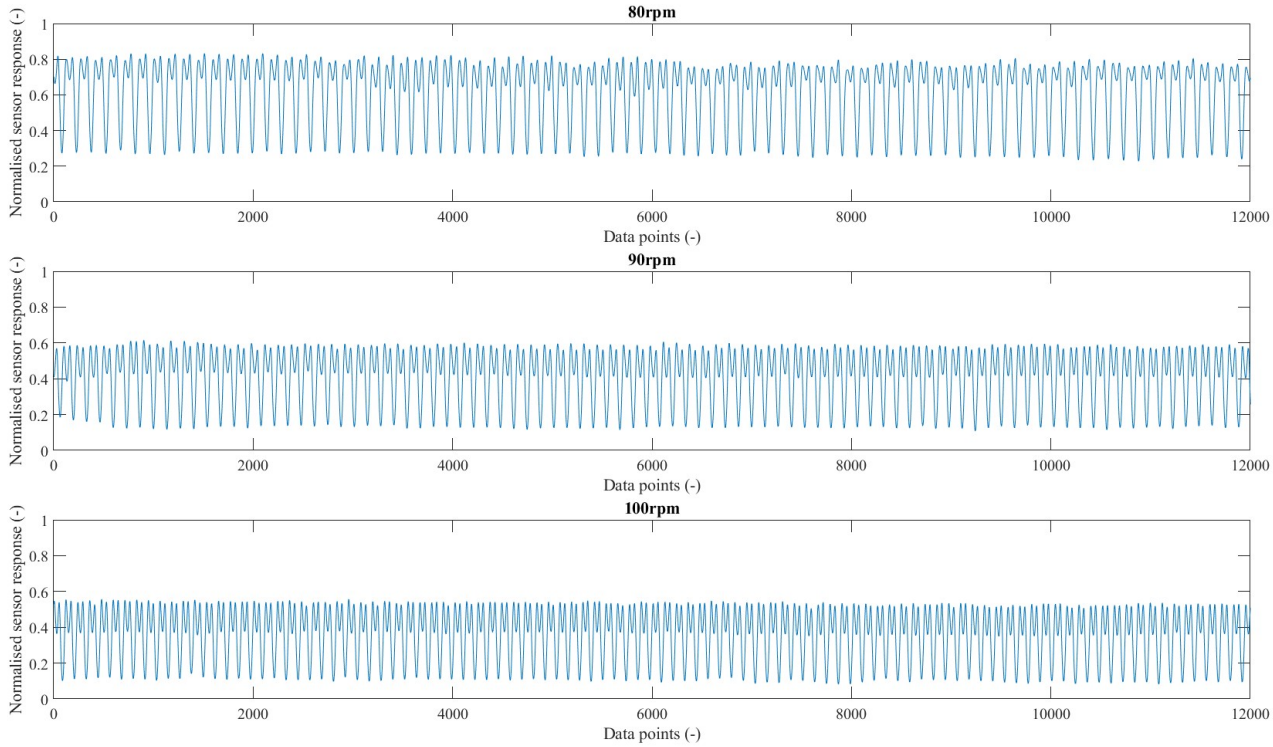


Figure 6.21: Normalised sensor response for 3 × 1-min segments at 80, 90 and 100 rpm during the cycling protocol, performed by participant 69013.

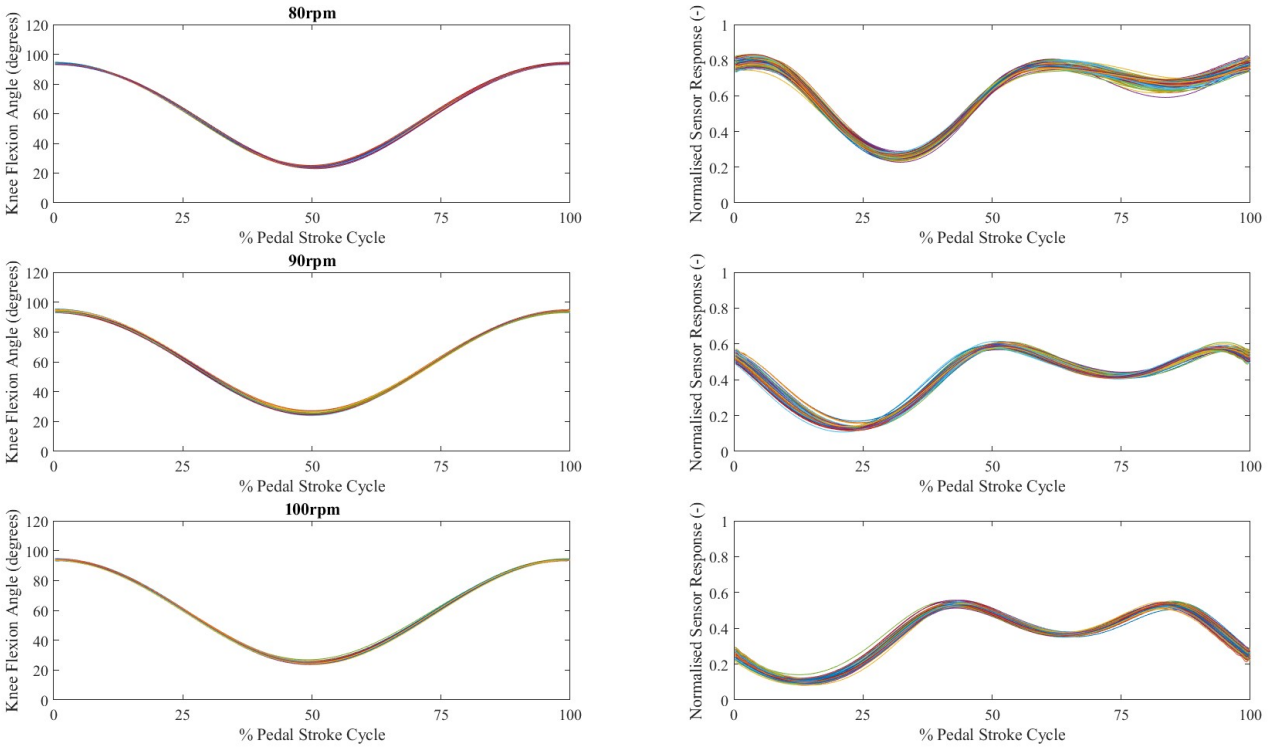


Figure 6.22: Overlaid time-normalised response for each pedal revolution for 3 × 1-min segments at 80, 90 and 100 rpm during the cycling protocol. Knee angles from Vicon on the left and strain sensor response on the right for participant 69013.

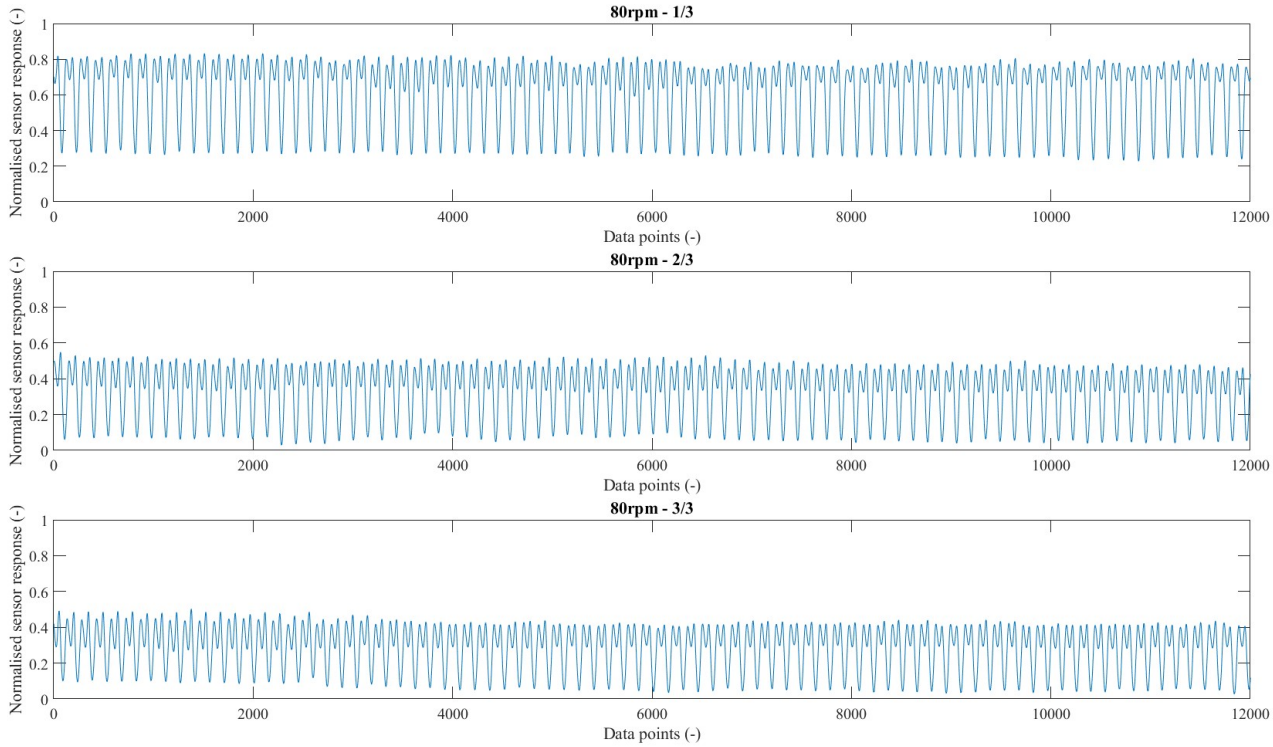


Figure 6.23: Normalised sensor response for for 3 × 1-min segments each at 80 rpm during the cycling protocol, performed by participant 69013.

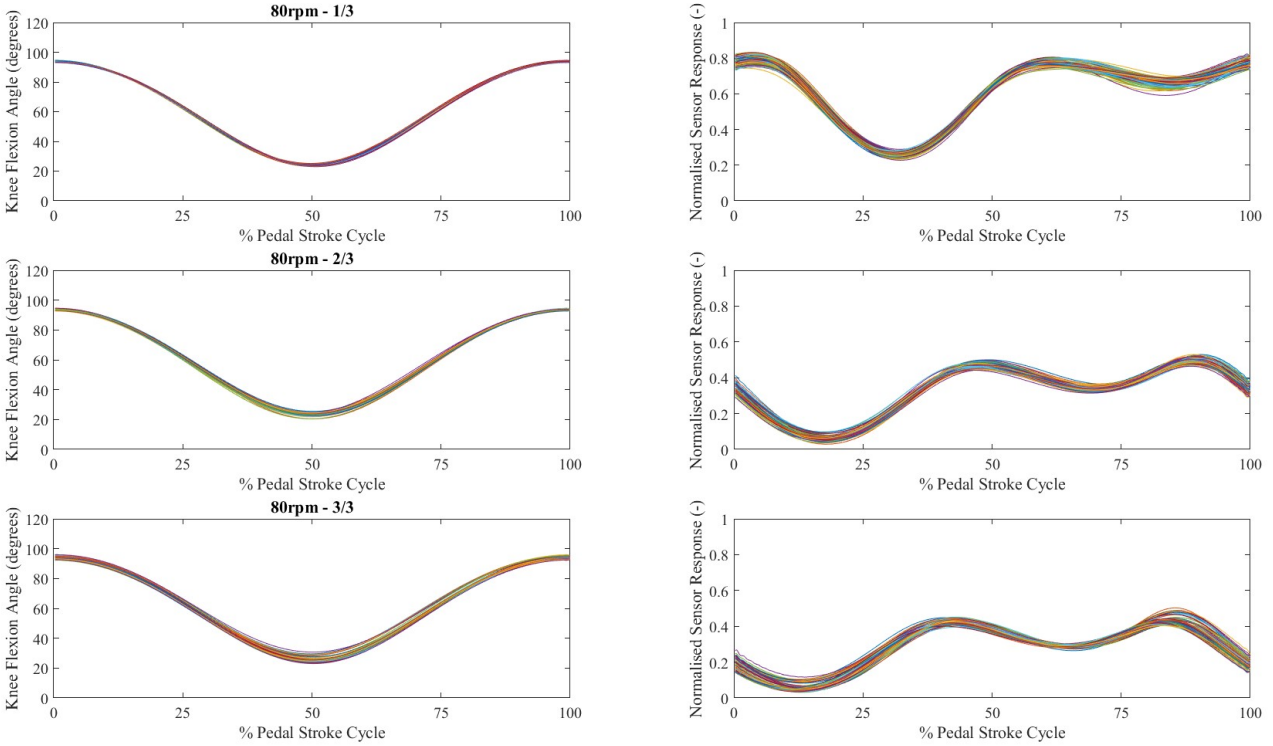


Figure 6.24: Overlaid time-normalised response for each each pedal revolution for 3 × 1-min segments each at 80 rpm during the cycling protocol. Knee angles from Vicon on the left and strain sensor response on the right for participant 69013.

6.4.2.1.4 Participant 60435 - visit 1/2

A different sensor was used for participant 60435, with this being the fourth use of this particular strain sensor (S3-004). The signal range remains consistent across the three different cadence extracts presented in Figure 6.25. There are double peaks, as featured in all previous signals, however these are much smaller and the second peak is slightly higher in amplitude than the first.

In Figure 6.26 the time-normalised strain sensor signal plots have the most similar profile to the corresponding Vicon plots out of all those presented so far (with the top of the curve being extended due to the double peaks). The overlaid pedal stroke cycles in these plots are also more similar to each other compared to previous plots, such as Figure 6.23 for participant 69013. The Vicon plots also have little difference throughout the pedal stroke at each of the three cadences.

Comparing the 80 rpm extracts in Figure 6.27, the double peaks continue to be less prominent as the testing protocol continues. By the final plot, the response range is almost halved to 0.4 in comparison to the first plot, producing the flattened time-normalised plot seen in Figure 6.28. The knee angles remain consistent throughout the pedal strokes at each of the repeats in Figure 6.28, but one outlier can be seen in the third 80 rpm repeat. This can also be spotted in the equivalent strain sensor plot.

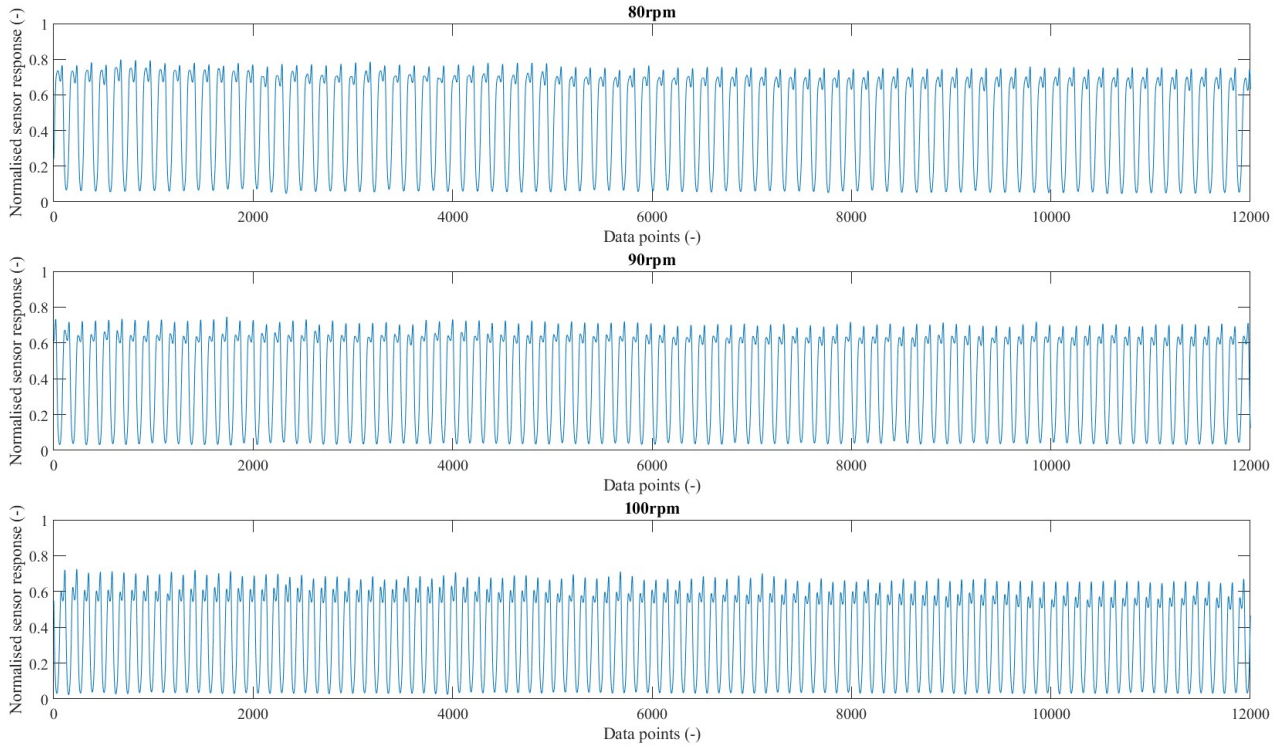


Figure 6.25: Normalised sensor response for 3 × 1-min segments at 80, 90 and 100 rpm during the cycling protocol, performed by participant 60435, visit 1/2.

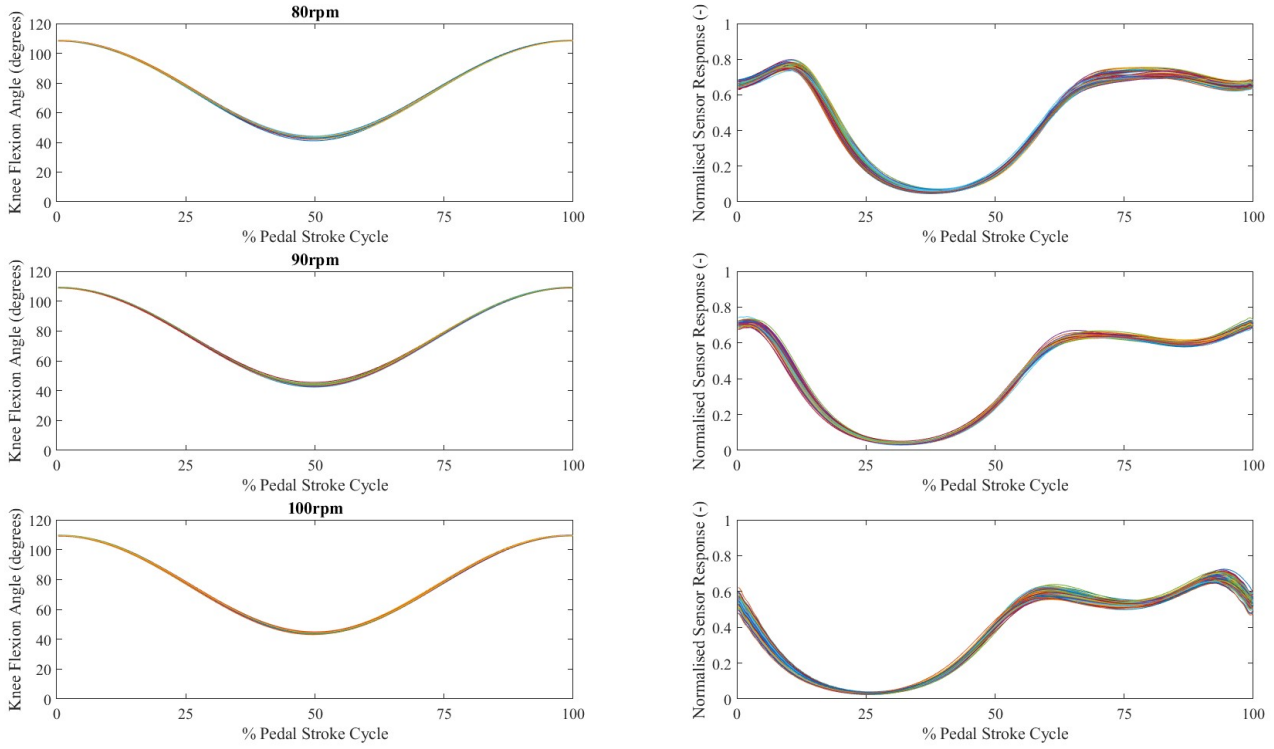


Figure 6.26: Overlaid time-normalised response for each pedal revolution for 3 × 1-min segments at 80, 90 and 100 rpm during the cycling protocol. Knee angles from Vicon on the left and strain sensor response on the right for participant 60435, visit 1/2.

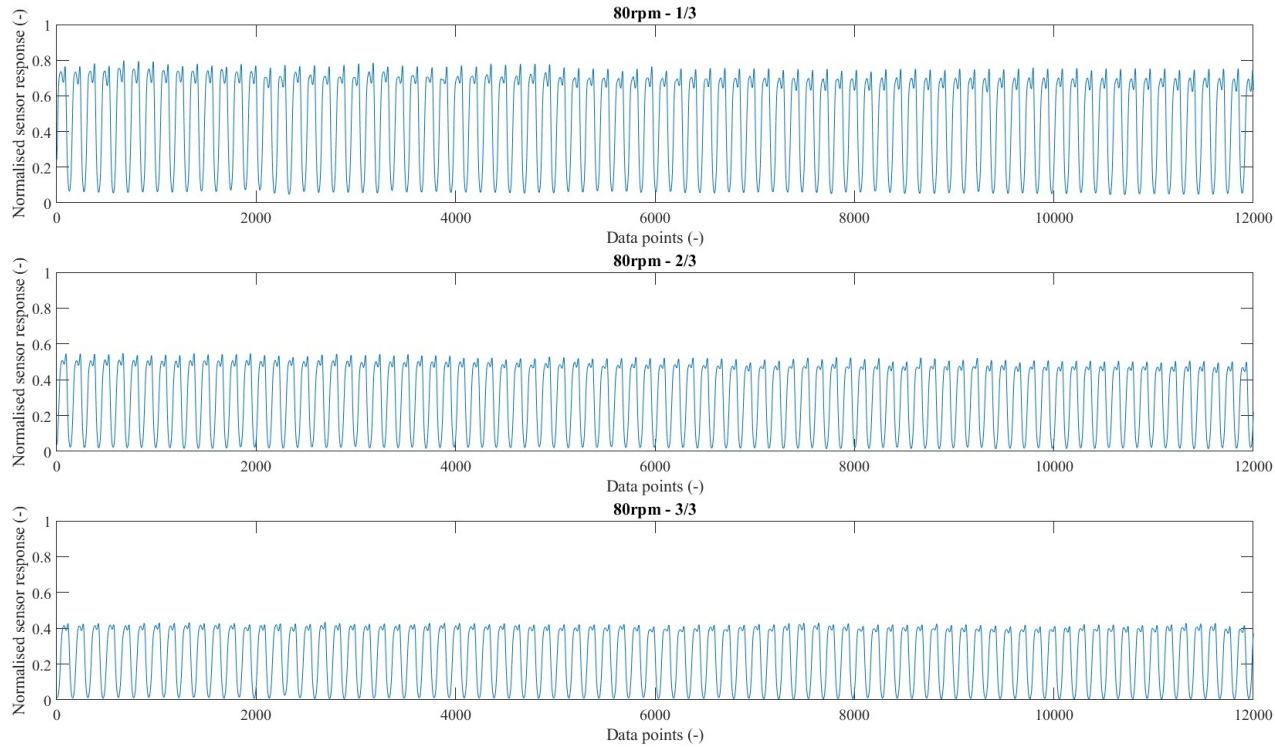


Figure 6.27: Normalised sensor response for for 3 × 1-min segments each at 80 rpm during the cycling protocol, performed by participant 60435, visit 1/2.

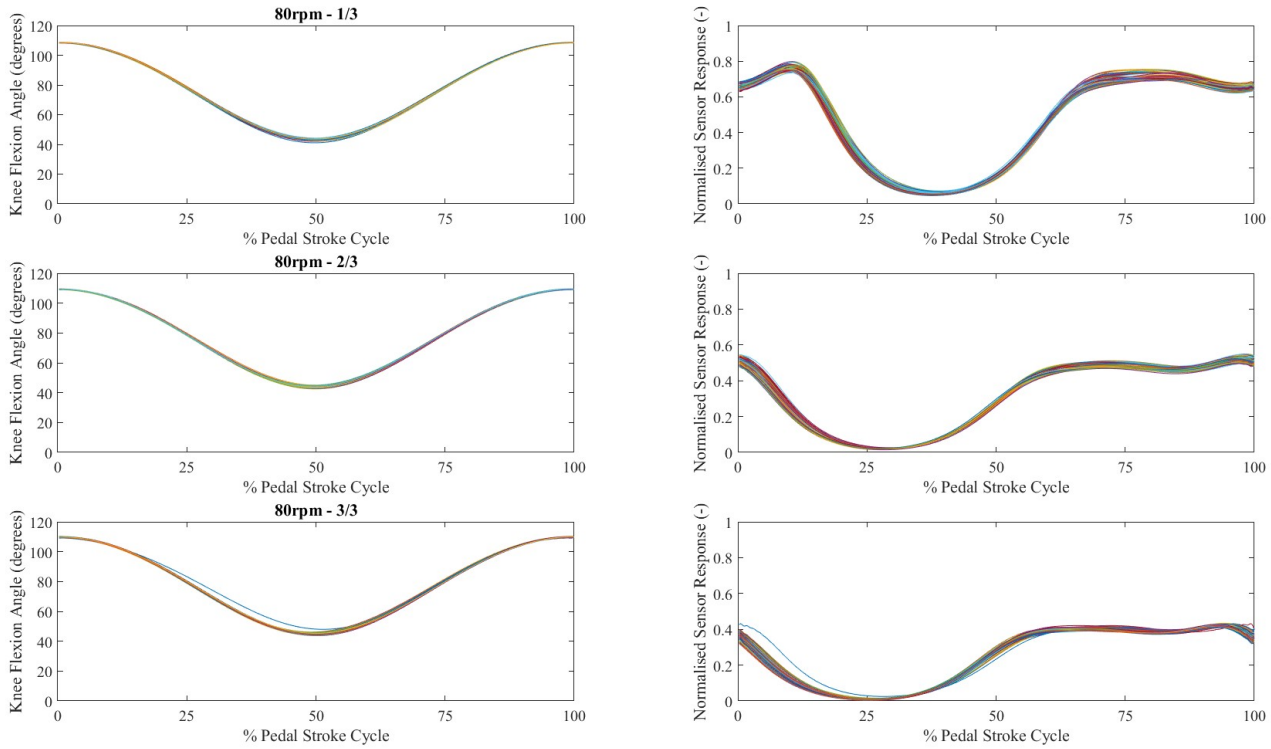


Figure 6.28: Overlaid time-normalised response for each each pedal revolution for 3 × 1-min segments each at 80 rpm during the cycling protocol. Knee angles from Vicon on the left and strain sensor response on the right for participant 60435, visit 1/2.

6.4.2.1.5 Participant 60435 - visit 2/2

The same strain sensor was used for this participant's second visit to complete the cycling protocol (S3-005). The normalised signal for the strain sensor response in Figure 6.29 is very similar to the first visit, with small double peaks present in each strain cycle. The overall range reduces between the 80 rpm and 90 rpm extracts (by approximately 0.1) and then remains constant between the 90 rpm and 100 rpm extracts. Similarities can also be seen in the time-normalised plots in Figure 6.30 for this visit and Figure 6.26 for the first visit with the overlaid cycles in the sensor signals being closer together and there being little change in knee angles at each cadence also.

During the testing protocol, the strain sensor response range in Figure 6.31 decreases from the first to second 80 rpm repeat by approximately 0.2, making it slightly lower than the 100 rpm extract in Figure 6.30 and following a similar pattern to the first visit. Again, this is reflected in the time-normalised plots in Figure 6.32.

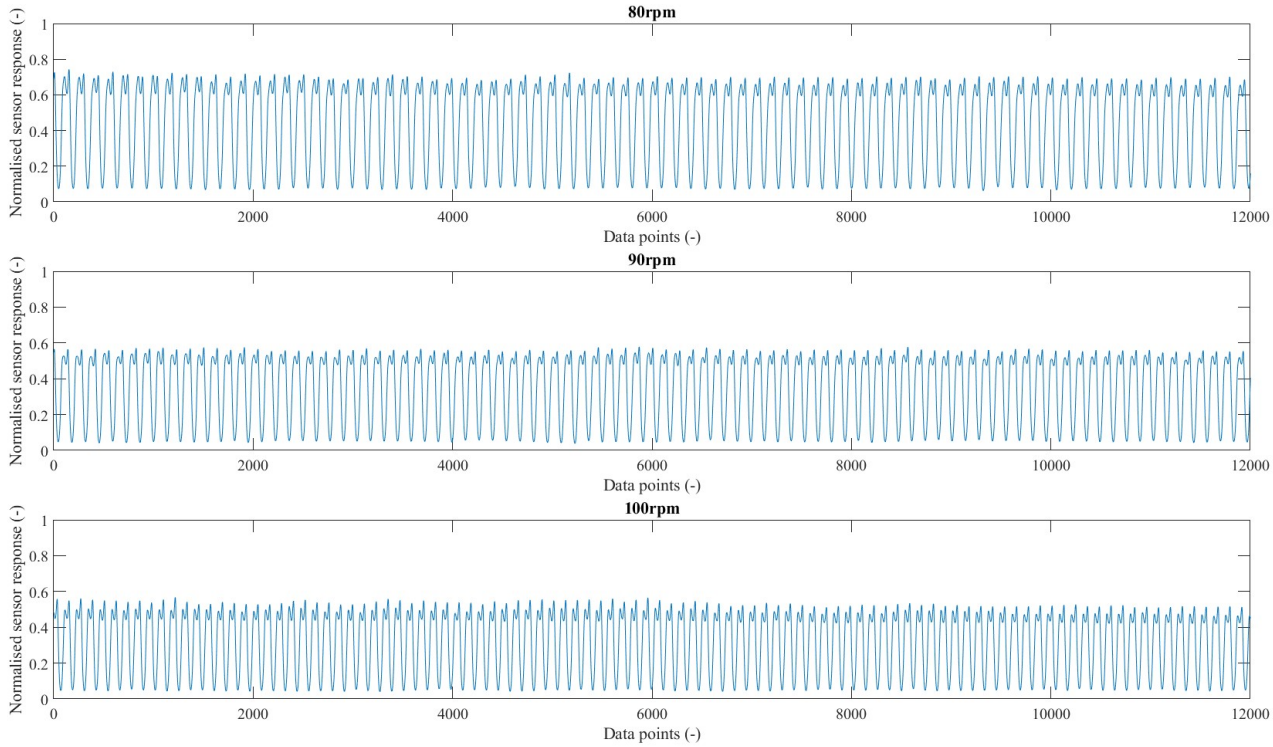


Figure 6.29: Normalised sensor response for 3 × 1-min segments at 80, 90 and 100 rpm during the cycling protocol, performed by participant 60435, visit 2/2.

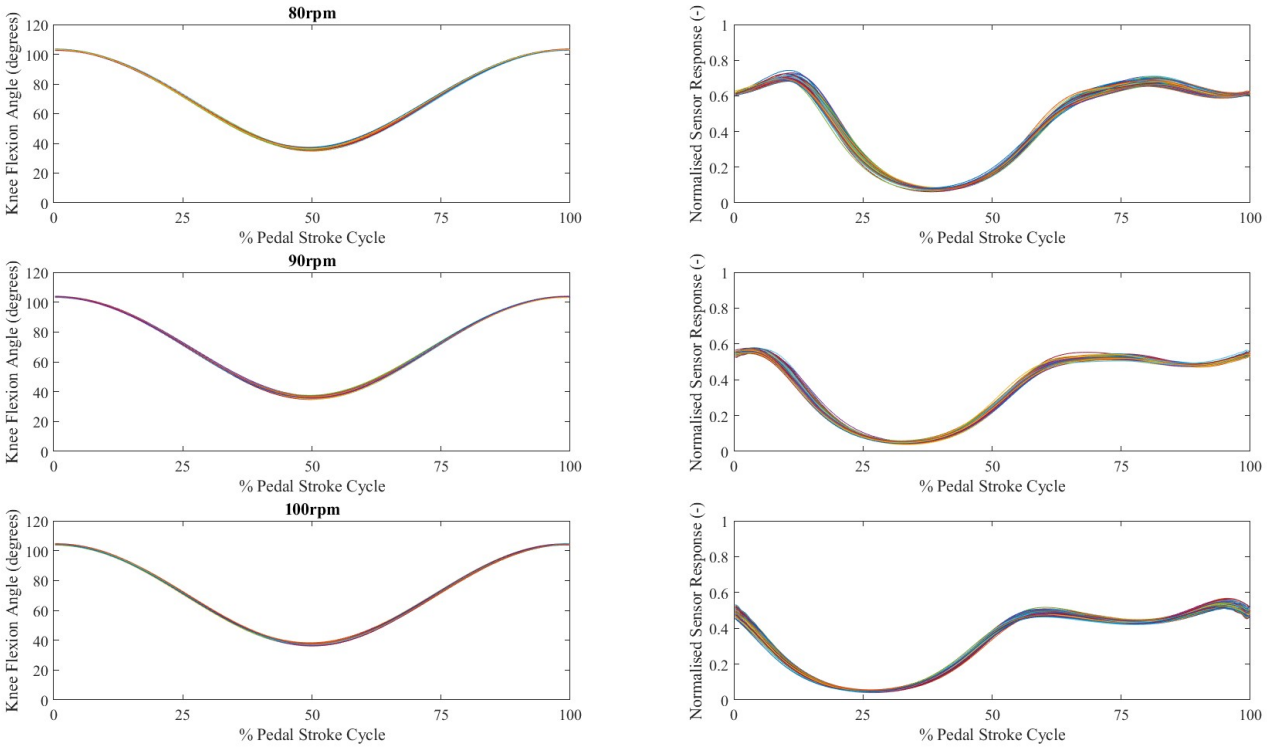


Figure 6.30: Overlaid time-normalised response for each pedal revolution for 3 × 1-min segments at 80, 90 and 100 rpm during the cycling protocol. Knee angles from Vicon on the left and strain sensor response on the right for participant 60435, visit 2/2.

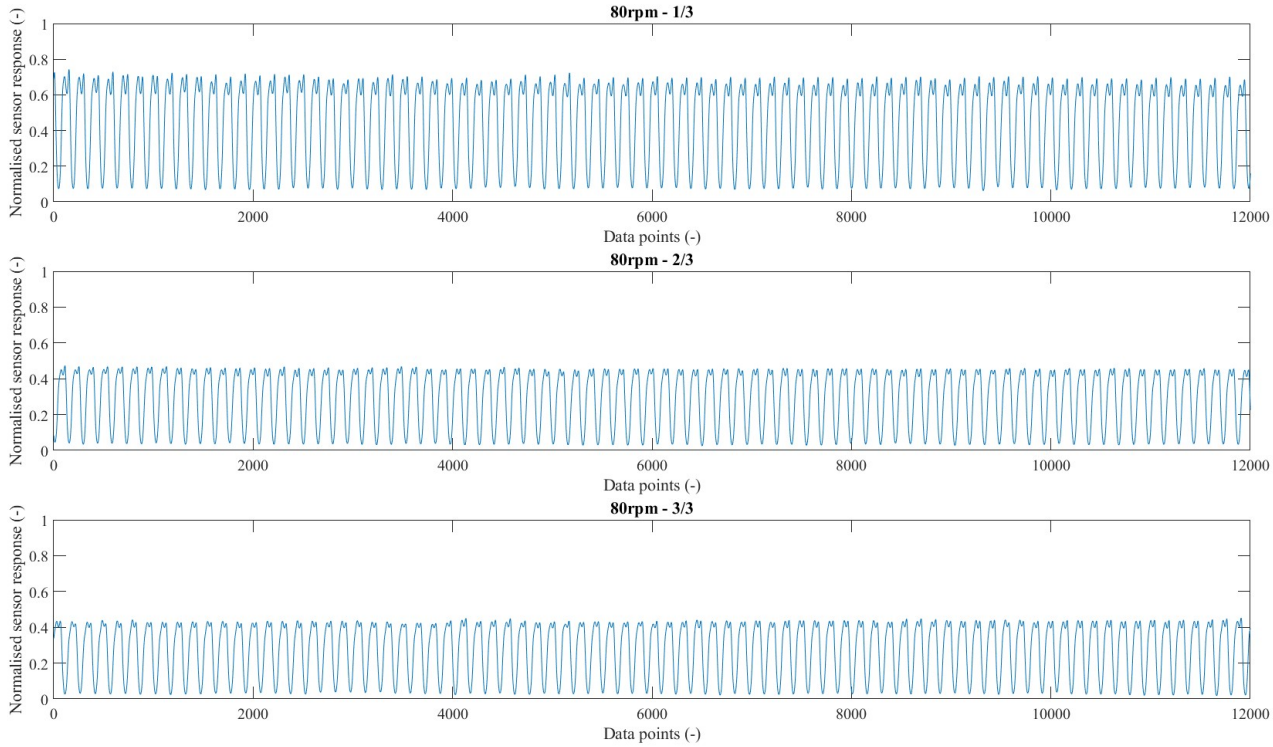


Figure 6.31: Normalised sensor response for for 3 × 1-min segments each at 80 rpm during the cycling protocol, performed by participant 60435, visit 2/2.

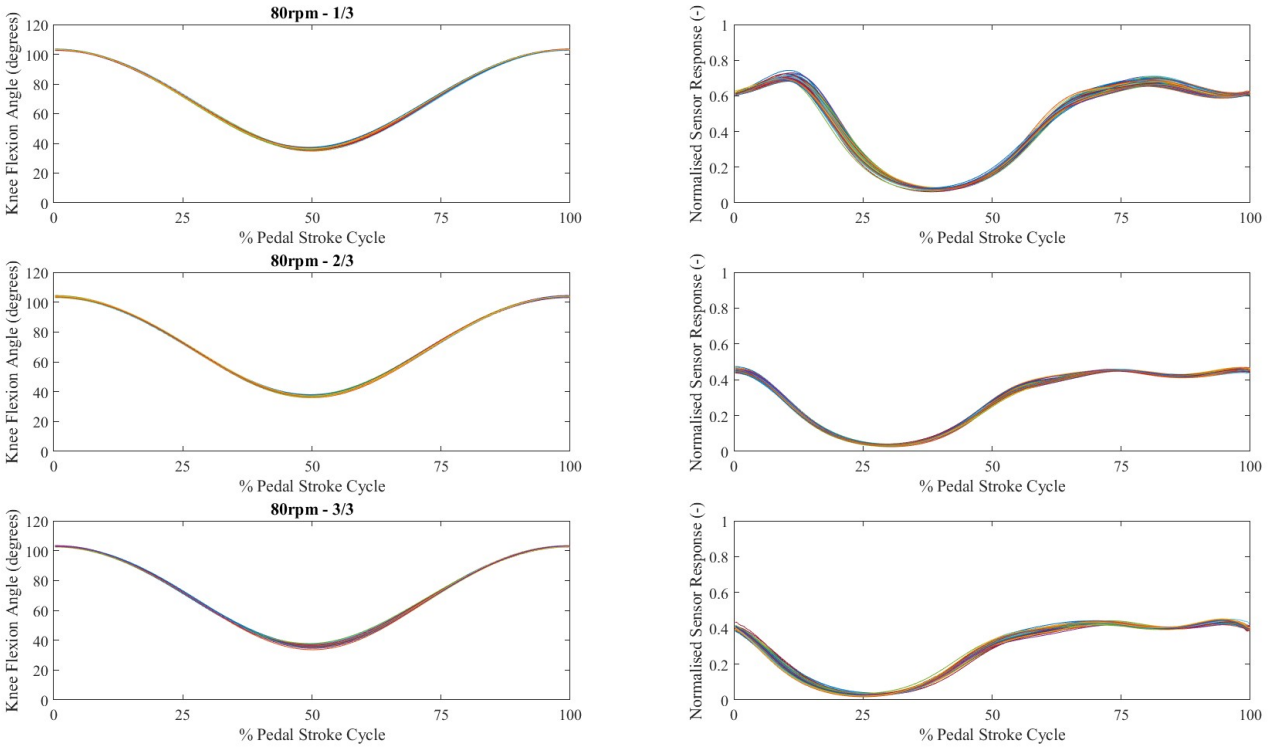


Figure 6.32: Overlaid time-normalised response for each each pedal revolution for 3 × 1-min segments each at 80 rpm during the cycling protocol. Knee angles from Vicon on the left and strain sensor response on the right for participant 60435, visit 2/2.

6.4.2.1.6 Participant 59445 - visit 1/2

The strain sensor used for this participant (59445) was the same as that used for the previous participant (60435) and this was the sixth use (S3-006). The features in Figure 6.33 are similar as those seen the normalised sensor response plots for participant 60435 (Figure 6.25 and Figure 6.29). The double peaks are small, with the second being slightly larger in amplitude. The signal range reduces from 0.8 at 80 rpm to 0.55 at 90 rpm.

There is more discrepancy in the second half of the pedal stroke cycle in the time-normalised plot at 80 rpm in Figure 6.34, corresponding to the upward phase of the pedal stroke. There is less discrepancy as the cadence increases to 90 rpm and the knee angles appear consistent throughout the pedal stroke as the cadence is further increased to 100 rpm. The strain sensor response appears to follow a similar pattern, with more variation between cycles at 80 rpm, that decreases as the cadence increases, but it should be noted that is occurs more when the knee is flexed and the sensor is being stretched at the top of the pedal stroke.

The double peaks are still present in the strain sensor when comparing the 80 rpm data extracts in Figure 6.35. In the second extract, the overall range steps up around 4000 data points in, from just below to just above 0.6. The Vicon time-normalised plot for the second extract in Figure 6.36 shows the most difference in knee angle throughout the pedal stroke for any of the participants presented so far, with one cycle an outlier when compared to the rest. By contrast, the final extract shows almost no variation in knee angle throughout the pedal stroke. Again, these patterns appear to be reflected in the sensor signal.

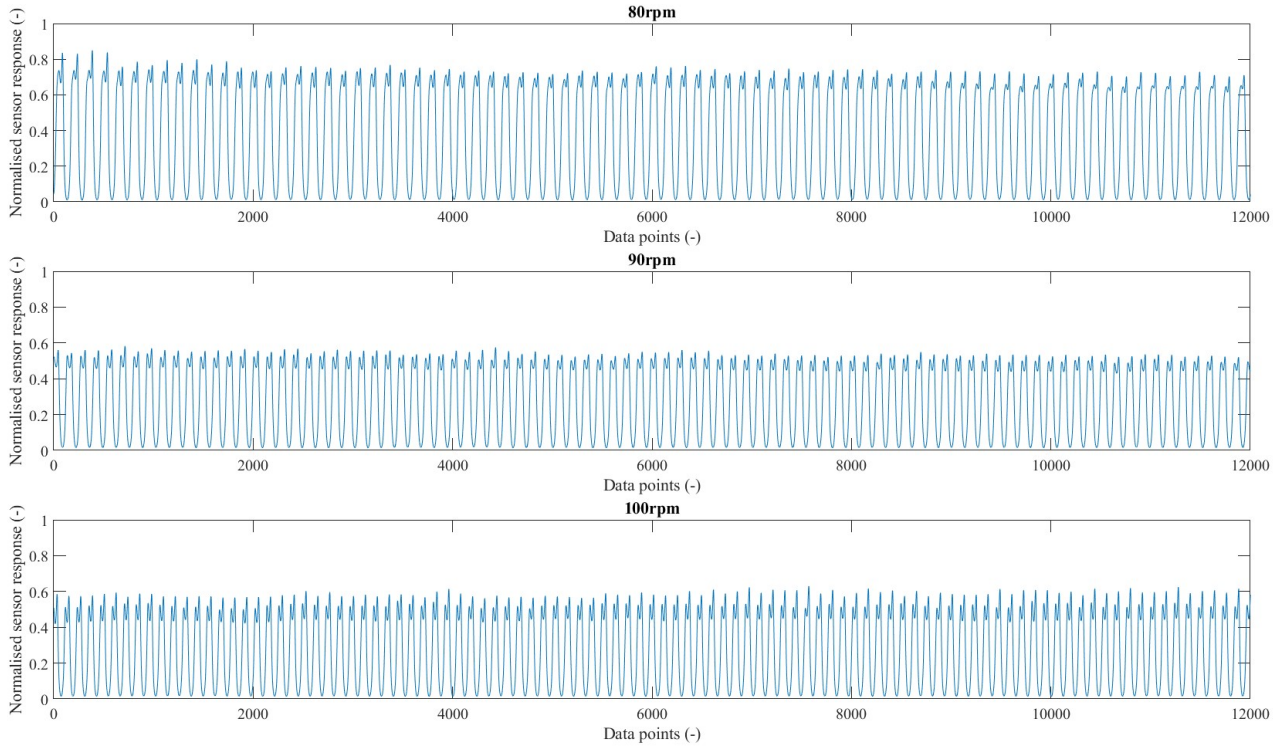


Figure 6.33: Normalised sensor response for 3 × 1-min segments at 80, 90 and 100 rpm during the cycling protocol, performed by participant 59445, visit 1/2.

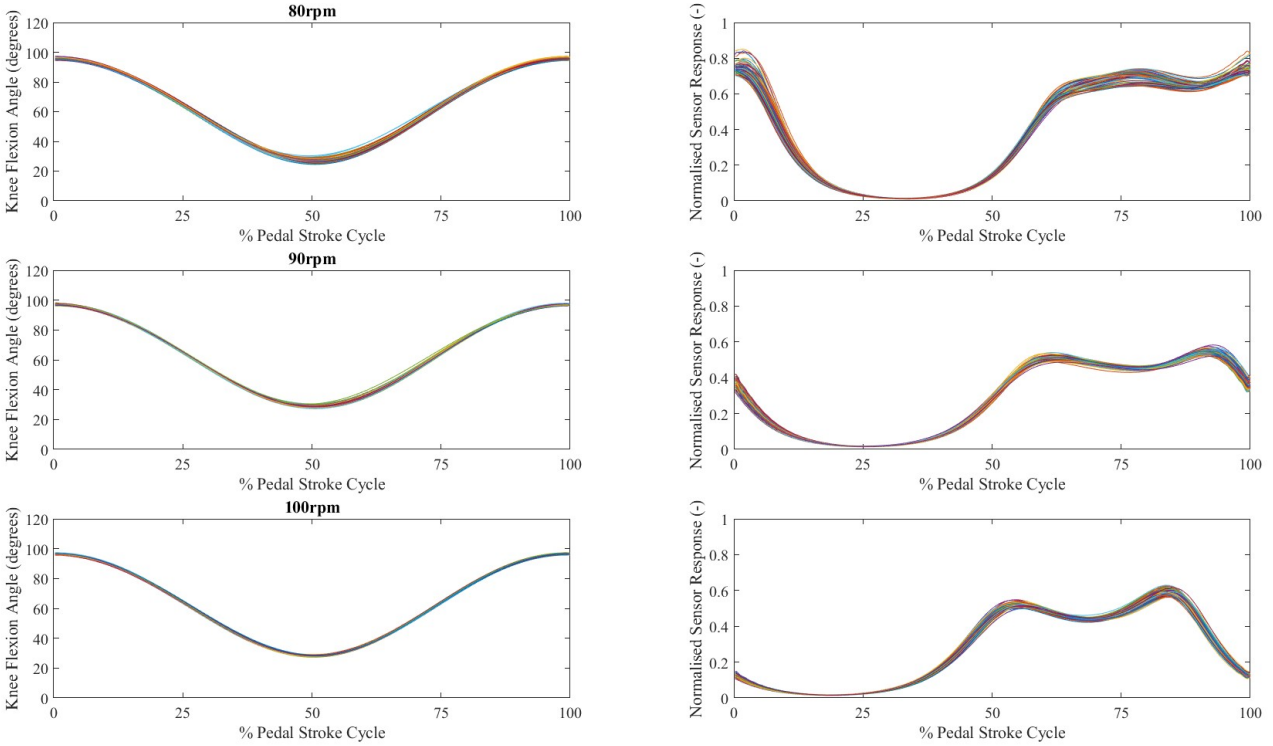


Figure 6.34: Overlaid time-normalised response for each pedal revolution for 3 × 1-min segments at 80, 90 and 100 rpm during the cycling protocol. Knee angles from Vicon on the left and strain sensor response on the right for participant 59445, visit 1/2.

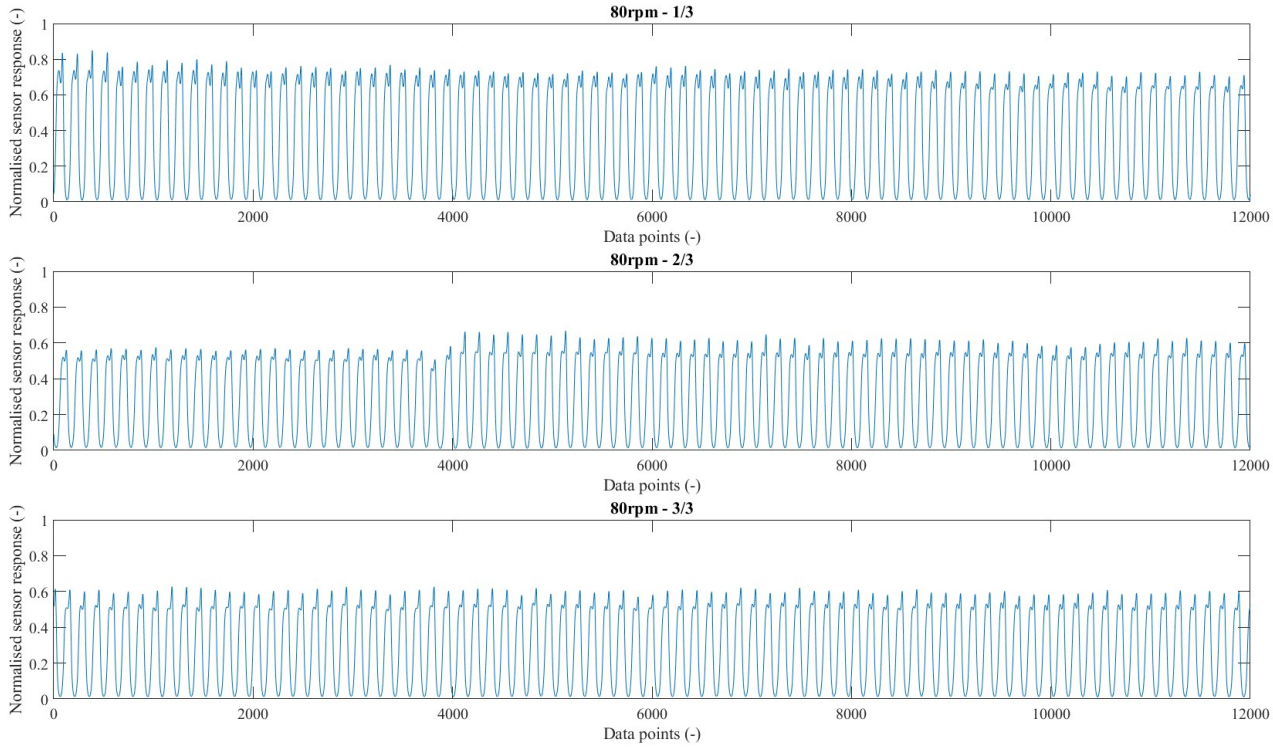


Figure 6.35: Normalised sensor response for for 3 × 1-min segments each at 80 rpm during the cycling protocol, performed by participant 59445, visit 1/2.

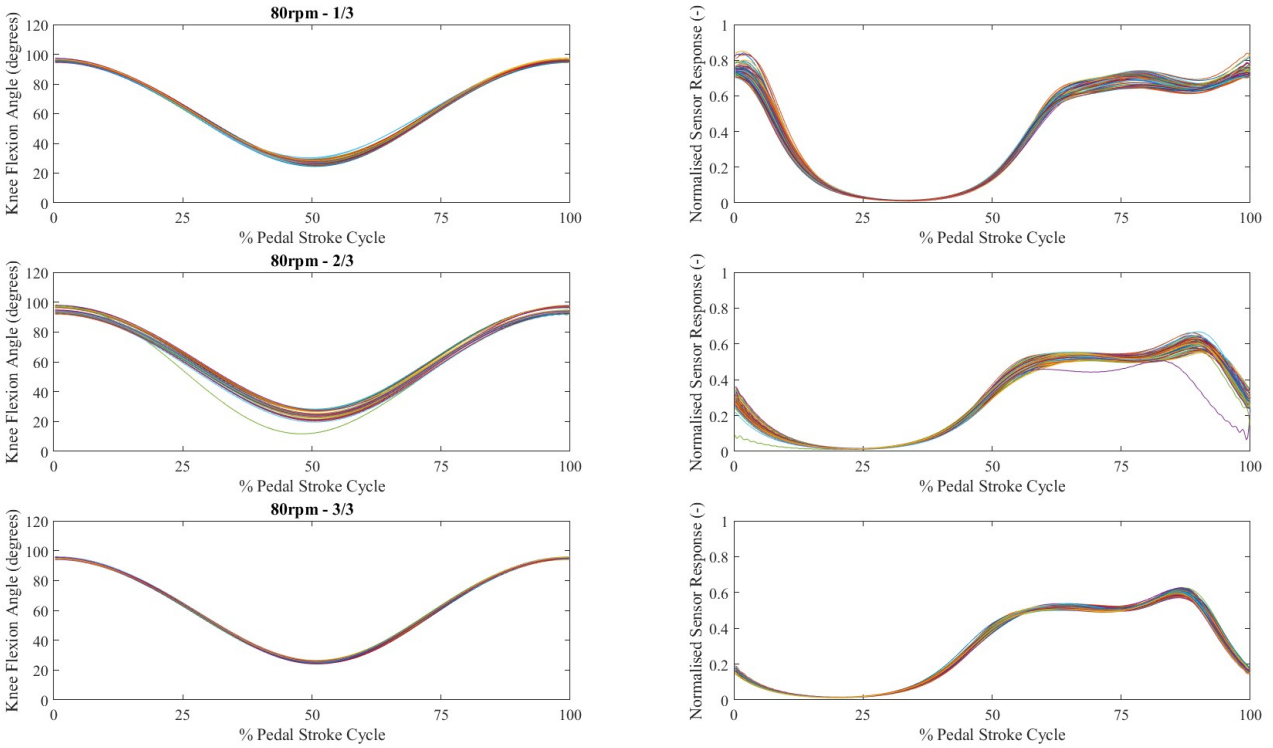


Figure 6.36: Overlaid time-normalised response for each each pedal revolution for 3 × 1-min segments each at 80 rpm during the cycling protocol. Knee angles from Vicon on the left and strain sensor response on the right for participant 59445, visit 1/2.

6.4.2.1.7 Participant 59445 - visit 2/2

The second visit for participant 59445 used the same strain sensor as the first and this was the seventh use (S3-007). There are small double peaks in each cycle across the three cadences presented in Figure 6.37, with the second peak being higher than the first. Looking at the time-normalised plots in Figure 6.38, the knee angles measured by Vicon are very similar at each of three cadence extracts. The strain sensor profile is similar to that in Figure 6.34, but the signal variation is similar across the different cadences in Figure 6.38.

The overall strain sensor signal range is slightly reduced from the first to second 80 rpm repeat in Figure 6.39 by approximately 0.1, and the first peak within the double peak in each cycle becomes less visible in the second and third repeats compared to the first. The second visit for this participant differs to the first when comparing the time-normalised Vicon plots in Figure 6.40 and Figure 6.36 respectively. In Figure 6.40 there is little difference in knee angles throughout the pedal stroke and this is observed across all of the 80 rpm repeats. The strain sensor curves are also similar with regards to profile and variation.

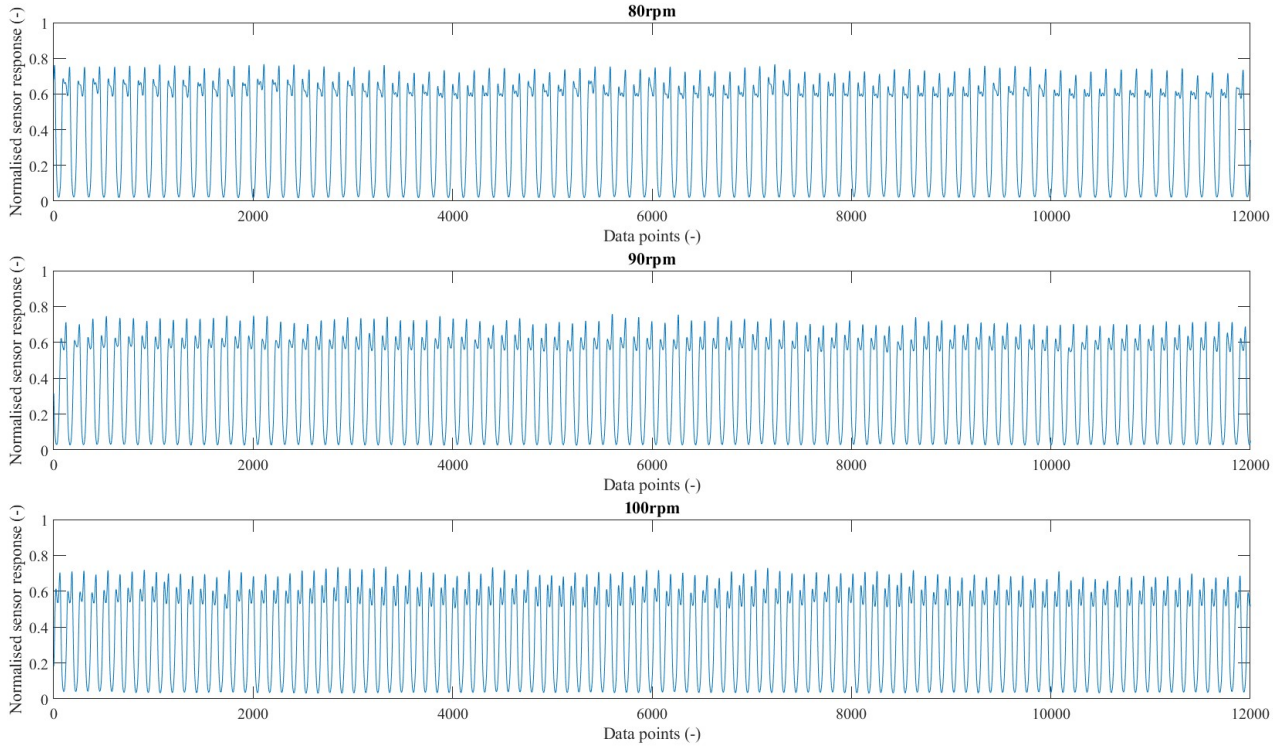


Figure 6.37: Normalised sensor response for 3 × 1-min segments at 80, 90 and 100 rpm during the cycling protocol, performed by participant 59445, visit 2/2.

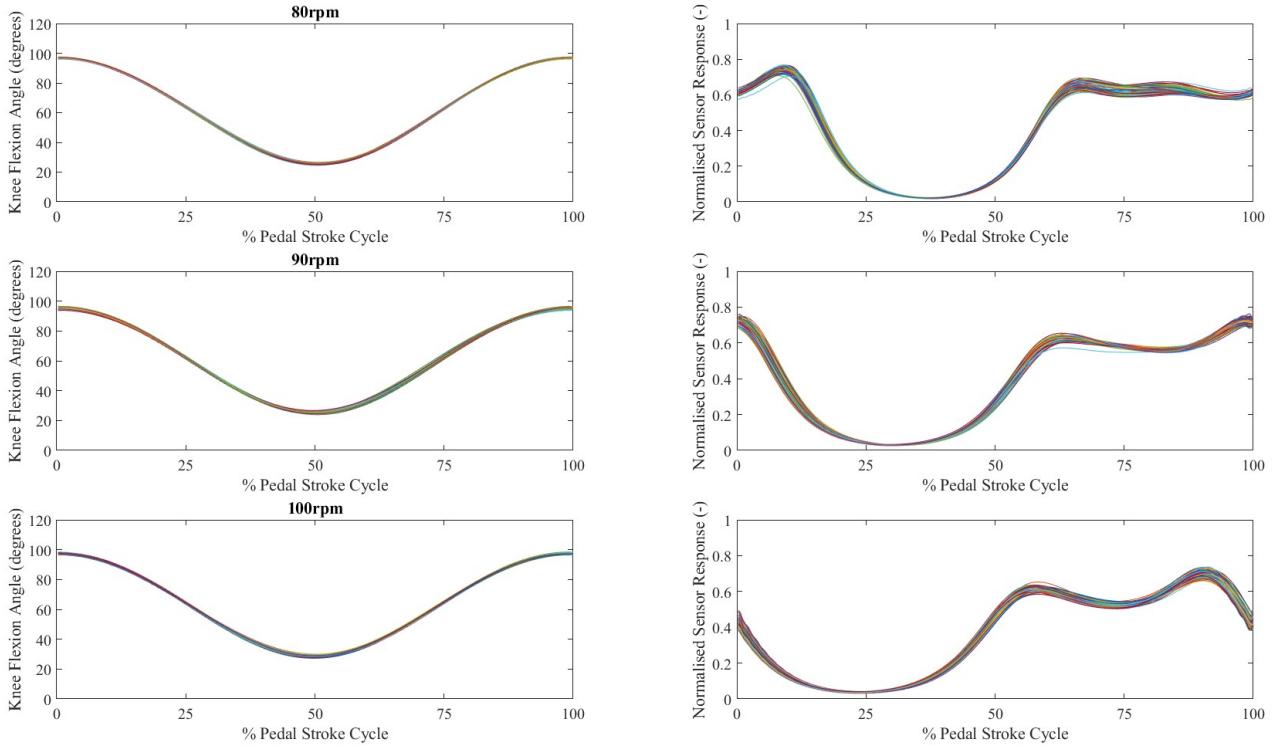


Figure 6.38: Overlaid time-normalised response for each pedal revolution for 3 × 1-min segments at 80, 90 and 100 rpm during the cycling protocol. Knee angles from Vicon on the left and strain sensor response on the right for participant 59445, visit 2/2.

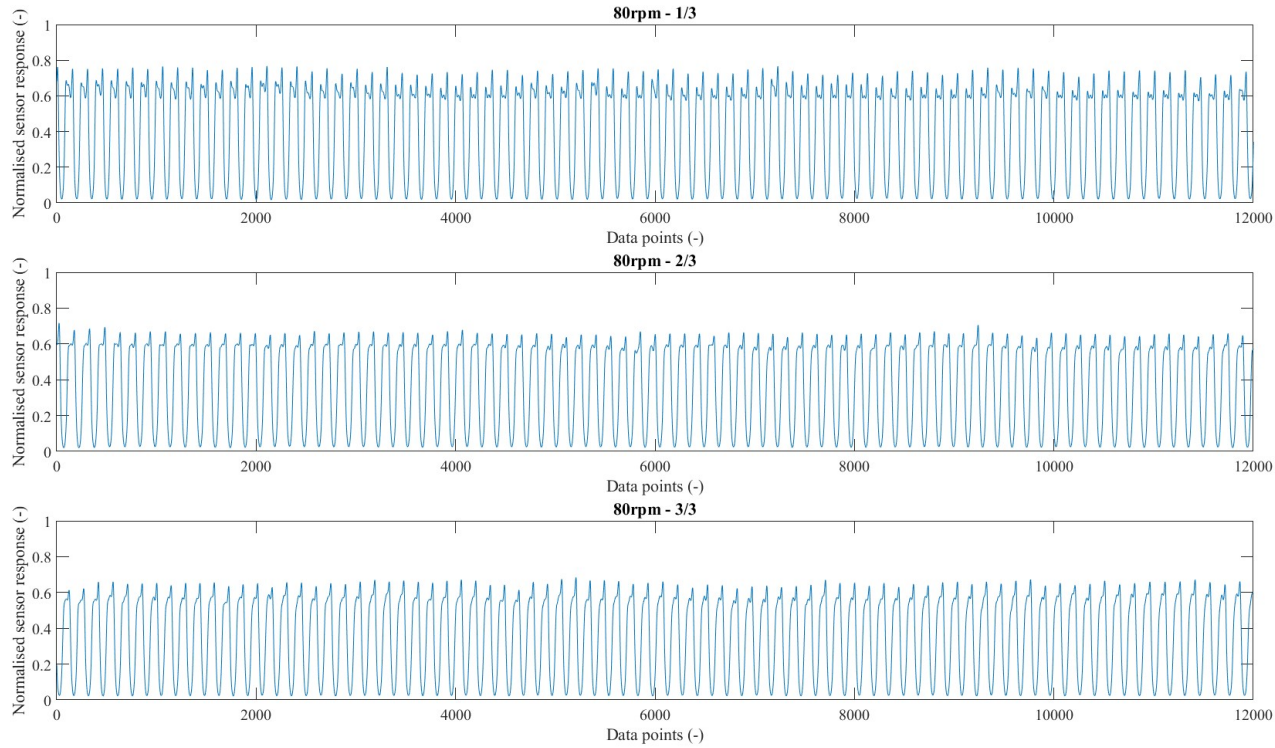


Figure 6.39: Normalised sensor response for for 3 × 1-min segments each at 80 rpm during the cycling protocol, performed by participant 59445, visit 2/2.

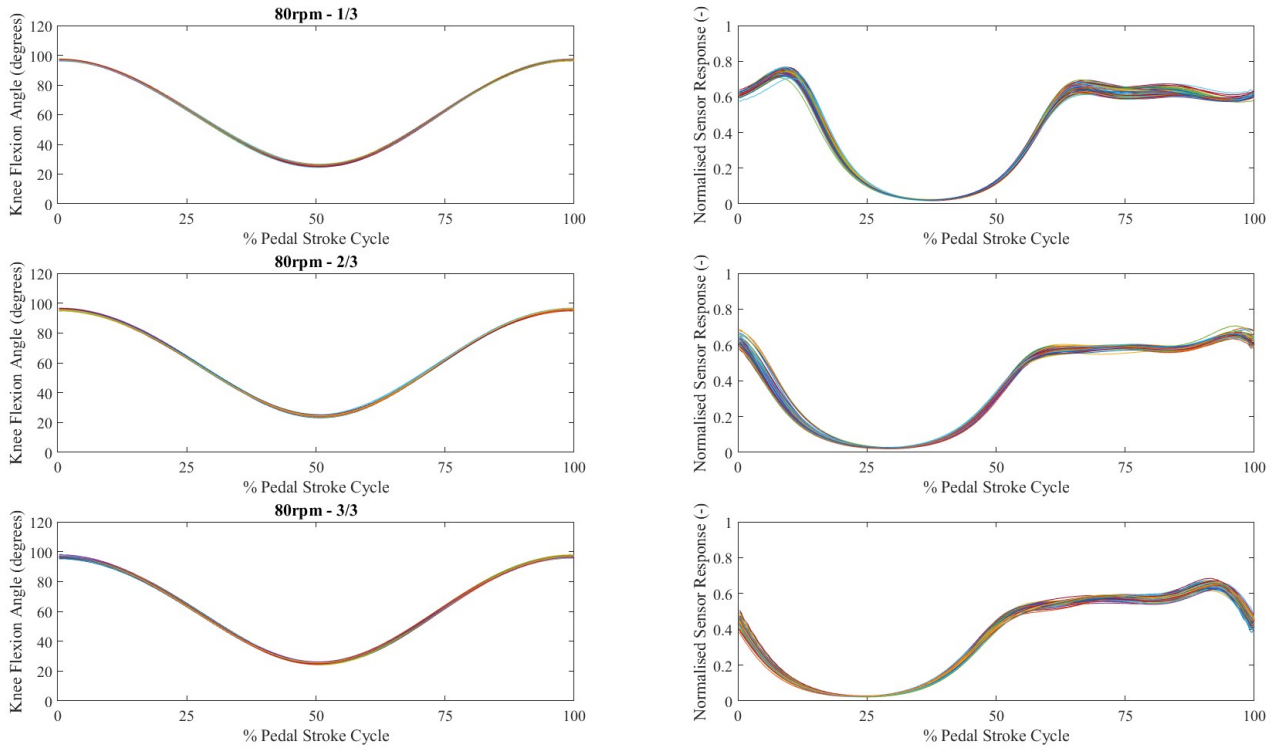


Figure 6.40: Overlaid time-normalised response for each each pedal revolution for 3 × 1-min segments each at 80 rpm during the cycling protocol. Knee angles from Vicon on the left and strain sensor response on the right for participant 59445, visit 2/2.

6.4.2.2 Kinematics Analysis of Vicon Signal

For each step and for each section of data extracted from the testing protocol, the mean maximum and minimum knee flexion angles were calculated for each participant, as well as the corresponding range of motion. These are displayed in Table 6.9 and Table 6.10 respectively. Standard deviation was generally higher at the bottom of the pedal stroke where the knee was minimally flexed (highest at 24.87 ± 2.40° for participant 59445 and 25.82 ± 1.85° for participant 69013) compared to the top of the pedal stroke where the knee was under the most flexion (highest at 95.06 ± 1.64° for participant 59445).

The maximum and minimum knee angles measured vary across the cohort, with the highest mean maximum and minimum knee flexion angles determined as 115.38 ± 0.42° for participant 39683 and 45.03 ± 0.58° for participant 60435 respectively. Meanwhile, the lowest mean maximum and minimum knee flexion angles were 93.73 ± 0.41° and 23.59 ± 0.90° respectively, both for participant 69013. Despite this, overall knee range of motion across the cohort was between 64.98 – 71.55° for all participants except for participant 39683 whose range of motion fell between 81.96 – 84.06°.

Table 6.9: Mean maximum and minimum knee flexion angles for each participant during each 1-min extract of cycling data.

Partici-pant ID	Test sess-ion	Mean knee flexion angle (degrees)									
		80 rpm (1)		90 rpm		100 rpm		80 rpm (2)		80 rpm (3)	
		Max	Min	Max	Min	Max	Min	Max	Min	Max	Min
50560	1	106.86 ± 0.24	38.59 ± 0.41	107.65 ± 0.20	40.88 ± 0.44	107.61 ± 0.21	42.03 ± 0.46	108.24 ± 0.28	40.87 ± 0.49	109.89 ± 0.39	42.08 ± 0.45
39683	2	112.77 ± 0.32	28.70 ± 1.20	113.89 ± 0.30	31.39 ± 0.80	115.05 ± 0.46	32.36 ± 0.85	114.32 ± 0.44	32.36 ± 1.05	115.38 ± 0.42	32.00 ± 1.13
69013	1	93.79 ± 0.22	24.08 ±0.44	93.92 ±0.38	25.05 ± 0.53	94.02 ± 0.24	24.98 ± 0.54	93.73 ± 0.41	23.59 ± 0.90	94.04 ± 1.00	25.82 ± 1.85
60435	1	108.52 ± 0.10	43.11 ± 0.51	109.06 ± 0.11	43.57 ± 0.50	109.53 ± 0.13	44.06 ± 0.38	109.40 ± 0.11	44.04 ± 0.51	110.01 ± 0.14	45.03 ± 0.58
60435	2	103.13 ± 0.13	36.14 ± 0.61	103.69 ± 0.14	36.50 ± 0.63	104.41 ± 0.18	37.23 ± 0.41	103.77 ± 0.25	37.00 ± 0.43	102.97 ± 0.22	36.07 ± 0.72
59445	1	96.11 ± 0.54	27.07 ± 1.10	97.09 ± 0.34	28.50 ± 0.70	96.75 ±0.34	28.19 ± 0.38	95.06 ± 1.64	24.87 ± 2.40	94.94 ± 0.41	25.35 ± 0.48
59445	2	96.96 ± 0.26	25.53 ± 0.46	95.40 ± 0.57	25.12 ± 0.55	97.50 ± 0.35	28.83 ± 0.46	95.82 ± 0.43	24.41 ± 0.36	96.80 ± 0.43	25.25 ± 0.43

Table 6.10: Mean knee flexion angle range for each participant during each 1-min extract of cycling data.

		Mean knee flexion angle range (degrees)				
ID		80 rpm (1)	90 rpm	100 rpm	80 rpm (2)	80 rpm (3)
50560	1	68.27	66.77	65.57	67.36	67.80
39683	2	84.06	82.50	82.69	81.96	83.38
69013	1	69.71	68.86	69.04	70.15	68.21
60435	1	65.41	65.50	65.47	65.37	64.98
60435	2	66.99	67.19	67.17	66.78	66.89
59445	1	69.04	68.59	68.56	70.19	69.59
59445	2	71.42	70.28	68.67	71.41	71.55

6.4.3 Discussion

The cycling protocol served to extend the knowledge about the strain sensors developed in this project and subject it to higher strain rates over longer periods of time (compared to the rowing protocol) with a different participant cohort. The continuous nature of the 20-minute warm up used in the cycling protocol enabled the entire strain sensor signal to be normalised by its range before extracting data at different cadences. This made it easier to interpret any signal variation throughout the test. As with the rowing study, the squats performed as a calibration step were not used to normalise the strain sensor signal due to the difference in strain rates and therefore sensor response.

Something that can be observed in the time-normalised plots for all participants is the shift in strain sensor signal in comparison to the one from Vicon. For example, in Figure 6.32 the knee is extended at the bottom of the pedal stroke at 50% of the stroke cycle. Looking at the corresponding sensor plots, the sensor response is at a minimum at 37.5%, 30% and then 25% for the first, second and third 80 rpm data extracts respectively. The viscoelastic behaviour of the sensors can explain this out-of-phase response, as it causes hysteresis, which leads to irreversible changes to the sensing performance over time with loading [140]. This is only enhanced by the already high strain rates associated with the cycling movement, further increased as the cadence is ramped up throughout the protocol. As observed in Chapter 4, when the strain sensor is constantly in motion, so are the CNTs that transfer charge and there is the possibility of a more erratic, out-of-phase response as the sensor does not have time to relax. If data is being analysed after the fact, then this delay is not problematic. However, when providing live feedback, then this delay must be considered alongside signal processing so that users can receive feedback within a suitable time frame to make any changes to their movements.

A feature observed in the range-normalised sensor plots was the double peaks present in every strain cycle. This is a known behaviour associated with CNT-based strain sensors during cyclic loading and is explained by the competing mechanisms that reform and deform conductive networks [238]. Even though this an inherent property of CNT-based strain sensors, the ideal scenario is to have the double peaks minimally distort the overall signal, unlike in Figure 6.13 for the 90 rpm plot where the double peaks have effectively split the strain cycle into two. If using this particular sensor to determine cadence, then it would double the value and it would also make it difficult to determine the position of the knee within the pedal stroke. For other tests using this particular sensor (S1), double peaks were highly prominent in each of the signals. However for the other sensor used (S3), the size of the double peaks were much smaller in amplitude and distorted the overall signal less, as seen in the time-normalised plot for participant 60435 in Figure 6.26. This suggests a difference in microstructure of these two sensors that has affected the quality of the response, with sensor S3 providing a much higher quality signal than sensor S1.

This difference in signal quality can be noticed in other aspects such as the range of the strain

sensor signal decreasing throughout the course of the 20-minute cycling protocol. This reduction in range was observed when originally characterising the strain sensors in Chapter 4, and happens as a result of the CNTs being reoriented when strain is repeatedly applied. The CNTs become more aligned and contact points (for charge transfer) are increased, leading to a lower resistance being measured. For sensor S1, in Figure 6.19 the overall range is almost halved from 0.8 to 0.4 from the first to third 80 rpm extract. This is compared to sensor S3 where the biggest reduction in range is seen in Figure 6.33 from approximately 0.8 to 0.55 as the cadence increases from 80 rpm to 90 rpm. Similar patterns can be seen for other tests using both of these sensors, with the signal range on the whole, being more stable for sensor S3, proposing again that there is a microstructural difference that makes sensor S3 more suitable for detecting knee range of motion due to its response stability. A screening method is therefore needed as part of the sensor fabrication process to ensure that only strain sensors meeting a minimum CNT uptake and providing a reliable signal that aligns with a known standard (in this case Vicon) are used for this application.

In one instance, the sensor response range increases over the course of testing after the initial decrease as for participant 50560 in Figure 6.15, and in another the minimum values of the sensor response increase over time as in Figure 6.17 for participant 39683. This can be attributed to the resistance of the sensor increasing over time as the conductive network is destroyed, likely due to material loss from the outer surfaces of the sensor. A coating that encompassed the strain sensor would prevent this material loss, while helping to stabilise the sensor response.

Focusing more on the response of sensor S3 and participant 60435 who completed the cycling protocol on two occasions, when looking at the knee motion as recorded by Vicon, there is minimal variation in its range across the different cadences as noted in Table 6.10 . For their first visit, the amount of knee flexion ranged between 64.89 – 65.50° and between 66.78 – 67.19° for the second visit, in both cases varying by less than 1°. Although there is more variation in the time—normalised sensor signal compared to Vicon, when comparing the sensor plots across the different cadences and the two visits they are consistent in Figures 6.26 and 6.30, indicating the response is repeatable between sessions for this particular sensor. This continues for participant 59445 who also completed the protocol using sensor S3, where the strain sensor is able to visually reflect the larger variation in knee angle range during the first visit in Figure 6.36, with the knee range varying between 68.56 – 70.19°. During the second visit, where the knee flexion range for the 80 rpm repeats is much smaller (between 71.41 – 71.55°), a difference can be seen in the time-normalised plots in Figure 6.40.

Although the mean knee flexion angle ranges vary by no more than 3° for each participant, at the bottom of the pedal stroke the standard deviation for the minimum knee flexion angle is higher than for the top of the pedal stroke and the maximum knee flexion angle, as highlighted in Table 9. Previous studies have shown that knee joint movement is related to movement occurring at the ankle joint: if the cycling shoes are attached to clipless pedals and the pelvis is stable on the saddle, then

plantar flexion must be responsible for changes in knee angle, with more variability for novice cyclists [137]. Decreased plantar flexion and increased knee extension have been reported as a result of higher cycling intensities, however these higher intensities have been achieved through increasing resistance [239, 240] and not necessarily increasing cadence as in this study.

For all participants presented in this chapter, the amount of knee extension decreased as the cadence was increased from 80 rpm to 100 rpm (see Table 6.9). Although a relationship cannot be determined between knee extension and cadence based on this small sample of data, it is an area to be considered, as well as the amount of variation in knee angles at different cadences. At this stage, a sensor such as sensor S3 has the ability to recognise variation in knee angles (see Figure 6.36) and so the WSS has potential to help determine an acceptable amount of variation in knee movement and act as a tool for monitoring improvement.

These improvements in pedalling technique would not only minimise injury risk, but help improve power application and ultimately cycling performance. Monitoring knee angle variation could supplement information provided by other sources, such as the polar view on the Wattbike that provides visual feedback on force applied through the pedal stroke. For individual users also, it has the potential to help them understand their own movements when riding in different environments or on different bikes that may require setting up in a particular way.

6.4.4 Summary

In this cohort study that observed the cycling movement, the strain sensors used in the wearable sensor system were subject to a much higher strain rate than in the rowing protocol, leading to the appearance of double peaks within each strain cycle. For the higher quality sensor used, these double peaks had a negligible effect on the overall signal and the profile had some similar features to the signal produced from Vicon.

For some participants, variations in the knee flexion angle throughout the pedal stroke and especially at the bottom of the pedal stroke cycle were observed, and this was recognised visually in the time-normalised sensor response at the different cadences extracted. Being able to understand and minimise this variation can aid in preventing injury from occurring at the knee joint.

6.5 Further Discussion

The rowing and cycling cohort studies provided different insights into the use of the strain sensors developed in this project. One common theme that was established was the quality of sensors used during testing and the difference that arose in the sensor response. To ensure that all data obtained from the strain sensors is representative of the knee joint movement and comparable to Vicon, a quality control step needs to be introduced in the fabrication process. Imaging a few sensors before and after

testing could provide a reference of what an ideal sensor structure is like for when future strain sensors are prepared. In addition to this, including a pre-conditioning step in the manufacturing process can help to overcome the orientation change of the CNT conductive filler (that can lower the resistance of the strain sensor over time).

Another common feature was the presence of double peaks within the sensor signal. The time taken for a strain cycle in each of the protocols can be calculated as follows:

$$time = 60\ seconds \div stroke\ rate \tag{6.1}$$

For rowing, and:

$$time = 60\ seconds \div cadence \tag{6.2}$$

For cycling. At the lowest stroke rate and cadence, the time taken for a strain cycle using the above equations were 3.3 seconds for rowing (at 18 spm) and 0.75 seconds for cycling (at 80 rpm). The strain cycle duration within the rowing stroke is over 4-times that in the cycling pedal stroke, however the double peaks are just as, if not more prominent. During characterisation of the strain sensor (see Chapter 4, the strain cycle at the highest strain rate of 350 mm/min took 4.4 seconds but double peaks were not present in the signal (see Figure 4.7. This indicates that for these piezoresistive CNT strain sensors, there is a threshold in strain cycle duration (or strain rate) that introduces these double peaks into the signal. As discussed earlier, some sensors provided a reliable response in line with Vicon and did not distort the signal when it came to be analysed, while others did not. The shortest strain cycle presented in this section was 0.6 seconds (at a cadence of 100 rpm in cycling) and this suggests that these sensors could be used in other applications where one strain cycle takes at least 0.6 seconds. For example in running, where the average step rate is 172.6 steps per minute (for both feet) at a speed of 10.8 km/h [241], the strain cycle duration for the WSS placed on one knee would be 0.7 seconds (at 86.3 steps per minute for one foot).

This exploratory phase of testing the strain sensors and WSS has shown what the current capability of this system is, with the main advantage being that the strain sensor is able to track the motion of the knee in both sporting movements. The profile of the sensor response can be used as the basis for movement recognition and the use of machine learning. Machine learning has been used in combination with inertial measurement units (IMUs) in tennis to classify tennis strokes [242] and to identify the experience level of different tennis players [93]. In this instance, machine learning could be used to classify different sports and differentiate between the rowing and cycling movements. In rowing where observations were made with regards to how early knee flexion occurred in the recovery phase of the rowing stroke (see Vicon time-normalised plots in Figure 6.7), machine learning could be used to build up a database to identify what constitutes "good and poor rowing technique" based on

this kinematic information and aligning with previous research on rowing technique [130, 243], aiding technical improvement within the sport.

Different forms of strain sensors for measuring human motion and physiological signals are continuing to be developed, with textiles and woven conductive elements being investigated over polymer-based composites. One such example is a graphene-based thermoplastic polyurethane (TPU)/textile composite that has been developed and characterised [244]. Characterisation included testing such as washability and durability. Durability investigations subjected the sensor to 10,000 cycles with the highest frequency testing (1 Hz = 1 strain cycle per second) taking place under 5% cyclical strain with the resistance being recorded at a sampling frequency of 25 Hz [244]. This is an impressive number of strain cycles with an 8% change in resistance over this duration, however in the sports investigated in this project the range of motion of the knee joint will subject any strain sensor to strains higher than 5% and with a low sampling frequency, there is the potential that certain features of the signal are being omitted during this cyclical testing process.

Laboratory and bench testing can give some indication of sensor performance but does not provide the full picture, as the work done in this project has shown. The strain sensors developed and tested in this project have been combined with electronics that accurately convey the signal produced with its high sampling frequency (of 200 Hz) and have been integrated into a real-life study. Although the low gauge factor means that this sensor currently cannot be used to determine absolute knee joint angles, it can be used to assess variation in knee joint movement over a period of time. Future work could include changing the saddle height in cycling or stroke length in rowing (both which will impact the overall knee flexion range), combined with improving the sensor sensitivity during fabrication, to determine the ability of the strain sensors to detect these larger changes in knee range of motion.

6.5.1 Limitations

There were some limitations that arose while conducting this study, the primary one being the size of the cohort and the number of repeat visits made by participants. Only ten participants were recruited for each study, which did not allow for sub-groups to be identified (whether by experience level or sex) and for generalisations to be made about the knee kinematics profile for each one. For the rowing study, only four out of the ten participants returned for a second visit, while in contrast this number was much higher for the cycling study at nine out of ten. This prevented comparisons being made between testing visits about the performance of the participant and the strain sensor.

Without a quality assessment of each strain sensor that was used, there was not a way of knowing how it would perform during the real-life testing process. This then had an impact on the data collected, as there was not consistency in the response of the different sensors used.

Each participant performed a series of squats before completing the cycling or rowing protocol, with the intention of using the squats to calibrate the subsequent data collected. However, while the squats

were being performed it became apparent that participants had differing amounts of mobility and not all were able to achieve their full knee range of motion while performing a squat that they would be able to achieve on a stationary bike or rowing machine. This, in conjunction with the fact that the speed of the squatting motion did not reflect the speed of the rowing and cycling motions, meant that in fact the range of the sensor response was larger during rowing and cycling (due to overshoot behaviour) and so the squats were not an appropriate calibration method. The best calibration would probably involve the actual sporting movement, and would serve as a baseline for the participant's knee range of motion.

6.6 Conclusion

The two cohort studies conducted showed that the carbon nanotube-rubber strain sensors that have been developed in this project and integrated into a wearable sensor system are able track knee range of motion in rowing and cycling. There was a difference in the quality of sensors used, but the better quality sensors were able to track the movement of the knee in line with the output produced by the Vicon motion capture system.

In both sports, a change in kinematics was observed as a result of increasing cadence or stroke rate: in cycling the standard deviation of the knee angle at the bottom of the pedal stroke decreased, while in rowing the amount of knee extension during the rowing stroke decreased. Having a method of monitoring these kinematics that cannot be observed by the naked eye is important as they can influence coaching that can help prevent injury or enhance performance. This is something that with further development, such as increased sensitivity and an improved calibration process, the wearable sensor system can help monitor.

Chapter 7

Cohort Study - Questionnaire Responses

Understanding the user experience of study participants and their interaction with the wearable sensor system

7.1 Introduction

The uptake of wearable technology relies not only on the information it can provide to the user but also on the experience of the user, particularly with respect to comfort and ease of set-up of the system. Literature regarding user preferences with respect to wearable devices for rehabilitation are limited. Papi et al. (2015) conducted focus groups with people with osteoarthritis to understand their needs and requirements for a knee monitoring device [245]. They noted differences in how long people would wear a device for (from a few hours to all day), but there was agreement that the device should be discreet, easy to use, compact and comfortable [245]. It was postulated that access to data could also help some participants adhere to and engage in rehabilitation protocols [245]. The findings of this worked highlighted the importance of liaising with end users to increase the uptake of a system. Bergmann et al. (2015) tested the feasibility of an attachable clothing sensing system to measure joint stability. Participants were also questioned about comfort while wearing the sensing system, as well as whether they would wear the sensing system to help with diagnostics, treatment, injury prevention and feedback [246]. The findings from this work suggested their sensing system was a suitable method to measure joint instability, with participants giving positive feedback about their interaction with it [246].

There are fewer references available in a sporting context that provide information about how study participants across different sports interacted with sensor systems and their thoughts on the use of such devices. A study by Makhni et al. (2018) requested users to complete an exit survey after testing a device to measure elbow torque in baseball [41]. The survey contained only close-ended questions and as such the richness of responses was limited and it was unclear why respondents replied the way they did. This was important as their exit survey indicated, "pitchers are unlikely to adopt the use of the

sleeve during real, in-game competition." [41]. However, it is unclear why it was not useable as this could be down to several reasons including design elements, obtrusion and comfort. This means that potentially a device was abandoned when issues with it could be overcome.

Therefore, a questionnaire was designed and incorporated into the testing protocol, which included both close-ended and open-ended questions that were analysed using descriptive statistics and a thematic analysis respectively.

Further motivation behind the development of this questionnaire and gathering information from participants included:

- Athletes being key stakeholders in this field, with their feedback being an important part of the development process of any new technology
- Engaging study participants in the development process to help them build a relationship with the wearable sensor system (WSS)
- Understanding how the needs of the study participants could be fulfilled
- Understanding the views already held by the study participants on wearable technology that is currently available
- Gathering perspectives from study participants on how they could use the WSS developed in this project

7.2 Methods

As part of the cohort study conducted, participants were invited to complete a questionnaire after their testing session, to gather information about their experience with the WSS and their opinions on wearable technology. The questionnaires were approved by the Imperial College Research Ethics Committee (ICREC Reference number: 17IC4173) and the Science Engineering Technology Research Ethics Committee (SETREC number: 21IC6651), copies of which are in Appendix D.

Participants were provided with a URL to access the relevant questionnaire comprising open- and closed-ended questions that had been set up in Qualtrics (Utah, United States), an online survey platform. Feedback was gained from participants about whether they noticed the WSS during testing and if they thought it had a negative impact on their performance. They were also asked if they would use it in training or in competition and if they would adjust their technique (rowing or cycling) based on feedback from the device. Questions were developed based on previous studies by Bergmann et al. (2012 and 2015), which sought to understand the user experience with and perceptions of wearable technology [246, 247]. Questionnaires were completed following data collection after each

testing session in the laboratory to determine whether there was a change in how the participants felt about the technology.

Table 7.1 shows a breakdown of the number of questionnaire responses received over both testing cohorts and for each session completed.

Table 7.1: Breakdown of questionnaire responses vs. total number of participants.

	Rowing		Cycling	
	Session 1	Session 2	Session 1	Session 2
Number of participants	10	4	10	9
Responses received	8*	2*	10	9

*Questionnaire introduced through ethics ammendement after two participants had already completed the study

7.2.1 Data Analysis

The first part of the questionnaire comprised closed-ended questions, with the aim of encouraging the participants to start consider different factors related to wearable technology. These were analysed separately for the rowing and cycling cohorts, using descriptive statistics in Matlab to determine which factors about wearable technology participants felt were the most important to consider and to compare responses across cohorts.

Responses from the open-ended questions were collated across both participant cohorts and a thematic analysis was conducted using the framework outlined by Braun and Clarke (2006): familiarisation, initial coding, theme searching, theme reviews, defining and naming themes, and reporting [248].

7.3 Results

7.3.1 Descriptive Statistics

7.3.1.1 Wearable Sensor System

Within the online questionnaire, participants were asked to rate their experience with the WSS after both testing sessions using a 10-point Likert scale, where 1 = very much and 10 = not at all. The distribution of scores across each cohort after each testing session are presented in Figures 7.1 and 7.2.

When asked if the WSS had a negative impact on their performance, the median score for cyclists and rowers were 9/10 and 10/10 respectively. The lowest score recorded for a cyclist was 6/10 and for a rower was 5/10. The maximum score across both cohorts was 10/10. Participants were also asked if they noticed the WSS while wearing it. Median scores were lower across both cohorts: this was 8/10 for cyclists and 6/10 for rowers. The range of scores was wider, with cyclists scoring as low as 3/10 for

noticing the WSS and rowers scoring as low as 4/10. Again, the maximum score across both cohorts was 10/10. These results are listed in Table 7.2.

Table 7.2: Overview of user experiences with the WSS. Outcomes for the 10-point Likert scale are given by the median and range.

	Cycling		Rowing	
Question	Median score	Score range	Median score	Score range
Do you think that the WSS negatively impacted your cycling performance? (Very much [1] – not at all [10])	9	6-10	10	5-10
Did you notice the WSS while wearing it? (Very much [1] – not at all [10])	8	3-10	6	4-10

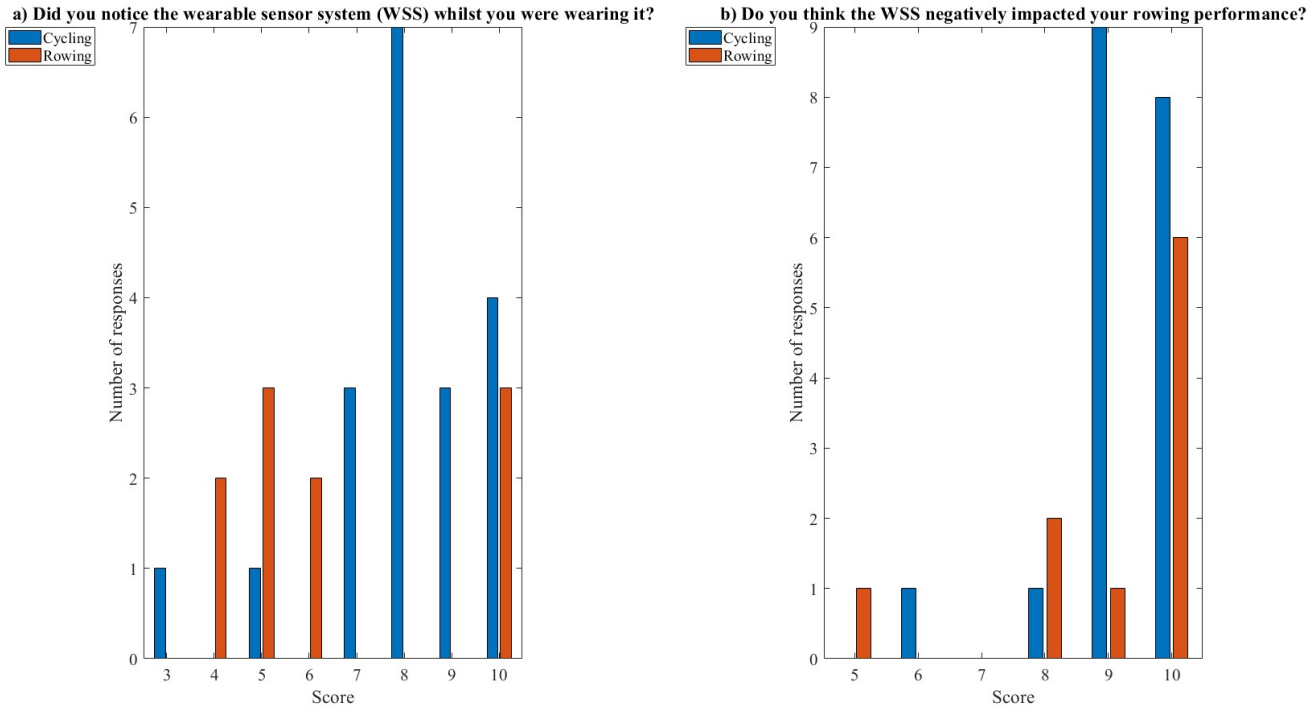


Figure 7.1: Participant experiences with WSS in a) cycling study and b) rowing study. The distribution of scores on the 10-point Likert scale are shown in each bar chart (very much [1] – not at all [10]).

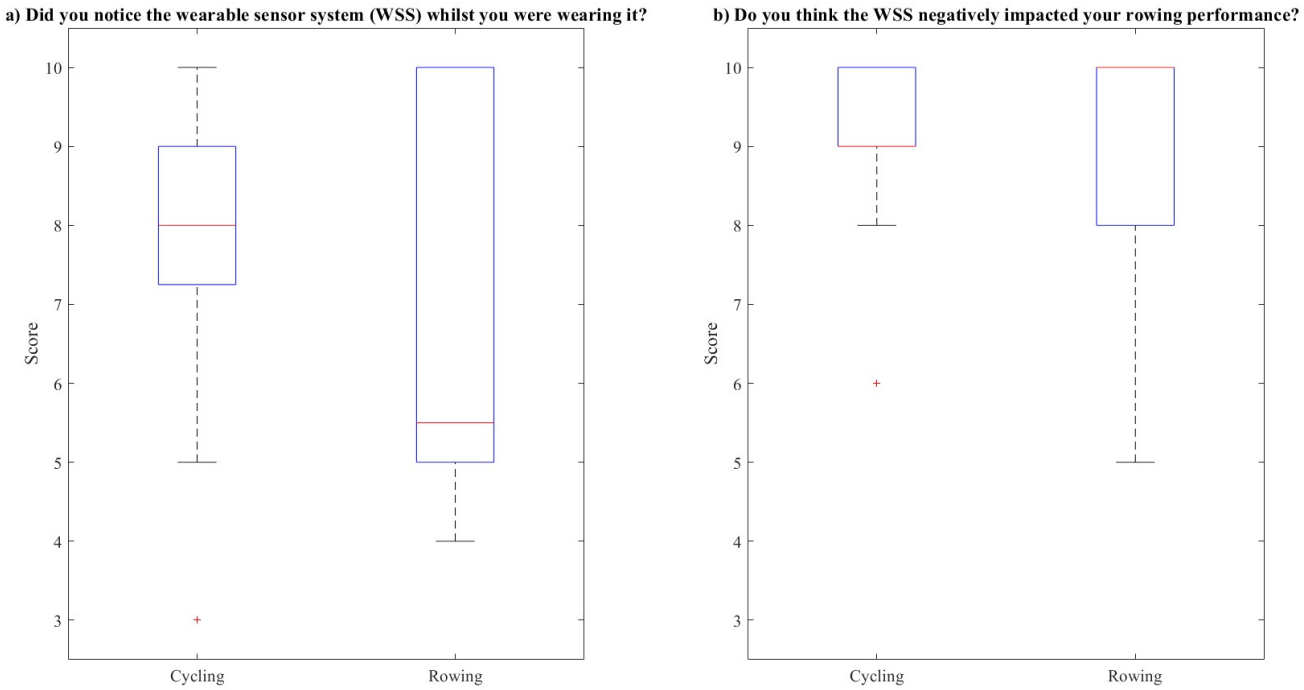


Figure 7.2: Box plots representing the distribution of scores from both cohorts - the red line represents the median, the top and bottom edges of the box are the 75th and 25th percentiles respectively. The whiskers extend to the extreme, non-outlier points. Outliers are represented by the + symbol.

Participants were asked to reflect on whether they would use the WSS in training or competition, and if they would adjust their technique based on any feedback provided by the system. For each question, responses were given on a 3-point Likert scale ("Yes", "No", and "Maybe") with an additional option of "I don't know". Results are displayed in Figure 7.3.

In both sports, the number of "Yes" responses increased for all questions when filling out the questionnaire for the second time, meaning that participants were more likely to use the WSS in training, competition and to adjust feedback after further exposure to the system. In both sports after the first session, participants were less sure about using the WSS in competition compared to training with the percentage of "Yes" responses decreasing from 60% to 13% in cycling and from 75% to 25% in rowing. Similar trends were observed after the second testing session with "Yes" responses decreasing from 67% to 14% among cyclists and from 100% to 50% among rowers. In all cases, rowers were more likely than cyclists to use the WSS in different environments.

The consideration to use the WSS to adjust technique was high in both cohorts with 78% of cyclists and 86% of rowers responding "Yes" after the first session. This increased to 100% for both rowers and cyclists after the second testing session.

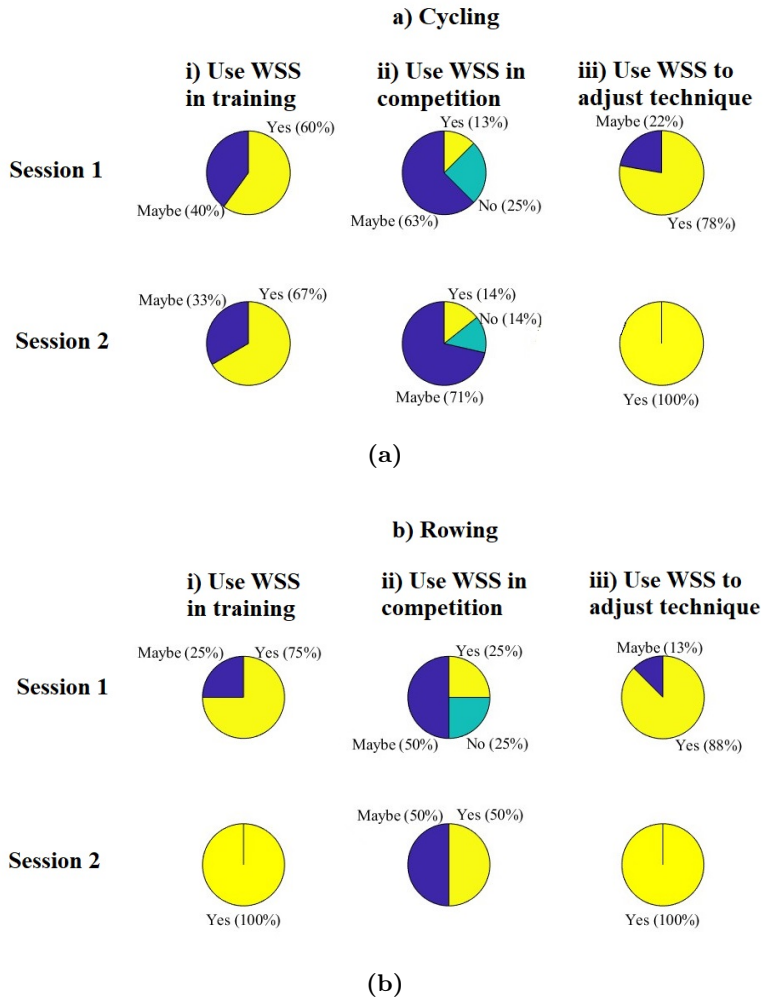


Figure 7.3: Results of participants using the WSS in a) cycling and b) rowing i) in training, ii) in competition and iii) to adjust their technique after the first testing session and iv-vi) after the second testing session.

7.3.1.2 Wearable Technology in General

Within the questionnaire after the first testing session, participants were asked to consider 13 factors on wearable technology in general, covering metrics, design, and interface with the user. These results are displayed in Figure 7.4 and Table 7.3 for both studies. Each factor was scored using a 10-point Likert scale, with a score of 10 stating that it was most important to the respondent.

Factors that achieved the highest median scores in both cohorts (participants gave a score of 10/10) were that wearable technology should "be comfortable", "not affect normal movements" and "not detach from the user unless needed". Factors where the median score differed by greater than one point were that wearable technology should "be recyclable" and "be discreet", with cyclists considering both factors more important than their rowing counterparts. The median score for cyclists on the importance of technology being recyclable and discreet were 8/10 and 7/10 respectively, while for rowing the scores were 5/10 and 4/10 respectively.

Table 7.3: Overview of participants' responses on wearable technology in general. . Outcomes for the 10-point Likert scale are given by the median and range.

	Cycling		Rowing	
Wearable technology in sport should... (Least important [1] – most important [10])	Median score	Score range	Median score	Score range
...be comfortable	10	9-10	10	7-10
...be compact (light and small)	9	8-10	8	7-10
...be discreet	7	3-9	4	2-10
...be easy to attach to the body	9	6-10	9	8-10
...be recyclable	8	5-10	5	3-8
...be reliable	9	8-10	10	8-10
...be simple to operate (and maintain)	9	7-10	9	4-10
...give instant feedback	8	5-10	7	4-10
...have clear and readable instructions	8	5-10	9	5-10
...not affect normal movements	10	10-10	10	9-10
...not detach from user unless needed	10	4-10	10	9-10
...provide clear and useful results	9	8-10	9	8-10
...work alongside any coaching input, instead of replacing it	9	5-10	8	5-10

Three further questions, which were asked after the first testing session, considered participants' views on whether they were happy for their data to be stored in a database; if they would use a device that they had to put on themselves; and if they would spend time learning to use a new device. Responses were given on a 3-point Likert scale ("Yes", "No", and "Maybe") with an additional option of "I don't know". 100% of rowers responded "Yes" to all three questions. 100% of cyclists responded "Yes" to applying a device themselves without assistance, but only 90% would consider their data being stored in a database or learn to use a new device. A summary of these results is displayed in Figure 7.5.

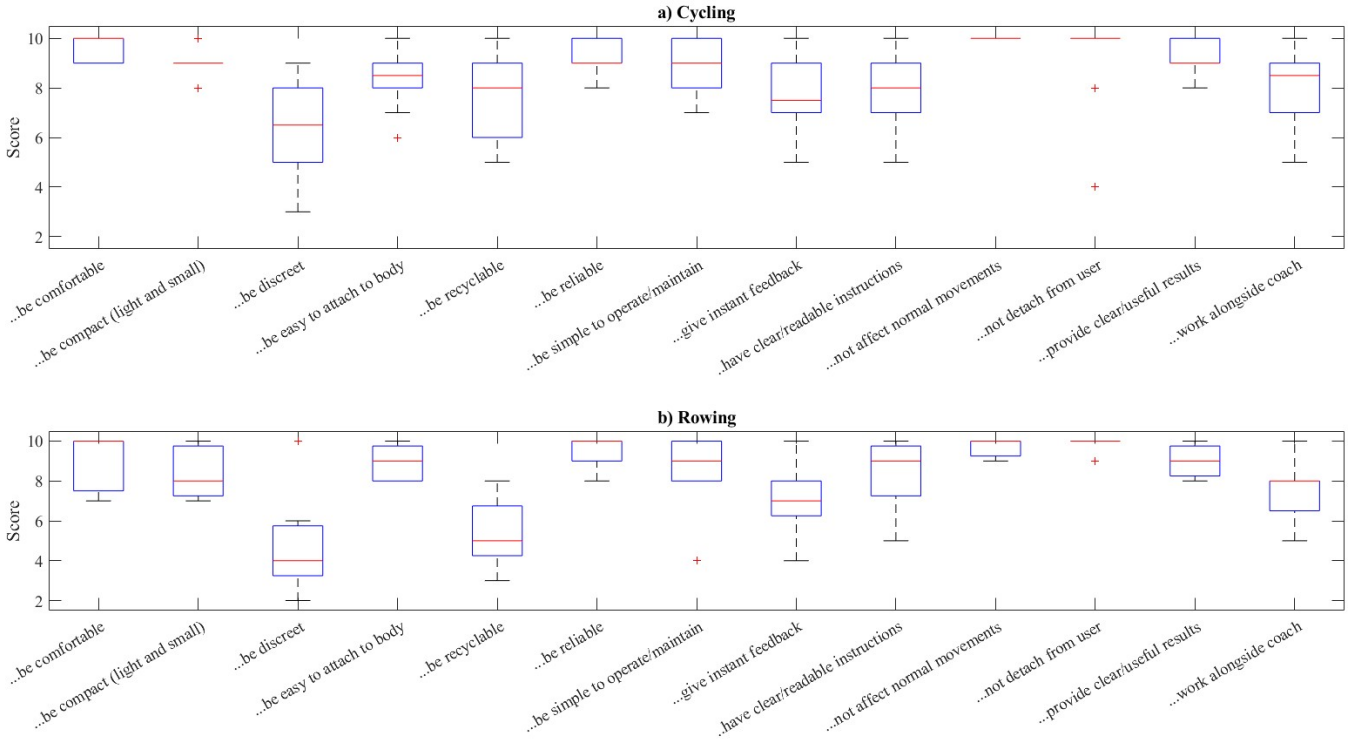


Figure 7.4: Box plots representing the distribution of scores from both cohorts - the red line represents the median, the top and bottom edges of the box are the 75th and 25th percentiles respectively. The whiskers extend to the extreme, non-outlier points. Outliers are represented by the + symbol.

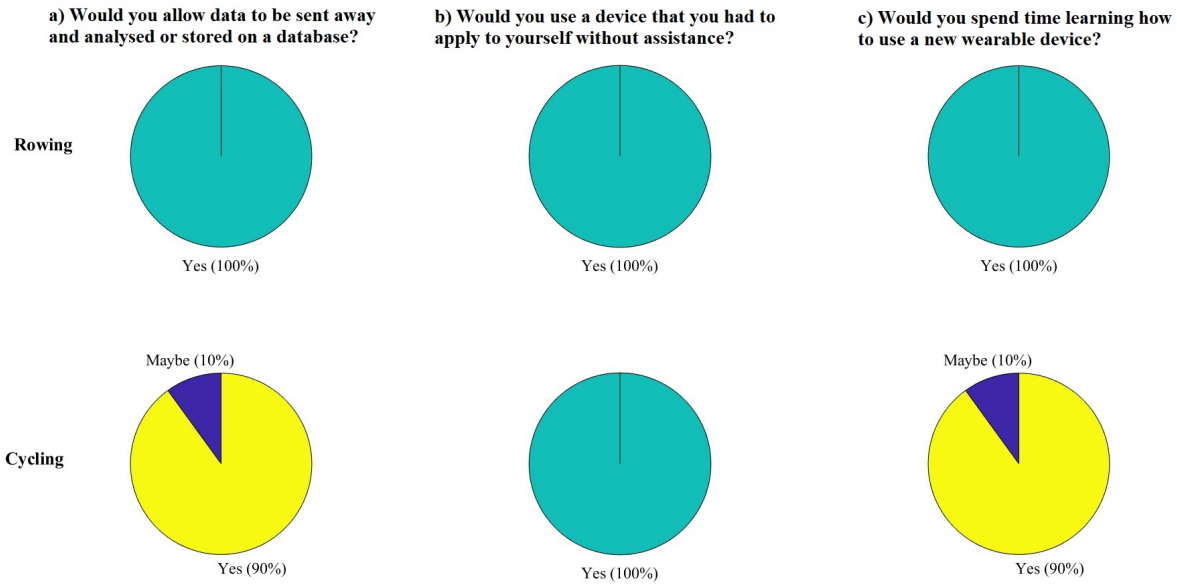


Figure 7.5: Participants' views on a) data storage, b) using a device without assistance and c) learning to use a new device.

7.3.1.3 Summary

There was a positive response from both study cohorts about the wearable sensor system – this included their interaction with the system and using it in different environments (training and/or competition). Both cohorts agreed that wearable technology in general should be comfortable but not obtrusive, while cyclists were more concerned about a device being recyclable and discreet than their rowing counterparts.

7.3.2 Thematic Analysis

Responses to the open-ended questions were collated from both sets of questionnaires, with a total of 18 participants (10 cyclists and 8 rowers). From analysing the responses, two overarching themes were identified: *Translational Factors* and *Monitoring*. Though there is a crossover within these main themes, several sub-themes were identified and considered essential to the discussion on the use of wearable technology in sports. Figure 7.6 displays the thematic map with main themes and sub-themes.

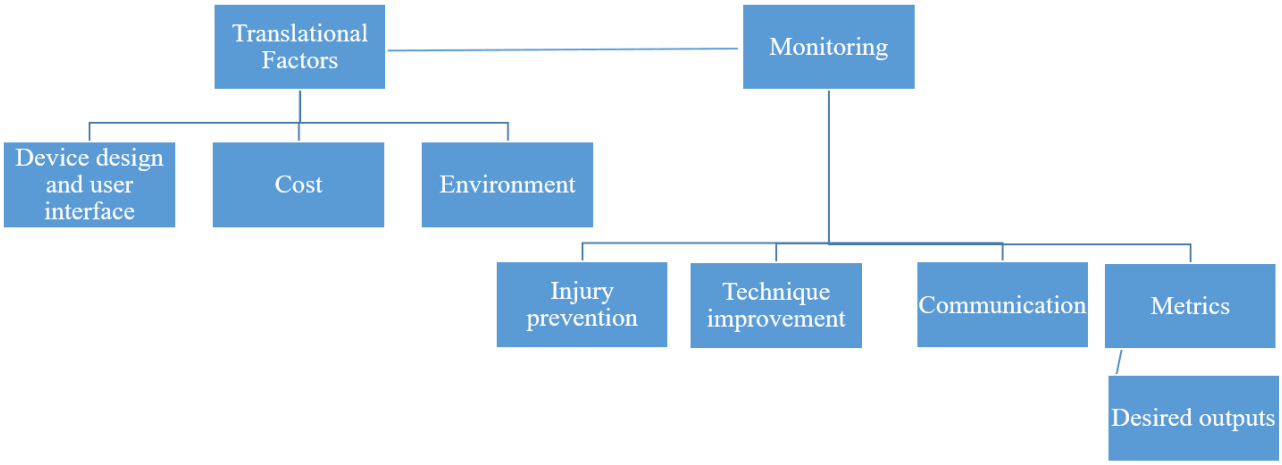


Figure 7.6: Thematic map showing the two main themes and linked sub-themes identified from the questionnaire responses.

Since the scope of this project focuses on developing strain sensors to monitor joint kinematics, both themes are discussed in detail. Where quotes are reported, they are extracted from the text responses, the type of athlete (rower or cyclist) is stated, along with their participation level (recreational or competitive) and their sex (male or female). Athletes were numbered to distinguish between respondents whilst maintaining confidentiality.

Overall, athletes expressed positive views about the WSS, offering opinions on how this specific system and wearable technology could help them in their chosen sport. The importance of the development process in this field was expressed by one rower:

"I feel like a lot of technology comes from companies just trying to make money so it's

nice / better to see a proof of concept coming from research rather than profit companies" (Rower 9 – Competitive, Female)

Another was excited by the prospect of wearable technology being able to aid the performance aspect of their sport:

> *"Look forward to future innovations to support and enhance performance in rowing on ergs and training on the water"* (Rower 6 – Competitive, Female)

7.3.2.1 Translational Factors

During the experimental process, participants were able to interact with the WSS and observe the set-up and data collection process. As a result of this, they were able to state factors that they felt were important to future designs and iterations of the system when in use outside of a laboratory environment. These were grouped together as *Translational Factors*.

The quotes included in the following text highlight the importance of considering user feedback during the research and design process to allow the wearable technology to have the best transfer to real-world use. Sub-themes identified were: *Device design and user interaction*, *Environment* and *Cost*.

7.3.2.1.1 Device Design and User Interface

Participants (predominantly from the cycling study) offered up different experiences on their interactions with the WSS, particularly around the printed circuit board (PCB) assembly component of the system. Some participants refer to the entirity of this assembly as an inertial measurement unit (IMU). Its size, placement and fixation to the knee warmer all gave rise to many comments. However, none of the athletes stated that this component affected their movements in any way:

> *"The sensors themselves weren't noticeable during wearing. The only noticeable thing was them [PCB assembly] falling off which is due to them being prototypes and fixed on in a temporary manner rather than being aware of the actual sensor itself."* (Cyclist 2 – Leisure, Female)

> *"I could feel the weight of the IMU a little bit pulling down on the knee warmer, but besides that it was fine and didn't get in the way of anything."* (Cyclist 10 – Competitive, Female)

The prototype nature of the WSS prompted design suggestions from two athletes. Improving the user experience and developing something that is not obtrusive is a key point that was made, alongside having a more discreet system. It was expressed by one athlete that the current design is holding the system back from making that transition from research to general use:

"I noticed the wearable device brush against my arm when rowing, so it being relatively thin would be ideal" (Rower 1 – Competitive, Male)

"Considering the WSS is in a development phase it was not disturbing to the cycling. However I would still be unsure whether to use it in a training environment. I would suggest creating a more compact sensor case (without long wires) and maybe placing the IMU in a strap that revolves around the moving leg. Overall it seemed an amazing device, with very interesting biomechanical data!" (Cyclist 4 – Competitive, Male)

The comfort of the knee warmer component of the WSS during the two testing sessions was also commented on by one cyclist. A preference was stated for having sensors integrated into kit that they were more accustomed to wearing if measurements were being made over longer durations of time than 20 minutes:

"Over a 20 minute period, wearing a knee warmer was okay, but over a longer period, especially cycling hard, it might get a bit uncomfortably warm." (Cyclist 5 – Leisure, Male)

"I think the majority of the discomfort was caused by the knee warmer. I'm personally not a fan of these as they tend to need to be quite tight to prevent them sliding down the leg, and the tightness leads to them folding together at the back of the knee, and I find that this feels like it's restricting blood flow. Perhaps if this system were built into some bib tights I wouldn't notice." (Cyclist 5 – Leisure, Male)

Finally, another key factor highlighted within the responses was the set-up time for the WSS, which involves putting on the knee warmer and sensor calibration. During data collection, this set-up time also included attaching markers used by the Vicon motion capture system and the calibration of this system, which took a number of minutes:

"As long as they are secure, no issues at all with them apart from time to fit for day to day training." (Cyclist 1 – Leisure, Male)

7.3.2.1.2 Environment

It is clear that device design and user interaction play an important part in whether athletes will use wearable technologies, with comfort and unobtrusiveness being important factors within this. For wearable technologies to have the most impact, athletes, and potentially coaches, should feel comfortable and confident in using them in a training environment and in competition if the sport allows.

With regards to this specific device, views fell on both sides of the argument for use outside of a research capacity, with the metrics available also coming into play:

"Didn't notice it all. Would use it in a training or racing environment if it provided feedback that improved my pedal stroke." (Cyclist 9 – Recreational, Male)

"Considering the WSS is in a development phase it was not disturbing to the cycling. However I would still be unsure whether to use it in a training environment. I would suggest creating a more compact sensor case (without long wires) and maybe placing the IMU in a strap that revolves around the moving leg. Overall it seemed an amazing device, with very interesting biomechanical data!" (Cyclist 4 – Competitive, Male)

7.3.2.1.3 Cost/investment

The high cost of wearable technology, particularly those that track biomechanical outcomes, can make it more difficult for the general public to access, becoming a barrier for potential users. One participant expressed that in general, wearable technology was not aimed at them. It is clear that cost is an important factor, with a subscription model being a solution to overcome this barrier:

"Usually aimed at higher level performance and can be expensive. For ones that do metrics such as mechanics it would be good to be able to 'rent' for a while to see performance but not necessarily invest in for wearing day-to-day." (Cyclist 2 - Leisure, Female)

"Affordability would be key to me" (Cyclist 6 – Competitive, Male)

7.3.2.2 Monitoring

The second major theme established in this analysis is *Monitoring*, encompassing several different factors about when, why and how athletes would use their devices. Monitoring was mentioned by participants in both sports, with the following sub-themes determined: *Injury prevention*, *Technique improvement*, *Metrics* and *Communication*, with enhancing performance underlying these different sub-themes. These sub-themes align with monitoring uses discussed in previous literature surrounding wearable technology [7, 249, 250].

7.3.2.2.1 Injury Prevention

Injury prevention was a key factor highlighted by rowers when asked how they would use information from the WSS developed in this project. There is an underlying awareness that avoiding injury is important for continuation in sport, but none of the participants were able to link this awareness to a common site of injury in their sport, particularly the knee:

"For injury prevention and to find areas for technical improvement" (Rower 1 – Competitive, Male)

"In its current form, for the measurement of power output, but I imagine it could be used to measure movements in different dimensions. This might highlight unnecessary movement in a different plane that wastes energy or that could potentially cause an injury" (Rower 5 – Competitive, Male)

7.3.2.2.2 Technique Improvement

Another factor highlighted, this time by both rowers and cyclists, was the use of the WSS for technical improvement in relation to other outcomes such as preventing injury, which was introduced above:

"Monitoring technique to prevent injury" (Rower 3 – Competitive, Male)

"Technical critique and improvement" (Rower 4 – Competitive, Female)

Participants had more confidence in specifying areas that they would like to see improvement in their own technique and movement patterns, and would therefore want the WSS to address. How the user receives this information is linked to how data is communicated from the WSS itself:

"Changing technique as required to maximise stroke efficiency" (Rower 7 – Competitive, Female)

"If the sensor implies something wrong about my rowing, eg rowing too long/too short I'd try to make adjustments to the stroke in order to reach a good length" (Rower 8 – Competitive, Male)

"Would use it in a training or racing environment if it provided feedback that improved my pedal stroke" (Cyclist 9 – Recreational, Male)

7.3.2.2.3 Communication

It is clear that participants want to be able to get something from a wearable device (including this one) and be able to interact with it so that they can adjust how they move:

"Didn't notice it at all. Would use it if provides useful feedback to improve my pedal stroke." (Cyclist 9 – Leisure, Male)

Wearable technology has the ability to facilitate conversations between athletes and coaches by supplementing, not replacing, any subjective feedback:

"Would share with coach for parallel input" (Rower 6 – Competitive, Female)

Care needs to be taken as to how data from a device is presented to the end user so that they are engaged with the outputs and understand the information that is being given to them:

> *"More data on different aspects of performance is good, but to be really useful it should be easily understood and be presentable in a manner such that it informs the wearer on how to improve."* (Rower 5 – Competitive, Male)

7.3.2.2.4 Metrics

This final sub-theme covers the outputs that participants would want from this particular system and from wearable technology in general. Users want to be able to have devices that provide data specific to their sport and it needs to be clear how this data is going to help them make improvements. This means for metrics to be appropriate, they need to be measuring something useful:

> *"More cycling specific stuff would be great"* (Cyclist 6 – Competitive, Male)

> *"I'm not sure what insights the sensor would be able to give. If it could help me train, I might wear one."* (Cyclist 5 – Recreational, Male)

7.3.2.2.5 Desired Outputs

A sub-sub-theme was identified, relating to desired outputs that were specific to the two sports rowing and cycling) tested in this project. Users want a better awareness of what their body is doing, whether that is in the form of a power measurement or understanding the kinematics of their motion:

> *"In its current form, for the measurement of power output, but I imagine it could be used to measure movements in different dimensions. This might highlight unnecessary movement in a different plane that wastes energy or that could potentially cause an injury"* (Rower 5 – Competitive, Male)

7.3.2.3 Summary

The open-ended questions offered a mix of responses that were positive and negative, but all contributed to furthering the understanding of consumer needs around wearable technology. In general, there was excitement around the potential of the system developed in this project, and the questionnaire allowed insight to be gained into design changes and how people would like to use this particular system.

7.4 Discussion

This questionnaire aimed to gain insight into the participants' views on wearable technology in general and to understand their experiences with the strain sensor and WSS developed in this project. This

information can inform the future development of this system and how it can aid people as they carry out their chosen sport. Similar themes arose from the descriptive statistics and thematic analysis, leading to a combined discussion centred around this particular system as well as the wider field of general wearable technology for sports.

A strong outcome from the thematic analysis is that research-backed technology can increase consumer trust: it gives the consumer the view that the technology they purchase will accurately measure any metrics it claims to. However, it is important to involve those that are within the sport, be it athletes, coaches or support staff, so that researchers can appreciate the metrics that are important to athletes. Involvement also allows those within the sport to understand how an objective input (from technology) can help them train and compete. This collaborative effort means that a product is developed that people will want to use and have confidence in.

7.4.1 System Design and Impact on Performance

Collecting responses from participants indicated how big a role the overall comfort and feel of wearable technology will play in its uptake. It is important that the participants did not feel like the WSS had a negative impact on their performance, increasing the likelihood that it will be used in the future. Wearable technology should be there to enhance performance and not take away from it. The views concerning this aspect of the WSS are positive, with a median score of 9/10 from cyclists and 10/10 from rowers, as presented in Table 7.2. The lower end of each score range is 6/10 for cyclists and 5/10 for rowers, however the low cycling score was deemed to be an outlier as displayed in Figure 7.2.

Common performance metrics in rowing and cycling are pacing (500-metre split time – time taken per 500 metres rowed) and power respectively. Comparing these metrics with and without the WSS would have a given objective feedback as to whether the WSS had an impact on the performance of the participants. However, the subjective feedback from the participants is still valid, as they would have had an idea as to where they expected their performance to be with regards to the common metrics. The high scoring in both testing cohorts suggests the potential for the WSS to be used in the two sports. The fact that participants felt that the WSS did not affect their performance aligns with the response from both cohorts that wearable technology should not affect normal movements, as shown in Table 7.3 and Figure 7.4.

Another considered factor was whether participants noticed the sensor system, Figure 7.1 suggests that rowing participants found the WSS more noticeable than their cycling counterparts. The difference between cohorts and the fact that cyclists also found the WSS somewhat noticeable could be for a number of reasons. For both cohorts, having a knee warmer on just one leg will create a different feeling compared to the other leg that does not have anything on it. This compounded with the participants knowing that they were there to test the WSS could have meant they were constantly thinking about it and trying not to disrupt any of the technology.

As indicated in Chapter 5, the basis for the WSS is a knee warmer, a piece of clothing that is typically used by cyclists. The unfamiliarity of this clothing with the rowers can explain why they noticed the system more. The knee warmer typically integrates better with cycling kit than rowing kit, with the grippers inside the bottom of the bib shorts worn in cycling helping to hold the knee warmer in place. Using a pair of knee warmers instead of just one could help alleviate this problem. Additionally, the current system allows for the strain sensor and PCB assembly to be easily removed – different base clothing could be used depending on the sport, without the assembly or strain sensor needing to be changed.

The open-ended questions offer more insight into where the design of the WSS could be improved as it is important for users. This WSS was used as a proof of concept, however, there are certain features that could be considered in future developments of the system. For example, the PCB assembly was particularly bulky relative to the developed strain sensor, but the advancements in thin film technologies could help reduce the profile of this component, leading to something lighter, thinner and more discreet. Discreetness was a more valued factor for cyclists than rowers as presented in Table 7.3, with aesthetics and aerodynamics leading cyclists to spend a lot of money on equipment and clothing to enhance speed and performance.

The jumper wires used to connect the sensor to the PCB assembly caused some difficulty during testing – 3M Transpore surgical tape was used to secure them to the knee warmer so that they were less disruptive but there was still a chance of them getting caught, particularly during the rowing motion. In addition, the connection to the electrodes was not always secure, leading to some loss of data. Custom-length jumper wires with loops built into the knee warmer to hold it in place could reduce the obtrusiveness of the system. Being able to reduce data loss is significant as wearable technology must be reliable, so being able to develop more secure connections is important. Rowers felt more so than cyclists that devices should not detach from the user unnecessarily (see Table 7.3) which relates to this, if a device does detach from the user then it stops being able to measure what it set out to.

The improved design is likely to promote uptake, but it is important to remember that development is an iterative process and requires this type of feedback from users in order to progress appropriately. It is also important to take into account the positives of the current design despite its prototype nature. Using knee warmers made the WSS easy to put on and take off, with the set-up time taking only a couple of minutes, compared to Vicon which took at least ten minutes with camera calibration and marker placement. With devices like power meters on bikes taking a matter of seconds to calibrate, keeping any set-up time low is key.

The knee warmers also allowed different sizes to be purchased, fitting a wide range of body proportions. Only one participant raised concern over the use of the knee warmer, with it being tight on the leg and the potential for it to get warm, suggesting that in general, this was not a problematic piece of clothing. The concerns raised are valid, however, in this proof-of-concept study, the use of a knee

warmer made it easier to transfer the system between users compared to integrating it into leggings or cycling bib tights.

7.4.2 Use Environment

The design of the WSS and its impact on user performance as discussed in the previous section will influence the environments that people are willing to use the system in, be it in training or competition. All participants were asked if they would use the WSS in training, in competition and to adjust their technique, with results presented in Figure 7.3. There were only two responses from rowers after the second testing session, so it is not appropriate to make comparisons between results from the first and second testing sessions. However, the shift in opinions for the cycling cohort, with people more likely to consider using the WSS in all scenarios, could suggest that some sort of adjustment time is needed for users to become more familiar with new technology. Fewer participants would use the WSS in competition compared to training – the fact that some only took part in their sport leisurely should be taken into account, but also athletes can be more particular about the equipment and clothing they compete with, not wanting to have any distractions. However, the majority of participants would consider using the WSS to adjust their technique (responding with "maybe" or "yes"), indicating that technical improvement is not just limited to those taking part in competitions and that wearable technology should not just be targeted at those at the highest level of their sport. For those taking part in sports recreationally, they are more likely to be doing so for the mental or physical health advantages [251] and so when it comes to how the WSS is used, the injury prevention aspect is more important than performance enhancement. Reducing the likelihood of injury results in longevity in the sport to reap the social, psychological, health and physical benefits [251].

Although some participants indicated that they would use the WSS in competition, rules and regulations in certain sports have limits on devices and data collection. In rowing, no data can be transmitted to or from the boat during racing, except using devices from World Rowing. Within the crew, there is "allowable data" that can be accessed: time, stroke rate, boat velocity/acceleration and heart rate [252]. No other data can be measured or recorded. A similar situation can be found in cycling, where the Union Cycliste Internationale (UCI – world governing body for cycling) regulations state that devices can capture and transmit the following types of data: positioning, image, mechanical information from the bike or its components, and some physiological data (heart rate, body temperature and sweat rate) [253]. Placing limits on where wearable technology can be used has quite big implications for the advancements in the field of sports biomechanics, with users, coaches and other support staff unable to make direct comparisons between training and competition. It can also give an insight into athlete mindset – is technique or power output changing under the pressure of competition? Regardless of whether people would use the WSS in competition or not, it is important that they would feel comfortable using it during training as observed in the thematic analysis. Taking someone out of a

laboratory environment and allowing them to do their sport somewhere that is more familiar to them means that they are more likely to perform their standard movement. Research and observation put people into a slightly different mindset and measuring conditions are not always realistic. The WSS has the potential to overcome this.

7.4.3 Cost, Investment and Accessibility

Questionnaire responses highlighted a perception that some people think that wearable technology, particularly those providing biomechanical outputs, is not for them and is instead aimed at higher-level performance. However, there is an interest from those that participate in sports leisurely and they should be able to get input from technology into how they perform. This perception likely derives from marketing and accessibility. Certain devices, including smartwatches and bike computers, that measure metrics such as physical activity, speed, distance and sometimes power, can be purchased quite easily and are stocked by different sports goods outlets in stores and online. However, wearable technology that can provide insight into kinetics and kinematics are less readily available and typically requires someone (like a biomechanist) to know what they want to measure and where to look for an appropriate device.

The cost of any wearable technology will also be an important factor in how it translates from research to commercial use, with one participant stating that affordability would be key to them. Another indicated that being able to rent the WSS would be a more viable option. The renting/subscription model is already seen with many goods such as cars, housing, phones and bikes. It can be popular for several reasons: people do not want to commit to something long-term and put lots of money in; it allows people to keep up-to-date with the newest version of a device/product, with some companies offering a trade-in service; this model gives the option for people to back out of a purchase, although sometimes at a cost. This model can potentially be more costly for consumers in the long-term but gives them a number of options to purchase a device.

This model is making its way into the sports and fitness industry, with companies like WHOOP (Boston, Massachusetts) offering a membership where the device is free and the monthly or annual membership fee allows access to the mobile app and analytics. This fitness tracker strap is popular with people in and outside of sports. It is clear then that newly developed wearable technology must appeal to consumers not only in aesthetics but also in cost. The prototype WSS was developed at a low cost and it would need to be ensured that any further developments took care to keep additional costs to a minimum.

7.4.4 Metrics and Communicaiton

Another area where consumer appeal is necessary is in the metrics offered by wearable technology and how data is communicated. The questionnaire revealed that some participants were not quite clear on

the potential outputs available from the WSS, therefore metrics related to each sport need to be clearly stated so that they can understand how it will benefit them. However, it is clear that participants are data-hungry but not quite sure what they want and how to use it. They do know that they want data to be reliable, alongside having clear and useful results as presented in Table 7.3.

The WSS has the ability to track knee movement in the sagittal plane, but additional strain sensors and utilising the data from the IMU within the PCB assembly could provide more than one-dimensional monitoring and estimate forces. For this project, knee flexion/extension was chosen as it is a parameter that has been reported in previous literature and has connections to performance in rowing in particular (Murphy, 2009). It is easy to choose a "new" metric to make a device stand out from those already on the market, but this can limit comparisons to other systems or any analysis in previous literature.

It was highlighted by one athlete that they would share information from the WSS with their coach, aligning with results from the descriptive statistics where study participants thought that wearable technology should not replace coaching input. Objective feedback provides a framework for athletes to understand how they are progressing, while for coaches it can be used to reign in or push an athlete, supplementing any subjective feedback they may give.

The WSS currently does not employ live feedback, but this is something that would be considered in any future development as it allows users to adjust their motion in real-time. Instant feedback was not rated as one of the most important factors in Table 7.3 (median score of 8/10 for cyclists and 7/10 for rowers) – having the data to interpret at any point is more important than doing it straight away. The output of the system is delivered post-testing but is still able to achieve the criteria of being easily understood as stated by one participant, by presenting knee kinematic data in a graphical format, which does not require much background knowledge. As discussed earlier, some consumers can be data hungry and to accommodate this then different user interfaces within a digital application could be considered depending on the type of user and how much insight they wanted.

7.4.4.1 Using WSS Outputs

Study participants were asked about how they would use outputs from the WSS, which included monitoring for injury prevention and technique improvement, both of which are linked to performance. Wearable technology provides a significant advantage over laboratory-based equipment as it can enable long-term monitoring, allowing trends and progress to be determined over time.

Participants were aware of injuries but not necessarily what causes them. For athletes working with coaches or physiotherapists who have that knowledge about movement patterns that can lead to injury (such as hyperflexion or hyperextension of the knee joint in rowing, or improper bike fit and/or cleat positioning in cycling that can lead to the knee tracking outside the sagittal plane), the use of WSS could empower them to take some responsibility for their own monitoring. It could also assist with rehabilitation, setting range of motion boundaries for an athlete to work within. Some education

alongside the WSS outputs could help users understand why certain movements are not ideal and how to avoid them. A similar argument could be made about technique improvement, with participants having an idea about what they would like to improve (pedal stroke in cycling or stroke length in rowing) but were not able to link this to kinetic or kinematic variables. Again, education would be needed to create that link between things like stroke length in rowing and knee range of motion in biomechanics. Having an understanding that a knee kinematics output can give you an indication of rowing too long or too short, will help the uptake of the WSS.

7.4.5 Further Perspectives on Wearable Technology

Some close-ended questions were able to provide further insight into some other factors that contribute to the uptake of wearable technology, with the responses presented in Figure 7.5. None of the participants in either cohort were against the idea of their data being analysed or stored in a database. This big data set can be beneficial in helping predict biomechanical patterns for different population groups, construct models of ideal movement patterns for different sports as discussed by Ae (2020) [6] and generally inform future research and development areas. However, it is important to respect people's privacy and assure them that their data will be protected – they are less likely to give it up if they can be identified from it.

Participants in both cohorts unanimously said that they would use a wearable device that they would have to apply themselves without assistance. This increases the environments that it can be used in as an expert is not needed to place it on the user, but the device needs to be developed in such a way that positioning by a non-expert will not have a drastic effect on its output and reduce the accuracy. Related to this, the majority of participants said that they would spend some time learning how to use a new wearable device. The fact they are willing to engage in this process means that it is unlikely to be a barrier to the uptake of the technology. In both cases though, the time taken to learn about a device and apply it must be short, in the order of minutes (to acquire a basic knowledge at least) or it will put users off wanting to purchase it or recommend it to others.

Thinking about wearable technology in the wider context of the use of instrumentation in sports, as discussed in Chapter 2, the majority of technology in rowing and cycling is placed on the boat or bike. There are disadvantages to this in both sports: in rowing, unless a crew is set and has use of a particular boat, there is the need to move equipment around to monitor the same person, which adds to the set-up time. In cycling, although bikes are more individual, a similar issue arises when the same person is moving between disciplines and therefore different bikes. Across both sports, there are compatibility issues between boats and bikes designed by different manufacturers and for different disciplines – oarlocks are different sizes for sculling and sweep rowing, while drop and flat handlebars are used across the cycling disciplines.

Therefore, the advantage in using a system like the WSS, is that by instrumenting a person means

that they can move between different boats or bikes without having to change how the system is set up. The same parameter, in this case knee kinematics, can be measured in the same way in different settings, whether that be indoor or outdoor. Smartwatches are a type of technology that allow this kind of continuous monitoring, acting as an external motivator or training companion [254]. The WSS, alongside the right feedback display, can empower users in the same way, to take more of an interest in their performance and injury prevention, in a way that instrumented equipment cannot.

7.4.6 Limitations

A limitation of the questionnaire distributed was not including the option of a follow-up interview to gain a deeper understanding of participants' thoughts. The use of a questionnaire which requires respondents to type text responses can lead to limited or no answers for some questions. A face-to-face or over-the-phone discussion scheduled for a certain duration would have perhaps given study participants an opportunity to go into more detail without feeling like they were in a rush to give feedback.

7.5 Conclusion

Valuable insights were gained from study participants through the distribution of a questionnaire. Participants were able to see the potential of the wearable sensor system, but some design changes and an overall low-cost system are needed in order for it to be more translatable to the real-world and not just a laboratory environment. It needs to be clearer to users what the wearable system can offer in terms of performance and injury prevention metrics, but continuing to involve them in the research and development process will ensure this device is appropriate for use in sports.

Chapter 8

Conclusions and Future Work

8.1 Introduction

The overarching aim of the work presented in this thesis was to develop and prototype a low-cost wearable technology system that could be used to measure knee range of motion in rowing and cycling. This was motivated by the current wearable technology landscape, where access to technology to measure biomechanics is largely prohibited by cost and the expertise required to interpret some performance-related metrics.

The use of wearable technology is becoming more prominent as it allows monitoring to take place outside of a laboratory environment. Sporting movements can be captured during training or competition, and these objective data can be fed back to athletes and coaches to enhance performance or prevent injury. The strain sensors developed in this project set out to address some of the limitations of systems such as inertial measurement units (IMUs) that are high-cost and require complex processing. These strain sensors were fabricated and characterised using mechanical testing machines, before assessing their potential translation to rowing and cycling.

This chapter will summarise the elements of work conducted as part of this project to achieve this aim, evaluating it in the context of sporting impact. It will also consider the avenues for future work, based on the limitations that arose throughout the project.

8.2 Summary of Work

8.2.1 Review of the Literature

In order to develop the strain sensors and the wearable sensor system (WSS), it was important to understand the current state of play with regards to the use of wearable technology in sport to measure biomechanics, particularly in relation to performance, the types of sensors used and the performance parameters that have been assessed. Systematic reviews were carried out, indicating that wearable technology had several uses in sports, including: assessing skill level, characterising movement and

acting as an injury prevention tool, all of which underpin performance enhancement.

Technology predominantly centred on IMUs, suggesting a gap in the market for a low-cost technology that needs to be addressed. Other requirements included being unobtrusive, and the ability to be used across multiple sports. Reviewing the literature also indicated the lack of wearable technologies in rowing and cycling, providing a focus for the development of a new system.

Different sensor classifications and material combinations were initially assessed, leading to pursuing a conductive polymer composite strain sensor based on piezoresistive technologies for this project. This technology was chosen because of the potential for low-cost fabrication, combined with its high stretchability which makes it suitable for measuring joint angles, particularly the knee.

The main findings of the systematic review around wearables in sport and the review on strain sensing technologies were that:

- The use of wearable technology in sport is becoming more prominent, with running and track athletics receiving the most focus
- More studies are being conducted outside of a laboratory environment, allowing a more realistic measurement of sporting movements
- IMUs are still the main type of technology used, with a number of commercially available systems that can be used across sports (e.g. MyoMOTION), as well as those that are sport-specific (e.g. Lumo Run and RunScribe)
- Alternate systems include pressure insoles, accelerometers and nanocomposite piezoresistive foam sensors, however the use of a flex sensor has only been reported once (included in the original systematic review)
- Technology is widely used in rowing and cycling, but these focus on performance metrics such as boat speed, power and stroke rate or cadence. There is little in the way of wearable technology for monitoring kinematics
- Strain sensors are being considered for healthcare monitoring and human motion detection as they can conform well to the shape of the human body, but there is limited evidence to show their use in sport
- Important performance parameters for strain sensors include: sensitivity, linearity, hysteresis, response and recovery time, and overshoot behaviour
- Piezoresistive-based strain sensors provide a suitable balance of these performance parameters, particularly when a carbon-based filler is used

8.2.2 Sensor Development and Characterisation

Composite strain sensors containing multi-walled carbon nanotubes (MWCNTs) and natural rubber were fabricated using a multi-stage method which included: preparation of the MWCNT dispersion, expansion of the rubber band matrix, and solvent exchange by which the MWCNTs entered the pores of the matrix. Scanning electron microscopy confirmed that the MWCNTs had entered the bulk of the rubber band, enhancing the sensing capabilities of the produced sensor by increasing the number of conductive pathways.

Steps within this fabrication were optimised such that it reduced the total time taken to produce sensors from over a week, to 2-3 days. In addition to this, a dispersion of concentration of 5 mg/mL provided the best uptake of MWCNTs into the rubber band matrix. This procedure was repeatable, however the random nature of the solvent exchange process meant that each strain sensor had its own unique microstructure.

This was confirmed during characterisation of fifteen strain sensors across two testing protocols, to determine the mechanical and electrical properties under cyclic strain. Through the first protocol in which ten sensors were tested over four test durations up to 1000 cycles and strain rates of up to 350 mm/min at 16% strain, it was determined that they had good durability with respect to structural integrity and sensor response when tested over 4800 cycles, except when stored in high temperature conditions. This testing protocol also exploited the properties of the strain sensor with the combination of strain rates and testing durations in a way that has not been previously attempted by others in the literature.

The adjusted gauge factor was calculated to be between 2-4; adjusted hysteresis was below 20% for eleven out of fifteen tests on one sensor; while coefficient of determination (R^2) values were above 0.9 in all but two tests on the same sensor. These results are comparable with other strain sensors reported in the literature, indicating their suitability to be used in real-life scenarios. However the hysteresis values and difference in R^2 between the loading and unloading phases of the strain cycle highlighted the complexity that would be introduced during sensor calibration.

The second protocol indicated that the strain sensor response does have some dependency on the strain rate that is applied, suggesting that normalising this response would provide a better method of comparing the strain sensor response between different tests. Both protocols enabled a comprehensive understanding of the strain sensor properties within a laboratory environment, before undergoing a cohort study to establish proof of concept.

To summarise the fabrication and characterisation processes:

- The manufacture of a flexible strain sensor from MWCNTs was optimised by considering different concentrations of the MWCNTs within the rubber band matrix and reducing the time of soaking in toluene, to retain the elastic properties of the rubber band

- The optimal concentration of the MWCNT dispersion used to fabricate the strain sensors was determined to be 5 mg/mL based on low resistance measurements of the strain sensor (when compared to those fabricated with 1 mg/mL and 10 mg/mL dispersions)
- Strain sensors were tested and found to be durable and able to withstand 4800 strain cycles, but hysteretic behaviour was observed in the resistance response
- This hysteretic behaviour during the mechanical testing and the strain-dependent response indicated the need for a sensor calibration procedure
- Future developments of this strain sensor are required to help increase the sensitivity and stability of the sensor response. The development of a protective coating will help aid the latter (minimising material loss), as well as preventing users from coming into contact with the nanomaterial filler. This was however beyond the scope of this thesis.

8.2.3 Wearable Technology Development and Cohort Testing

In order to use the strain sensor developed in this project to measure knee range of motion, it required integration into clothing or an accessory that the participants could wear. The sensor, alongside a printed circuit board (PCB) assembly (containing an IMU and data logger), was integrated into a knee warmer that is a common accessory used in cycling. This was deemed to be a low-cost solution, with different sized knee warmers being able to accommodate a wide range of participants. The easy removal of the strain sensor allowed it to be transferred between these different knee warmers, as well as reducing the amount of time it would take to replace a sensor if it failed. This combination of these elements was called the wearable sensor system (WSS).

The prototype nature of the WSS meant that there were some issues that arose during cohort testing predominately with respect to comfort and security of the sensing elements. However, this provided an opportunity for feedback to be gained from participants about how the WSS could be improved. The preliminary testing on rowing and cycling cohorts (both containing ten participants) indicated that the strain sensors were able to track knee range of motion in both sports (including counting the number of strokes or pedal revolutions), as well as variation in this range as stroke rate or cadence were increased. Data obtained from some participants were more comparable to the data collected from the Vicon motion capture system than others. With the same protocols and equipment used, it is likely that the quality of the sensor response was influenced by its microstructure and the concentration and orientation of the MWCNTs that form the conductive network. Future work should therefore focus on ensuring continuity of sensor fabrication.

The use of a questionnaire also provided insight into how participants perceived wearable technology and this particular system, an element of research and development that is often omitted but can be highly valuable and can optimise future translation and device use. Participants in both cohorts agreed

that wearable technology should be unobtrusive and provide useful metrics, but not cost prohibitive. The feedback surrounding the WSS was largely positive, with views shared on how the system could be improved with respect to comfort. There are limitations in rowing and cycling on data that can be collected during competition due to sporting rules, however the WSS can be used as a training tool to help athletes and coaches understand how they are moving, making technical changes that can prevent them from becoming injured and to enhance their performance. Given the increasing narrow margins to success in elite support this is an important area and one that has received limited attention in many sports. There is also the potential for such measures to support athlete health and wellbeing through injury prevention.

8.3 Future Work

Limitations have already been discussed in detail in earlier chapters of this thesis, including the stability of the sensor response due the lack of a coating, as well as the quality of each sensor that was fabricated and used in a small testing cohort. The suggested future work therefore sets out to address some of these limitations. Considering that development of wearable technology is a multi-disciplinary challenge, there are various projects that can run alongside each other to help move this wearable sensor system forward.

8.3.1 Sensor Coating

The need for the strain sensor used in this project to be coated was recognised, however it was not within the scope of this project to fully explore potential coatings before the cohort testing because of disruption due to Covid-19 and the time frames available. Preliminary coating investigations indicated that polyvinyl alcohol (PVA) and polyvinylpyrrolidine (PVP) were not suitable with the former not matching the elastic properties of the strain sensor and delaminating under strain, and the latter not curing well. Polydimethylsiloxane has been used in previously literature as a sensor matrix and also as a coating, and has impressive elastic properties. The drop casting technique or a mould could be used to apply the coating, with curing taking place at a low temperature so as not to degrade the natural rubber matrix of the strain sensor.

The presence of a coating would encapsulate the composite strain sensor and prevent the loss of any MWNCTs, which could help stabilise the sensor response over multiple uses. Any resistance changes would be as a result of the change in orientation of MWCNTs within the sensor matrix, not as a result of MWCNTs being lost from the surface due to contact with other materials (which would increase the overall resistance. However, if the coating cannot meet the elastic properties of the strain sensor (as with PVA and PVP) then this can cause early failure of the sensor and reduce its lifetime. Another advantage to the presence of the coating is protecting any users from the nanomaterials embedded

within the strain sensor. Exposure to nanomaterials is not without its health risks, and so the coating would help reduce this and also aid the commercial viability of the WSS.

8.3.2 Further Sensor Characterisation

The presence of a coating would require additional mechanical and electrical characterisation to take place, to understand whether the sensor response is altered by the coating. Considering the temperature response of the strain sensor, as well as how it interacts with sweat, would help improve how the sensor is calibrated and the design of the wearable sensor system. The current design of the WSS allows the removal of the strain sensor from the knee warmer, meaning that the knee warmer can be washed independently between uses. As such, the resilience of the combined strain sensor and coating to washing do not need to be investigated for this reason. However, rowing and cycling are outdoor sports and can be practised in wet conditions, so understanding the waterproof nature of the coated strain sensor would be important.

More imaging using scanning electron microscopy would be employed, before and after mechanical testing, to observe whether there have been changes in the microstructure and how this may have influenced sensor performance. The cohort testing highlighted the need to for a quality control step to make sure that the sensors used will respond in line with the movements carried out. The imaging, alongside resistance measurements, could form part of this step.

8.3.3 Wider Cohort Testing

Refinements can be made to the WSS, such as the profile and placement of the PCB assembly, as well as the attachment of the strain sensor to knee warmers, or other items of clothing as considered in the qualitative analysis of the questionnaire responses from participants. Miniaturisation of the PCB assembly would make it less obtrusive and users would be less aware of its presence. In order to make the WSS translatable for real-life use, an interactive tool should be developed and tested that can provide feedback to users. Live feedback is desirable an can come in the form of visual, auditory or haptic feedback – this can be tested to determine which method users respond to best when considering their knee range of motion. The Bluetooth module within the PCB assembly means that the WSS already has the capabilities to transmit live data and so the focus would be on the appropriate format of this data.

In this project, the IMU data was not analysed as this was beyond the scope of this thesis, but the information collected from that can be considered in relation to the strain sensor response. With the help of machine learning, the orientation of the IMU could be used to distinguish between the rowing and cycling movements. As determined in the mechanical characterisation of the strain sensor, the response is strain rate dependent – the accelerations and angular velocities as measured by the IMU could help overcome this factor during sensor characterisation, aiding its ability to measure knee

angles at different speeds of movement.

Ultimately, the advantage of wearable technology is that it can be used outside of a laboratory environment, and so testing should be conducted in-field by rowers and cyclists to understand the ease of system set-up and data collection, as well as whether the views expressed are altered, positively or negatively, by these different surroundings. Increasing the cohort size would help understanding of distinctions in technique that can be made between different experience levels using the WSS and gather more data to assess the practicality of its use.

The WSS has shown application in two sports, but other sports where motion of the knee is significant to movement can be considered. An example of this is weightlifting, where knee extension is important when performing the Olympic lifts, but also knee flexion can be monitored to determine range of motion in supplementary lifts such as the back squat. Whichever sport is considered, it is important to be aware of the metrics that relate to performance that the WSS can measure, and that the users have a good understanding of being able to use the WSS in this way.

8.4 Research Contributions

To summarise, this thesis has evaluated the use of wearable technology in sports to measure biomechanics, and has developed and characterised a conductive polymer composite strain sensor that can be used as a lower cost alternative to currently available technologies to measure knee range of motion. A prototype sensor system was created and tested on rowing and cycling cohorts, with data collected able to inform future development of the system. The main scientific contributions are:

- Assessment of how wearable technology is used in sports biomechanics and the requirements for new technology that is being developed
- Development and characterisation of a carbon nanotube-natural rubber composite strain sensor
- Integration of the strain sensor into a wearable sensor system for measuring knee range of motion in rowing and cycling
- Evaluation of the capabilities of the wearable sensor system to monitor knee range of motion, when compared to a motion capture system
- Consideration of the perspectives held by participants surrounding wearable technology and their experiences with the developed sensor system used in this project

Bibliography

[1] M. Dehghani, K. J. Kim, and R. M. Dangelico. Will smartwatches last? factors contributing to intention to keep using smart wearable technology. *Telematics and Informatics*, 35(2):480–490, 2018. doi:10.1016/j.tele.2018.01.007.

[2] J. M. Peake, G. Kerr, and J. P. Sullivan. A critical review of consumer wearables, mobile applications, and equipment for providing biofeedback, monitoring stress, and sleep in physically active populations. *Frontiers in Physiology*, 9:743, 2018. doi:10.3389/fphys.2018.00743.

[3] M. Cardinale and M. C. Varley. Wearable training-monitoring technology: Applications, challenges, and opportunities. *International Journal of Sports Physiolgy and Performance*, 12(Suppl 2):S255–s262, 2017. doi:10.1123/ijspp.2016-0423.

[4] X. Zhang, G. Shan, Y. Wang, B. Wan, and H. Li. Wearables, biomechanical feedback and human motor-skills', learning & optimization, 2019. doi:10.3390/app9020226.

[5] J. Zhang, Y. Cao, M. Qiao, L. Ai, K. Sun, Q. Mi, S. Zang, Y. Zuo, X. Yuan, and Q. Wang. Human motion monitoring in sports using wearable graphene-coated fiber sensors. *Sensors and Actuators, A: Physical*, 274:132–140, 2018. doi:10.1016/j.sna.2018.03.011.

[6] M. Ae. The next steps for expanding and developing sport biomechanics. *Sports Biomechanics*, 19(6):701–722, 2020. doi:10.1080/14763141.2020.1743745.

[7] Y. Adesida, E. Papi, and A. H. McGregor. Exploring the role of wearable technology in sport kinematics and kinetics: A systematic review. *Sensors*, 19(7), 2019. doi:10.3390/s19071597.

[8] A. Waters, E. Phillips, D. Panchuk, and A. Dawson. The coach–scientist relationship in high-performance sport: Biomechanics and sprint coaches. *International Journal of Sports Science & Coaching*, 14(5):617–628, 2019. doi:10.1177/1747954119859100.

[9] S. McDevitt, H. Hernandez, J. Hicks, R. Lowell, H. Bentahaikt, R. Burch, J. Ball, H. Chander, C. Freeman, C. Taylor, and B. Anderson. Wearables for biomechanical performance optimization and risk assessment in industrial and sports applications. *Bioengineering*, 9(1), 2022. doi:10.3390/bioengineering9010033.

[10] J. Zhao. A review of wearable IMU (inertial-measurement-unit)-based pose estimation and drift reduction technologies. In *Journal of Physics: Conference Series*, volume 1087, 2018. doi:10.1088/1742-6596/1087/4/042003.

[11] X. Robert-Lachaine, H. Mecheri, C. Larue, and A. Plamondon. Validation of inertial measurement units with an optoelectronic system for whole-body motion analysis. *Medical & Biological Engineering & Computing*, 55(4):609–619, 2017. doi:10.1007/s11517-016-1537-2.

[12] H. Nakamoto, T. Yamaji, I. Hirata, H. Ootaka, and F. Kobayashi. Joint angle measurement by stretchable strain sensor. *Journal of Ambient Intelligence and Humanized Computing*, 2018. doi:10.1007/s12652-018-0915-z.

[13] J. Ren, C. Wang, X. Zhang, T. Carey, K. Chen, Y. Yin, and F. Torrisi. Environmentally-friendly conductive cotton fabric as flexible strain sensor based on hot press reduced graphene oxide. *Carbon*, 111:622–630, 2017. doi:10.1016/j.carbon.2016.10.045.

[14] L. Duan, D. R. D'Hooge, and L. Cardon. Recent progress on flexible and stretchable piezoresistive strain sensors: From design to application. *Progress in Materials Science*, 114:100617, 2020. doi:10.1016/j.pmatsci.2019.100617.

[15] A. J. Murphy. *Elite Rowing: Technique and Performance*. Thesis, University of London, 2009. URL: https://ethos.bl.uk/OrderDetails.do?uin=uk.bl.ethos.511989.

[16] R. L. Jones and M. Wallace. Another bad day at the training ground: Coping with ambiguity in the coaching context. *Sport, Education and Society*, 10(1):119–134, 2005. doi:10.1080/1357332052000308792.

[17] A. Lees. Biochemical assessment of individual sports for improved performance. *Sports Medicine*, 28(5):299–305, 1999. doi:10.2165/00007256-199928050-00001.

[18] A. Ito. Analysis of techniques for world-top sprinters (in japanese). in h. sasaki, k. kobayashi, & m. ae (eds.), techniques of world-top athletes. *Baseball Magazine Co. Ltd.*, pages 31–49, 1994.

[19] M. Doyle, A. Lyttle, and B. Elliott. Comparison of force-related performance indicators between heavyweight and lightweight rowers. *Sports Biomechanics*, 9:178–92, 2010. doi:10.1080/14763141.2010.511678.

[20] L. Rum, O. Sten, E. Vendrame, V. Belluscio, V. Camomilla, G. Vannozzi, L. Truppa, M. Notarantonio, T. Sciarra, A. Lazich, A. Mannini, and E. Bergamini. Wearable sensors in sports for persons with disability: A systematic review. *Sensors*, 21(5), 2021. doi:10.3390/s21051858.

[21] P. Taboga, R. Kram, and A. M. Grabowski. Maximum-speed curve-running biomechanics of sprinters with and without unilateral leg amputations. *Journal of Experimental Biology*, 219(6):851–858, 2016. doi:10.1242/jeb.133488.

[22] J. R. Fletcher, T. Gallinger, and F. Prince. How can biomechanics improve physical preparation and performance in paralympic athletes? A narrative review. *Sports*, 9(7), 2021. doi:10.3390/sports9070089.

[23] R. Martindale and C. Nash. Sport science relevance and application: Perceptions of UK coaches. *Journal of Sports Sciences*, 31(8):807–819, 2013. doi:10.1080/02640414.2012.754924.

[24] J. J. Malone, L. D. Harper, B. Jones, J. Perry, C. Barnes, and C. Towlson. Perspectives of applied collaborative sport science research within professional team sports. *European Journal of Sport Science*, 19(2):147–155, 2019. doi:10.1080/17461391.2018.1492632.

[25] E. van der Kruk and M. M. Reijne. Accuracy of human motion capture systems for sport applications; state-of-the-art review. *European Journal of Sport Science*, 18(6):806–819, 2018. doi:10.1080/17461391.2018.1463397.

[26] J. Taborri, J. Keogh, A. Kos, A. Santuz, A. Umek, C. Urbanczyk, E. van der Kruk, and S. Rossi. Sport biomechanics applications using inertial, force, and emg sensors: A literature overview. *Applied Bionics and Biomechanics*, 2020:2041549, 2020. doi:10.1155/2020/2041549.

[27] B. Pueo and J. Jimenez-Olmedo. Application of motion capture technology for sport performance analysis. *Retos*, 32:241–247, 2017. doi:10.47197/retos.v0i32.56072.

[28] E. Mencarini, C. Leonardi, A. De Angeli, and M. Zancanaro. Design opportunities for wearable devices in learning to climb. In *ACM International Conference Proceeding Series*, volume 23-27-October-2016, 2016. doi:10.1145/2971485.2971509.

[29] E. Mencarini, A. Rapp, L. Tirabeni, and M. Zancanaro. Designing wearable systems for sports: A review of trends and opportunities in human–computer interaction. *IEEE Transactions on Human-Machine Systems*, 49(4):314–325, 2019. doi:10.1109/THMS.2019.2919702.

[30] P. Düking, F. K. Fuss, H-C. Holmberg, and B. Sperlich. Recommendations for assessment of the reliability, sensitivity, and validity of data provided by wearable sensors designed for monitoring physical activity. *JMIR Mhealth Uhealth*, 6(4):e102, 2018. doi:10.2196/mhealth.9341.

[31] D. T. McMaster, N. Gill, J. Cronin, and M. McGuigan. A brief review of strength and ballistic assessment methodologies in sport. *Sports Medicine*, 44(5):603–623, 2014. doi:10.1007/s40279-014-0145-2.

[32] J. Hamill, G. E. Caldwell, and T. R. Derrick. Reconstructing digital signals using shannon's sampling theorem. *Journal of Applied Biomechanics*, 13(2):226–238, 1997. doi:10.1123/jab.13.2.226.

[33] R. Li, Z. Cai, W. Lee, and D. T. H. Lai. A wearable biofeedback control system based body area network for freestyle swimming. *Conference Proceedings: ... Annual International Conference of the IEEE Engineering in Medicine & Biology Society*, 2016:1866–1869, 2016. doi:10.1109/EMBC.2016.7591084.

[34] J. Reenalda, E. Maartens, L. Homan, and J. H. J. Buurke. Continuous three dimensional analysis of running mechanics during a marathon by means of inertial magnetic measurement units to objectify changes in running mechanics. *Journal of Biomechanics*, 49(14):3362–3367, 2016. doi:10.1016/j.jbiomech.2016.08.032.

[35] W. Kim and M. Kim. Soccer kick detection using a wearable sensor. In *2016 International Conference on Information and Communication Technology Convergence (ICTC)*, pages 1207–1209, 2016. doi:10.1109/ICTC.2016.7763408.

[36] S. Fantozzi, A. Giovanardi, F. A. Magalhaes, R. Di Michele, M. Cortesi, and G. Gatta. Assessment of three-dimensional joint kinematics of the upper limb during simulated swimming using wearable inertial-magnetic measurement units. *Journal of Sports Sciences*, 34(11):1073–1080, 2016. doi:10.1080/02640414.2015.1088659.

[37] M. Patterson, J. Doyle, E. Cahill, B. Caulfield, and U. M. Persson. Quantifying show jumping horse rider expertise using imus. In *2010 32nd Annual International Conference of the IEEE Engineering in Medicine and Biology Society (EMBC 2010), 31 Aug.-4 Sept. 2010*, pages 684–7, 2010. doi:10.1109/IEMBS.2010.5626214.

[38] A. Munz, F. Eckardt, C. Heipertz-Hengst, C. Peham, and K. Witte. A preliminary study of an inertial sensor-based method for the assessment of human pelvis kinematics in dressage riding. *Journal of Equine Veterinary Science*, 33(11):950–955, 2013. doi:10.1016/j.jevs.2013.02.002.

[39] L. K. Philpott, S. Weaver, D. Gordon, P. P. Conway, and A. A. West. Assessing wireless inertia measurement units for monitoring athletics sprint performance. In *SENSORS, 2014 IEEE*, pages 2199–2202, 2014. doi:10.1109/ICSENS.2014.6985476.

[40] R. C. King, D. G. McIlwraith, B. Lo, J. Pansiot, A. H. McGregor, and G. Z. Yang. Body sensor networks for monitoring rowing technique. In *2009 Sixth International Workshop on Wearable and Implantable Body Sensor Networks*, pages 251–255, 2009. doi:10.1109/BSN.2009.60.

[41] E. C. Makhni, V. A. Lizzio, F. Meta, J. P. Stephens, K. R. Okoroha, and V. Moutzouros. Assessment of elbow torque and other parameters during the pitching motion: Comparison of fastball, curveball, and change-up. *Arthroscopy : The journal of Arthroscopic & Related Surgery*, 34(3):816–822, 2018. doi:10.1016/j.arthro.2017.09.045.

[42] Michael Lapinski, Eric Berkson, Thomas Gill, Mike Reinold, and Joseph A. Paradiso. A distributed wearable, wireless sensor system for evaluating professional baseball pitchers and batters. In *2009 International Symposium on Wearable Computers, ISWC 2009, September 4, 2009 - September 7, 2009*, Proceedings - International Symposium on Wearable Computers, ISWC, pages 131–138. IEEE Computer Society, 2009. doi:10.1109/ISWC.2009.27.

[43] J. B. Shepherd, G. Giblin, G. J. Pepping, D. Thiel, and D. Rowlands. Development and validation of a single wrist mounted inertial sensor for biomechanical performance analysis of an elite netball shot. *IEEE Sensors Letters*, 1(5):600100 (4 pp.), 2017. doi:10.1109/LSENS.2017.2750695.

[44] Y. Wang, Y. Zhao, R. H. M. Chan, and W. J. Li. Volleyball skill assessment using a single wearable micro inertial measurement unit at wrist. *IEEE Access*, 6:13758–13765, 2018. doi:10.1109/ACCESS.2018.2792220.

[45] Z. Wang, J. Wang, H. Zhao, N. Yang, and G. Fortino. Canoesense: Monitoring canoe sprint motion using wearable sensors. In *2016 IEEE International Conference on Systems, Man, and Cybernetics, SMC 2016 - Conference Proceedings*, pages 644–649, 2016. doi:10.1109/SMC.2016.7844313.

[46] A. Krüger and J. Edelmann-Nusser. Biomechanical analysis in freestyle snowboarding: Application of a full-body inertial measurement system and a bilateral insole measurement system. *Sports Technology*, 2(1-2):17–23, 2009. doi:10.1080/19346182.2009.9648494.

[47] J. Chardonnens, J. Favre, F. Cuendet, G. Gremion, and K. Aminian. Characterization of lower-limbs inter-segment coordination during the take-off extension in ski jumping. *Human Movement Science*, 32(4):741–52, 2013. doi:10.1016/j.humov.2013.01.010.

[48] S. Blair, G. Duthie, S. Robertson, W. Hopkins, and K. Ball. Concurrent validation of an inertial measurement system to quantify kicking biomechanics in four football codes. *Journal of Biomechanics*, 73:24–32, 2018. doi:10.1016/j.jbiomech.2018.03.031.

[49] E. A. Gandy, A. Bondi, R. Hogg, and T. M. C. Pigott. A preliminary investigation of the use of inertial sensing technology for the measurement of hip rotation asymmetry in horse riders. *Sports Technology*, 7(1-2):79–88, 2014. doi:10.1080/19346182.2014.905949.

[50] H. Koda, K. Sagawa, K. Kuroshima, T. Tsukamoto, K. Urita, and Y. Ishibashi. 3d measurement of forearm and upper arm during throwing motion using body mounted sensor. *Journal of*

Advanced Mechanical Design Systems and Manufacturing, 4(1):167–178, 2010. doi:10.1299/jamdsm.4.167.

[51] D. Kiernan, D. A. Hawkins, M. A. C. Manoukian, M. McKallip, L. Oelsner, C. F. Caskey, and C. L. Coolbaugh. Accelerometer-based prediction of running injury in national collegiate athletic association track athletes. *Journal of Biomechanics*, 73:201–209, 2018. doi:10.1016/j.jbiomech.2018.04.001.

[52] Y. W. Guo, G. Z. Liu, B. Y. Huang, G. R. Zhao, Z. Y. Mei, and L. Wang. A pilot study on quantitative analysis for table tennis block using a 3d accelerometer. In *Proceedings of the IEEE/EMBS Region 8 International Conference on Information Technology Applications in Biomedicine, ITAB*, 2010. doi:10.1109/ITAB.2010.5687806.

[53] M. Bachlin and G. Troster. Swimming performance and technique evaluation with wearable acceleration sensors. *Pervasive and Mobile Computing*, 8(1):68–81, 2012. doi:10.1016/j.pmcj.2011.05.003.

[54] F. Mocera, G. Aquilino, and A. Somà. Nordic walking performance analysis with an integrated monitoring system. *Sensors*, 18(5), 2018. doi:10.3390/s18051505.

[55] J. S. Akins, N. R. Heebner, M. Lovalekar, and T. C. Sell. Reliability and validity of instrumented soccer equipment. *Journal of Applied Biomechanics*, 31(3):195–201, 2015. doi:10.1123/jab.2014-0191.

[56] S. Gawsalyan, T. S. Janarthanan, N. Thiruthanikan, R. Shahintha, and P. Silva. Upper limb analysis using wearable sensors for cricket. In *Proceedings of the 2017 2nd IEEE International Conference on Electrical, Computer and Communication Technologies, ICECCT 2017*, 2017. doi:10.1109/ICECCT.2017.8118010.

[57] K. Nakazato, P. Scheiber, and E. Müller. A comparison of ground reaction forces determined by portable force-plate and pressure-insole systems in alpine skiing. *Journal of Sports Science and Medicine*, 10(4):754–762, 2011. URL: https://www.ncbi.nlm.nih.gov/pmc/articles/PMC3761512/.

[58] K. Nakazato, P. Scheiber, and E. Müller. Comparison between the force application point determined by portable force plate system and the center of pressure determined by pressure insole system during alpine skiing. *Sports Engineering*, 16(4):297–307, 2013. doi:10.1007/s12283-013-0119-x.

[59] A. Jacob, W. N. W. Zakaria, M. R. B. Tomari, T. K. Sek, and A. A. M. Suberi. Wearable flex sensor system for multiple badminton player grip identification. In *Advances in Electri-*

cal and Electronic Engineering: From Theory to Applications, volume 1883 of *AIP Conference Proceedings*, 2017. doi:10.1063/1.5002054.

[60] C. M. Wood and K. Kipp. Use of audio biofeedback to reduce tibial impact accelerations during running. *Journal of Biomechanics*, 47(7):1739–41, 2014. doi:10.1016/j.jbiomech.2014.03.008.

[61] T. Mitsui, S. Tang, and S. Obana. Support system for improving golf swing by using wearable sensors. In *2015 Eighth International Conference on Mobile Computing and Ubiquitous Networking (ICMU)*, pages 100–101, 2015. doi:10.1109/ICMU.2015.7061049.

[62] S. Lee, K. Kim, Y. H. Kim, and S. S. Lee. Motion anlaysis in lower extremity joints during ski carving turns using wearble inertial sensors and plantar pressure sensors. In *2017 Ieee International Conference on Systems, Man, and Cybernetics*, IEEE International Conference on Systems Man and Cybernetics Conference Proceedings, pages 695–698, 2017. doi:10.1109/SMC.2017.8122688.

[63] M. J. Page, J. E. McKenzie, P. M. Bossuyt, I. Boutron, T. C. Hoffmann, C. D. Mulrow, L. Shamseer, J. M. Tetzlaff, E. A. Akl, S. E. Brennan, R. Chou, J. Glanville, J. M. Grimshaw, A. Hróbjartsson, M. M. Lalu, T. Li, E. W. Loder, E. Mayo-Wilson, S. McDonald, L. A. McGuinness, L. A. Stewart, J. Thomas, A. C. Tricco, V. A. Welch, P. Whiting, and D. Moher. The PRISMA 2020 statement: an updated guideline for reporting systematic reviews. *BMJ*, 372:n71, 2021. doi:10.1136/bmj.n71.

[64] Y. W. Bai and I. H. Hsieh. Using a wearable device to assist the training of the throwing motion of baseball players. In *2019 IEEE Canadian Conference of Electrical and Computer Engineering, CCECE 2019*, 2019. doi:10.1109/CCECE.2019.8861566.

[65] V. Cigrovski, M. Ocic, I. Bon, T. Rupcic, and I. Bozic. Does the sequential teaching of elements of alpine ski school follow the increase of pressure beneath the skier's foot? *Acta Kinesiologica*, 14(2):42–46, 2020. URL: https://www.bib.irb.hr/1096671/download/1096671.06-Cigrovski-V.-et.-alpdf.

[66] T. Menzel and W. Potthast. Validation of a novel boxing monitoring system to detect and analyse the centre of pressure movement on the boxer's fist. *Sensors*, 21(24), 2021. doi:10.3390/s21248394.

[67] S. Shankar, R. P. Suresh, V. Talasila, V. Sridhar, and Ieee. Performance measurement and analysis of shooting form of basketball players using a wearable iot system. In *2018 3rd International Conference on Circuits, Control, Communication and Computing (I4C)*, 2018. doi:10.1109/CIMCA.2018.8739721.

[68] A. Patoz, T. Lussiana, B. Breine, C. Gindre, and D. Malatesta. A single sacral-mounted inertial measurement unit to estimate peak vertical ground reaction force, contact time, and flight time in running. *Sensors*, 22(3), 2022. doi:10.3390/s22030784.

[69] M. Kos and I. Kramberger. Tennis stroke consistency analysis using miniature wearable IMU. In *2018 25th International Conference on Systems, Signals and Image Processing (IWSSIP)*, 2018. doi:10.1109/IWSSIP.2018.8439382.

[70] Z. Bańkosz and S. Winiarski. Using wearable inertial sensors to estimate kinematic parameters and variability in the table tennis topspin forehand stroke. *Applied Bionics and Biomechanics*, 2020, 2020. doi:10.1155/2020/8413948.

[71] X. Sha, G. Wei, X. Zhang, X. Ren, S. Wang, Z. He, and Y. Zhao. Accurate recognition of player identity and stroke performance in table tennis using a smart wristband. *IEEE Sensors Journal*, 21(9):10923–10932, 2021. doi:10.1109/JSEN.2021.3060914.

[72] M. Shang and Y. Cheng. Elite male freestyle swimmers hip roll characteristics research. In *2021 International Conference on Health Big Data and Smart Sports, HBDSS 2021, October 29, 2021 - October 31, 2021*, pages 206–209, 2021. doi:10.1109/HBDSS54392.2021.00047.

[73] M. Lapinski, C. Brum Medeiros, D. Moxley Scarborough, E. Berkson, T. J. Gill, T. Kepple, and J. A. Paradiso. A wide-range, wireless wearable inertial motion sensing system for capturing fast athletic biomechanics in overhead pitching. *Sensors*, 19(17), 2019. doi:10.3390/s19173637.

[74] D. S. Cottam, A. C. Campbell, M. P. C. Davey, P. Kent, B. C. Elliott, and J. A. Alderson. Measurement of uni-planar and sport specific trunk motion using magneto-inertial measurement units: The concurrent validity of Noraxon and Xsens systems relative to a retro-reflective system. *Gait and Posture*, 92:129–134, 2022. doi:10.1016/j.gaitpost.2021.11.012.

[75] C. A. Clermont, L. C. Benson, W. B. Edwards, B. A. Hettinga, and R. Ferber. New considerations for wearable technology data: Changes in running biomechanics during a marathon. *Journal of Applied Biomechanics*, 35(6):401–409, 2019. doi:10.1123/jab.2018-0453.

[76] N. U. Ahamed, D. Kobsar, L. Benson, C. Clermont, R. Kohrs, S. T. Osis, and R. Ferber. Using wearable sensors to classify subject-specific running biomechanical gait patterns based on changes in environmental weather conditions. *PLoS ONE*, 13(9):e0203839, 2018. doi:10.1371/journal.pone.0203839.

[77] L. C. Benson, N. U. Ahamed, D. Kobsar, and R. Ferber. New considerations for collecting biomechanical data using wearable sensors: Number of level runs to define a stable running pattern with a single imu. *Journal of Biomechanics*, 85:187–192, 2019. doi:10.1016/j.jbiomech.2019.01.004.

[78] D. H. K. Chow, L. Tremblay, C. Y. Lam, A. W. Y. Yeung, W. H. W. Cheng, and P. T. W. Tse. Comparison between accelerometer and gyroscope in predicting level-ground running kinematics by treadmill running kinematics using a single wearable sensor. *Sensors*, 21(14), 2021. doi:10.3390/s21144633.

[79] Y. Tomita, T. Iizuka, K. Irisawa, and S. Imura. Detection of movement events of long-track speed skating using wearable inertial sensors. *Sensors*, 21(11), 2021. doi:10.3390/s21113649.

[80] D. J. Epifano, S. Ryan, A. C. Clarke, and K. J. Middleton. Objective assessment of fast bowling delivery intensity in amateur male cricketers. *Journal of Sports Sciences*, 40(4):442–449, 2022. doi:10.1080/02640414.2021.1996987.

[81] Y. Chen, J. X. Li, Y. Hong, and L. Wang. Plantar stress-related injuries in male basketball players: Variations on plantar loads during different maximum-effort maneuvers. *BioMed Research International*, 2018, 2018. doi:10.1155/2018/4523849.

[82] C. Chen, Z. Liang, and S. Li. The plantar pressure analysis of open stance forehand in female tennis players. *Physical Activity and Health*, 3(1):63–70, 2019. doi:10.5334/paah.37.

[83] S. Jandova, M. Sparks, P. Olesniewicz, J. Charousek, M. Chrastkova, and J. Markiewicz. Changes in the foot strike pattern and pressure distribution when running in minimalist and traditional sport shoes. *Medicina dello Sport*, 71(2):257–267, 2018. doi:10.23736/S0025-7826.18.03029-6.

[84] S. Matsumura, K. Ohta, S. I. Yamamoto, Y. Koike, and T. Kimura. Comfortable and convenient turning skill assessment for alpine skiers using IMU and plantar pressure distribution sensors. *Sensors (Switzerland)*, 21(3):1–12, 2021. doi:10.3390/s21030834.

[85] T. Purevsuren, B. Khuyagbaatar, K. Kim, and Y. H. Kim. Investigation of knee joint forces and moments during short-track speed skating using wearable motion analysis system. *International Journal of Precision Engineering and Manufacturing*, 19(7):1055–1060, 2018. URL: https://rdcu.be/c4rdT.

[86] V. Bessone, J. Petrat, and A. Schwirtz. Ski position during the flight and landing preparation phases in ski jumping detected with inertial sensors. *Sensors*, 19(11), 2019. doi:10.3390/s19112575.

[87] V. Bessone, J. Petrat, and A. Schwirtz. Ground reaction forces and kinematics of ski jump landing using wearable sensors. *Sensors*, 19(9), 2019. doi:10.3390/s19092011.

[88] M. K. Seeley, A. Evans-Pickett, G. Q. Collins, J. B. Tracy, N. J. Tuttle, P. G. Rosquist, A. J. Merrell, W. F. Christensen, D. T. Fullwood, and A. E. Bowden. Predicting vertical ground

reaction force during running using novel piezoresponsive sensors and accelerometry. *Journal of Sports Sciences*, 38(16):1844–1858, 2020. doi:10.1080/02640414.2020.1757361.

[89] T. Menzel and W. Potthast. Application of a validated innovative smart wearable for performance analysis by experienced and non-experienced athletes in boxing. *Sensors*, 21(23), 2021. doi:10.3390/s21237882.

[90] R. S. Alcantara, E. M. Day, M. E. Hahn, and A. M. Grabowski. Sacral acceleration can predict whole-body kinetics and stride kinematics across running speeds. *PeerJ*, 9, 2021. doi:10.7717/peerj.11199.

[91] P. Macadam, J. B. Cronin, A. M. Uthoff, R. Nagahara, J. Zois, S. Diewald, F. Tinwala, and J. Neville. Thigh loaded wearable resistance increases sagittal plane rotational work of the thigh resulting in slower 50-m sprint times. *Sports Biomechanics*, pages 1–12, 2020. doi:10.1080/14763141.2020.1762720.

[92] S. M. Brice, M. Hurley, and E. J. Phillips. Use of inertial measurement units for measuring torso and pelvis orientation, and shoulder-pelvis separation angle in the discus throw. *International Journal of Sports Science & Coaching*, 13(6):985–992, 2018. doi:10.1177/1747954118778664.

[93] Y. Wang, M. Chen, X. Wang, R. H. M. Chan, and W. J. Li. IoT for next-generation racket sports training. *IEEE Internet of Things Journal*, 5(6):4558–4566, 2018. doi:10.1109/JIOT.2018.2837347.

[94] E. M. Day, R. S. Alcantara, M. A. McGeehan, A. M. Grabowski, and M. E. Hahn. Low-pass filter cutoff frequency affects sacral-mounted inertial measurement unit estimations of peak vertical ground reaction force and contact time during treadmill running. *Journal of Biomechanics*, 119, 2021. doi:10.1016/j.jbiomech.2021.110323.

[95] C. L. Camp, S. Loushin, S. Nezlek, A. P. Fiegen, D. Christoffer, and K. Kaufman. Are wearable sensors valid and reliable for studying the baseball pitching motion? an independent comparison with marker-based motion capture. *The American Journal of Sports Medicine*, 49(11):3094–3101, 2021. doi:10.1177/03635465211029017.

[96] N. D. Leafblad, D. R. Larson, G. S. Fleisig, S. Conte, S. A. Fealy, J. S. Dines, J. D'Angelo, and C. L. Camp. Variability in baseball throwing metrics during a structured long-toss program: Does one size fit all or should programs be individualized? *Sports Health*, 11(6):535–542, 2019. doi:10.1177/1941738119869945.

[97] Y. C. Choi, B. Khuyagbaatar, M. Cheon, T. Batbayar, S. Lee, and Y. H. Kim. Kinematic comparison of double poling techniques between national and college level cross-country skiers

using wearable inertial measurement unit sensors. *International Journal of Precision Engineering and Manufacturing*, 22(6):1105–1112, 2021. doi:10.1007/s12541-021-00511-3.

[98] Y. H. Kim, B. Khuyagbaatar, J. Lee, M. Cheon, T. Batbayar, and Y. C. Choi. Kinematic comparison of national and college level cross-country skiers during double poling technique. *Gait & Posture*, 73(Supplement 1):461–462, 2019. doi:10.1016/j.gaitpost.2019.07.352.

[99] M. Colapietro, J. J. Fraser, J. E. Resch, and J. Hertel. Running mechanics during 1600 meter track runs in young adults with and without chronic ankle instability. *Physical Therapy in Sport*, 42:16–25, 2020. doi:10.1016/j.ptsp.2019.11.010.

[100] C. Gregory, R. M. Koldenhoven, M. Higgins, and J. Hertel. External ankle supports alter running biomechanics: a field-based study using wearable sensors. *Physiological measurement*, 40(4):044003, 2019. doi:10.1088/1361-6579/ab15ad.

[101] C. R. Hollis, R. M. Koldenhoven, J. E. Resch, and J. Hertel. Running biomechanics as measured by wearable sensors: effects of speed and surface. *Sports biomechanics*, 20(5):521–531, 2021. doi:10.1080/14763141.2019.1579366.

[102] R. M. Koldenhoven and J. Hertel. Validation of a wearable sensor for measuring running biomechanics. *Digital Biomarkers*, 2(2):74–78, 2018. doi:10.1159/000491645.

[103] Z. Kozinc, D. Smajla, and N. Šarabon. The reliability of wearable commercial sensors for outdoor assessment of running biomechanics: the effect of surface and running speed. *Sports biomechanics*, pages 1–14, 2022. doi:10.1080/14763141.2021.2022746.

[104] X. Wu, Z. Zhou, and Q. Wang. Real-time kinematics measurement of human lower-limb underwater motions based on inertial units. In *2021 27th International Conference on Mechatronics and Machine Vision in Practice, M2VIP 2021*, pages 715–720, 2021. doi:10.1109/M2VIP49856.2021.9665010.

[105] F. J. Wouda, M. Giuberti, G. Bellusci, E. Maartens, J. Reenalda, B. F. van Beijnum, and P. H. Veltink. Estimation of vertical ground reaction forces and sagittal knee kinematics during running using three inertial sensors. *Frontiers in Physiology*, 9:218, 2018. doi:10.3389/fphys.2018.00218.

[106] B. Fasel, J. Sporri, J. Chardonnens, J. Kroll, E. Muller, and K. Aminian. Joint inertial sensor orientation drift reduction for highly dynamic movements. *IEEE Journal of Biomedical and Health Informatics*, 22(1):77–86, 2018. doi:10.1109/JBHI.2017.2659758.

[107] B. Muniz-Pardos, S. Sutehall, J. Gellaerts, M. Falbriard, B. Mariani, A. Bosch, M. Asrat, J. Schaible, and Y. P. Pitsiladis. Integration of wearable sensors into the evaluation of running

economy and foot mechanics in elite runners. *Current Sports Medicine Reports*, 17(12):480–488, 2018. doi:10.1249/JSR.0000000000000550.

[108] R. Li, Q. Ye, and D. T. H. Lai. A real-time fuzzy logic biofeedback controller for freestyle swimming body posture adjustment. In *2020 42nd Annual International Conference of the IEEE Engineering in Medicine & Biology Society (EMBC)*, pages 4620–4623, 2020. doi:10.1109/EMBC44109.2020.9176237.

[109] Y. Nagano, S. Sasaki, A. Higashihara, and H. Ichikawa. Movements with greater trunk accelerations and their properties during badminton games. *Sports Biomechanics*, 19(3):342–352, 2020. doi:10.1080/14763141.2018.1478989.

[110] N. G. Punchihewa, H. Arakawa, E. Chosa, and G. Yamako. A hand-worn inertial measurement unit for detection of bat-ball impact during baseball hitting. *Sensors*, 21(9), 2021. doi:10.3390/s21093002.

[111] I. N. Moltó, J. P. Albiach, J. J. Amer-Cuenca, E. Segura-Orti, W. Gabriel, and J. Martínez-Gramage. Wearable sensors detect differences between the sexes in lower limb electromyographic activity and pelvis 3D kinematics during running. *Sensors*, 20(22), 2020. doi:10.3390/s20226478.

[112] B. Nyoni, M. Nleya, and B. Mtunzi. A training utility for estimating the bowling speed of a cricketer using accelerometer data. In *2018 International Conference on Intelligent and Innovative Computing Applications, ICONIC 2018, December 6, 2018 - December 7, 2018*, 2018. doi:10.1109/ICONIC.2018.8601232.

[113] J. M. Oliva-Lozano, E. F. Maraver, V. Fortes, and J. M. Muyor. Kinematic analysis of the postural demands in professional soccer match play using inertial measurement units. *Sensors*, 20(21):1–11, 2020. doi:10.3390/s20215971.

[114] R. Pimentel, M. N. Potter, J. J. Carollo, D. R. Howell, and E. A. Sweeney. Peak sagittal plane spine kinematics in female gymnasts with and without a history of low back pain. *Clinical Biomechanics*, 76, 2020. doi:10.1016/j.clinbiomech.2020.105019.

[115] M. Zrenner, C. Feldner, U. Jensen, N. Roth, R. Richer, and B. M. Eskofier. Evaluation of foot kinematics during endurance running on different surfaces in real-world environments. In *Proceedings of the 12th International Symposium on Computer Science in Sport (IACSS 2019)*, pages 106–113, 2020. doi:10.1007/978-3-030-35048-2_13.

[116] Z. Wang, X. Shi, J. Wang, F. Gao, J. Li, M. Guo, H. Zhao, and S. Qiu. Swimming motion analysis and posture recognition based on wearable inertial sensors. In *Conference Proceedings*

- *IEEE International Conference on Systems, Man and Cybernetics*, pages 3371–3376, 2019. doi:10.1109/SMC.2019.8913847.

[117] Z. Wang, J. Wang, H. Zhao, S. Qiu, J. Li, F. Gao, and X. Shi. Using wearable sensors to capture posture of the human lumbar spine in competitive swimming. *IEEE Transactions on Human-Machine Systems*, 49(2):194–205, 2019. doi:10.1109/THMS.2019.2892318.

[118] A. I. Cuesta-Vargas, A. Galán-Mercant, and J. M. Williams. The use of inertial sensors system for human motion analysis. *Physical Therapy Reviews*, 15(6):462–473, 2010. doi:10.1179/1743288X11Y.0000000006.

[119] S. Lee, K. Kim, Y. H. Kim, and S. S. Lee. Motion anlaysis in lower extremity joints during ski carving turns using wearble inertial sensors and plantar pressure sensors. In *2017 IEEE International Conference on Systems, Man, and Cybernetics, SMC 2017*, pages 695–698, 2017. doi:10.1109/SMC.2017.8122688.

[120] Movesense. Movesense developer kit 2.0. Access date: 30/09/2022. URL: https://www.movesense.com/product/movesense-developer-kit-2-0/.

[121] RunScribe. Runscribe. Access date: 30/09/2022. URL: https://runscribe.com/.

[122] IMeasureU. Imeasureu imu-step plans and pricing. Access date: 30/09/2022. URL: https://imeasureu.com/pricing/#plan-features.

[123] A. Donaldson, D. G. Lloyd, B. J. Gabbe, J. Cook, W. Young, P. White, and C. F. Finch. Scientific evidence is just the starting point: A generalizable process for developing sports injury prevention interventions. *Journal of Sport and Health Science*, 5(3):334–341, 2016. doi:10.1016/j.jshs.2016.08.003.

[124] J. M. Plaza-Bravo, Mateo-March M., Sanchis-Sanchis R., Pérez-Soriano P., Zabala M., and Encarnación-Martínez A. Validity and reliability of the leomo motion-tracking device based on inertial measurement unit with an optoelectronic camera system for cycling pedaling, evaluation. *International Journal of Environmental Research and Public Health*, 19(14), 2022. doi:10.3390/ijerph19148375.

[125] T. Černe, R. Kamnik, and M. Munih. The measurement setup for real-time biomechanical analysis of rowing on an ergometer. *Measurement*, 44(10):1819–1827, 2011. doi:10.1016/j.measurement.2011.09.006.

[126] R. R. Steer, A. H. McGregor, and A. M. Bull. A comparison of kinematics and performance measures of two rowing ergometers. *Journal of Sports Science & Medicine*, 5(1):52–9, 2006. URL: https://www.ncbi.nlm.nih.gov/pmc/articles/PMC3818674/.

[127] E. M. Buckeridge, A. M. Bull, and A. H. McGregor. Foot force production and asymmetries in elite rowers. *Sports Biomechanics*, 13(1):47–61, 2014. doi:10.1080/14763141.2013.861013.

[128] A. J. Murphy, S. T. H. Chee, A. M. J. Bull, and A. H. McGregor. The calibration and application of a force-measuring apparatus on the seat of a rowing ergometer. *Proceedings of the Institution of Mechanical Engineers, Part P: Journal of Sports Engineering and Technology*, 224(1):109–116, 2009. doi:10.1243/17543371JSET39.

[129] A. M. Bull and A. H. McGregor. Measuring spinal motion in rowers: the use of an electromagnetic device. *Clinical Biomechanics*, 15(10):772–6, 2000. doi:10.1016/s0268-0033(00)00043-7.

[130] P. J. Holt, A. M. Bull, P. M. Cashman, and A. H. McGregor. Kinematics of spinal motion during prolonged rowing. *International Journal of Sports Medicine*, 24(8):597–602, 2003. doi:10.1055/s-2003-43273.

[131] R. Geng, J. Li, and Y. Gu. Biomechanical evaluation of two rowing training methods. *Applied Mechanics and Materials*, 105-107, 2011. doi:10.4028/www.scientific.net/AMM.105-107.283.

[132] D. Perić, N. Ilić, and Z. Ahmetovićvić. Kinematic and dynamic stroke variables of elite and sub-elite rowers. *International Journal of Performance Analysis in Sport*, 19(1):65–75, 2019. doi:10.1080/24748668.2018.1563857.

[133] N. A. Turpin and B. Watier. Cycling biomechanics and its relationship to performance. *Applied Sciences*, 10(12), 2020. doi:10.3390/app10124112.

[134] D. J. S. Wadsworth and P. Weinrauch. The role of a bike fit in cyclists with hip pain. A clinical commentary. *International Journal of Sports Physical Therapy*, 14(3):468–486, 2019. URL: https://www.ncbi.nlm.nih.gov/pmc/articles/PMC6818133/.

[135] V. Rodríguez-Rielves, Lillo-Beviá J. R., Buendía-Romero A., Martínez-Cava A., Hernández-Belmonte A., and Courel-Ibáñez J. Pallarés J. G. Are the Assioma Favero power meter pedals a reliable tool for monitoring, 2021. doi:10.3390/s21082789.

[136] W. W. Peveler, J. D. Pounders, and P. A. Bishop. Effects of saddle height on anaerobic power production in cycling. *The Journal of Strength & Conditioning Research*, 21(4), 2007. doi:10.1519/00124278-200711000-00007.

[137] W. W. Peveler, B. Shew, S. Johnson, and T. G. Palmer. A kinematic comparison of alterations to knee and ankle angles from resting measures to active pedaling during a graded exercise protocol. *The Journal of Strength & Conditioning Research*, 26(11), 2012. doi:10.1519/JSC.0b013e318243fdcb.

[138] K. A. Karlson. Rowing: sport-specific concerns for the team physician. *Current Sports Medicine Reports*, 11(5):257–61, 2012. doi:10.1249/JSR.0b013e3182699154.

[139] E. M. Buckeridge, A. M. Bull, and A. H. McGregor. Biomechanical determinants of elite rowing technique and performance. *Scandinavian Journal of Medicine & Science in Sports*, 25(2):e176–83, 2015. doi:10.1111/sms.12264.

[140] M. Amjadi, K. Kyung, I. Park, and M. Sitti. Stretchable, skin-mountable, and wearable strain sensors and their potential applications: A review. *Advanced Functional Materials*, 26(11):1678–1698, 2016. doi:10.1002/adfm.201504755.

[141] S. Ryu, P. Lee, J. B. Chou, R. Xu, R. Zhao, A. J. Hart, and S. Kim. Extremely elastic wearable carbon nanotube fiber strain sensor for monitoring of human motion. *ACS Nano*, 9(6):5929–5936, 2015. doi:10.1021/acsnano.5b00599.

[142] D. J. Cohen, D. Mitra, K. Peterson, and M. M. Maharbiz. A highly elastic, capacitive strain gauge based on percolating nanotube networks. *Nano Letters*, 12(4):1821–1825, 2012. doi:10.1021/nl204052z.

[143] J. Park, I. You, S. Shin, and U. Jeong. Material approaches to stretchable strain sensors. *ChemPhysChem*, 16(6):1155–1163, 2015. doi:10.1002/cphc.201402810.

[144] W. Obitayo and T. Liu. A review: Carbon nanotube-based piezoresistive strain sensors. *Journal of Sensors*, 2012:652438, 2012. doi:10.1155/2012/652438.

[145] L. Cai, L. Song, P. Luan, Q. Zhang, N. Zhang, Q. Gao, D. Zhao, X. Zhang, M. Tu, F. Yang, W. Zhou, Q. Fan, J. Luo, W. Zhou, P. M. Ajayan, and S. Xie. Super-stretchable, transparent carbon nanotube-based capacitive strain sensors for human motion detection. *Scientific Reports*, 3:3048, 2013. doi:10.1038/srep03048.

[146] T. Yamada, Y. Hayamizu, Y. Yamamoto, Y. Yomogida, A. Izadi-Najafabadi, D. N. Futaba, and K. Hata. A stretchable carbon nanotube strain sensor for human-motion detection. *Nature Nanotechnology*, 6(5):296–301, 2011. doi:10.1038/nnano.2011.36.

[147] V. Giurgiutiu. *Chapter 8 - Other Sensors for SHM of Aerospace Composites*, pages 297–315. Academic Press, Oxford, 2016. doi:10.1016/B978-0-12-409605-9.00008-8.

[148] W. Montero, R. Farag, V. Díaz, M. Ramirez, and B. L. Boada. Uncertainties associated with strain-measuring systems using resistance strain gauges. *The Journal of Strain Analysis for Engineering Design*, 46(1):1–13, 2010. doi:10.1243/03093247JSA661.

[149] Y. Wang, D. Thomas, P. Zhang, H. Yokota, and L. Yang. Whole field strain measurement on complex surfaces by digital speckle pattern interferometry. *Materials Evaluation*, 66(5):507–512, 2008. URL: https://www.ncbi.nlm.nih.gov/pmc/articles/PMC3122977/.

[150] M. I. Tiwana, S. J. Redmond, and N. H. Lovell. A review of tactile sensing technologies with applications in biomedical engineering. *Sensors and Actuators A: Physical*, 179:17–31, 2012. doi:10.1016/j.sna.2012.02.051.

[151] E. A. Al-Fakih, N. A. Abu Osman, and F. R. Mahmad Adikan. Techniques for interface stress measurements within prosthetic sockets of transtibial amputees: A review of the past 50 years of research. *Sensors*, 16(7):1119, 2016. doi:10.3390/s16071119.

[152] H. Souri, H. Banerjee, A. Jusufi, N. Radacsi, A. A. Stokes, I. Park, M. Sitti, and M. Amjadi. Wearable and stretchable strain sensors: Materials, sensing mechanisms, and applications. *Advanced Intelligent Systems*, 2(8):2000039, 2020. doi:10.1002/aisy.202000039.

[153] C. S. Boland, U. Khan, C. Backes, A. O'Neill, J. McCauley, S. Duane, R. Shanker, Y. Liu, I. Jurewicz, A. B. Dalton, and J. N. Coleman. Sensitive, high-strain, high-rate bodily motion sensors based on graphene–rubber composites. *ACS Nano*, 8(9):8819–8830, 2014. doi:10.1021/nn503454h.

[154] R. Rahimi, M. Ochoa, W. Yu, and B. Ziaie. Highly stretchable and sensitive unidirectional strain sensor via laser carbonization. *ACS Applied Materials & Interfaces*, 7(8):4463–4470, 2015. doi:10.1021/am509087u.

[155] D. G. Callister, W. D.and Rethwisch. *Materials Science and Engineering, Eighth Edition SI Version*. John Wiley & Sons Pte Ltd, 2011.

[156] R. Nur, N. Matsuhisa, Z. Jiang, M. O. G. Nayeem, T. Yokota, and T. Someya. A highly sensitive capacitive-type strain sensor using wrinkled ultrathin gold films. *Nano Letters*, 18(9):5610–5617, 2018. doi:10.1021/acs.nanolett.8b02088.

[157] A. Atalay, V. Sanchez, O. Atalay, D. M. Vogt, F. Haufe, R. J. Wood, and C. J. Walsh. Batch fabrication of customizable silicone-textile composite capacitive strain sensors for human motion tracking. *Advanced Materials Technologies*, 2(9):1700136, 2017. doi:10.1002/admt.201700136.

[158] J. Guo, B. Zhou, R. Zong, L. Pan, X. Li, X. Yu, C. Yang, L. Kong, and Q. Dai. Stretchable and highly sensitive optical strain sensors for human-activity monitoring and healthcare. *ACS Applied Materials & Interfaces*, 11(37):33589–33598, 2019. doi:10.1021/acsami.9b09815.

[159] W. Zheng, X. Tao, B. Zhu, G. Wang, and C. Hui. Fabrication and evaluation of a notched

polymer optical fiber fabric strain sensor and its application in human respiration monitoring. *Textile Research Journal*, 84(17):1791–1802, 2014. doi:10.1177/0040517514528560.

[160] C. E. Campanella, A. Cuccovillo, C. Campanella, A. Yurt, and V. M. N. Passaro. Fibre Bragg grating based strain sensors: Review of technology and applications. *Sensors*, 18(9):3115, 2018. doi:10.3390/s18093115.

[161] P. Roriz, L. Carvalho, O. Frazão, J. L. Santos, and J. A. Simões. From conventional sensors to fibre optic sensors for strain and force measurements in biomechanics applications: A review. *Journal of Biomechanics*, 47(6):1251–1261, 2014. doi:10.1016/j.jbiomech.2014.01.054.

[162] R. C. Allil and M. M. Werneck. Optical high-voltage sensor based on fiber Bragg grating and pzt piezoelectric ceramics. *IEEE Transactions on Instrumentation and Measurement*, 60(6):2118–2125, 2011. doi:10.1109/TIM.2011.2115470.

[163] J. Li, J. Liu, C. Li, H. Zhang, and Y. Li. Wearable wrist movement monitoring using dual surface-treated plastic optical fibers. *Materials*, 13(15):3291, 2020. doi:10.3390/ma13153291.

[164] T. Fresvig, P. Ludvigsen, H. Steen, and O. Reikerås. Fibre optic Bragg grating sensors: An alternative method to strain gauges for measuring deformation in bone. *Medical Engineering & Physics*, 30(1):104–108, 2008. doi:10.1016/j.medengphy.2007.01.006.

[165] R. P. Rocha, A. F. Silva, J. P. Carmo, and J. H. Correia. FBG in PVC foils for monitoring the knee joint movement during the rehabilitation process. In *2011 Annual International Conference of the IEEE Engineering in Medicine and Biology Society*, pages 458–461, 2011. doi:10.1109/IEMBS.2011.6090064.

[166] M. Anwar Zawawi, S. O'Keffe, and E. Lewis. Intensity-modulated fiber optic sensor for health monitoring applications: a comparative review. *Sensor Review*, 33(1):57–67, 2013. doi:10.1108/02602281311294351.

[167] Z. L. Wang and W. Wu. Piezotronics and piezo-phototronics: fundamentals and applications. *National Science Review*, 1(1):62–90, 2013. doi:10.1093/nsr/nwt002.

[168] K. K. Sappati and S. Bhadra. Piezoelectric polymer and paper substrates: A review. *Sensors*, 18(11):3605, 2018. doi:10.3390/s18113605.

[169] X. Chen, K. Parida, J. Wang, J. Xiong, M. Lin, J. Shao, and P. S. Lee. A stretchable and transparent nanocomposite nanogenerator for self-powered physiological monitoring. *ACS Applied Materials & Interfaces*, 9(48):42200–42209, 2017. doi:10.1021/acsami.7b13767.

[170] T. Chen, Q. Shi, Z. Yang, J. Liu, H. Liu, L. Sun, and C. Lee. A self-powered six-axis tactile sensor by using triboelectric mechanism. *Nanomaterials*, 8(7):503, 2018. doi:10.3390/nano8070503.

[171] Z. L. Wang. Triboelectric nanogenerators as new energy technology and self-powered sensors – principles, problems and perspectives. *Faraday Discussions*, 176(0):447–458, 2014. doi:10.1039/C4FD00159A.

[172] H. Zou, Y. Zhang, L. Guo, P. Wang, X. He, G. Dai, H. Zheng, C. Chen, A. C. Wang, C. Xu, and Z. L. Wang. Quantifying the triboelectric series. *Nature Communications*, 10(1):1427, 2019. doi:10.1038/s41467-019-09461-x.

[173] D. J. Lacks and T. Shinbrot. Long-standing and unresolved issues in triboelectric charging. *Nature Reviews Chemistry*, 3(8):465–476, 2019. doi:10.1038/s41570-019-0115-1.

[174] F. Fan, Z. Tian, and Z. Lin Wang. Flexible triboelectric generator. *Nano Energy*, 1(2):328–334, 2012. doi:10.1016/j.nanoen.2012.01.004.

[175] L. Jin, J. Tao, R. Bao, L. Sun, and C. Pan. Self-powered real-time movement monitoring sensor using triboelectric nanogenerator technology. *Scientific Reports*, 7(1):10521, 2017. doi:10.1038/s41598-017-10990-y.

[176] H. Zhao, K. O'Brien, S. Li, and R. F. Shepherd. Optoelectronically innervated soft prosthetic hand via stretchable optical waveguides. *Science Robotics*, 1(1), 2016. doi:10.1126/scirobotics.aai7529.

[177] M. T. Almansoori, L. Xuan, and L. Zheng. A brief review on e-skin and its multifunctional sensing applications. *Current Smart Materials*, 4(1):3–14, 2019. doi:10.2174/2405465804666190313154903.

[178] J. Li, L. Fang, B. Sun, X. Li, and S. H. Kang. Review—recent progress in flexible and stretchable piezoresistive sensors and their applications. *Journal of The Electrochemical Society*, 167(3):037561, 2020. doi:10.1149/1945-7111/ab6828.

[179] Y. Cheng, D. Wu, S. Hao, Y. Jie, X. Cao, N. Wang, and Z. L. Wang. Highly stretchable triboelectric tactile sensor for electronic skin. *Nano Energy*, 64:103907, 2019. doi:10.1016/j.nanoen.2019.103907.

[180] M. Zhu, Q. Shi, T. He, Z. Yi, Y. Ma, B. Yang, T. Chen, and C. Lee. Self-powered and self-functional cotton sock using piezoelectric and triboelectric hybrid mechanism for healthcare and sports monitoring. *ACS Nano*, 13(2):1940–1952, 2019. doi:10.1021/acsnano.8b08329.

[181] L. M. Zhang, Y. He, S. Cheng, H. Sheng, K. Dai, W. J. Zheng, M. X. Wang, Z. S. Chen, Y. M. Chen, and Z. Suo. Self-healing, adhesive, and highly stretchable ionogel as a strain sensor for extremely large deformation. *Small*, 15(21):1804651, 2019. doi:10.1002/smll.201804651.

[182] Y. Zhou, P. Zhan, M. Ren, G. Zheng, K. Dai, L. Mi, C. Liu, and C. Shen. Significant stretchability enhancement of a crack-based strain sensor combined with high sensitivity and superior durability for motion monitoring. *ACS Applied Materials & Interfaces*, 11(7):7405–7414, 2019. doi:10.1021/acsami.8b20768.

[183] J. Shintake, E. Piskarev, S. H. Jeong, and D. Floreano. Ultrastretchable strain sensors using carbon black-filled elastomer composites and comparison of capacitive versus resistive sensors. *Advanced Materials Technologies*, 3(3):1700284, 2018. doi:10.1002/admt.201700284.

[184] H. Liu, Q. Li, S. Zhang, R. Yin, X. Liu, Y. He, K. Dai, C. Shan, J. Guo, C. Liu, C. Shen, X. Wang, N. Wang, Z. Wang, R. Wei, and Z. Guo. Electrically conductive polymer composites for smart flexible strain sensors: a critical review. *Journal of Materials Chemistry C*, 6(45):12121–12141, 2018. doi:10.1039/C8TC04079F.

[185] B. Liang, Z. Lin, W. Chen, Z. He, J. Zhong, H. Zhu, Z. Tang, and X. Gui. Ultra-stretchable and highly sensitive strain sensor based on gradient structure carbon nanotubes. *Nanoscale*, 10(28):13599–13606, 2018. doi:10.1039/C8NR02528B.

[186] R.J. Young and P.A. Lovell. *Introduction to Polymers, Second Edition*. Taylor & Francis, 1991. URL: https://books.google.co.uk/books?id=-IhIzD4NQXAC.

[187] H. Souri and D. Bhattacharyya. Highly sensitive, stretchable and wearable strain sensors using fragmented conductive cotton fabric. *Journal of Materials Chemistry C*, 6(39):10524–10531, 2018. doi:10.1039/C8TC03702G.

[188] M. Amjadi and I. Park. Carbon nanotubes-ecoflex nanocomposite for strain sensing with ultra-high stretchability. In *2015 28th IEEE International Conference on Micro Electro Mechanical Systems (MEMS)*, pages 744–747, 2015. doi:10.1109/MEMSYS.2015.7051065.

[189] K. Kim, N. Jang, S. Ha, J. H. Cho, and J. Kim. Highly sensitive and stretchable resistive strain sensors based on microstructured metal nanowire/elastomer composite films. *Small*, 14(14):1704232, 2018. doi:10.1002/smll.201704232.

[190] M. H. G. Wichmann, S. T. Buschhorn, J. Gehrmann, and K. Schulte. Piezoresistive response of epoxy composites with carbon nanoparticles under tensile load. *Physical Review B*, 80(24):245437, 2009. doi:10.1103/PhysRevB.80.245437.

[191] K. P. Sau, T. K. Chaki, and D. Khastgir. The change in conductivity of a rubber-carbon black composite subjected to different modes of pre-strain. *Composites Part A: Applied Science and Manufacturing*, 29(4):363–370, 1998. doi:10.1016/S1359-835X(97)00100-0.

[192] B. Wang, A. Thukral, Z. Xie, L. Liu, X. Zhang, W. Huang, X. Yu, C. Yu, T. J. Marks, and A. Facchetti. Flexible and stretchable metal oxide nanofiber networks for multimodal and monolithically integrated wearable electronics. *Nature Communications*, 11(1):2405, 2020. doi:10.1038/s41467-020-16268-8.

[193] M. Amjadi, A. Pichitpajongkit, S. Lee, S. Ryu, and I. Park. Highly stretchable and sensitive strain sensor based on silver nanowire–elastomer nanocomposite. *ACS Nano*, 8(5):5154–5163, 2014. doi:10.1021/nn501204t.

[194] T. Yang, D. Xie, Z. Li, and H. Zhu. Recent advances in wearable tactile sensors: Materials, sensing mechanisms, and device performance. *Materials Science and Engineering: R: Reports*, 115:1–37, 2017. doi:10.1016/j.mser.2017.02.001.

[195] M. Li, H. Li, W. Zhong, Q. Zhao, and D. Wang. Stretchable conductive polypyrrole/polyurethane (ppy/pu) strain sensor with netlike microcracks for human breath detection. *ACS Applied Materials & Interfaces*, 6(2):1313–1319, 2014. doi:10.1021/am4053305.

[196] T. del Castillo-Castro, M. M. Castillo-Ortega, J. C. Encinas, P. J. Herrera Franco, and H. J. Carrillo-Escalante. Piezo-resistance effect in composite based on cross-linked polydimethylsiloxane and polyaniline: potential pressure sensor application. *Journal of Materials Science*, 47(4):1794–1802, 2012. doi:10.1007/s10853-011-5965-y.

[197] P. Lee, J. Ham, J. Lee, S. Hong, S. Han, Y. D. Suh, S. E. Lee, J. Yeo, S. S. Lee, D. Lee, and S. H. Ko. Highly stretchable or transparent conductor fabrication by a hierarchical multiscale hybrid nanocomposite. *Advanced Functional Materials*, 24(36):5671–5678, 2014. doi:10.1002/adfm.201400972.

[198] N. C. Das, T. K. Chaki, and D. Khastgir. Effect of axial stretching on electrical resistivity of short carbon fibre and carbon black filled conductive rubber composites. *Polymer International*, 51(2):156–163, 2002. doi:10.1002/pi.811.

[199] J. Zhao, K. Dai, C. Liu, G. Zheng, B. Wang, C. Liu, J. Chen, and C. Shen. A comparison between strain sensing behaviors of carbon black/polypropylene and carbon nanotubes/polypropylene electrically conductive composites. *Composites Part A: Applied Science and Manufacturing*, 48:129–136, 2013. doi:10.1016/j.compositesa.2013.01.004.

[200] Y. Zheng, Y. Li, Y. Zhou, K. Dai, G. Zheng, B. Zhang, C. Liu, and C. Shen. High-performance wearable strain sensor based on graphene/cotton fabric with high durability and low detection limit. *ACS Applied Materials & Interfaces*, 12(1):1474–1485, 2020. doi:10.1021/acsami.9b17173.

[201] S. Bae, Y. Lee, B. K. Sharma, H. Lee, J. Kim, and J. Ahn. Graphene-based transparent strain sensor. *Carbon*, 51:236–242, 2013. doi:10.1016/j.carbon.2012.08.048.

[202] Z. Berk. *Chapter 11 - Extraction*, pages 287–309. Academic Press, 2013. doi:10.1016/B978-0-12-415923-5.00011-3.

[203] P. May, U. Khan, J. M. Hughes, and J. N. Coleman. Role of solubility parameters in understanding the steric stabilization of exfoliated two-dimensional nanosheets by adsorbed polymers. *The Journal of Physical Chemistry C*, 116(20):11393–11400, 2012. doi:10.1021/jp302365w.

[204] C. Hansen. *Hansen Solubility Parameters*. CRC Press, 2007. doi:10.1201/9781420006834.

[205] G. Wypych. *Handbook of Plasticizers*. Elsevier Science, 2017. URL: https://books.google.co.uk/books?id=FSJ2DQAAQBAJ.

[206] Y. Hernandez, M. Lotya, D. Rickard, S. D. Bergin, and J. N. Coleman. Measurement of multicomponent solubility parameters for graphene facilitates solvent discovery. *Langmuir*, 26(5):3208–3213, 2010. doi:10.1021/la903188a.

[207] H. J. Lim, K. Lee, Y. S. Cho, Y. S. Kim, T. Kim, and C. R. Park. Experimental consideration of the hansen solubility parameters of as-produced multi-walled carbon nanotubes by inverse gas chromatography. *Physical Chemistry Chemical Physics*, 16(33):17466–17472, 2014. doi:10.1039/C4CP02319F.

[208] K. Sridharan and K. Elangovan. Investigation on the swelling characteristics of NR/BR rubber blends. *Journal of Chemical and Pharmaceutical Research*, 8(1):553–557, 2016. URL: http://www.jocpr.com/articles/investigation-on-the-swelling-characteristics-of-nrbr-rubber-blends.pdf.

[209] Alamusi, Y. Li, N. Hu, L. Wu, W. Yuan, X. Peng, B. Gu, C. Chang, Y. Liu, H. Ning, J. Li, Surina, S. Atobe, and H. Fukunaga. Temperature-dependent piezoresistivity in an mwcnt/epoxy nanocomposite temperature sensor with ultrahigh performance. *Nanotechnology*, 24(45):455501, 2013. doi:10.1088/0957-4484/24/45/455501.

[210] M. Amjadi, Y. J. Yoon, and I. Park. Ultra-stretchable and skin-mountable strain sensors using carbon nanotubes-ecoflex nanocomposites. *Nanotechnology*, 26(37), 2015. doi:10.1088/0957-4484/26/37/375501.

[211] X. Fu, M. Ramos, A. M. Al-Jumaily, A. Meshkinzar, and X. Huang. Stretchable strain sensor facilely fabricated based on multi-wall carbon nanotube composites with excellent performance. *Journal of Materials Science*, 54(3):2170–2180, 2019. doi:10.1007/s10853-018-2954-4.

[212] F. M. Guo, X. Cui, K. L. Wang, and J. Q. Wei. Stretchable and compressible strain sensors based on carbon nanotube meshes. *Nanoscale*, 8(46):19352–19358, 2016. doi:10.1039/C6NR06804A.

[213] S. A. Khan, M. Gao, Y. Zhu, Z. Yan, and Y. Lin. Mwcnts based flexible and stretchable strain sensors. *Journal of Semiconductors*, 38(5):053003, 2017. doi:10.1088/1674-4926/38/5/053003.

[214] J. H. Kim, J. Hwang, H. R. Hwang, H. S. Kim, J. H. Lee, J. Seo, U. S. Shin, and S. Lee. Simple and cost-effective method of highly conductive and elastic carbon nanotube/polydimethylsiloxane composite for wearable electronics. *Scientific Reports*, 8(1):1375, 2018. doi:10.1038/s41598-017-18209-w.

[215] B. M. Lee and K. J. Loh. Carbon nanotube thin film strain sensors: comparison between experimental tests and numerical simulations. *Nanotechnology*, 28(15):155502, 2017. doi:10.1088/1361-6528/aa6382.

[216] C. Lee, L. Jug, and E. Meng. High strain biocompatible polydimethylsiloxane-based conductive graphene and multiwalled carbon nanotube nanocomposite strain sensors. *Applied Physics Letters*, 102(18):183511, 2013. doi:10.1063/1.4804580.

[217] L. Lin, S. Liu, Q. Zhang, X. Li, M. Ji, H. Deng, and Q. Fu. Towards tunable sensitivity of electrical property to strain for conductive polymer composites based on thermoplastic elastomer. *ACS Applied Materials & Interfaces*, 5(12):5815–5824, 2013. doi:10.1021/am401402x.

[218] D. J. Lipomi, M. Vosgueritchian, B. C. Tee, S. L. Hellstrom, J. A. Lee, C. H. Fox, and Z. Bao. Skin-like pressure and strain sensors based on transparent elastic films of carbon nanotubes. *Nature Nanotechnology*, 6(12):788–92, 2011. doi:10.1038/nnano.2011.184.

[219] J. Lu, M. Lu, A. Bermak, and Y. Lee. Study of piezoresistance effect of carbon nanotube-pdms composite materials for nanosensors. In *2007 7th IEEE Conference on Nanotechnology (IEEE NANO)*, pages 1240–1243, 2007. doi:10.1109/NANO.2007.4601407.

[220] T. Ogasawara, T. Tsuda, and N. Takeda. Stress–strain behavior of multi-walled carbon nanotube/peek composites. *Composites Science and Technology*, 71(2):73–78, 2011. doi:10.1016/j.compscitech.2010.10.001.

[221] X. Wang, J. Li, H. Song, H. Huang, and J. Gou. Highly stretchable and wearable strain sensor based on printable carbon nanotube layers/polydimethylsiloxane composites with adjustable sensitivity. *ACS Applied Materials & Interfaces*, 10(8):7371–7380, 2018. doi:10.1021/acsami.7b17766.

[222] S. Seyedin, P. Zhang, M. Naebe, S. Qin, J. Chen, X. Wang, and J. M. Razal. Textile strain sensors:

a review of the fabrication technologies, performance evaluation and applications. *Materials Horizons*, 6(2):219–249, 2019. doi:10.1039/C8MH01062E.

[223] B. Zhou, C. Li, Z. Liu, X. Zhang, Q. Li, H. He, Y. Zhou, and L. Jiang. A highly sensitive and flexible strain sensor based on dopamine-modified electrospun styrene-ethylene-butylene-styrene block copolymer yarns and multi walled carbon nanotubes, 2022. doi:10.3390/polym14153030.

[224] Y. Yang, H. Wang, Y. Hou, S. Nan, Y. Di, Y. Dai, F. Li, and J. Zhang. Mwcnts/pdms composite enabled printed flexible omnidirectional strain sensors for wearable electronics. *Composites Science and Technology*, 226:109518, 2022. doi:10.1016/j.compscitech.2022.109518.

[225] E. Papi, Y. N. Bo, and A. H. McGregor. A flexible wearable sensor for knee flexion assessment during gait. *Gait & Posture*, 62:480–483, 2018. doi:10.1016/j.gaitpost.2018.04.015.

[226] H. Nakamoto, H. Ootaka, M. Tada, I. Hirata, F. Kobayashi, and F. Kojima. Stretchable strain sensor based on areal change of carbon nanotube electrode. *IEEE Sensors Journal*, 15(4):2212–2218, 2015. doi:10.1109/JSEN.2014.2377022.

[227] B. J. Munro, T. E. Campbell, G. G. Wallace, and J. R. Steele. The intelligent knee sleeve: A wearable biofeedback device. *Sensors and Actuators B: Chemical*, 131(2):541–547, 2008. doi:10.1016/j.snb.2007.12.041.

[228] R. Helmer, I. Blanchonette, D. Farrow, K. Ball, and Callum Mackay. Preliminary development of a reconfigurable garment system for interactive biomechanics. In *31 International Conference on Biomechanics in Sports (2013)*, 2013. URL: https://ojs.ub.uni-konstanz.de/cpa/article/view/5694.

[229] G. Saggio, L. R. Quitadamo, and L. Albero. Development and evaluation of a novel low-cost sensor-based knee flexion angle measurement system. *Knee*, 21(5):896–901, 2014. doi:10.1016/j.knee.2014.04.014.

[230] S. Hu, M. Dai, T. Dong, and T. Liu. A textile sensor for long durations of human motion capture. *Sensors*, 19(10), 2019. doi:10.3390/s19102369.

[231] E. Papi, D. Osei-Kuffour, Y. M. Chen, and A. H. McGregor. Use of wearable technology for performance assessment: a validation study. *Medical Engineering & Physics*, 37(7):698–704, 2015. doi:10.1016/j.medengphy.2015.03.017.

[232] J. H. M. Bergmann, S. Anastasova-Ivanova, I. Spulber, V. Gulati, P. Georgiou, and A. McGregor. An attachable clothing sensor system for measuring knee joint angles. *IEEE Sensors Journal*, 13(10):4090–4097, 2013. doi:10.1109/JSEN.2013.2277697.

[233] A. Hermann, J. Ostarhild, Y. Mirabito, N. Bauer, and V. Senner. Stretchable piezoresistive vs. capacitive silicon sensors integrated into ski base layer pants for measuring the knee flexion angle. *Sports Engineering*, 23(1), 2020. doi:10.1007/s12283-020-00336-9.

[234] M. Hopkins. *Smart sockets for lower limb prostheses*. Thesis, 2019. doi:https://doi.org/10.25560/78771.

[235] Erica M. Buckeridge, Anthony M. J. Bull, and Alison H. McGregor. Incremental training intensities increases loads on the lower back of elite female rowers. *Journal of Sports Sciences*, 34(4):369–378, 2016. doi:10.1080/02640414.2015.1056821.

[236] British Cycling. Indoor/outdoor session 20 minute warm-up. Date accessed: 09/01/2023. URL: https://www.britishcycling.org.uk/zuvvi/media/bc_files/sportivetrainingplans/20_MINUTE_WARM_UP.pdf.

[237] E. Buckeridge, S. Hislop, A. Bull, and A. McGregor. Kinematic asymmetries of the lower limbs during ergometer rowing. *Medicine & Science in Sports & Exercise*, 44(11):2147–53, 2012. doi:10.1249/MSS.0b013e3182625231.

[238] R. Zhang, H. Deng, R. Valenca, J. Jin, Q. Fu, E. Bilotti, and T. Peijs. Carbon nanotube polymer coatings for textile yarns with good strain sensing capability. *Sensors and Actuators A: Physical*, 179:83–91, 2012. doi:https://doi.org/10.1016/j.sna.2012.03.029.

[239] W. Holliday, R. Theo, J. Fisher, and J. Swart. Cycling: joint kinematics and muscle activity during differing intensities. *Sports Biomechanics*, pages 1–15, 2019. doi:10.1080/14763141.2019.1640279.

[240] J. Swart and W. Holliday. Cycling biomechanics optimization—the (R) evolution of bicycle fitting. *Current Sports Medicine Reports*, 18(12):490–496, 2019. doi:10.1249/jsr.0000000000000665.

[241] Bryan C. Heiderscheit, Elizabeth S. Chumanov, Max P. Michalski, Christa M. Wille, and Michael B. Ryan. Effects of step rate manipulation on joint mechanics during running. *Medicine & Science in Sports & Exercise*, 43(2), 2011. doi:10.1249/MSS.0b013e3181ebedf4.

[242] D. Whiteside, O. Cant, M. Connolly, and M. Reid. Monitoring hitting load in tennis using inertial sensors and machine learning. *International Journal of Sports Physiology and Performance*, 12(9):1212–1217, 2017. doi:10.1123/ijspp.2016-0683.

[243] A. H. McGregor, A. M. J. Bull, and R. Byng-Maddick. A comparison of rowing technique at different stroke rates: A description of sequencing, force production and kinematics. *Int J Sports Med*, 25(06):465–470, 2004. doi:10.1055/s-2004-820936.

[244] Y. Zhou and R. Stewart. Highly flexible, durable, uv resistant, and electrically conductive graphene based tpu/textile composite sensor. *Polymers for Advanced Technologies*, 33(12):4250–4264, 2022. doi:https://doi.org/10.1002/pat.5856.

[245] E. Papi, A. Belsi, and A. H. McGregor. A knee monitoring device and the preferences of patients living with osteoarthritis: a qualitative study. *BMJ Open*, 5(9):e007980, 2015. doi:10.1136/bmjopen-2015-007980.

[246] J. H. M. Bergmann, H. Goodier, I. Spulber, S. Anastasova, P. Georgiou, and A. H. McGregor. The "wear and measure" approach: Linking joint stability measurements from a smart clothing system to optical tracking. *Journal of Sensors*, 2015:8, 2015. doi:10.1155/2015/762869.

[247] J. Bergmann, V. Chandaria, and A. McGregor. Wearable and implantable sensors: The patient's perspective. *Sensors*, 12(12):16695, 2012. doi:10.3390/s121216695.

[248] V. Braun and V. Clarke. Using thematic analysis in psychology. *Qualitative Research in Psychology*, 3(2):77–101, 2006. doi:10.1191/1478088706qp063oa.

[249] V. Camomilla, E. Bergamini, S. Fantozzi, and G. Vannozzi. Trends supporting the in-field use of wearable inertial sensors for sport performance evaluation: A systematic review. *Sensors*, 18(3), 2018. doi:10.3390/s18030873.

[250] P. Düking, H. C. Holmberg, and B. Sperlich. Instant biofeedback provided by wearable sensor technology can help to optimize exercise and prevent injury and overuse. *Frontiers in Physiology*, 8(APR), 2017. doi:10.3389/fphys.2017.00167.

[251] E. Caglar, Y. Canlan, and M. Demir. Recreational exercise motives of adolescents and young adults. *Journal of Human Kinetics*, 22(1):83–89, 2009. doi:10.2478/v10078-009-0027-0.

[252] World Rowing. World Rowing Rule Book, 2021. Accessed: 12/12/2022. URL: https://worldrowing.com/technical/rules/2021-rule-book/.

[253] Union Cycliste Internationale. Uci cycling regulations, 2022. Accessed: 03/01/2023. URL: https://assets.ctfassets.net/761l7gh5x5an/wQympSG6EWlKq6o6HKw9E/e721b3a612383790a42bdcae8fb3839a/1-GEN-20230101-E.pdf.

[254] A. Rapp and L. Tirabeni. Self-tracking while doing sport: Comfort, motivation, attention and lifestyle of athletes using personal informatics tools. *International Journal of Human-Computer Studies*, 140:102434, 2020. doi:10.1016/j.ijhcs.2020.102434.

Appendix A

Systematic Review Published in 2019

sensors

MDPI

Review

Exploring the Role of Wearable Technology in Sport Kinematics and Kinetics: A Systematic Review

Yewande Adesida *, Enrica Papi and Alison H. McGregor

Department of Surgery and Cancer, Imperial College London, Charing Cross Campus, London W6 8RP, UK; e.papi@imperial.ac.uk (E.P.); a.mcgregor@imperial.ac.uk (A.H.M.)
* Correspondence: yewande.adesida12@imperial.ac.uk

Received: 7 February 2019; Accepted: 26 March 2019; Published: 2 April 2019

check for updates

Abstract: The aim of this review was to understand the use of wearable technology in sport in order to enhance performance and prevent injury. Understanding sports biomechanics is important for injury prevention and performance enhancement and is traditionally assessed using optical motion capture. However, such approaches are limited by capture volume restricting assessment to a laboratory environment, a factor that can be overcome by wearable technology. A systematic search was carried out across seven databases where wearable technology was employed to assess kinetic and kinematic variables in sport. Articles were excluded if they focused on sensor design and did not measure kinetic or kinematic variables or apply the technology on targeted participants. A total of 33 articles were included for full-text analysis where participants took part in a sport and performed dynamic movements relating to performance monitored by wearable technologies. Inertial measurement units, flex sensors and magnetic field and angular rate sensors were among the devices used in over 15 sports to quantify motion. Wearable technology usage is still in an exploratory phase, but there is potential for this technology to positively influence coaching practice and athletes' technique.

Keywords: wearables; sports performance; kinematics; sensors; motion analysis; athlete; coaching

1. Introduction

1.1. Background

The role of feedback in sport is of great importance, and both coaches and athletes can benefit from it as a means of improving athletic performance or minimizing injury risk. The coaching process can be highly subjective, as Jones and Wallace (2005) state: 'Every coach or athlete brings personal interests to the coaching setting' [1]. Ambiguity can arise in how best to develop and optimize an athlete's performance, with the technique and approach used by the coach being reliant on their own expertise, experience and background. Rising interest and research into technology is helping to overcome this subjectivity; for example, video analysis where videos can be annotated to measure angles, allowing performance to be quantified objectively rather than be dependent on the coach's critical eye. However, whilst such approaches provide objectivity there is a desire to provide athletes with real-time feedback.

1.2. Types of Systems

Motion capture systems have the ability to analyse the biomechanics of many functional and sporting tasks. Optical systems consist of cameras used to track passive or active markers placed on anatomical landmarks in order to obtain full-body capture. A systematic review by Pueo et al. (2017) stated Vicon (Oxford Metrics, Oxford, UK) and Qualisys (Qualisys AB, Göteborg, Sweden) as being the most commonly used systems in a number of different sports, from tennis to swimming to

taekwondo [2]. However, due to camera set-up, these systems are limited by their capture volume, generally being confined to laboratory settings. Furthermore, the large number of markers frequently required has implications on time and can impede the performance of the tasks under investigation and, conversely, the complexity of sporting tasks frequently leads to marker occlusion.

Wearable technology, however, is an alternative approach that has the potential to overcome these limitations. There is a range of different types of sensors, including inertial measurement units (IMUs) and microelectromechanical sensors (MEMS), containing a combination of magnetometers, accelerometers and gyroscopes. In addition, there are also flex sensors, such as those produced by Spectra Symbol (Salt Lake City, UT, USA), capable of tracking joint motion through means of changes in resistance when a force is applied to the sensor.

A significant advantage of these wearable systems is the ability to monitor athletes in a real sport environment to provide real-time feedback, a feature not offered by video analysis. Furthermore, they are designed to be small, lightweight, wireless and unobtrusive permitting full movements while participating in a sport. This gives rise to the potential for athletes to be observed outside a laboratory setting and in their natural training environment. Sensors have been used in sports such as skiing, snowboarding and swimming that take place in extreme conditions and have the added features of being waterproof or being able to withstand cold temperatures while recording data [3–8]. However, they are not without limitations: the presence of ferromagnetic objects can distort measurements from inertial-based systems [9], and precise positioning may affect data accuracy as well as data integration introducing errors when trying to extrapolate positional data from acceleration measures [10,11]. Furthermore, using a wireless method to transfer data has the potential for loss of signal during recording time or interference from mobile phones or other devices that may be on the same transmission frequency [12].

1.3. The Adoption of Wearable Technology in Sport

A number of sports are now being seen to use wearable sensors. Monitoring player workloads in Australian football using Global Positioning System (GPS) devices has allowed energy expenditure to be analysed, a process previously done using heart rate monitors [13]. Using heart rate alone is not an accurate method of determining workload as it does not factor in speed and distance travelled during a game [13]. GPS tracking devices placed on the upper back are used to quantify the difference in the amount of work done in different player positions as well as the game intensities [13,14]. An inverse relationship was proposed by Wisbey et al. (2007) between the success of a team and the workload of the players from the use of these devices [14].

Wearable sensors have been used in American football to monitor concussions by measuring linear and angular head accelerations upon impact [15]. Sensors have been integrated into helmet linings and mouth guards, highlighting their unobtrusiveness, a key factor in their use in training and competition. Siegmund et al. (2015) tested two such systems, which were found to detect over 95% of impacts, providing data that would have been otherwise unobtainable [15]. Injury prevention has also been considered in baseball and volleyball where there is a problem with shoulder over-use injuries. A study performed by Rawashdeh et al. (2016) was able to classify movements of the shoulder joint, giving athletes and coaches quantifiable information [16].

By moving away from visual approaches, coaches are able to monitor several athletes in volleyball at once and in real-time, using the VERT inertial measurement unit (IMU) system (Version 2.0, Mayfonk Inc., Fort Lauderdale, FL, USA) to quantify jump height accurately [17] without the concern of markers being obstructed from the view of a camera. The VERT IMU is commercially available, as are other systems such as the KINEXON sensor (Kinexon Sports and Media Gmbh, Munich, Germany) used in sports such as basketball to measure player acceleration and the Nadi × yoga pants (Wearable X, New York City, NY, USA) which uses a combination of motion sensors and haptic feedback to guide yoga technique.

1.4. Requirements for Wearable Technology in Sport

Optical systems are widely considered to be a gold-standard method for motion capture [18], so wearable technology should be validated against such systems and tested for reliability in order to replace them. Recommendations have been suggested by Düking et al. (2018) including confirming both inter-device and intra-device reliability, simulating the movements in the sport intended for the sensor to be used in and selecting a study population that is reflective of the ultimate intended user [19]. Concurrent criterion validity is an easy way of determining similarities or differences between the data obtained through wearable technology and a gold-standard reference. Test-retest and intra-subject reliability are important when assessing the sensor performance with relation to the participants, while sensor sensitivity is essential when considering the change of parameters with respect to time, as any sensors used need to be able to track these changes [19].

The sampling frequency of a wearable device is also important for tracking changes and is dependent on the assessed movement and variables of interest, with recommendations based on the Nyquist-Shannon sampling theorem [20]. This states that the critical sampling frequency must be a minimum of two times the highest frequency in the signal of interest to obtain all the information found in the original signal [21,22]. A consequence of having too low a sampling frequency is that relevant information can be lost.

With sensors being wireless and having their own power source that is not connected to a mains supply adds a recording lifetime to the system used. Any wearable technology needs to last at least the duration of a training or testing session or the length of a race or match.

The increasing use of wearable sensors in sport cannot be ignored. The unobtrusive measurement systems are able to provide athletes and coaches with information regarding the range of motion, accelerations and impacts, among other indicators of performance or injury risk in real-time. The provision of objective data takes coaching to a new level, allowing more informed decision-making, yet the information collected from these sensors needs to be delivered in a format that is easy to interpret for it to be of use.

Previous reviews have focused on inertial sensors only, such as those by Chambers et al. (2015) and Camomilla et al. (2018) despite other technologies such as pressure insoles or flex sensors which could find application in sport scenarios [23,24]. Their use is not as widespread as inertial sensors and some may require further development, but have the ability to measure biomechanical variables of use to athletes and support staff. Several reviews also exist targeting the validity, reliability and use of activity monitors to quantify energy expenditure, measure heart rate and count steps [25–27]. However, these measures are not able to provide indications as to how the movement was performed, thus limiting their ability to intervene to improve performance or prevent injury in a sporting population.

The aim of this study was to identify the use of wearable technology in sports as a means of measuring kinetic or kinematic variables that could be used to enhance performance or prevent injury. The focus was on sport-specific movements being performed by people who participated in these sports, while wearing a form of wearable technology. In addition to looking at the measures obtained by the devices, the collection and processing of data was also considered, as well as the lifetime of the devices and how some compared to gold standard measurements.

2. Materials and Methods

2.1. Search Strategy

The following databases were used to carry out a systematic search from inception up until 31st October 2018: Scopus, Medline, Embase, Cochrane Library, IEEE Xplore, Web of Science (Core Collection) and Engineering Village. The search terms were grouped under the following headings: 'wearable', 'sensor' and 'sport', with the Boolean search strategy used being 'wearable AND sensor AND sport'. The search strategy is detailed in Tables 1 and 2. Hand searches and screening the references of relevant articles were also performed to identify studies that may have been overlooked

by the electronic searches. Retrieved articles were imported into Endnote X8 software (Clarivate Analytics, Philadelphia, PA, USA).

Table 1. Boolean search strategy.

General	Specific	
Wearable	Portable OR worn OR cloth*3 [1] OR "body-mounted" OR "non-invasive" OR mobile OR wearable* OR apparel OR textile OR "electronic skin"	
	Cochrane Library MeSH terms	Wearable electronic devices (exp)
	Embase MeSH terms	Non-invasive monitoring
		Clothing
	Medline MeSH terms	Clothing
		Wearable electronic devices
Sensor	Sens*3 OR goniomet* OR acceleromet* OR monitor* OR inertia* OR gyroscope* OR device* OR magnet* OR imu OR telemet* OR pressure OR strain OR conductive OR stretch* OR flexible OR smart OR electronic*1 OR electromagnetic OR microsensor*1 OR microelectronic*1	
	Cochrane Library MeSH terms	Monitoring, ambulatory
	Embase MeSH terms	Ambulatory monitoring
		Sensor
		Devices
		Monitoring
	Medline MeSH terms	Monitoring, ambulatory
Sport	Athlete*3 OR sport* OR (List of Olympic Sports, see Table 2)	
	Cochrane Library MeSH terms	Athletes
		Sports
		Exercise
		Athletic performance
		Motor activity
	Embase MeSH terms	Athletes
		Sports
		Exercise
		Training
		Sports medicine
		Motor activity
		Athletic performance
	Medline MeSH terms	Athletes
		Sports
		Exercise
		Motor activity
		Sports medicine

[1] The asterisk (*) after the initial letters 'cloth' expands the search to include all terms beginning with cloth, while the number '3' limits the number of characters after 'cloth' of the included terms.

Table 2. List of Olympic sports.

Olympic Sports
archery OR run*4 [1] OR badminton OR basketball OR boxing OR canoe* OR cycl*4 OR bik*3 OR bicycl* OR bmx OR div*3 OR equestrian OR dressage OR fencing OR football OR soccer OR golf OR gymnastics OR handball OR hockey OR judo OR pentathlon OR row*3 OR rugby OR sail*3 OR shoot*3 OR swim*4 OR taekwondo OR tennis OR trampoline OR triathlon OR volleyball OR "water polo" OR weightlifting OR wrestling OR skiing OR biathlon OR bobsleigh OR curling OR skat*3 OR luge OR "Nordic combined" OR skeleton OR snowboard*

[1] The asterisk (*) after the initial letters 'run' expands the search to include all terms beginning with run, while the number '4' limits the number of characters after 'run' of the included terms.

2.2. Eligibility Criteria

Articles were included if they were: published in English; included at least one of the following outcome measures: kinematics, kinetics as obtained from wearable technology; participants took part in a sport (defined as an organized physical activity done alone or with a group); dynamic

movement tasks were performed related to performance in the sport studied. Articles were excluded if they were a review or case study; were a conference abstract (except peer-reviewed abstracts); used only non-wearable devices; wearable technology was used to only quantify physical activity or spatio-temporal parameters of the sport performed; or described a potential technology not validated/used with human subjects.

2.3. Selection Process

Duplicates arising from searches in multiple databases were removed, and the titles and abstracts were reviewed for inclusion by two independent reviewers (Y.A. and E.P.) against the inclusion and exclusion criteria. Results from both reviewers were compared through discussion, with any conflicts being resolved by a third reviewer (A.H.M). Full texts of the remaining articles were retrieved, and these were evaluated against the inclusion criteria.

2.4. Data Extraction

The details used for data extraction were modified from a review published by Papi et al. (2017) looking at the use of wearable technology to assess spinal kinematics [28]. The following details were extracted from each study: aim; sport studied; sample size; participants' demographics (e.g., population type, age, gender, mass, height); tasks conducted; measuring system used; data acquisition/sampling; participant set-up (e.g., position of the sensors, fixation method); data processing (e.g., filter used for the signal); kinematic and kinetic variables evaluated from the sensor signals (performance indicators); statistical analysis technique; and reliability/evaluation.

2.5. Quality Appraisal

The review by Papi et al. (2017) was used as a basis for forming a quality assessment checklist [28]. This was based on previous reviews on motion analysis and relating to the use of technology [29,30]. 17 items were included in the checklist and each was rated between zero and two (0 = no, 1 = limited and 2 = good detail), listed in Table 3.

Table 3. Criteria used for the quality assessment of included articles.

Quality Assessment Criteria
1. Were the research objectives or aims clearly stated?
2. Was the study design clearly described?
3. Was the study population adequately described?
4. Were the eligibility criteria specified?
5. Was the sampling methodology appropriately described?
6. Was the sample size used justified?
7. Did the method description enable accurate replication of the measurement procedures?
8. Was the equipment design and set up clearly described?
9. Were sensors locations accurately and clearly described?
10. Was sensor attachment method clearly described?
11. Was the signal/data handling described?
12. Were the main outcomes measured and the related calculations (if applicable) clearly described?
13. Was the system compared to an acknowledged gold standard?
14. Were measures of reliability/accuracy of the equipment used reported?
15. Were the main findings of the study stated?
16. Were the statistical tests appropriate?
17. Were limitations of the study clearly described?

3. Results

A total of 44,220 articles were obtained from the search, five further articles were identified from another review [23] and one from a search in Sensors. After duplicates were removed, 27,767 articles

remained for title and abstract screening using the eligibility criteria set out in Section 2.2. From there, 46 full texts were assessed for eligibility.

Thirty-four articles satisfied the inclusion criteria. The selection process and reasons for exclusion are presented in Figure 1. The details extracted from these articles can be found in the Supplementary Materials, Table S1: Data extracted from included articles. Studies were conducted across a range of sports: football and rugby (n = 4) [9,31–33], swimming (n = 3) [4,6,34], skiing (n = 6) [5,7,8,35–37], equestrian (n = 3) [38–40], cricket (n = 1) [41], table tennis (n = 1) [42], badminton (n = 1) [43], athletics and running (n = 4) [12,44–46], rowing (n = 1) [47], baseball (n = 3) [48–50], snowboarding (n = 1) [3], golf (n = 1) [51], netball (n = 1) [52], archery (n = 1) [53], volleyball (n = 1) [54], canoeing (n = 1) [55] and Nordic walking [56].

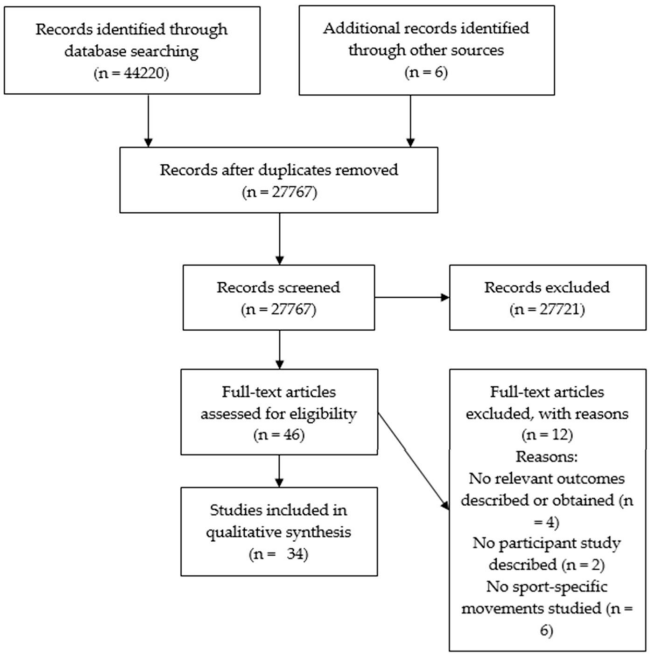


Figure 1. PRISMA chart detailing the article selection process [57].

3.1. Article Quality

The quality of the included papers was rated according to the following scale: low (score $\leq$ 33.3%), medium (33.4–66.7%) and high (score $\geq$ 66.8%) [28]. Four articles were deemed to be of low quality [51,53,55,56], 19 of medium quality [4–8,12,31,32,37–39,41–44,47,49,50,54] and 11 of high quality [3,9,33–36,40,45,46,48,52]. The results from this assessment are detailed in Appendix A, Table A1. None of the articles described a sampling methodology and only one article out of the 34 that were included attempted to justify the sample size [33]. Sample size was not reported in two articles [41,51] and ranged from 1 [43] to 37 [48] in the remaining articles, with the average number of participants at 10. Twelve studies had participants equal to or greater than this [4,5,7–9,31,33,35,36,42,48,54]. Seventeen articles described the method in enough detail to enable it to be replicated accurately [4,6,9,31–36,38–40,42,44,45,48,52]. All studies gave a description

of where the sensors were located, with 19 of them giving a description that was clear and accurate [4–9,12,31,32,34–36,40,43,44,46–48,52].

Eleven of the papers compared the wearable systems to a gold-standard measurement during their testing [3,9,33–36,45,47,49,50,52]. A further four papers compared observed parameter results to values that had been reported in previous literature as means of sensor data validation [5,7,31,39].

3.2. Types of Measuring Systems Used and Evaluated Variables

Inertial sensors were the most common type of system used in these studies in the form of individual sensor nodes or as part of a body suit. Individual inertial sensors were used in 13 articles [6,12,32,34,38,39,45,47–49,52,54,55], body suits in five articles [3,6,8,9,40] and a combination in two articles [5,7].

Body suits mentioned in the included articles were produced by different companies: suits by Xsens Technologies B.V. (Enschede, The Netherlands) contained 16–17 sensor units, allowing full body coverage [3,9,37,40]; while the Physilog inertial measurement units (IMUs) (GaitUp, Lausanne, Switzerland) were incorporated into an underwear suit and contained five to seven sensors [5,7,8]. Blair et al. (2018) used the MVN Link IMS from Xsens Technologies B.V. (Enschede, The Netherlands) to determine lower body kinetics and kinematics including sagittal plane angles for the shank and pelvis during football and rugby kicks [9]; Gandy et al. (2018) also used an MVN suit to determine hip and ankle joints, as well as their moments and forces [40]; while in snowboarding the suit was used to determine knee and ankle joint angles [3]. The Physilog IMU suits (GaitUp, Lausanne, Switzerland) were all used in skiing studies by Chardonnens et al. (2013a, 2013b, 2014) measuring lower body joint angles and velocities, ski angles and centre of mass (CoM) position, force and velocity [5,7,8].

In archery, athletics, swimming, table tennis, baseball, football and golf, tri-axial accelerometers were used on their own to measure different kinematic and kinetic variables. Peak positive acceleration of the tibia was evaluated in runners [44]; three-dimensional acceleration and angular velocity during the golf swing using accelerometers weighing as little as 22 g [51,58]; linear and angular velocity and acceleration of the shank and thigh, as well as angular momentum, power and impulse during the football instep kick [31]. The sensor module used in football by Meamarbashi et al. had the largest dimensions of 23 cm × 2.3 cm × 2.5 cm and weighed 80 g, alongside a data logger weighing 70 g and dimensions of 6 cm × 7 cm × 2.5 cm; the placement of both components was controlled after each kick [31]. Koda et al. (2010) used the tri-axial accelerometers, weighing 93 g, to evaluate kinematics of the arm in baseball [50]. Kiernan et al. (2018) used accelerations to determine the peak vertical ground reaction force in male middle distance runners, with the accelerometer contained within an activity monitor and fixed to the lateral right iliac crest with a neoprene belt by the participants themselves [46]. In table tennis, the average peak plus acceleration value was determined with a BSN node board small enough for use on most parts of the body (23 mm in diameter) [42] and in swimming, accelerometers were used to determine roll and pitch angles (body rotation) as well as body acceleration [4]. The devices used in swimming were reported as unobtrusive and compared to every day accessories such as wristwatches and belts [4]. A tri-axial accelerometer was used alongside a load cell by Mocera et al. (2018) in Nordic walking to characterize the different phases of the cyclic arm movement [56]. The authors stated that the system must have the 'lowest possible influence on the users' movements in order to avoid undesirable compensations', in a sport where the walking poles weigh as little as 180 g [56]. An accelerometer was also used in archery to measure arm displacement [53] but the type was not stated.

Magnetic, angular rate and gravity (MARG) sensors were used in football to study angle range of motion [33] and in cricket to observe the elbow extension angle [41]. The x-IMU (x-io Technologies, Bristol, UK) MARG sensors used in football weigh 49g with a battery and encased in a plastic housing (57 mm × 38 mm × 21 mm) [59]. The Pedar Pressure Insole System (novel gmbh, Munich, Germany) was used in two studies by Nakazato et al (2011, 2013) to measure the vertical ground reaction force [36] and foot centre of pressure [35] in comparison to Kistler force plates (Kistler Instruments Ltd.,

Hampshire, UK). The insoles have a thickness of 1.9mm and require an analyzer weighing 400 g [60]. T and T Medilogic (T and T Medilogic Medizintechnik GmbH, Schönefeld, Germany) bilateral insole measurements were used in snowboarding to determine foot force alongside an inertial suit measuring lower limb kinematics [3].

A flex sensor produced by Spectra Symbol (Salt Lake City, UT, USA) and incorporated into a glove-like hand monitoring module was used by a badminton coach in order to determine the different types of hand grips by measuring the flexion angle of the thumb, index and middle fingers [43]. In this device, the flex sensors were connected to the battery and microcontroller, which were also situated on the glove, by cables.

The specification for each technology and how each was fixed onto the study participants can be found in the Supplementary Materials (Table S1).

3.3. Testing Environment

Only five studies took place in a laboratory setting [9,33,34,44,47], most likely to allow the use of a gold-standard measurement as a reference, which was the case in four articles [9,33,34,47]. Fantozzi et al. (2016) had participants simulate the upper-body portion of the swimming stroke while the lower limbs were held against a rigid box by an operator instead of performing experiments in the water [34]. Reliable measurements were produced (RMSE = 5° and 7° for breaststroke and front-crawl, respectively), but this method had its limitations as participants were required to use their lumbar muscles to support themselves and range of motion of the body was reduced in comparison to normal kinematics in the water [34]. Additionally, studies conducted by Wood et al. (2014) and King et al. (2009) used treadmills and rowing machines but both authors mentioned the need to test the wearable systems in a normal running environment and on the water [44,47].

Three articles did not state the environment that the experiments took place in [32,43,51] and the remaining studies were conducted in field, with the skiing studies by Chardonnens et al. (2013a, 2013b, 2014) and a distance running study by Kiernan et al. (2018) monitoring participants during general training [5,7,8,46].

3.4. Data Sampling, Collection and Processing

Four articles did not state the sampling frequency of the devices that were used [38,43,48,54] but for those that did, this ranged between 10 Hz and 1000 Hz, with the most common frequency used being 100 Hz by eight systems [32,35–37,39,49,52,55]. Sampling frequency was justified in four articles: 25 Hz was deemed 'competent for obtaining enough knowledge of performance' with regards to table tennis blocks by Guo et al. (2010) [42], and the accelerometers used by Kiernan et al. (2018) had a frequency that was double that of observed vertical ground reaction forces (vGRFs) in running [46]. The SportSemble nodes in baseball contained accelerometers with differing sampling frequencies (1000 Hz and 100 Hz) in order to record slow and fast motion [49]. This was recognized as a limitation of optical motion trackers. The higher sampling frequency of the SportSemble nodes enabled more detail about the pitching movement to be obtained compared to an optical motion analysis system sampling at 180 Hz, which is important when considering variables such as peak acceleration. In contrast, an inertial measurement unit (IMU) developed at Loughborough University was used by Philpott et al. (2014) to assess sprint starts in athletics had a much lower sampling frequency compared to Vicon (Oxford Metrics, Oxford, UK) (50 Hz and 250 Hz, respectively) [45]. The few data points collected by the IMU do not make it suitable for the explosive nature of the sprint start sequence. However, a sampling frequency of 50 Hz was deemed suitable for capturing the dynamics of the pole movement in Nordic walking [56].

Some of the systems recorded the output of the sensor onto a memory card (including micro and mini SD cards) (n = 7) [6,8,31,46,52,54,56], used data loggers (n = 3) [5,7,36] and microcontrollers (n = 3) [4,41,49]. In these cases, data was visualised and processed after testing. Some systems employed wireless data transfer (n = 11) [3,12,32,38,40,42,43,47,51,53,55], meaning that there was

potential for data to be received and analysed in real-time, with five specifically stating the use of Bluetooth [38,40,43,51,53] but still data was processed after data collection.

Real-time feedback was used in only 2 articles [25,46]. Wood et al. (2014) used auditory feedback in order to reduce tibial peak-positive acceleration (PPA) in runners [44], while the "ISWIM" system used by Li et al. (2016) provided live feedback in the form of vibrations [6]. In both cases, participants were instructed to modify running or swimming biomechanics based solely on the feedback produced from the devices. Runners were able to significantly reduce PPAs throughout a 25 min testing period from 5.9 $\pm$ 0.7 g to 5.4 $\pm$ 0.7 g [44]. The case was similar with the "ISWIM" system—the vibratory feedback improved body rotation angles and as a result increased stroke rate and improved session times in three out of four participants [6]. Feedback in both systems led to a change in biomechanics without any technical input from coaches, indicating that these are systems that athletes could use on their own.

The elbow torque-measurement device (ETD) studied by Makhni et al. (2018) used data transmission via Bluetooth to display the output of the sensor, including parameters such as arm speed, shoulder rotation and torque across the medial elbow, on a smartphone application [48]. However, the authors were not concerned with the feedback produced from the device, so there is not any indication as to its utility. This type of setup is also mentioned by Mitsui et al. (2015) to improve a golfer's swing [51] but it was unclear whether the output was displayed in real-time or not and the impact of feedback on improving performance.

Fifteen studies mentioned data being filtered before being subject to analysis and a variety of filters were used: second- [4,34], third- [39] and fifth- [45] order Butterworth filters; a low-pass median filter [5,7]; a second-order low-pass filter [3]; the Madgwick Altitude and Heading Reference System (AHRS) orientation filter [41,52]; a band pass filter [42]; a first-order analogue filter [49]; Kalman filtering and algorithms [9,12,34]; and a three-point moving average filter [54]. Kalman filtering was used when a wearable system contained multiple sensors in order to fuse the data, however, it is limited at higher speeds, with Blair et al. (2018) noting higher measurement errors in segments experiencing higher movement velocities in different kicking codes, but a good concurrent validity was observed when comparing the IMS to Vicon (Oxford Metrics, Oxford, UK) [9]. In three instances, commercially available data processing software from Xsens (MVN Biomech Studio, MVN Studio and MT Manager 4.2.1, Xsesns Technologies B.V.m Enschede, The Netherlands) was used to process data which uses Kalman filters to fuse sensor data [9,12,40]. In all other cases, custom-made scripts were used to process data.

3.5. Recording and Usage Lifetime of Wearable Systems

Systems employed different recording methods, leading to a variation in the amount of data that could be recorded and the usage lifetime. Lithium ion polymer batteries (LiPo) were found in many accelerometers, IMUs and inertial and magnetic measurement units (IMMUs) [33,49,55,61–63]. The exact Physilog sensors (GaitUp, Lausanne, Switzerland) used by Chardonnens et al. (2013a, 2013b, 2014) were not stated [5,7,8] but data on Physilog 4 measurement units (GaitUp, Lausanne, Switzerland) state the use of rechargeable LiPo batteries. Nickel-metal hydride (NiMH) batteries were also used, chosen for their cost-efficiency and availability [35,36,43]. The highest storage capacity listed was of the Opal IMMUs (APDM Wearable Technologies, Portland, OR, USA) which are able to store approximately 720 h of data internally used by Fantozzi et al. (2016) [34,64]. The SwimMaster system is able to record continuously for up to 48 h [4]. A summary of the battery and storage features of the devices used is listed in Table 4.

Table 4. Battery and storage features of the wearable device systems.

Device	Battery Type	Battery Life	Storage Capacity	Application
MVN Link IMS (Xsens Technologies B.V., Enschede, The Netherlands)	One battery	Ten hours	-	Rugby and football [9]
Moven suit (Xsens Technologies B.V., Enschede, The Netherlands)	-	Approximately three hours [65]		Snowboarding [3]
Opal IMMUs (APDM Wearable Technologies, Portland, OR, USA)	-	Up to 16 h depending on whether data is logged or streamed	Internal storage of up to 8GB (approximately 720 h) [64]	Swimming [34]
Physilog 4 inertial measurement unit (IMU) (GaitUp, Lausanne, Switzerland)	LiPo battery	Up to 23 h	Internal storage of 4GB, providing 9 days of storage at 200 Hz [63]	Skiing [5,7,8]
SportSemble node	145 mAh LiPo rechargeable battery	Up to three hours	Flash memory of 116 kB (allowing each node to store around 11 seconds of data)	Baseball [49]
x-IMU magnetic, angular rate and gravity (MARG) sensors (x-io Technologies Limited, Bristol, UK)	LiPo battery (on-board charging via USB) [59]	-	-	Football [33]
G-Link-LXRS tri-axial accelerometer (LORD MicroStrain, Williston, VT, USA)	22 mAh LiPo battery (at 3.7 V)	-	2 MB [61]	Running [44]
Motus sensor (Motus Global, Rockville Centre, NY, USA)	10 mAH lithium ion battery (rapid charging using a microUSB)	Up to eight hours	Store 450+ throws	Baseball [48]
SABELSense IMU	High density LiPo battery	Approximately three hours	8 GB on a micro SD card [62]	Netball [52]
IMU nodes in CanoeSense system	1200 mAHh LiPo batteries	More than six hours	-	Canoeing [55]
Hand Monitoring Module	1500 mAh NiMh batteries (at 1.5 V per cell)	-	-	Badminton [43]
Pedar pressure insole system (novel gmbh, Munich, Germany)	NiMh batteries	-	2 GB SD card [60]	Skiing [35,36]
TSND121 wearable sensors (ATR-Promotion, Kyoto, Japan)	-	Approximately six hours	5.8 h of memory storage at 100 Hz [58]	Golf [51]
SwimMaster System	250 mAh battery at 3.7 V)	Up to 48 h	1 GB of flash memory	Swimming [4]
BSN nodes	-	-	512 kB of flash memory	Rowing [47]
XSens MTw IMMUs (Xsens Technologies B.V., Enschede, The Netherlands)	-	Approximately three hours	-	Running [12]

3.6. Validation and Reliability Using Gold-Standard Measurements

The Vicon motion capture system (Oxford Metrics, Oxford, UK) was used as a gold-standard reference for wearable systems used in football [9,33], rugby [9], baseball [50], athletics [45] and netball [52]. Philpott et al. (2014) used Kistler force platforms (Kistler Instruments Ltd., Hampshire, UK) alongside the Vicon (Oxford Metrics, Oxford, UK) camera set-up [45] when looking at sprinting in athletics. Optical based systems, such as BTS Bioengineering stereo-photogrammetric system (BTS Bioengineering Corp., Quincy, MA, USA) and XOS Technologies (Wilmington, MA, USA) optical motion analysis system), were also used as gold standards when observing movement in swimming [34], rowing [47] and baseball [49]. Kistler force plates (Kistler Instruments Ltd., Hampshire, UK) were also used in snowboarding by Krüger et al. and in skiing by Nakazato et al. (2011, 2013) [3,35,36]. The reliability of the wearable systems in comparison to the gold-standard references are detailed in Table 5. Results obtained from experimentation by Chardonnens et al. (2013a, 2014),

Gandy et al. (2018), Meamarbashi et al. (2010) and Munz et al. (2013) were compared to values reported in literature [5,7,31,39], detailed in Table 6.

Table 5. Wearable systems compared to a gold-standard reference.

Article and Sport	System Used	Gold Standard	Reliability
Akins et al. (2015)—Football [33]	Two x-IMU magnetic, angular rate and gravity (MARG) sensors (x-io Technologies Limited, Bristol, UK)	8 camera Vicon motion capture system (Oxford Metrics, Oxford, UK)	Concurrent criterion validity was assessed by comparing ankle plantar flexion, inversion and internal rotation angles between the MARG sensors and Vicon (Oxford Metrics, Oxford, UK). High correlation between sagittal plane data (r = 0.900 to 0.975) for all manoeuvres and RMSE was <5° for drop landing, drop jump and stop jump manoeuvres. Poor correlation between frontal plane data (r = −0.074 to 0.562) and RMSE > 3° for all manoeuvres. Poor correlation between transverse plane data and RMSE > 3° for all manoeuvres.
Blair et al. (2018)—Australian football, football and rugby [9]	MVN Link IMS—17 inertial sensors (Xsens Technologies B.V., Enschede, The Netherlands)	12 camera Vicon motion capture system (Oxford Metrics, Oxford, UK)	Trivial to small errors between the IMS and Vicon (Oxford Metrics, Oxford, UK) in all kinematic parameters (0.1 to 5.8%). Trivial to small differences were found (0.2 to 5.8%) were found between linear velocities (foot and pelvis), angular velocities (knee, shank and thigh), sagittal joint (knee and hip) and segment angle (shank and pelvis) means.
Fantozzi et al. (2016)—Swimming [34]	Seven Opal IMMU units (APDM Wearable Technologies, Portland, OR, USA)	7 camera SMART-DX 7000 stereo-photogrammetric system (BTS Bioengineering Corp., Quincy, MA, USA)	Better agreement between the two systems was found during breaststroke compared to front crawl (CMC = 0.99 compared to 0.97, R = 0.99 compared to 0.95 and RMSE = 5° compared to 7°).
King et al. (2009)—Rowing [47]	Three BSN nodes with inertial sensors	SMART-D system (BTS Bioengineering Corp., Quincy, MA, USA)	Mean error between the BSN nodes and BTS system: 3.6° in femur rotation, 4.0° for thoraco-lumbar rotation and 4.1° in sacrum rotation. Accuracy of BSN nodes not as fine as BTS system resolution.
Koda et al. (2010)—Baseball [50]	3D sensor containing two types of accelerometer and gyroscope	Vicon motion capture system (Vicon460, Oxford Metrics, Oxford, UK))	Correlation coefficient (R) and RMS of error calculated between estimated position by 3D sensor and position measured by the Vicon system (Oxford Metrics, Oxford, UK). For the shoulder, elbow and wrist, R in the x and y direction showed excellent agreement (>0.95) but was smaller for the z direction (0.73 to 0.92). However RMS was less than 10 cm for the z direction and between 13 cm to 18 cm for the x and y directions.
Krüger et al. (2009)—Snowboarding [3]	Moven IMS—16 sensor units (Xsens Technologies B.V., Enschede, The Netherlands); T and T Medilogic bilateral insole measurement (T and T Medilogic Medizintechnik GmbH, Schönefeld, Germany)	Three synchronized cameras; Kistler force plate (Kistler Instruments Ltd., Hampshire, UK)	The IMS system had a moderate accuracy when compared to the cameras. Mean deviation in knee angles for left leg and right leg were 4.8° and 3.1° respectively. Correlation coefficients were high (0.96 for the left knee angle and 0.77 for the right knee angle). The insoles had a milted accuracy with a mean RMSE of 28%.
Lapinski et al. (2009)—Baseball [49]	Five SportSemble nodes—inertial measurement units (IMUs)	10 camera XOS Technologies (Wilmington, MA, USA) optical motion analysis system	No statistical difference between average shoulder internal rotation velocity in pitching measured by the IMUs and XOS Technologies system was found. Average standard deviation for IMUs was 6% compared to 15% for the optical system. In batting, the average error of bat speed at time of impact was 4.8%.
Nakazato et al. (2011)—Skiing [36]	Pedar pressure insole system (novel gmbh, Munich, Germany)	Two Kistler portable force plates (Kistler Instruments Ltd., Hampshire, UK)	The mean absolute difference of the vertical ground reaction force (vGRF) mean between the two systems ranged from 0.45 to −0.23 N/BW on the outside leg, from −0.19 to −0.10 N/BW on the inside leg and from −0.25 to 0.13 N/BW during the edge changing phase. Differences were influenced by the skier's level, skiing mode and pitch.
Nakazato et al. (2013)—kiing [35]	Pedar pressure insole system (novel gmbh, Munich, Germany)	Two Kistler portable force plates (Kistler Instruments Ltd., Hampshire, UK)	Similarity coefficients between the two systems were contrary or low in the x direction during the outside and inside phases (−0.95 to 0.26 and −0.53 to 0.40 respectively). Highly similar time characteristics were indicated in the y direction for the outside phase (0.92 to 0.96) and were lower for the inside phase (0.15 to 0.78).
Philpott et al. (2014)—Athletics [45]	Wireless IMU	14 Vicon T-Series cameras (Oxford Metrics, Oxford, UK); two Kistler force platforms (Kistler Instruments Ltd., Hampshire, UK)	The mean correlation coefficient between the IMU and Vicon (Oxford Metrics, Oxford, UK) was 0.907. The timing accuracy of the IMU was 1.26 frames and the acceleration mean accuracy was 1.81 m/s^2.
Shepherd et al. (2017)—Netball [52]	SABELSense IMU sensor	10 camera Vicon motion capture system (Oxford Metrics, Oxford, UK)	The IMU overestimated the Vicon (Oxford Metrics, Oxford, UK) angle of the forearm at release by 4.03°, which was deemed an appropriate level of accuracy.

Table 6. Wearable systems compared to values reported in literature.

Article and Sport	System Used	Reliability
Chardonnens et al. (2013a)—Skiing [7]	Seven Physilog inertial measurement units (IMUs) (GaitUp, Lausanne, Switzerland)	Validity of the system was assessed by comparing ski horizontal angle at landing impact to hill slope: $-0.2 \pm 4.8^{\circ}$, max value 11.5°. When compared to literature data, differences were smaller than 6° for 75% of the angles and smaller than 15° for 90% of the angles.
Chardonnens et al. (2014)—Skiing [5]	Seven Physilog IMUs (GaitUp, Lausanne, Switzerland)	Maximum centre of mass (CoM) velocity for Group 1 was 2.51 ± 0.83 m/s and for Group 2 was 2.23 ± 0.28 m/s compared to 2.3 m/s reported in literature.
Meamarbashi et al. (2010)—Football [31]	Sensor module and data logger	Angular velocity of the shank in the x-axis of $1911.2 \pm 241.6^{\circ}$/s is comparable with the widely accepted value reported by Nunome et al. (2006) of $2257 \pm 224.6^{\circ}$ [66]
Munz et al. (2013)—Equestrian [39]	Two MTx inertial sensors (Xsens Technologies B.V., Enschede, The Netherlands)	Inter-individual differences were found for anterior-posterior (AP) and lateral (LT) angles in sitting trot ($13.3 \pm 2.3^{\circ}$ and $6.4 \pm 1.1^{\circ}$ respectively), corresponding well with values in literature ($13.9 \pm 2.2^{\circ}$ and $5.1 \pm 1.1^{\circ}$ respectively) reported by Byström et al. (2009) [67]

Accuracy of the systems used were reported using different measures in other articles. The inertial measurement units (IMU) sensors in the MVN system used by Gandy et al. (2018) were stated to have a 3-dimensional orientation accuracy within 1° [40]. Gawsalyan et al. (2017) reported a typical RMSE of around 7° for the magnetic, angular rate and gravity (MARG) sensors used in upper limb motion detection in cricket [41]. The "ISWIM" system was compared to a stopwatch, not considered a gold standard, reporting an average difference of 0.56 seconds between timings [6]. Jacob et al. (2017) reported accuracy of the flex sensors as a detection percentage, displaying a 70% detection ability in identifying five badminton grips [43]. The accuracy of the elbow torque-measurement device for monitoring baseball pitches was much higher, being able to detect 97.4% of pitches thrown by a given player [48]. A wearable sensor detecting football kicks only failed to detect six kicks out of a total of 450 [32]. The IMU for assessing skill level in volleyball had an average accuracy of 94% [54].

3.7. Application of Technology

Different applications were reported for the wearable systems and included injury prevention; quantifying skill level and expertise; improving technique; and characterizing movements. Injury prevention was the motivation behind twelve studies [3,12,33,35–37,40,44,46,48–50]. For instance, in running, high tibial peak-positive accelerations (PPAs) are linked to the risk of tibial stress fracture and as mentioned in Section 3.4, the provision of auditory feedback was able to temporarily reduce PPAs in participants [44]. By correlating the pitch of the signal output to the magnitude of PPAs, athletes were able to audibly understand the impact they were generating during each step. Fatigue is considered as another risk factor in relation to injury and the change in running mechanics was observed during a marathon [12]. Despite being ideal conditions to monitor fatigue and significant changes in mechanics, data was only collected from three participants, which is not enough to produce an analysis representative of runners in general. Yet another variable was considered as an indication of injury risk by Kiernan et al. (2018)—peak vertical ground reaction force (vGRF) was measured in injured and non-injured runners during every day training [46]. A higher peak vGRF was produced by injured runners, which is something that could be used by coaches and support staff to generate a threshold for injury potential.

Injury prevention was also considered in baseball [48–50], with three authors of included articles assessing different parameters. Lapinski et al. (2009) studied a combination of kinetics and kinematics of the upper body [49], Makhni et al. (2018) focused on elbow torque [48] and Koda et al. (2010) observed kinematics of the upper limb [50]. A combination of accelerometers and gyroscopes was used in all three articles.

In other studies, authors were able to accurately measure parameters that were connected to injury-risk, such as high forces produced in middle-turns in skiing [37] and hip asymmetry in horse riders [40], suggesting their possibility of influencing rehabilitation or aiding elite coaches and athletes. However, there was no indication on the utility of the results in making biomechanical changes to

reduce injuries risk. Magnetic, angular rate and gravity (MARG) sensors used by Akins et al. (2015) in football showed promise of clinical utility with regards to sagittal plane movement only [33] but the impact of these measures was not demonstrated in practice.

Wearable technology was used to quantify skill level and expertise by five authors [5,7,8,38,54]. The inertial measurement units (IMUs) used to assess the skill level of volleyball players had a 94% accuracy in determining a players' ability. The data was also compiled into a database, increasing the impact of the sensor as this information could be used by sports scientists and professional coaches [54]. Patterson et al. (2010) also used IMUs to quantify the expertise of show jumping horse riders. The authors came to the conclusion that their hypothesis was confirmed in that novice riders were more unbalanced during jumps and differences were recorded between experienced and novice riders in the variables measured [38], but there was not any statistical analysis performed to support this or explain the significance of these differences.

Movement recognition using sensors was also explored in sports such as dressage, cricket, football, rugby, badminton, rowing, swimming and table tennis [9,32,34,39,41–43,47]. In dressage authors reported kinematic differences between two riders with similar levels of experience [39] and in rowing, King et al. (2009) were able to distinguish between poor and good technique but this was not quantified [39,47]. Yet in the study by Guo et al. (2010), accelerations were used to characterize the table tennis block movement as well as distinguish between different athlete levels by comparing the standard deviation in acceleration [42]. Acceleration and force values were also used to characterize Nordic walking phases by Mocera et al. (2018) [56]. The hand monitoring module (HMM) for monitoring the grip in badminton had only a 70% detection ability between the five different grips [43]. Accuracy of the wearable sensor used by Kim et al. (2016) was also reported: out of 450 kicks, only six were not detected and the sensor was also able to discriminate kicking from other motion such as walking [32]. In cricket, MARG sensors were used to analyse upper limb motion in cricketers to detect potentially illegal bowling actions.

4. Discussion

The aim of this review was to determine the use and application of wearable technology in sport. From the reviewed articles it can be seen that a variety of wearable systems (including inertial sensors, pressure insoles and flex sensors) were able to measure kinetic and kinematic parameters in over 15 different sports. The common themes were injury prevention, performance assessment, movement recognition and skill level classification.

Out of these themes, injury prevention is an area with great potential when the cost of injuries and harm to athletes is considered. However, this potential has not been realised when compared to the other themes. Difficulties are presented by the many definitions of sports injury in literature and the barriers to describing their incidence: defining and gaining access to the population of interest and obtaining a suitable measure of exposure time [68]. Anecdotal experience is often the basis for preventive measures, such as strength training and stretching [69]; little of it is evidence-based as there are few randomised controlled trials reported in the literature [68,69] and this is especially the case for overuse injuries [70]. Moreover, there is a lack in the use of biomechanical measures as a means of objectively preventing injury as it is not clear which measures should be used.

However, data and technology have the potential to be used to predict injury, forming the basis for individualised programmes and allowing monitoring over a period of time, as demonstrated by Kiernan et al. (2018) who studied participants over a 60-day period [46]. To fully exploit this potential in injury prevention, however, there is still a need of identifying which biomechanical data obtained from wearable technology is the most useful as a predictor of injury.

4.1. Quality of Articles

The quality of the included papers varied greatly, with regards to descriptions of methods, sensor location and processing techniques. The population studied also varied, with participants ranging

from an amateur to professional level. As stated by Düking et al. (2018), the study population should reflect the intended user of the wearable technology as different populations behave differently [19]. There was no standardization within each sport in terms of population size and experience. Swimming was studied by Bächlin et al. (2012) and Fantozzi et al. (2016) with 16 participants (from occasional to elite swimmers) in the former article and 8 (no experience level stated) in the latter [4,34]. Smaller sample sizes can create population bias in the results, making it difficult to trust the output.

There was also a discrepancy in detail given for the tasks conducted by study participants and the description of the location of the sensors. The amount of detail given affects the ability of a study to be accurately replicated by another person. When multiple IMUs are used, the output can be combined using a model to reconstruct human motion and trajectories, but often this is dependent on using specific anatomical landmarks, so sensor placement can affect the reliability and accuracy of the reconstruction [71].

4.2. Wearable Systems Used

Commercially available sensors were used in the majority of studies, the most popular being those produced by Xsens Technologies B.V. (Enschede, The Netherlands) in the form of individual sensor nodes and sensor suits in seven articles in skiing, equestrian, football, rugby, running and snowboarding [3,9,12,37–40]. A possible explanation for this could be the accuracy of these inertial sensors in comparison to a gold-standard reference. The MVN Link IMS used by Blair et al. (2018) [9] was compared to the Vicon motion capture system (Oxford Metrics, Oxford, UK) and small errors were reported (0.1 to 5.8%) between the two systems. Results from MTx inertial sensors analysing pelvis motion corresponded well with previously reported values in the literature where reflective markers and infrared cameras were used to study the same movement [39,67].

The cost of these devices is what makes them prohibitive for widespread use. The MTw Awinda 3DOF Wireless Motion Tracker (Xsens Technologies B.V., Enschede, The Netherlands) costs €400 per unit [72], while the Physilog 5 inertial measurement unit (IMU) (GaitUp, Lausanne, Switzerland) is slightly more at €499 per unit [73]. When you consider that Chardonnens et al. (2013, 2014) [5,7] used seven Physilog sensors to monitor skiing kinematics just of the lower limbs, the total cost associated with the setup rises dramatically. This limits the technology to high performance or private organizations that have a budget to spend on equipment, but this is only representative of a small section of the sporting population.

An alternative to commercially available sensors are those that have been developed in-house, which have also been shown to be comparable to motion capture systems. ADXL193 and ADXL320 accelerometers from Analog Devices were components in the 3D sensor used by Koda et al. (2010) [50] with estimation errors of about 10% but are a fraction of the cost of the x-io Technologies IMU (Bristol, UK) used by Akins et al. (2015) [33,59,74]. The ADXL193 is being sold for £18 by one supplier [75], while the x-IMU has a cost of £309 with housing and battery [59]. Other comparable features between the two devices included sampling frequency and battery lifetimes.

The ease of use of wearable systems must be considered. Sensors requiring complex set ups or technicians are not providing additional benefit compared to motion capture systems. For instance, the elbow torque-measurement device (ETD) studied by Makhni et al. (2018) [48] and the compression sleeve housing it were positioned by technicians and this positioning was constantly monitored. However, this process takes approximately a minute and if it is easy for coaches or other baseball players to learn and carry out it could contribute to device uptake. The fact that the activity monitor employed by Kiernan et al. (2018) [46] was placed by the participants themselves demonstrates its ease of use and indicates that small changes in positioning will not have a significant impact on the device output. The ease of using the Xsens MVN suit (Xsens Technologies B.V., Enschede, The Netherlands) was mentioned by Gandy et al. (2014) [40]. As the inertial sensors are embedded in the suit, it allowed for quicker changes between participants during the study.

Only three studies considered the impact of the technology used on participants [48,52,56] and two did so in a quantitative manner [48,52]. In a sport such as Nordic walking where the equipment is so light (180 g per pole), any technological additions must have minimal impact in terms of weight which was considered by the authors [56]. However, no indication of the weight of the acquisition system was given nor a comparison between this setup and poles that had not been equipped with any technology. This would have provided a clear indication of its impact on the participant's movements. An important result from the study by Shepherd et al. (2017) [52] in netball was the comparison of player performance when wearing the IMU and when not wearing it. The Pearson's correlation coefficient, used for measuring the linear dependence between the conditions of wearing the IMU or not, was approximately equal to one [52], meaning that there was no significant impact on performance when wearing the IMU, an indicator of unobtrusiveness which could help with increasing the uptake of the device. Makhni et al. (2018) [48] followed up with participants after testing and 95% indicated that they thought it was important to monitor the stress on the arm when throwing and 73% indicated that they would alter their technique based on the results of the ETD. However, there was a significant difference between the percentage of those surveyed as to whether they would use the ETD in a practice or game setting (91% compared to 41%) [48]. Further information as to why this was the case would have been useful as for understanding what athletes expect from wearable devices if they are to use them in a competition setting.

4.3. Data Collection and Processing

Motion capture systems and wearable devices are able to provide athletes and coaches with more detailed analysis of the biomechanics involved in a certain sport, enhancing the methods already employed such as video analysis. However, systems such as Vicon (Oxford Metrics, Oxford, UK) have lengthy data processing times and require familiarity with how the system works. This is being considered by researchers, who recognize the importance of making data easy to interpret and also providing simple real-time feedback to athletes. The benefits of this can be seen in the systems studied by Li et al. (2016) [6] and Wood et al. (2014) [44] where vibratory and audible feedback is provided to the athletes and has been able to change movement biomechanics by reducing tibial impact and body rotation but this type of feedback is still novel.

Both Bächlin et al. (2012) [4] and Wang et al. (2016) [55] were aware of the importance of being able to provide real-time feedback for the SwimMaster and CanoeSense monitoring systems, respectively, and this was indicated in plans for further work, which would allow continuous monitoring and swimmers to make changes without a coach [4] or a coach to assess synchronicity between athletes and its impact on canoe propulsion [55].

As feedback from the "ISWIM" system was provided by the device itself and not an external source, there was not a concern for signal loss. For other wearable technology considering real-time feedback as grounds or future work, wireless data transfer was employed and some devices were affected by interference and signal loss. In the case of Reenalda et al. (2016), data was transferred wirelessly from inertial and magnetic measurement units (IMMUs) to a base station (Awinda Master, Xsens Technologies B.V., Enschede, The Netherlands)) while runners completed a marathon [12]. This base station was mounted on the handlebars of a bike that travelled alongside the athlete, with the antenna raised up to make sure that elements such as road signs and other runners did not interfere. Despite this, signal loss meant that data could only be collected for three out of the five initial participants [12]. A similar problem was encountered by Gandy et al. (2014) where wireless signals were lost at a consistent location during testing, potentially due to the presence of a radio mast [40]. Wireless data transfer has been pursued as a means of providing a less invasive system, however signal loss in outdoor environments or due to other objects causing interference limits its potential.

4.4. Testing Environment

Only five studies were conducted in a laboratory setting [9,33,34,44,47]. The remaining studies were conducted in a sporting environment [3–8,12,31,35–42,45,46,48–50,52–55] with the exception of three, where the location was not stated [32,43,51]. The conditions of testing are really important as revealed by the study conducted by Fantozzi et al. (2016) where simulated swimming altered the swimmers' biomechanics [34]. Although this is suitable for testing the reliability of the inertial and magnetic measurement units (IMMUs), it is not necessarily suitable for considering kinematic and kinetic factors relating to injury or performance. The unpredictability of the conditions in an outdoor environment in sports such as running can influence the biomechanical motions of an athlete, therefore, it is important for wearable systems to be tested in these scenarios and allow more accurate kinetic and kinematic measures to be obtained.

Conducting tests in a sports setting has the advantage of being able to factor in elements that may affect readings, such as drag in swimming, as well as having a better understanding of how an athlete moves in their chosen sport. Furthermore, monitoring an athlete in a training or competition environment is a good test of whether or not a system is unobtrusive as its performance is under scrutiny. Under laboratory conditions, participants may expect sensors to be uncomfortable but would generally not put up with them causing discomfort or affecting their range of motion during training or competition.

4.5. Application of Wearable Technology

The potential of wearable technology is huge. Across the included articles different applications were reported: the prevention of injury; characterizing movements; analysing technique and performance; and identifying skill level. Participants from a recreational to elite level were selected in the various studies, demonstrating that these devices are not just for athletes at the top of their game but have a wider target audience, increasing the impact of wearables.

There was a crossover between themes, such as the combination of movement classification and performance in the study by Shepherd et al. (2017) in netball [52], as kinematic observations can be used to influence coaching practices to achieve a more consistent forearm angle at ball release, which would increase the likelihood of scoring during a game. Addressing more than one theme elevates the utility of a technology as it means more people can benefit from it in different ways.

The demand for wearable devices is there, especially where injury is concerned: twelve studies considered factors related to injury [3,12,33,35–37,40,44,46,48–50]. When you consider injury statistics reported by Lapinski et al. (2009) in baseball [49], where the percentage of pitchers with injuries sufficient enough to prevent them from throwing increased from 50% in 1973 [76] to over 75% in 1999 [77], there is hope that technology can reverse this trend.

Both running and baseball injuries were each studied by three different authors, each looking at different parameters. However, in each sport, only one author was able to convey the effect of the device on study participants [44,48]. It was clear to see the influence of providing feedback in the form of audible beeps directly to athletes in the case of Wood et al. (2014) [44]. This simple method is beneficial as it allows athletes to still have an awareness of their training environment without looking at visual information in the form of figures or numbers. As discussed in Section 4.2, Makhni et al. (2018) was the closest to demonstrating buy-in from athletes in terms of using the device in training [48]. Furthermore, the elbow torque-measurement device (ETD) used was linked to a smartphone application, where quantified data may be more beneficial for coaches who can use the readouts to compare athletes. There is an advantage of smartphone applications to all users in that it is integrated into a device that is used every day, additional equipment is not needed besides the sensor.

What this information demonstrates is that we are still at an exploratory phase of using wearable technology in sports. Despite all studies being able to measure kinematic and kinetic parameters with these devices, only a few were able to translate the output into something suitable for actual use by coaches and athletes [6,44,48,51]. This opens up the possibility to future studies to explore how to take

a device from the research stage to the sporting environment by considering athlete comfort and ease of interpreting device output.

It is also evident from reviewing these articles that there is a wearable technology market for both athletes and coaches. Devices that are able to give audible and vibratory feedback are more useful for athletes who can then focus on the movements they are performing and their environment, also enabling them to make biomechanical changes without the presence of a coach. Where the device output can be displayed as readout on a smartphone or tablet is more suitable for coaches, but when developing these accompanying applications, care must be taken to only provide data that is useful and easy to interpret.

4.6. Review Limitations

Limitations must be considered when interpreting the findings of this review. The search was limited to seven databases, albeit integrated by reference lists and hand searches to identify other relevant papers. The results of this review are also limited by the choice of search terms and inclusion criteria—using different terms and criteria may have changed the number of articles included. However, the search terms and criteria were guided by similar reviews that have been published previously. Included articles were restricted to those published in English, posing a language bias to article selection. The quality assessment checklist was formed based on a review of wearable technology for spine movement assessment [28] as a standardized tool was not found because study quality was not reported in similar reviews.

5. Conclusions

This review highlighted the increase in research surrounding wearable technology as a means to measure kinetic and kinematic parameters in sport to understand movement and differentiate between skill levels. However, it is still not at a stage where there is a good translation to general usage.

The most common type of device used were inertial measurement units, however, authors explored stand-alone accelerometers and flex sensors also, both those commercially produced and developed in-house. Devices were developed in-house as a way to reduce their cost, which will ultimately have an impact on uptake when reaching the general market. Different applications were reported, from injury prevention to assessing performance, with the long-term vision of influencing coaching practices and athlete technique. There is potential for wearable technology to be used for long-term monitoring, especially beneficial in injury prevention as it provides coaches and athletes with the capacity to observe and analyse biomechanical risk factors over a defined exposure time, with the ability to influence injury prevention models.

A significant advantage of these devices is the ability to monitor athletes in-field instead of inside a laboratory. Laboratory testing introduces many limitations, while normal sports environments are able to provide a more accurate setting for biomechanical measurements. Furthermore, a number of studies validated the wearable technology against gold-standard reference, showing good concurrent validity. Despite the measurement errors associated with inertial measurement units, they are able to provide reliable measurements of joint kinematics and as a result, are a popular choice across different sports.

Providing real-time feedback has been shown to influence technique in swimmers and runners, but this is not yet a common feature across all sports. Wireless data transfer is a necessity but signal loss needs to be minimized in order for data to be beneficial. Any output must also be easy to interpret if it is going to be adopted by athletes and coaches who may have limited experience when analysing movement biomechanics data. Wireless data transfer has been addressed in a few studies, where data was transferred to and displayed in smartphone applications.

There have been discrepancies in the amount of detail given in the studies carried out and the wearable sensors that were used, but it is clear that they are able to provide accurate information regarding biomechanics that can be exploited in a number of ways in sport.

Supplementary Materials: The following are available online at http://www.mdpi.com/1424-8220/19/7/1597/s1, **Table S1.** Data extracted from included articles.

Author Contributions: All authors contributed to conceive and design the study; Y.A. performed the data retrieval; Y.A. and E.P. evaluated title and abstracts of the retrieved papers for inclusion and compared results through discussion. Any conflicts were resolved by A.H.M. Y.A. and E.P. analysed the included papers and extracted useful information. Y.A. prepared the original draft and E.P. and A.H.M. assisted in reviewing and editing the manuscript.

Funding: This research received no external funding

Conflicts of Interest: The authors declare no conflict of interest.

Appendix A

Table A1. Quality assessment of included articles (L: Low, M: Medium, H: High).

Quality Index Item Number	Akins et al. (2015)	Bächlin et al. (2012)	Blair et al. (2018)	Chardonnens et al. (2013a)	Chardonnens et al. (2013b)	Chardonnens et al. (2014)	Fantozzi et al. (2016)	Gandy et al. (2018)	Gawsalyan et al. (2017)
1	2	1	2	2	2	1	2	2	1
2	2	1	2	1	1	1	2	1	0
3	2	1	2	1	2	2	2	2	1
4	2	0	0	0	0	0	0	1	0
5	2	0	0	0	0	0	0	0	0
6	2	0	0	0	0	0	0	0	0
7	2	2	2	0	0	0	2	2	0
8	1	2	2	2	2	2	2	1	1
9	1	2	2	2	2	2	2	2	1
10	1	2	2	2	2	2	2	1	0
11	0	2	1	2	1	2	2	2	1
12	2	2	2	2	2	2	2	1	1
13	2	0	2	0	0	0	2	0	0
14	2	0	2	2	0	0	2	2	2
15	2	2	2	2	2	2	2	2	1
16	2	0	2	2	2	2	2	2	1
17	2	1	2	1	2	0	2	2	2
Total score/ out of 34	29	18	27	21	20	18	28	23	12
Percentage score/%	85.3	52.9	79.4	61.8	58.8	52.9	82.4	67.6	35.3
Quality category	H	M	H	M	M	M	H	H	M

Table A1. *Cont.*

Quality Index Item Number	Guo et al. (2010)	Jacob et al. (2017)	Kiernan et al (2018)	Kim et al. (2016)	King et al. (2009)	Koda et al. (2010)	Krüger et al. (2009)	Lapinski et al. (2009)	Lee et al. (2017)
1	1	2	2	1	1	2	2	2	1
2	1	0	2	0	0	2	2	1	0
3	1	1	2	1	0	2	1	1	2
4	0	0	2	0	0	0	0	0	0
5	0	0	0	0	0	0	0	0	0
6	0	0	0	0	0	0	0	0	0
7	2	1	1	2	0	1	1	1	1
8	2	2	2	2	2	2	2	1	2
9	1	2	2	2	2	1	1	1	1
10	1	2	2	1	0	2	2	2	1
11	2	0	1	0	0	0	2	2	0
12	2	2	2	2	2	2	2	2	2
13	0	0	0	0	2	2	2	2	0
14	0	1	0	1	2	2	2	2	0
15	1	1	2	2	1	2	2	1	2
16	1	0	2	0	1	2	1	0	0
17	1	1	2	1	0	0	2	2	0
Total score/ out of 34	16	15	24	15	13	22	24	20	12
Percentage score/%	47.1	44.1	70.6	44.1	38.2	64.7	70.6	58.8	35.3
Quality category	M	M	H	M	M	M	H	M	M

Table A1. *Cont.*

Quality Index Item Number	Li et al. (2016)	Makhni et al. (2018)	Meamarbashi et al. (2010)	Mitsui et al. (2015)	Mocera et al. (2018)	Munz et al. (2013)	Nakazato et al. (2011)	Nakazto et al. (2013)
1	1	2	2	1	1	2	2	2
2	0	2	1	0	0	1	2	2
3	1	2	2	0	2	2	2	1
4	0	2	1	0	0	0	0	0
5	0	0	0	0	0	0	0	0
6	0	0	0	0	0	0	0	0
7	2	2	2	0	0	2	2	2
8	2	2	2	1	1	2	2	2
9	2	2	2	1	1	1	2	2
10	1	2	2	0	0	2	1	1
11	0	0	0	0	1	2	0	0
12	2	2	2	2	2	2	2	2
13	0	0	0	0	0	0	2	2
14	0	2	0	0	0	0	2	2
15	2	2	2	1	2	2	2	2
16	0	2	2	0	0	2	2	2
17	0	2	0	0	1	2	2	2
Total score/ out of 34	13	26	20	6	11	22	25	24
Percentage score/%	38.2	76.5	58.8	17.6	32.4	64.7	73.5	70.6
Quality category	M	H	M	L	L	M	H	H

Table A1. *Cont.*

Quality Index Item Number	Patterson et al. (2010)	Philpott et al. (2014)	Reenalda et al. (2016)	Shepherd et al. (2017)	Taha et al. (2016)	Wang et al. (2018)	Wang et al. (2016)	Wood et al. (2014)
1	2	2	2	2	2	1	1	2
2	1	1	1	1	0	1	0	2
3	1	2	2	2	1	2	1	2
4	0	0	0	0	0	0	0	1
5	0	0	0	0	0	0	0	0
6	0	0	0	0	0	0	0	0
7	2	2	1	2	1	1	1	2
8	2	1	2	2	1	2	2	2
9	1	1	2	2	1	1	1	2
10	2	0	2	2	0	0	0	0
11	2	2	1	1	0	2	1	0
12	2	2	2	2	2	2	2	2
13	0	2	0	2	0	0	0	0
14	0	2	0	2	0	2	0	0
15	2	2	2	2	1	2	1	2
16	0	2	2	2	0	2	0	2
17	1	2	2	0	1	1	0	1
Total score/ out of 34	18	23	21	24	10	19	10	20
Percentage score/%	52.9	67.6	61.8	70.6	29.4	55.9	29.4	58.8
Quality category	M	H	M	H	L	M	L	M

References

1. Jones, R.L.; Wallace, M. Another bad day at the training ground: Coping with ambiguity in the coaching context. *Sport Educ. Soc.* **2005**, *10*, 119–134. [CrossRef]
2. Pueo, B.; Jimenez-Olmedo, J. Application of motion capture technology for sport performance analysis. *Retos* **2017**, *32*, 241–247.
3. Krüger, A.; Edelmann-Nusser, J. Biomechanical analysis in freestyle snowboarding: Application of a full-body inertial measurement system and a bilateral insole measurement system. *Sports Technol.* **2009**, *2*, 17–23. [CrossRef]
4. Bachlin, M.; Troster, G. Swimming performance and technique evaluation with wearable acceleration sensors. *Pervasive Mob. Comput.* **2012**, *8*, 68–81. [CrossRef]
5. Chardonnens, J.; Favre, J.; Cuendet, F.; Gremion, G.; Aminian, K. Measurement of the dynamics in ski jumping using a wearable inertial sensor-based system. *J. Sports Sci.* **2014**, *32*, 591–600. [CrossRef]
6. Li, R.; Zibo, C.; WeeSit, L.; Lai, D.T. A wearable biofeedback control system based body area network for freestyle swimming. In Proceedings of the 2016 38th Annual International Conference of the IEEE Engineering in Medicine and Biology Society (EMBC), Orlando, FL, USA, 16–20 August 2016; Volume 2016, pp. 1866–1869. [CrossRef]
7. Chardonnens, J.; Favre, J.; Cuendet, F.; Gremion, G.; Aminian, K. A system to measure the kinematics during the entire ski jump sequence using inertial sensors. *J. Biomech.* **2013**, *46*, 56–62. [CrossRef] [PubMed]
8. Chardonnens, J.; Favre, J.; Cuendet, F.; Gremion, G.; Aminian, K. Characterization of lower-limbs inter-segment coordination during the take-off extension in ski jumping. *Hum. Mov. Sci.* **2013**, *32*, 741–752. [CrossRef]
9. Blair, S.; Duthie, G.; Robertson, S.; Hopkins, W.; Ball, K. Concurrent validation of an inertial measurement system to quantify kicking biomechanics in four football codes. *J. Biomech.* **2018**, *73*, 24–32. [CrossRef]
10. Alonge, F.; Cucco, E.; Ippolito, F.; Pulizzotto, A. The use of accelerometers and gyroscopes to estimate hip and knee angles on gait analysis. *Sensors* **2014**, *14*, 8430. [CrossRef]
11. Papi, E.; Spulber, I.; Kotti, M.; Georgiou, P.; McGregor, A.H. Smart sensing system for combined activity classification and estimation of knee range of motion. *IEEE Sens. J.* **2015**, *15*, 5535–5544. [CrossRef]
12. Reenalda, J.; Maartens, E.; Homan, L.; Buurke, J.H. Continuous three dimensional analysis of running mechanics during a marathon by means of inertial magnetic measurement units to objectify changes in running mechanics. *J. Biomech.* **2016**, *49*, 3362–3367. [CrossRef] [PubMed]
13. Wisbey, B.; Rattray, B.; Pyne, D. *Quantifying Changes in AFL Player Game Demands Using GPS Tracking 2006 AFL Season*; FitSense Australia: Florey, Australia, 2007.
14. Wisbey, B.; Montgomery, P.; Pyne, D. *Quantifying Changes in AFL Player Game Demands Using GPS Tracking 2007 AFL Season*; FitSense Australia: Florey, Australia, 2008.
15. Siegmund, G.P.; Guskiewicz, K.M.; Marshall, S.W.; DeMarco, A.L.; Bonin, S.J. Laboratory validation of two wearable sensor systems for measuring head impact severity in football players. *Ann. Biomed. Eng.* **2016**, *44*, 1257–1274. [CrossRef] [PubMed]
16. Rawashdeh, S.A.; Rafeldt, D.A.; Uhl, T.L. Wearable imu for shoulder injury prevention in overhead sports. *Sensors* **2016**, *16*, 1847. [CrossRef] [PubMed]
17. MacDonald, K.; Bahr, R.; Baltich, J.; Whittaker, J.L.; Meeuwisse, W.H. Validation of an inertial measurement unit for the measurement of jump count and height. *Phys. Ther. Sport* **2017**, *25*, 15–19. [CrossRef] [PubMed]
18. van der Kruk, E.; Reijne, M.M. Accuracy of human motion capture systems for sport applications; state-of-the-art review. *Eur. J. Sport Sci.* **2018**, *18*, 806–819. [CrossRef] [PubMed]
19. Düking, P.; Fuss, F.K.; Holmberg, H.-C.; Sperlich, B. Recommendations for assessment of the reliability, sensitivity, and validity of data provided by wearable sensors designed for monitoring physical activity. *JMIR mHealth uHealth* **2018**, *6*, e102. [CrossRef] [PubMed]
20. McMaster, D.T.; Gill, N.; Cronin, J.; McGuigan, M. A brief review of strength and ballistic assessment methodologies in sport. *Sports Med.* **2014**, *44*, 603–623. [CrossRef] [PubMed]
21. Hamill, J.; Caldwell, G.E.; Derrick, T.R. Reconstructing digital signals using shannon's sampling theorem. *J. Appl. Biomech.* **1997**, *13*, 226–238. [CrossRef]
22. Robertson, G.E.; Caldwell, G.E.; Hamill, J.; Kamen, G.; Whittlesey, S. *Research Methods in Biomechanics*; Human Kinetics: Champaign, IL, USA, 2004.

23. Camomilla, V.; Bergamini, E.; Fantozzi, S.; Vannozzi, G. Trends supporting the in-field use of wearable inertial sensors for sport performance evaluation: A systematic review. *Sensors* **2018**, *18*, 873. [CrossRef] [PubMed]
24. Chambers, R.; Gabbett, T.J.; Cole, M.H.; Beard, A. The use of wearable microsensors to quantify sport-specific movements. *Sports Med.* **2015**, *45*, 1065–1081. [CrossRef] [PubMed]
25. Bunn, J.A.; Navalta, J.W.; Fountaine, C.J.; Reece, J.D. Current state of commercial wearable technology in physical activity monitoring 2015–2017. *Int. J. Exerc. Sci.* **2018**, *11*, 503–515. [PubMed]
26. O'Driscoll, R.; Turicchi, J.; Beaulieu, K.; Scott, S.; Matu, J.; Deighton, K.; Finlayson, G.; Stubbs, J. How well do activity monitors estimate energy expenditure? A systematic review and meta-analysis of the validity of current technologies. *Br. J. Sports Med.* **2018**. [CrossRef] [PubMed]
27. Evenson, K.R.; Goto, M.M.; Furberg, R.D. Systematic review of the validity and reliability of consumer-wearable activity trackers. *Int. J. Behav. Nutr. Phys. Act.* **2015**, *12*, 159. [CrossRef]
28. Papi, E.; Koh, W.S.; McGregor, A.H. Wearable technology for spine movement assessment: A systematic review. *J. Biomech.* **2017**, *64*, 186–197. [CrossRef] [PubMed]
29. Dobson, F.; Morris, M.E.; Baker, R.; Graham, H.K. Gait classification in children with cerebral palsy: A systematic review. *Gait Posture* **2007**, *25*, 140–152. [CrossRef] [PubMed]
30. Needham, R.; Stebbins, J.; Chockalingam, N. Three-dimensional kinematics of the lumbar spine during gait using marker-based systems: A systematic review. *J. Med. Eng. Technol.* **2016**, *40*, 172–185. [CrossRef] [PubMed]
31. Meamarbashi, A.; Reza, S.; Hosseini, S. Application of novel inertial technique to compare the kinematics and kinetics of the legs in the soccer instep kick. *J. Hum. Kinet.* **2010**, *23*, 5–13. [CrossRef]
32. Kim, W.; Kim, M. Soccer kick detection using a wearable sensor. In Proceedings of the 2016 International Conference on Information and Communication Technology Convergence (ICTC), Jeju Island, Korea, 19–21 October 2016; pp. 1207–1209.
33. Akins, J.S.; Heebner, N.R.; Lovalekar, M.; Sell, T.C. Reliability and validity of instrumented soccer equipment. *J. Appl. Biomech.* **2015**, *31*, 195–201. [CrossRef] [PubMed]
34. Fantozzi, S.; Giovanardi, A.; Magalhães, F.A.; Di Michele, R.; Cortesi, M.; Gatta, G. Assessment of three-dimensional joint kinematics of the upper limb during simulated swimming using wearable inertial-magnetic measurement units. *J. Sports Sci.* **2016**, *34*, 1073–1080. [CrossRef]
35. Nakazato, K.; Scheiber, P.; Müller, E. Comparison between the force application point determined by portable force plate system and the center of pressure determined by pressure insole system during alpine skiing. *Sports Eng.* **2013**, *16*, 297–307. [CrossRef]
36. Nakazato, K.; Scheiber, P.; Müller, E. A comparison of ground reaction forces determined by portable force-plate and pressure-insole systems in alpine skiing. *J. Sports Sci. Med.* **2011**, *10*, 754–762. [PubMed]
37. Lee, S.; Kim, K.; Kim, Y.H.; Lee, S.S. Motion anlaysis in lower extremity joints during ski carving turns using wearble inertial sensors and plantar pressure sensors. In Proceedings of the 2017 IEEE International Conference on Systems, Man, and Cybernetics, Banff, AB, Canada, 5–8 October 2017; pp. 695–698.
38. Patterson, M.; Doyle, J.; Cahill, E.; Caulfield, B.; McCarthy Persson, U. Quantifying show jumping horse rider expertise using imus. In Proceedings of the 2010 Annual International Conference of the IEEE Engineering in Medicine and Biology Society, EMBC'10, Buenos Aires, Argentina, 31 August–4 September 2010; pp. 684–687.
39. Munz, A.; Eckardt, F.; Heipertz-Hengst, C.; Peham, C.; Witte, K. A preliminary study of an inertial sensor-based method for the assessment of human pelvis kinematics in dressage riding. *J. Equine Vet. Sci.* **2013**, *33*, 950–955. [CrossRef]
40. Gandy, E.A.; Bondi, A.; Hogg, R.; Pigott, T.M.C. A preliminary investigation of the use of inertial sensing technology for the measurement of hip rotation asymmetry in horse riders. *Sports Technol.* **2014**, *7*, 79–88. [CrossRef]
41. Gawsalyan, S.; Janarthanan, T.S.; Thiruthanikan, N.; Shahintha, R.; Silva, P. Upper limb analysis using wearable sensors for cricket. In Proceedings of the 2017 2nd IEEE International Conference on Electrical, Computer and Communication Technologies, ICECCT 2017, Coimbatore, India, 22–24 February 2017.
42. Guo, Y.W.; Liu, G.Z.; Huang, B.Y.; Zhao, G.R.; Mei, Z.Y.; Wang, L. A pilot study on quantitative analysis for table tennis block using a 3d accelerometer. In Proceedings of the IEEE/EMBS Region 8 International Conference on Information Technology Applications in Biomedicine, ITAB, Corfu, Greece, 3–5 November 2010.

43. Jacob, A.; Zakaria, W.N.W.; Tomari, M.R.B.; Sek, T.K.; Suberi, A.A.M. Wearable flex sensor system for multiple badminton player grip identification. In *Advances in Electrical and Electronic Engineering: From Theory to Applications*; AIP Publishing: College Park, MD, USA, 2017; Volume 1883.
44. Wood, C.M.; Kipp, K. Use of audio biofeedback to reduce tibial impact accelerations during running. *J. Biomech.* **2014**, *47*, 1739–1741. [CrossRef]
45. Philpott, L.K.; Weaver, S.; Gordon, D.; Conway, P.P.; West, A.A. Assessing wireless inertia measurement units for monitoring athletics sprint performance. In Proceedings of the Sensors, Valencia, Spain, 2–5 November 2014; pp. 2199–2202.
46. Kiernan, D.; Hawkins, D.A.; Manoukian, M.A.C.; McKallip, M.; Oelsner, L.; Caskey, C.F.; Coolbaugh, C.L. Accelerometer-based prediction of running injury in national collegiate athletic association track athletes. *J. Biomech.* **2018**, *73*, 201–209. [CrossRef]
47. King, R.C.; McIlwraith, D.G.; Lo, B.; Pansiot, J.; McGregor, A.H.; Yang, G.-Z. Body sensor networks for monitoring rowing technique. In Proceedings of the 2009 6th International Workshop on Wearable and Implantable Body Sensor Networks, BSN 2009, Berkeley, CA, USA, 3–5 June 2009; pp. 251–255.
48. Makhni, E.C.; Lizzio, V.A.; Meta, F.; Stephens, J.P.; Okoroha, K.R.; Moutzouros, V. Assessment of elbow torque and other parameters during the pitching motion: Comparison of fastball, curveball, and change-up. *Arthroscopy* **2018**, *34*, 816–822. [CrossRef] [PubMed]
49. Lapinski, M.; Berkson, E.; Gill, T.; Reinold, M.; Paradiso, J.A. A distributed wearable, wireless sensor system for evaluating professional baseball pitchers and batters. In Proceedings of the 2009 International Symposium on Wearable Computers, ISWC 2009, Linz, Austria, 4–7 September 2009; pp. 131–138.
50. Koda, H.; Sagawa, K.; Kuroshima, K.; Tsukamoto, T.; Urita, K.; Ishibashi, Y. 3d measurement of forearm and upper arm during throwing motion using body mounted sensor. *J. Adv. Mech. Des. Syst. Manuf.* **2010**, *4*, 167–178. [CrossRef]
51. Mitsui, T.; Tang, S.; Obana, S. Support system for improving golf swing by using wearable sensors. In Proceedings of the 2015 Eighth International Conference on Mobile Computing and Ubiquitous Networking (ICMU), Hakodate, Japan, 20–22 January 2015; pp. 100–101.
52. Shepherd, J.B.; Giblin, G.; Pepping, G.J.; Thiel, D.; Rowlands, D. Development and validation of a single wrist mounted inertial sensor for biomechanical performance analysis of an elite netball shot. *IEEE Sens. Lett.* **2017**, *1*. [CrossRef]
53. Taha, Z.; Mat-Jizat, J.A.; Omar, S.F.S.; Suwarganda, E. Correlation between archer's hands movement while shooting and its score. *Eng. Sport* **2016**, *147*, 145–150. [CrossRef]
54. Wang, Y.; Zhao, Y.; Chan, R.H.M.; Li, W.J. Volleyball skill assessment using a single wearable micro inertial measurement unit at wrist. *IEEE Access* **2018**, *6*, 13758–13765. [CrossRef]
55. Wang, Z.; Wang, J.; Zhao, H.; Yang, N.; Fortino, G. Canoesense: Monitoring canoe sprint motion using wearable sensors. In Proceedings of the 2016 IEEE International Conference on Systems, Man, and Cybernetics, SMC 2016, Budapest, Hungary, 9–12 October 2016; pp. 644–649.
56. Mocera, F.; Aquilino, G.; Somà, A. Nordic walking performance analysis with an integrated monitoring system. *Sensors* **2018**, *18*, 1505. [CrossRef]
57. Moher, D.; Liberati, A.; Tetzlaff, J.; Altman, D.G.; The, P.G. Preferred reporting items for systematic reviews and meta-analyses: The prisma statement. *PLoS Med.* **2009**, *6*, e1000097. [CrossRef] [PubMed]
58. Small Wireless Multi-Function Sensor "tsnd121/151". Available online: https://www.atr-p.com/products/TSND121.html (accessed on 24 December 2018).
59. X-IMU Our Original Versatile IMU Board. Available online: http://x-io.co.uk/x-imu/ (accessed on 24 December 2018).
60. The Pedar®System—The Quality In-Shoe Dynamic Pressure Measuring System. Available online: http://novel.de/novelcontent/pedar (accessed on 24 December 2018).
61. G-link®-lxrs®Low-Cost Integrated Accelerometer Node. Available online: https://www.microstrain.com/wireless/g-link (accessed on 24 December 2018).
62. Wireless Mems Inertial Sensor. Available online: https://sabelsport.files.wordpress.com/2014/03/sabel_sense_270214a.pdf (accessed on 24 December 2018).
63. User Manual and Specifications. Available online: https://gaitup.com/wp-content/uploads/Physilog-User-manual_RA.pdf (accessed on 24 December 2018).

64. Research-Grade Wearable Sensors. Available online: https://www.apdm.com/wearable-sensors/ (accessed on 24 December 2018).
65. Moven User Manual. Available online: http://cs.unc.edu/Research/stc/FAQs/Xsens/Moven/Moven%20User%20Manual.pdf (accessed on 24 December 2018).
66. Nunome, H.; Ikegami, Y.; Kozakai, R.; Apriantono, T.; Sano, S. Segmental dynamics of soccer instep kicking with the preferred and non-preferred leg. *J. Sports Sci.* **2006**, *24*, 529–541. [CrossRef] [PubMed]
67. Byström, A.; Rhodin, M.; Von Peinen, K.; Weishaupt, M.A.; Roepstorff, L. Basic kinematics of the saddle and rider in high-level dressage horses trotting on a treadmill. *Equine Vet. J.* **2009**, *41*, 280–284. [CrossRef] [PubMed]
68. Chalmers, D.J. Injury prevention in sport: Not yet part of the game? *Inj. Prev.* **2002**, *8*, iv22–iv25. [CrossRef] [PubMed]
69. Donaldson, A.; Lloyd, D.G.; Gabbe, B.J.; Cook, J.; Young, W.; White, P.; Finch, C.F. Scientific evidence is just the starting point: A generalizable process for developing sports injury prevention interventions. *J. Sport Health Sci.* **2016**, *5*, 334–341. [CrossRef] [PubMed]
70. Schiff, M.A.; Caine, D.J.; O'Halloran, R. Injury prevention in sports. *Am. J. Lifestyle Med.* **2010**, *4*, 42–64. [CrossRef]
71. Cuesta-Vargas, A.I.; Galán-Mercant, A.; Williams, J.M. The use of inertial sensors system for human motion analysis. *Phys. Ther. Rev.* **2010**, *15*, 462–473. [CrossRef]
72. Mtw Awinda Wireless 3dof Motion Tracker. Available online: https://shop.xsens.com/shop/xsens-mvn/mtw-awinda-wireless-3dof-motion-tracker (accessed on 29 January 2019).
73. Physilog®5: Motion Sensor. Available online: https://shop.gaitup.com/index.php?id_product=1&controller=product (accessed on 29 January 2019).
74. Adxl330 Small, Low Power, 3-axis ±3 g i Mems®Accelerometer Data Sheet (Rev. 0). Available online: https://www.sparkfun.com/datasheets/Components/ADXL330_0.pdf (accessed on 1 January 2019).
75. Single Axis Accelerometer Breakout—ADXL193 (±250 g). Available online: https://www.proto-pic.co.uk/single-axis-accelerometer-breakout-adxl193-250g.html (accessed on 29 January 2019).
76. Tullos, H.S.; King, J.W. Throwing mechanism in sports. *Orthop. Clin. N. Am.* **1973**, *4*, 709–720.
77. Conte, S.; Requa, R.K.; Garrick, J.G. Disability days in major league baseball. *Am. J. Sports Med.* **2001**, *29*, 431–436. [CrossRef]



© 2019 by the authors. Licensee MDPI, Basel, Switzerland. This article is an open access article distributed under the terms and conditions of the Creative Commons Attribution (CC BY) license (http://creativecommons.org/licenses/by/4.0/).

Appendix B

Inter-test variability results for all strain sensors

B.1 Sensor S1

Table B.1: Mean of the sensor resistance range, standard deviation and percent deviation for sensor S1

Test	Mean (Ohms)	Standard deviation (Ohms)	Percent deviation (%)
100 cycles at 350mm/min, test 1	396.95	4.67	1.18
200 cycles at 350mm/min	394.18	2.67	0.68
500 cycles at 350mm/min	389.27	2.44	0.63
100 cycles at 50mm/min	370.82	4.04	1.09
100c cycles at 100mm/min	376.04	0.38	0.10
100 cycles at 350mm/min, test 2	392.70	2.00	0.51
100 cycles at 350mm/min, test 3	392.74	2.25	0.57
200 cycles at 50mm/min	450.92	5.98	1.33
1000 cycles at 350mm/min	474.69	2.62	0.55
200c cycles at 100mm/min	531.22	13.03	2.45
1000 cycles at 100mm/min	515.46	3.11	0.60
100 cycles at 350mm/min, test 4	841.81	18.00	2.14
500 cycles at 100mm/min	805.87	8.33	1.03
100 cycles at 350mm/min, test 5	838.72	8.05	0.96

Table B.2: Inter-test variability results from comparisons between tests of the same cycle length on sensor S1 (including post-hoc analysis). Significant values have been highlighted in red and non-significant values in green. The test number within Protocol 1 has been used to distinguish between comparisons.

	100 cycles	200 cycles	500 cycles	1000 cycles
No. tests	7	3	2	2
No. comparisons	21	3	1	1
Stats test	Friedman	Friedman	Wilcoxon	Wilcoxon
p-value	0	0	0	0
Post-hoc	Wilcoxon	Wilcoxon		
Adjusted α	0.002	0.017		
p-value	(12,14)=0.797			
	rest=0	All comparisons =0		

B.2 Sensor S2

Table B.3: Mean of the sensor resistance range, standard deviation and percent deviation for sensor S2

Test	Mean (Ohms)	Standard deviation (Ohms)	Percent deviation (%)
100 cycles at 350mm/min, test 1	125.66	7.13	5.67
100 cycles at 350mm/min, test 2	137.18	1.54	1.12
100 cycles at 350mm/min, test 3	143.29	2.38	1.66
100 cycles at 350mm/min, test 4	144.93	2.90	2.00
100 cycles at 350mm/min, test 5	146.70	2.31	1.57
200 cycles at 350mm/min	268.45	21.74	8.10
500 cycles at 350mm/min	288.49	17.26	5.98
1000 cycles at 350mm/min	283.70	19.81	6.98
100c cycles at 100mm/min	151.84	5.67	3.74
200c cycles at 100mm/min	149.78	3.22	2.15
500 cycles at 100mm/min	323.48	4.44	1.37
1000 cycles at 100mm/min	462.71	19.98	4.32
100 cycles at 50mm/min	1302.89	48.60	3.73
200 cycles at 50mm/min	1283.22	69.64	5.43
500 cycles at 50mm/min	987.65	127.93	12.95

Table B.4: Inter-test variability results from comparisons between tests of the same cycle length on sensor S2 (including post-hoc analysis). Significant values have been highlighted in red and non-significant values in green. The test number within Protocol 1 has been used to distinguish between comparisons.

	100 cycles	200 cycles	500 cycles	1000 cycles
No. tests	7	3	3	2
No. comparisons	21	3	3	1
Stats test	Friedman	Friedman	Friedman	Wilcoxon
p-value	0	0	0	0
Post-hoc	Wilcoxon	Wilcoxon	Wilcoxon	
Adjusted α	0.002	0.017	0.017	
p-value				
	(3,4)=0.001, (4,5)=0.002, rest=0	All comparisons =0	All comparisons =0	

B.3 Sensor S3

Table B.5: Mean of the sensor resistance range, standard deviation and percent deviation for sensor S3

Test	Mean (Ohms)	Standard deviation (Ohms)	Percent deviation (%)
100 cycles at 350mm/min, test 1	796.73	206.29	25.89
100 cycles at 350mm/min, test 2	798.96	194.37	24.33
100 cycles at 350mm/min, test 3	694.15	195.20	28.12
100 cycles at 350mm/min, test 4	721.09	179.74	24.93
100 cycles at 350mm/min, test 5	711.68	201.76	28.35
200 cycles at 350mm/min	658.00	236.09	35.88
500 cycles at 350mm/min	582.00	154.37	26.52
1000 cycles at 350mm/min	1681.26	52.33	3.11
100c cycles at 100mm/min	1476.51	48.23	3.27
200c cycles at 100mm/min	1357.57	45.79	3.37
500 cycles at 100mm/min	1411.68	105.89	7.50
1000 cycles at 100mm/min	2012.01	212.70	10.57
100 cycles at 50mm/min	1671.45	72.55	4.34
200 cycles at 50mm/min	2351.65	160.00	6.80
500 cycles at 50mm/min	1930.40	143.62	7.44

Table B.6: Inter-test variability results from comparisons between tests of the same cycle length on sensor S3 (including post-hoc analysis). Significant values have been highlighted in red and non-significant values in green. The test number within Protocol 1 has been used to distinguish between comparisons.

	100 cycles	200 cycles	500 cycles	1000 cycles
No. tests	7	3	3	2
No. comparisons	21	3	3	1
Stats test	Friedman	Friedman	Friedman	Wilcoxon
p-value	0	0	0	0
Post-hoc	Wilcoxon	Wilcoxon	Wilcoxon	
Adjusted α	0.002	0.017	0.017	
p-value	(1,2)=0.877,			
	(1,3)=0.057,			
	(1,4)=0.125,			
	(1,5)=0.12,			
	(2,3)=0.027,			
	(2,4)=0.221,			
	(2,5)=0.063,			
	(3,4)=0.558,			
	(3,5)=0.688,			
	(4,5)=0.781			
	rest=0	All comparisons =0	All comparisons =0	

B.4 Sensor S4

Table B.7: Mean of the sensor resistance range, standard deviation and percent deviation for sensor S4

Test	Mean (Ohms)	Standard deviation (Ohms)	Percent deviation (%)
100 cycles at 350mm/min, test 1	597.06	36.28	6.08
100 cycles at 350mm/min, test 2	796.50	78.37	9.84
100 cycles at 350mm/min, test 3	862.62	87.29	10.12
100 cycles at 350mm/min, test 4	874.62	86.24	9.86
100 cycles at 350mm/min, test 5	853.70	85.56	10.02
200 cycles at 350mm/min	823.16	97.62	11.86
500 cycles at 350mm/min	1067.62	121.43	11.37
1000 cycles at 350mm/min	1004.58	89.03	8.86
100c cycles at 100mm/min	1187.27	80.88	6.81
200c cycles at 100mm/min	1078.05	398.92	37.00
500 cycles at 100mm/min	1611.57	92.88	5.76
1000 cycles at 100mm/min	4575.80	743.73	16.25
100 cycles at 50mm/min	N/A	N/A	N/A
200 cycles at 50mm/min	N/A	N/A	N/A
500 cycles at 50mm/min	N/A	N/A	N/A

Table B.8: Inter-test variability results from comparisons between tests of the same cycle length on sensor S4 (including post-hoc analysis). Significant values have been highlighted in red and non-significant values in green. The test number within Protocol 1 has been used to distinguish between comparisons.

	100 cycles	200 cycles	500 cycles	1000 cycles
No. tests	6	2	2	2
No. comparisons	15	3	3	1
Stats test	Friedman	Wilcoxon	Wilcoxon	Wilcoxon
p-value	0	0.003	0	0
Post-hoc	Wilcoxon			
Adjusted α	0.003			
p-value	(3,4)=0.861,			
	(3,5)=0.975,			
	(4,5)=0.959			
	rest=0			

B.5 Sensor S5

Table B.9: Mean of the sensor resistance range, standard deviation and percent deviation for sensor S5

Test	Mean (Ohms)	Standard deviation (Ohms)	Percent deviation (%)
100 cycles at 350mm/min, test 1	2424.79	133.00	5.49
100 cycles at 350mm/min, test 2	2583.47	160.46	6.21
100 cycles at 350mm/min, test 3	2521.88	69.14	2.74
100 cycles at 350mm/min, test 4	3981.72	221.75	5.57
100 cycles at 350mm/min, test 5	6109.69	345.50	5.65
200 cycles at 350mm/min	6049.63	272.72	4.51
500 cycles at 350mm/min	34212.99	10140.09	29.64
1000 cycles at 350mm/min	77530.81	33067.85	42.65
100c cycles at 100mm/min	5249.67	396.92	7.56
200c cycles at 100mm/min	6189.42	448.58	7.25
500 cycles at 100mm/min	N/A	N/A	N/A
1000 cycles at 100mm/min	N/A	N/A	N/A
100 cycles at 50mm/min	N/A	N/A	N/A
200 cycles at 50mm/min	N/A	N/A	N/A
500 cycles at 50mm/min	N/A	N/A	N/A

Table B.10: Inter-test variability results from comparisons between tests of the same cycle length on sensor S5 (including post-hoc analysis). Significant values have been highlighted in red and non-significant values in green. The test number within Protocol 1 has been used to distinguish between comparisons.

	100 cycles	200 cycles	500 cycles	1000 cycles
No. tests	6	2	2	1
No. comparisons	15	1	1	0
Stats test	Friedman	Wilcoxon	Wilcoxon	
p-value	0	0.119	0	
Post-hoc	Wilcoxon			
Adjusted α	0.003			
p-value	(2,3)=0.04			
	(1,2)=0.001,			
	(1,3)=0.001, rest=0			

B.6 Sensor S6

Table B.11: Mean of the sensor resistance range, standard deviation and percent deviation for sensor S6

Test	Mean (Ohms)	Standard deviation (Ohms)	Percent deviation (%)
100 cycles at 350mm/min, test 1	1184.78	364.30	30.75
100 cycles at 350mm/min, test 2	1124.66	252.24	22.43
100 cycles at 350mm/min, test 3	1163.98	196.32	16.87
100 cycles at 350mm/min, test 4	963.50	150.40	15.61
100 cycles at 350mm/min, test 5	1026.92	138.78	13.51
200 cycles at 350mm/min	932.20	124.19	13.32
500 cycles at 350mm/min	936.76	118.50	12.65
1000 cycles at 350mm/min	916.67	111.55	12.17
100c cycles at 100mm/min	724.74	43.67	6.03
200c cycles at 100mm/min	729.81	32.41	4.44
500 cycles at 100mm/min	762.09	29.62	3.89
1000 cycles at 100mm/min	N/A	N/A	N/A
100 cycles at 50mm/min	753.51	193.38	25.66
200 cycles at 50mm/min	1017.13	46.69	4.59
500 cycles at 50mm/min	1108.49	33.84	3.05

Table B.12: Inter-test variability results from comparisons between tests of the same cycle length on sensor S6 (including post-hoc analysis). Significant values have been highlighted in red and non-significant values in green. The test number within Protocol 1 has been used to distinguish between comparisons.

	100 cycles	200 cycles	500 cycles	1000 cycles
No. tests	7	3	3	1
No. comparisons	21	3	3	0
Stats test	Friedman	Friedman	Friedman	
p-value	0	0	0	
Post-hoc	Wilcoxon	Wilcoxon	Wilcoxon	
Adjusted α	0.002	0.017	0.017	
p-value	(1,2)=0.221,			
	(1,3)=0.992,			
	(1,5)=0.009,			
	(2,3)=0.318,			
	(2,5)=0.039,			
	(4,5)=0.153,			
	(9,13)=0.015			
	(1,4)=0.001,	All compar-		
	(2,4)=0.002,	isons =0		
	(3,5)=0.001, rest=0			

B.7 Sensor S7

Table B.13: Mean of the sensor resistance range, standard deviation and percent deviation for sensor S7

Test	Mean (Ohms)	Standard deviation (Ohms)	Percent deviation (%)
100 cycles at 350mm/min, test 1	1090.33	269.86	24.75
100 cycles at 350mm/min, test 2	1053.23	176.28	16.74
100 cycles at 350mm/min, test 3	1058.56	127.93	12.09
100 cycles at 350mm/min, test 4	1048.16	84.00	8.01
100 cycles at 350mm/min, test 5	1050.77	150.99	14.37
200 cycles at 350mm/min	1021.21	137.72	13.49
500 cycles at 350mm/min	1133.32	209.22	18.46
1000 cycles at 350mm/min	1222.45	224.87	18.40
100c cycles at 100mm/min	648.30	42.46	6.55
200c cycles at 100mm/min	678.40	25.35	3.74
500 cycles at 100mm/min	645.17	19.27	2.99
1000 cycles at 100mm/min	632.54	19.15	3.03
100 cycles at 50mm/min	900.55	27.37	3.04
200 cycles at 50mm/min	888.08	34.11	3.84
500 cycles at 50mm/min	851.34	83.13	9.76

Table B.14: Inter-test variability results from comparisons between tests of the same cycle length on sensor S7 (including post-hoc analysis). Significant values have been highlighted in red and non-significant values in green. The test number within Protocol 1 has been used to distinguish between comparisons.

	100 cycles	200 cycles	500 cycles	1000 cycles
No. tests	7	3	3	2
No. comparisons	21	3	3	1
Stats test	Friedman	Friedman	Friedman	Wilcoxon
p-value	0	0	0	0
Post-hoc	Wilcoxon	Wilcoxon	Wilcoxon	
Adjusted α	0.002	0.017	0.017	
p-value	(1,4)=0.012,			
	(1,5)=0.098,			
	(2,3)=0.53,			
	(2,4)=0.125,			
	(2,5)=0.028,			
	(3,4)=0.023,			
	(3,5)=0.01,			
	(4,5)=0.382			
	(1,2)=0.001, rest=0	All comparisons =0	All comparisons =0	

B.8 Sensor S8

Table B.15: Mean of the sensor resistance range, standard deviation and percent deviation for sensor S8

Test	Mean (Ohms)	Standard deviation (Ohms)	Percent deviation (%)
100 cycles at 350mm/min, test 1	1640.74	179.97	10.97
100 cycles at 350mm/min, test 2	1459.07	189.25	12.97
100 cycles at 350mm/min, test 3	1466.52	183.63	12.52
100 cycles at 350mm/min, test 4	1539.34	130.40	8.47
100 cycles at 350mm/min, test 5	1576.99	165.79	10.51
200 cycles at 350mm/min	1473.31	173.51	11.78
500 cycles at 350mm/min	1648.10	270.53	16.41
1000 cycles at 350mm/min	1425.62	182.49	12.80
100c cycles at 100mm/min	762.93	43.80	5.74
200c cycles at 100mm/min	738.31	19.80	2.68
500 cycles at 100mm/min	727.96	24.95	3.43
1000 cycles at 100mm/min	878.54	25.79	2.94
100 cycles at 50mm/min	837.24	46.97	5.61
200 cycles at 50mm/min	844.38	24.86	2.94
500 cycles at 50mm/min	1473.30	80.94	5.49

Table B.16: Inter-test variability results from comparisons between tests of the same cycle length on sensor S8 (including post-hoc analysis). Significant values have been highlighted in red and non-significant values in green. The test number within Protocol 1 has been used to distinguish between comparisons.

	100 cycles	200 cycles	500 cycles	1000 cycles
No. tests	7	3	3	2
No. comparisons	21	3	3	1
Stats test	Friedman	Friedman	Friedman	Wilcoxon
p-value	0	0	0	0
Post-hoc	Wilcoxon	Wilcoxon	Wilcoxon	
Adjusted α	0.002	0.017	0.017	
p-value	(1,4)=0.012,			
	(1,5)=0.098,			
	(2,3)=0.53,			
	(2,4)=0.125,			
	(2,5)=0.028,			
	(3,4)=0.023,			
	(3,5)=0.01,			
	(4,5)=0.382			
	(1,2)=0.001, rest=0	All comparisons =0	All comparisons =0	

B.9 Sensor S9

Table B.17: Mean of the sensor resistance range, standard deviation and percent deviation for sensor S9

Test	Mean (Ohms)	Standard deviation (Ohms)	Percent deviation (%)
100 cycles at 350mm/min, test 1	873.40	203.80	23.33
100 cycles at 350mm/min, test 2	1034.13	303.21	29.32
100 cycles at 350mm/min, test 3	834.75	131.80	15.79
100 cycles at 350mm/min, test 4	826.99	178.77	21.62
100 cycles at 350mm/min, test 5	830.41	157.48	18.96
200 cycles at 350mm/min	826.97	237.24	28.69
500 cycles at 350mm/min	802.11	167.65	20.90
1000 cycles at 350mm/min	777.41	145.73	18.75
100c cycles at 100mm/min	302.14	15.53	5.14
200c cycles at 100mm/min	380.81	12.64	3.32
500 cycles at 100mm/min	393.57	10.39	2.64
1000 cycles at 100mm/min	401.53	9.61	2.39
100 cycles at 50mm/min	404.83	11.11	2.74
200 cycles at 50mm/min	488.85	13.14	2.69
500 cycles at 50mm/min	501.56	100.16	19.97

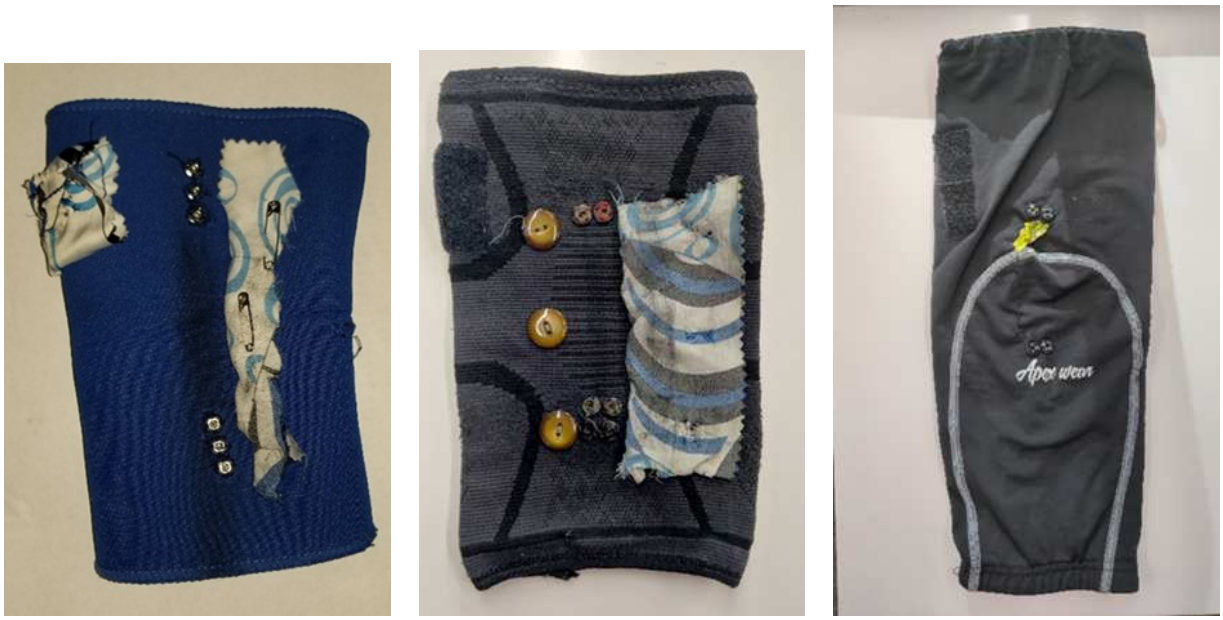
Table B.18: Inter-test variability results from comparisons between tests of the same cycle length on sensor S9 (including post-hoc analysis). Significant values have been highlighted in red and non-significant values in green. The test number within Protocol 1 has been used to distinguish between comparisons.

	100 cycles	200 cycles	500 cycles	1000 cycles
No. tests	7	3	3	2
No. comparisons	21	3	3	1
Stats test	Friedman	Friedman	Friedman	Wilcoxon
p-value	0	0	0	0
Post-hoc	Wilcoxon	Wilcoxon	Wilcoxon	
Adjusted α	0.002	0.017	0.017	
p-value	(1,2)=0.006, (1,3)=0.544,(1,4)=0.393, (1,5)=0.28, (2,3)=0.003, (2,5)=0.002, (3,4)=0.719, (3,5)=0.797. (4,5)=0.658 (2,4)=0.002, rest=0	All comparisons =0	All comparisons =0	

Appendix C

Wearable Sensor System Design Iterations

C.1 Knee Sleeve Design



(a) Iteration 1 **(b)** Iteration 2 **(c)** Iteration 3

Figure C.1: Different designs trialled for the WSS a) iteration 1, b) iteration 2 and c) iteration 3.

C.1.1 Iteration 1

Table C.1: Summary of main features of design iteration 1.

Feature	Details
Base knee sleeve	Neoprene knee support sleeve
IMU attachment	Pocket sewn to outer side of support
Strain sensor attachment	One snap fastener attached to each electrode
Sensor protection	Thin cotton cover

Table C.2: Summary of the positive and negative factors of design iteration 1.

Positives	Negatives
Covering over sensor	IMU pocket not secure
Snap fasteners allow easy modification	Not enough purchase with snap fasteners
	Not much stretch from knee sleeve
	Lack of grippers on knee sleeve causes bunching

C.1.2 Iteration 2

Table C.3: Summary of main features of design iteration 2.

Feature	Details
Base knee sleeve	Compression sleeve (material composition: 75% nylon, 15% spandex and 10% all-natural rubber)
IMU attachment	Hook and loop tape
Strain sensor attachment	Two snap fasteners attached to each electrode, along with microporous tape
Sensor protection	Thin cotton cover

Table C.4: Summary of the positive and negative factors of design iteration 2.

Positives	Negatives
Knee sleeve more flexible and conformed better to knee	Still bunching of knee sleeve
Grippers mean knee sleeve is more likely to stay in place	
Better purchase with two snap fasteners	
IMU attached with hook and loop tape, better fixation and consistency with orientation	

C.1.3 Iteration 3

Table C.5: Summary of main features of design iteration 3.

Feature	Details
Base knee sleeve	Cycling knee warmer
IMU attachment	Hook and loop tape
Strain sensor attachment	Two snap fasteners attached to each electrode, along with microporous tape
Sensor protection	Theraband

Table C.6: Summary of the positive and negative factors of design iteration 3.

Positives	Negatives
Multiple sizes purchased	Theraband does not wash well
Longer length means shorts can also hold knee warmer in place	
Theraband cover stretches with knee warmer and strain sensor	

C.2 Sensor Configuration

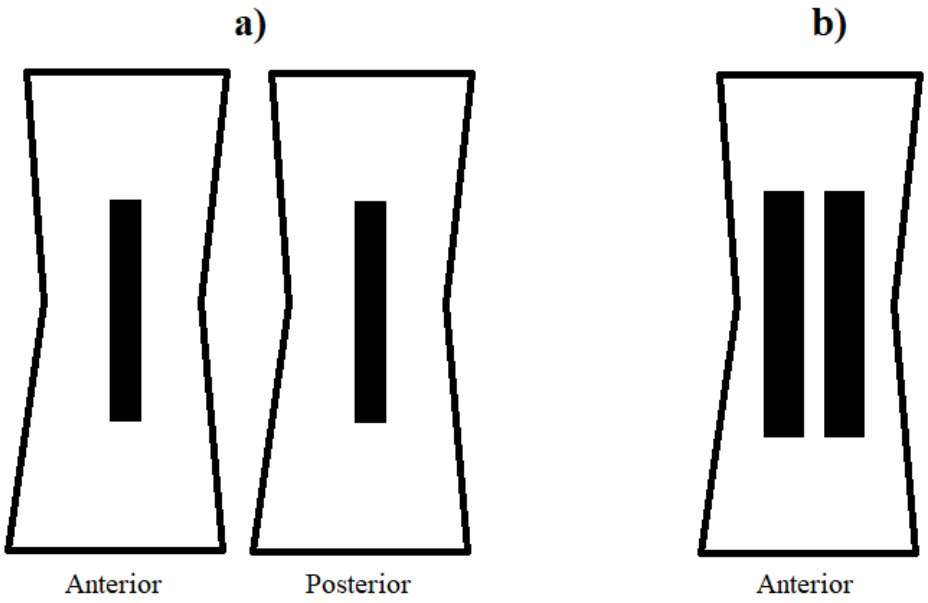


Figure C.2: Schematic of the two sensor configurations tested on the knee warmer a) one sensor was placed on the anterior and the second on the posterior b) both sensors were placed side-by-side on the anterior.

C.2.1 Configuration 1

Table C.7: Summary of the positive and negative factors of sensor configuration 1.

Positives	Negatives
Two sensors to obtain a signal from	Signals produced were out of phase
Sensors positioned in middle of knee joint for most amount of stretch	Calibration more complex with out of phase signals
	Posterior sensor would buckle, despite covering, prodcing a noisy signal

C.2.2 Configuration 2

Table C.8: Summary of the positive and negative factors of sensor configuration 2.

Positives	Negatives
Two sensors to obtain a signal from	Reduced amount of sensor stretching and increased amount of buckling with knee flexion
Both sensor signals in phase	
Potential to detect medial and lateral movement of the knee joint	

Appendix D

Ethics Documents

D.1 Cycling Documents

D.1.1 Approval Letter

Imperial College London

Science Engineering Technology Research Ethics Committee
Imperial College London
Room 221
Medical School Building
St Marys Campus
London
W2 1PG
Tel: +44 (0)207 594 1882

researchethicscommittee@imperial.ac.uk

10 March 2021

Dear Prof. Alison McGregor

Study Title: Study of the Applicability of a Flexible Strain Sensor for Measuring Knee Kinematics in Cyclists

SETREC number: 21IC6651

The above study was approved by your Head of Department on 17/02/21 and by the Research Governance and Integrity Team on 11/03/21.

Under the Science Engineering Technology Research Ethics Committee process, a study that has been reviewed by the Research Governance and Integrity Team and Head of Division/Department, where no significant ethical issues have been identified in the protocol or ethics application, can be given RGIT approval without requiring it to go to full committee.

Documents
The documents reviewed were:

- Application form (v2.1 09/03/2021)
- Protocol (v2.1 09/03/2021)
- Participant Information Sheet (v2.1 09/03/2021)
- Consent Form (v2.1 09/03/2021)
- Recruitment Wording (v2.0 01/03/2021)
- Feedback Questions (v2.1 09/03/2021)

Yours sincerely,

[redacted]

Ruth Nicholson,
Head of Research Governance and Integrity,
Imperial College London

D.1.2 Participant Information Sheet

Imperial College London

Participant Information Sheet

Study of the Applicability of a Flexible Strain Sensor for Measuring Knee Kinematics in Cyclists

Chief Investigator: Professor Alison McGregor (a.mcgregor@imperial.ac.uk)
Co-Investigator: Yewande Adesida (Yewande.adesida12@imperial.ac.uk)

You are being invited to take part in a research study. Before you decide it is important for you to understand why the research is being done and what it will involve. Please take time to read the following information carefully and discuss it with others if you wish.

Ask us if there is anything that is not clear or if you would like more information.
Take time to decide whether or not you wish to take part.

Thank you for reading this.

What is the purpose of the study?
Wearable technology is increasing in popularity and usage, for those looking to track their day to day activities, as well as those looking for those marginal gains. Wearables have the ability to measure biomechanics in a training or competition environment, where movements are not constrained by being in a lab. This can be essential for preventing injury or improving performance.

The overall aim of this study is to determine if a wearable sensor system, containing flexible stretch sensors, can be used to measure knee angles during cycling and to validate it against a gold standard motion capture system and/or commercially available cycling sensors.

We would also like to investigate the repeatability of the measurements and determine the effects of cadence on the motion of the knee joint. The development of this tool can be used to both aid injury prevention and improve performance in cyclists.

Why have I been invited?
We are inviting you to join the study as you have been cycling for at least a year and can help validate this system. We are inviting 20 volunteers to take part in the study.

© Imperial College of Science, Technology and Medicine

Imperial College London

Who are we looking for?

You can take part in the study if you:

- Are 18 years or older
- Have a good understanding of written and spoken English
- Have been cycling for at least a year
- Are in good physical condition and health – no serious injuries or illnesses in the past 3 months
- Are fit – able to complete a 20 minute progressive warm up on the bike
- Have access to an indoor cycling trainer, cadence sensor and cycling computer (for the remote study)

You cannot take part in this study if you:

- Have had serious injuries or illnesses in the past 3 months
- Are pregnant

Do I have to take part?

It is up to you to decide whether or not to take part. If you do decide to take part you will be given this information sheet to keep and be asked to sign a consent form. If you decide to take part you are still free to withdraw at any time and without giving a reason. As the data is anonymised, your contributions will not be deleted but all personal data will be.

What will happen to me if I take part?

Once you have read this document, and have decided to participate, you will be asked to provide your consent via an online form and complete a pre-testing questionnaire, recording details such as: age, gender, height, and body mass and your cycling experience. You will then be asked to come to the Biodynamics Lab (MSk Lab, Imperial College London, White City Campus) for two sessions with the research team on the same day or within two days, or complete the study at remotely at a time that suits you on at least two occasions (within two weeks). For the remote study, you will be provided with an instruction manual that will inform you how to wear the wearable sensor system and how to collect the data.

The study should last no longer than one hour, including participant set-up and completing the progressive warm up.

Assessment steps to take place:

Lab study only:

- Reflective markers and clusters will be positioned over your waist and lower limbs. This is so we can use the VICON motion capture system to also record you knee joint movement and validate the sensor

Remote study:

- You are required to find a suitable place indoors (this can be your normal indoor training environment) to carry out the study

Both studies:

- You will be asked to wear a pair of cycling knee warmers with a wearable sensor system attached to the right knee warmer
- You will be asked to stand still and then perform bodyweight squats in order to calibrate the sensor. For the remote study you will be required to film the squat motion focusing on your lower limbs (your face does not need to be visible). For the lab study this will be recorded using the VICON system
- You will be asked to perform a 20-minute progressive warm up developed by British Cycling on your indoor training set up or our lab set up (Wattibke indoor trainer) while data is collected from the wearable sensor system. Details of the warm up can be found here: https://www.britishcycling.org.uk/zuvvi/media/bc_files/sportivetrainingplans/20_MINUTE_WARM_UP.pdf The warm up will start at a cadence of 80rpm instead of 90rpm as written.
- You will be asked to complete a follow up questionnaire, documenting your experience with the wearable sensor system

The same protocol will be used for each testing session.

You are not required to avoid anything before taking part in the study. Treat it as you would a normal training session, and eat/take medicine beforehand as necessary.

Patient confidentiality will be maintained at all times. Your data will be anonymised for analysis and all data collected will be stored using the reference number on a password-protected computer. Only the research team will be able to access the data from this study.

If you are travelling to Imperial College White City Campus, unfortunately reimbursement for your travel will not be covered. If you are taking part in the remote study, the wearable sensor system will be posted to you and you will be required to

return it once you have completed the study. Unfortunately, we are unable to cover postage costs.

COVID-19 precautions for lab participants: We will be following the university and government guidelines at all times. The university and NHS track and trace will be used, and social distancing will be maintained. Where this is not possible, such as when applying motion capture markers, you will be required to a wear a mask. The research team will be wearing a mask at all times.

What are the possible disadvantages and risks of taking part?

The assessment techniques are entirely safe and non-invasive. There are no known risks from performing these tests. All tests will be performed within your own fitness limits. Care will be taken to ensure your comfort throughout marker placement and removal in the lab study. We will be attaching reflective markers using non-allergenic adhesive tape. These may cause redness to the skin. If you have allergies or skin conditions, please inform the researcher, and other material will be used over the skin to which these markers will be attached to instead. You may also suffer from delayed onset muscle soreness for a few days after testing but you should be able to recover swiftly, being used to such training protocols.

What are the possible benefits of taking part?

There are no direct benefits to you by taking part in the study, however the collective results of the study may contribute to greater insight into knee kinematics in cycling and the use of sensors as an injury prevention and/or performance tool.

What if something goes wrong?

Imperial College London holds insurance policies which apply to this study. If you experience harm or injury as a result of taking part in this study, you will be eligible to claim compensation without having to prove that Imperial College is at fault. This does not affect your legal rights to seek compensation.

If you are harmed due to someone's negligence, then you may have grounds for a legal action. Regardless of this, if you wish to complain, or have any concerns about any aspect of the way you have been treated during the course of this study then you should immediately inform the Investigator (Prof Alison McGregor a.mcgregor@imperial.ac.uk) If you are still not satisfied with the response, you may contact the Imperial College Research Governance Integrity Team.

What will happen to the results of the research study?

The results of the study will be analysed by the research team and presented at health care and scientific conferences and published in peer-reviewed journals. No individual participant will be identified in any report or presentation arising from the research.

Who is organising and funding the research?
EPRSC have supported the researchers' PhD studentship.
This study will be run by a research team based at Imperial College London.

Who has reviewed the study?
This study was reviewed by the Head of Department and the Research Governance and Integrity Team (RGIT).

Confidentiality/Anonymization
Patient confidentiality will be maintained at all times. All staff involved in the study will be required to abide by the Data Protection Act (2018). You will be issued with a unique reference number, which will be used to name and store scientific measures. All data collected will be stored using the reference number on a password-protected computer that belongs to the College. Paper documents will be stored in a locked room and only the principal and co-investigators will have access. Data collected during the study from the sensor and cycling computer device or indoor cycling trainer will be pseudo-anonymised. Any personal data such as: name address and telephone number will be stored separately to the anonymised data.
Data will be stored directly onto a password protected computer. Only the research team will have access to any data collected during the study. Any identifiable data will be kept for 10 years before being destroyed.

Contact for Further Information
If you would like further information about the study, please contact Yewande Adesida (yewande.adesida12@imperial.ac.uk)

Imperial College London

How will we use this information about you?
Research Study Title: Study of the Applicability of a Flexible Strain Sensor for Measuring Knee Kinematics in Cyclists

Imperial College London is the sponsor for this study and will act as the data controller for this study. This means that we are responsible for looking after your information and using it properly. Imperial College London will keep your personal data for:

- 10 years after the study has finished in relation to data subject consent forms.
- 10 years after the study has completed in relation to primary research data.

Legal Basis
As a university we use personally-identifiable information to conduct research to improve health, care and services. As a publicly-funded organisation, we have to ensure that it is in the public interest when we use personally-identifiable information from people who have agreed to take part in research. This means that when you agree to take part in a research study, we will use your data in the ways needed to conduct and analyse the research study.
Health and care research should serve the public interest, which means that we have to demonstrate that our research serves the interests of society as a whole. We do this by following the UK Policy Framework for Health and Social Care Research

International Transfers
There may be a requirement to transfer information to countries outside the European Economic Area (for example, to a research partner). Where this information contains your personal data, Imperial College London will ensure that it is transferred in accordance with data protection legislation. If the data is transferred to a country which is not subject to a European Commission (**EC**) adequacy decision in respect of its data protection standards, Imperial College London will enter into a data sharing agreement with the recipient organisation that incorporates EC approved standard contractual clauses that safeguard how your personal data is processed.

Sharing your information with others
For the purposes referred to in this privacy notice and relying on the bases for processing as set out above, we will share your personal data with certain third parties.

- Other College employees, agents, contractors and service providers (for example, suppliers of printing and mailing services, email communication services or web services, or suppliers who help us carry out any of the activities described above). Our third party service providers are required to enter into data processing agreements with us. We only permit them to process your personal data for specified purposes and in accordance with our policies.

What are your choices about how your information is used?
You can stop being part of the study at any time, without giving a reason, but we will keep information about you that we already have.

- We need to manage your records in specific ways for the research to be reliable. This means that we won't be able to let you see or change the data we hold about you.

Where can you find out more about how your information is used?
You can find out more about how we use your information

- by asking one of the research team
- by sending an email to Prof Alison McGregor (a.mcgregor@imperial.ac.uk), or
- by ringing us on +44 (0)20 7594 2972.

Complaint
If you wish to raise a complaint on how we have handled your personal data, please contact Imperial College London's Data Protection Officer via email at dpo@imperial.ac.uk, via telephone on 020 7594 3502 and/or via post at Imperial College London, Data Protection Officer, Faculty Building Level 4, London SW7 2AZ.

If you are not satisfied with our response or believe we are processing your personal data in a way that is not lawful you can complain to the Information Commissioner's Office (ICO). The ICO does recommend that you seek to resolve matters with the data controller (us) first before involving the regulator.

D.1.3 Feedback Questions

All participants will be required to answer the pre-testing and post-testing questions.

Qualtrics will be used to set up questionnaires, providing links to the PIS. Consent will be taken online from all participants (ICREC_ConsentForm V1 14012021) at the beginning of the questionnaire.

Pre-Testing Questions

The statements on the consent form document (ICREC_ConsentForm V1 14012021) will be listed as with a check box next to each one. Below this, a box will be provided for participants to print their name, which will be taken as consent.

1. Preference for remote or lab study
2. Do you have access to an indoor training set-up (e.g. turbo trainer, rollers or Wattbike AND cadence sensor as minimum)? Please provide details (Remote participants only)
3. Name
4. Age
5. Height
6. Weight
7. Sex
8. No. years cycling
9. Main discipline (Options: Road, Track, MTB, BMX, Cyclocross, Other)
10. Cycling experience level (Options: Commuter, Leisure rider, Competitive, Other)
11. No. training hours per week

Post-Testing Questions

1. Name (to match to pre-testing questions)
2. Were you familiar with the BC warm up prior to the study? Yes/No

Questions specific to this wearable system

Remote participants only:

1. How was it to set up the data collection? (Difficult [1]–very easy [10])
2. How was it to put on/take off the wearable sensor system (WSS)? (Difficult [1]–very easy [10])

All participants:

3. Did you notice the WSS whilst you were wearing it? (Very much [1]–not at all [10])
4. Do you think the WSS negatively impacted your cycling performance? (Very much [1]–not at all [10])

5. Would you use the WSS in a training environment? Yes/No/Maybe/I don't know
6. Would you use the WSS in a competition environment? Yes/No/Maybe/I don't know
7. Would you adjust your cycling based on feedback from this WSS? Yes/No/Maybe/I don't know

V2 01/03/2021

8. Please provide any other details you had on your experience. Open

Questions on wearable systems in general

On a scale 1-10, 10 being most important: wearable technology worn in sport should...

...be comfortable

...be compact (light and small)

...be discrete

...be easy to attach to the body

...be recyclable

...be reliable

...be simple to operate (and maintain)

...give instant feedback

...have clear and readable instructions

...not affect normal movements

...not detach from user unless needed

...provide clear and useful results

...work alongside any coaching input, instead of replacing it

9. Would you allow data to be sent away and analysed or stored on a database?
   Yes/no/maybe/don't know
10. Would you use a device that you had to apply yourself without assistance?
    Yes/no/maybe/don't know
11. Would you spend time learning how to use a new wearable device?
    Yes/no/maybe/don't know

12. Are there any further comments you'd like to make on the general use of wearable technology in sport? Open

V2 01/03/2021

D.2 Rowing Documents

D.2.1 Approval Letter

Imperial College London

Imperial College Research Ethics Committee
Imperial College London
Room 221
Medical School Building
St Marys Campus
London
W2 1PG
Tel: +44 (0)207 594 1862

researchethicscommittee@imperial.ac.uk

17/09/2021

Dear Alison McGregor,

Study Title: A validation study of a flexible strain sensor for monitoring knee flexion in rowers

ICREC Reference number: 17IC4173

The above Notice of Amendment was reviewed by the Research Governance and Integrity Team (RGIT) on 17/09/2021.

The Research Governance and Integrity Team have reviewed the revised documents you submitted and would like to grant RGIT approval to this study on the basis described in the Notice of Amendment.

Documents
The documents reviewed were:

- Notice of Amendment 3 14/09/2021
- Protocol v3.1 07/09/2021
- Participant Information Sheet v5.2 07/09/2021
- Consent Form v4 07/09/2021
- Participant Data Sheet v1 30/08/2021
- Advert v3 07/09/2021
- Email invitation v3 07/09/2021
- Feedback Questions v1 15/07/2021

Yours sincerely,

[redacted]

Ruth Nicholson,
Head of Research Governance and Integrity,
Imperial College London

D.2.2 Participant Information Sheet

Imperial College London

MSk LAB
Advancing musculoskeletal research and treatment

Department of Surgery and Cancer
Imperial College London
Biodynamics laboratory, 2nd Floor
Sir Michael Uren Hub
86 Wood Lane
London W12 0BZ
Tel: 020 3313 8833
www.imperial.ac.uk

Chief Investigator: Professor Alison McGregor (a.mcgregor@imperial.ac.uk)
Co-Investigator: Miss Yewande Adesida (yewande.adesida12@imperial.ac.uk)

A validation study of a flexible strain sensor for monitoring knee flexion in rowing

Participant Information Sheet
Version 5.2, 07.09.2021

We would like to invite you to join a research study. Before you decide it is important for you to understand why the research is being done and what it will involve. Please take time to read the following information carefully and discuss it with others if you wish. Ask us if there is anything that is not clear or if you would like more information. Take time to decide whether or not you wish to take part.

What is the purpose of the study?
The overall goal of the study is to determine if a flexible strain sensor can be used to measure knee angles during the rowing stroke and to validate it against a gold standard motion capture system. We would also like to investigate the repeatability of the measurements and determine whether the range of motion of the knee joint changes at different speeds. The development of this tool can be used as an injury prevention method but also for performance in terms of looking at stroke length.

Why have I been invited?
We are asking you to think about joining this study because you have been rowing for at least two years. We are inviting 30 volunteers to take part in this study.

Who are we looking for?
You can take part in the study if you:

- Are aged 18 and over
- Have been rowing for a minimum of two years
- Are in good physical condition and have not been injured in the past six months
- Are fit and able to complete a 12-minute step test on the rowing machine

You cannot take part in this study if you:

- Currently have any episode of lower back pain or any other serious illnesses or injuries
- Have had any knee injuries in the past 12 months
- Have a history of knee surgery
- Are pregnant

Do I have to take part?
No. It is entirely up to you whether or not you would like to take part. If you decide to take part, you will be given this information sheet to keep and be asked to sign a consent form. Even after you have signed this consent form and agreed to join the study, you are free to withdraw at any time. A decision to withdraw at any time, or a decision not to take part, will not affect

the standard of care you receive, your education or grades should you be a student at Imperial College London. If you chose to withdraw from the study at any time, the information collected up until that point will be retained and used in the study; however, no further data will be collected. Please inform any member of the research team if you no longer wish to participate in the study.

What will I have to do if I take part?
Once you have decided to take part in this research, you will be asked to come to the Biodynamics Laboratory (the address of which is shown above), where a member of our research team will discuss the study with you and answer any questions you may have. If you are still happy to take part, we will ask you to sign the consent form.
You will be required to attend the Biodynamics Laboratory (MSk laboratory, Imperial College, White City Campus), for a total of two sessions, lasting approximately 60 minutes each.

Assessment steps taking place within the Biodynamics Lab:

- Your height, weight, gender and age will be recorded on your first visit to the Lab.
- The following assessments will be the same for both sessions.
    - Reflective markers and clusters will be positioned over your waist and lower limbs. This is so that we can use the VICON Motion System to also record your knee joint movement and validate the sensor
    - You will be asked to wear a knee sleeve which will have the flexible strain sensors positioned over the knee joint
    - You will be asked to complete a step test on the rowing machine: 4x3 minutes at increasing stroke rates (r18, r24, r28 and free rate). The actual rate, average 500m split and distance covered will be recorded for each one. You will be allowed time to rest between each step and recover as needed

You will be asked to complete a follow up questionnaire, recording details such as: your rowing background and experience with the wearable sensor system. You will be provided with a link to the questionnaire on Qualtrics by a member of the research team after each testing session and it will take no more than five minutes to complete.

Note: You will be asked to wear appropriate kit for using the rowing machine such as an all in one and trainers.

What are the side effects and are there any risks in taking part?
The assessment techniques are entirely safe and non-invasive. There are no known risks from having these tests or exercises performed. All tests will be performed within your own fitness limits. Care will be taken to ensure you comfort throughout marker placement and removal. We will be attaching reflective markers to your skin using non allergenic adhesive tape. These may cause redness to the skin. If you have allergies or skin conditions, please inform the researcher, and other material will be used over the skin to which the markers will be attached to instead. You may also suffer from delayed onset muscle soreness in the few days after testing but you should be able recover swiftly being used to such training method.

What are the possible benefits of taking part?
There is no direct benefit to research participants. However, the collective results of the study may contribute to greater insight into knee kinematics in rowing and the use of sensors as an injury prevention and/or performance tool.

What if something goes wrong?
If you are harmed by taking part in this research project, there are no special compensation arrangements. If you are harmed due to someone's negligence, then you may have grounds for a legal action. Regardless of this, if you wish to complain, or have any concerns about any aspect of the way you have been treated during the course of this study then you should immediately inform the Investigator (Prof. Alison McGregor, a.mcgregor@imperial.ac.uk). If

you are still not satisfied with the response, you may contact the Imperial College Research Governance and Integrity Team.

What happens when the research study stops?
The results of the study will be analysed by the research team and presented at health care and scientific conferences and published in peer-reviewed journals. No individual participant will be identified in any report or presentation arising from the research.

Who is organising and funding the research?
EPRSC have supported the researchers' PhD studentship.
This study will be run by a research team based at Imperial College London.

Will I be paid for taking part in the study?
You will not be paid for your participation in the study.

Who has reviewed the study?
This study was reviewed by the Head of Department and the Research Governance and Integrity Team (RGIT).

Contacts for further information
If you would like further information about the study, please contact Yewande Adesida (yewande.adesida12@imperial.ac.uk)

How will your information be used about you?

Research Study Title: A validation study of a flexible strain sensor for monitoring knee flexion in rowing
Study number: 17IC4173
Imperial College London is the sponsor for this study and will act as the data controller for this study. This means that we are responsible for looking after your information and using it properly. Imperial College London will keep your personal data for:

- 10 years after the study has finished in relation to data subject consent forms.
- 10 years after the study has completed in relation to primary research data.

We will need to use information from you for this research project. This information will include your name. People will use this information to do the research or to check your records to make sure that the research is being done properly. People who do not need to know who you are will not be able to see your name or contact details. Your data will have a code number instead. We will keep all information about you safe and secure. Once we have finished the study, we will keep some of the data so we can check the results. We will write our reports in a way that no-one can work out that you took part in the study.

Legal Basis
As a university we use personal information to conduct research that will either be in the public interest, or the legitimate interests of the College.
As a publicly-funded organisation we have to ensure that when we use personally-identifiable information from people who have agreed to take part in research, it is either in the public interest, or that our legitimate purposes are both properly notified to you and are not overridden by your rights.
We will conduct scientific research in compliance with the law and the recommendations and guidance published by the UK Information Commissioners Office (ICO). This will follow similar rules to health and care research but may not meet the definition of the College's public

interest task. In such cases we will be holding and using your data for what are deemed our "legitimate interests".

International Transfers
There may be a requirement to transfer information to countries outside the European Economic Area (for example, to a research partner). Where this information contains your personal data, Imperial College London will ensure that it is transferred in accordance with data protection legislation. If the data is transferred to a country which is not subject to a European Commission (**EC**) adequacy decision in respect of its data protection standards, Imperial College London will enter into a data sharing agreement with the recipient organisation that incorporates EC approved standard contractual clauses that safeguard how your personal data is processed.

Sharing your information with others
For the purposes referred to in this privacy notice and relying on the bases for processing as set out above, we will share your personal data with certain third parties.

- Other College employees, agents, contractors and service providers (for example, suppliers of printing and mailing services, email communication services or web services, or suppliers who help us carry out any of the activities described above). Our third party service providers are required to enter into data processing agreements with us. We only permit them to process your personal data for specified purposes and in accordance with our policies.

What are your choices about how your information is used?
You can stop being part of the study at any time, without giving a reason, but we will keep information about you that we already have.

- We need to manage your records in specific ways for the research to be reliable. This means that we won't be able to let you see or change the data we hold about you. (this must be consistent with the protocol document, amend if needed)

Where can you find out more about how your information is used?
You can find out more about how we use your information

- by asking one of the research team
- by sending an email to Prof Alison McGregor (a.mcgregor@imperial.ac.uk), or
- by ringing us on +44 (0)20 7594 2972.

Complaint
If you wish to raise a complaint on how we have handled your personal data, please contact Imperial College London's Data Protection Officer via email at dpo@imperial.ac.uk, via telephone on 020 7594 3502 and/or via post at Imperial College London, Data Protection Officer, Faculty Building Level 4, London SW7 2AZ.

If you are not satisfied with our response or believe we are processing your personal data in a way that is not lawful you can complain to the Information Commissioner's Office (ICO). The ICO does recommend that you seek to resolve matters with the data controller (us) first before involving the regulator.

Thank you
We would like to thank you for taking the time to read through this information sheet and for possibly participating in the study.

D.2.3 Feedback Questions

All participants will be required to answer the post-testing questions.

Qualtrics will be used to set up questionnaires.

Post-Testing Questions

1. Name
2. No. years rowing
3. Main discipline (Options: Sweep, Sculling, Fixed Seat, Coastal, Indoor, Other)
4. Rowing experience level (Options: Recreational, Competitive, Other)

Questions specific to this wearable system

All participants:

1. Did you notice the wearable sensor system (WSS) whilst you were wearing it? (Very much [1]–not at all [10])
2. Do you think the WSS negatively impacted your rowing performance? (Very much [1]–not at all [10])

3. Would you use the WSS in a training environment? Yes/No/Maybe/I don't know
4. Would you use the WSS in a competition environment? Yes/No/Maybe/I don't know
5. Would you adjust your rowing based on feedback from this WSS? Yes/No/Maybe/I don't know

6. How would you use the information from this system?

7. Please provide any other details you had on your experience. Open

Questions on wearable systems in general

On a scale 1-10, 10 being most important: wearable technology worn in sport should...

...be comfortable

...be compact (light and small)

...be discrete

...be easy to attach to the body

...be recyclable

...be reliable

...be simple to operate (and maintain)

V1 15/07/2021

...give instant feedback

...have clear and readable instructions

...not affect normal movements

...not detach from user unless needed

...provide clear and useful results

...work alongside any coaching input, instead of replacing it

8. Would you allow data to be sent away and analysed or stored on a database? Yes/no/maybe/don't know
9. Would you use a device that you had to apply yourself without assistance? Yes/no/maybe/don't know
10. Would you spend time learning how to use a new wearable device? Yes/no/maybe/don't know

11. Are there any further comments you'd like to make on the general use of wearable technology in sport? Open

V1 15/07/2021

Appendix E

Squat Calibration

E.1 Participant 34943, visit 1

Table E.1: Mean max and min knee flexion angles during squatting and rowing trials (Participant 34943)

	Mean knee flexion angle (degrees)	
	Max	Min
Squats	132.20 ± 0.74	6.35 ± 1.71
Rowing step 1	120.96 ± 0.93	-3.55 ± 0.83
Rowing step 2	127.95 ± 0.65	0.87 ± 0.92
Rowing step 3	133.52 ± 0.75	3.50 ± 1.00
Rowing step 4	135.66 ± 0.57	5.06 ± 1.33

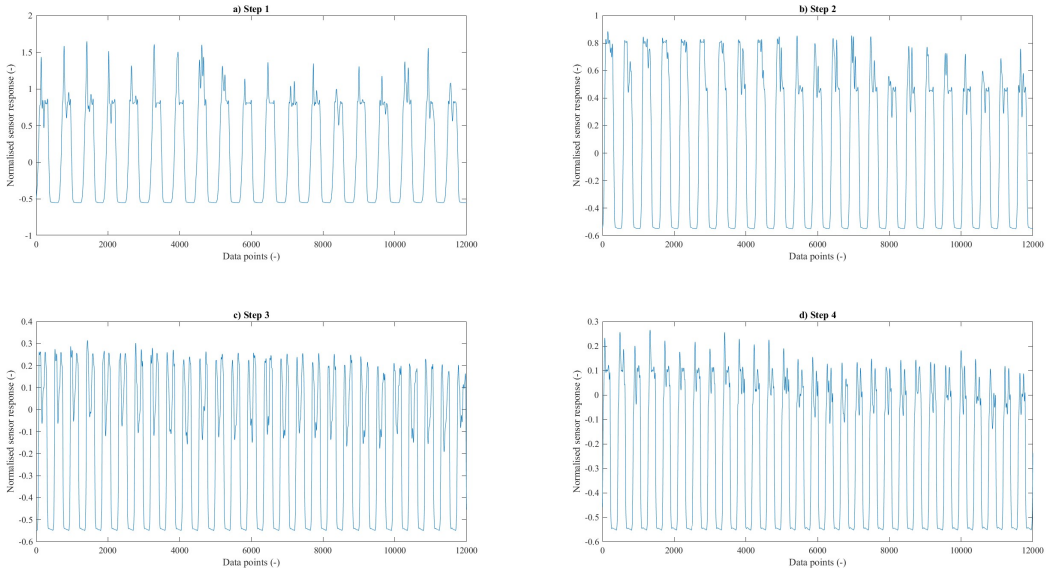


Figure E.1: Example of sensor response normalised by the sensor signal range in dynamic squat trial performed at the beginning of the testing protocol (Participant 34943)

E.2 Participant 77344, visit 1

Table E.2: Mean max and min knee flexion angles during squatting and rowing trials (Participant 77344)

	Mean knee flexion angle (degrees)	
	Max	Min
Squats	137.07 ± 0.70	6.35 ± 0.65
Rowing step 1	141.29 ± 0.30	-3.55 ± 0.65
Rowing step 2	142.45 ± 0.25	0.87 ± 0.88
Rowing step 3	140.09 ± 0.33	3.50 ± 0.37
Rowing step 4	136.03 ± 0.69	5.06 ± 0.56

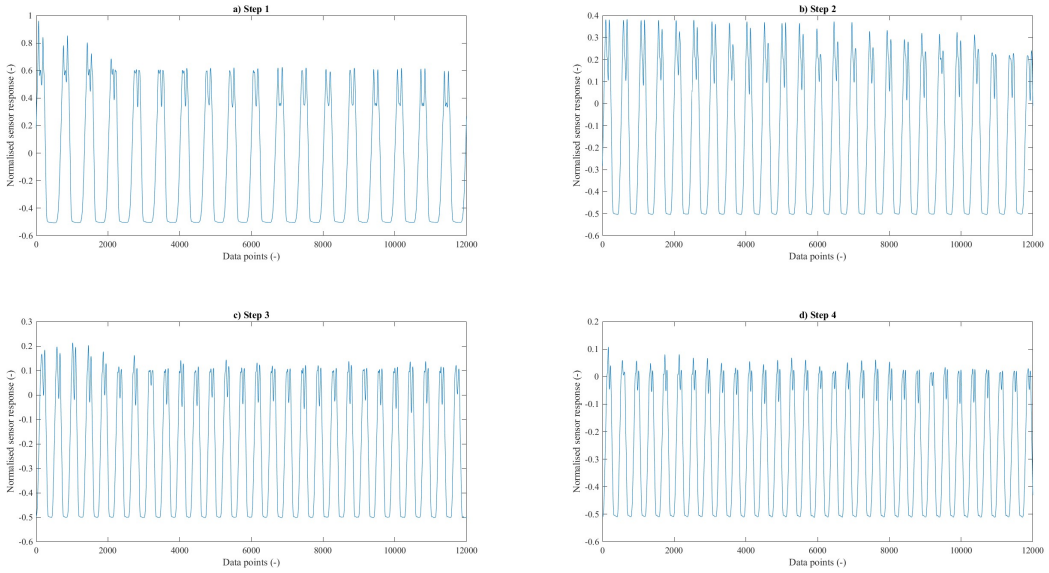


Figure E.2: Example of sensor response normalised by the sensor signal range in dynamic squat trial performed at the beginning of the testing protocol (Participant 77344)

E.3 Participant 48896, visit 2

Table E.3: Mean max and min knee flexion angles during squatting and rowing trials (Participant 48896)

	Mean knee flexion angle (degrees)	
	Max	Min
Squats	100.92 ± 2.8	-7.92 ± 0.80
Rowing step 1	129.16 ± 0.45	-0.17 ± 1.19
Rowing step 2	127.51 ± 0.55	3.55 ± 1.43
Rowing step 3	129.07 ± 0.66	2.48 ± 0.96
Rowing step 4	129.06 ± 0.62	3.46 ± 1.52

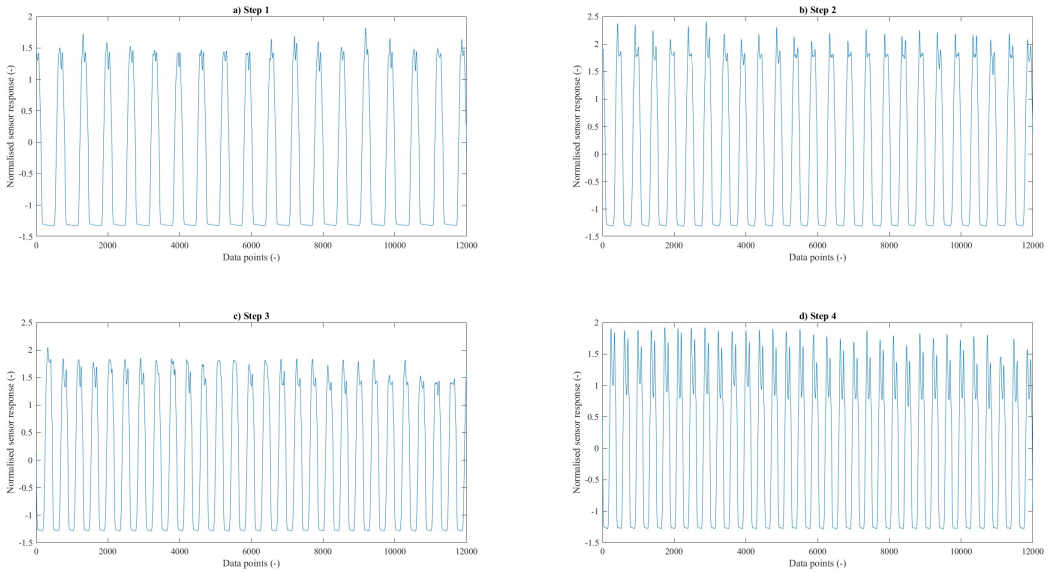


Figure E.3: Example of sensor response normalised by the sensor signal range in dynamic squat trial performed at the beginning of the testing protocol (Participant 48896)